Application of geochemical characterization, multivariate statistics and geological modelling in assessment and prediction studies on selected coal and gold mine waste in South Africa

by

Oluseyi Blessed Abegunde

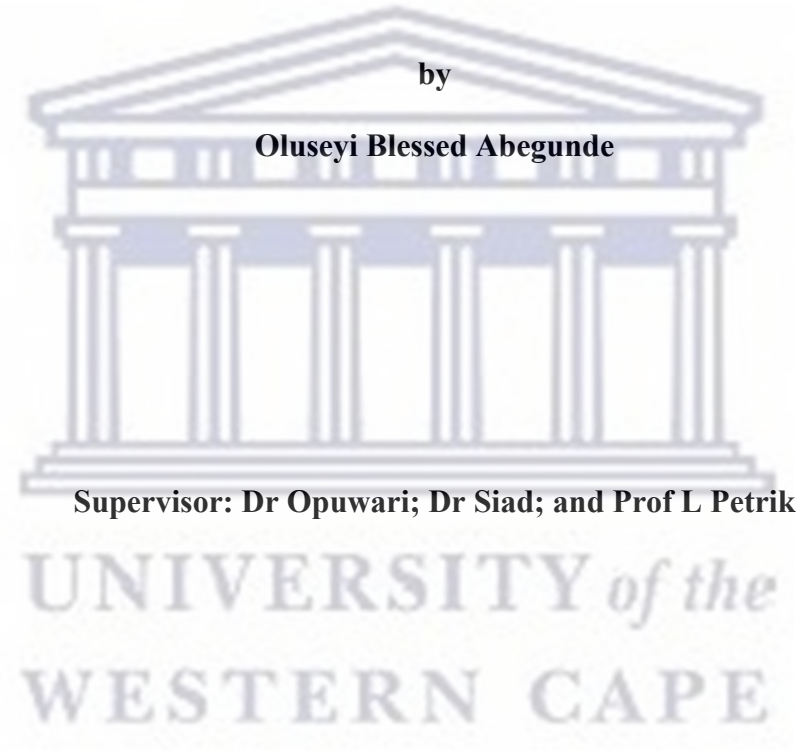

Supervisor: Dr Opuwari; Dr Siad; and Prof L Petrik

UNIVERSITY of the
WESTERN CAPE

A thesis submitted in fulfilment of the requirements for the degree of Doctor of Philosophy of Science in Applied Geology in the Faculty of Natural Sciences at the University of the Western Cape

http://etd.uwc.ac.za/

DECLARATION

I therefore declare that this thesis report is my own, unaided work. It is being submitted for the degree of PhD in Applied geology at the Department of Earth Science, Faculty of Natural Sciences, University of the Western Cape, Bellville. It has not been submitted before for any degree or examination in any other University.

……..

Student Signature

UNIVERSITY of the
WESTERN CAPE

http://etd.uwc.ac.za/

ABSTRACT

Over the years, South Africa has generated vast amounts of coal fly ash and gold slime tailings, constituting over 70% of the country's waste materials. These by-products contain elevated levels of trace metals, posing a potential threat to the environment upon release. Addressing this issue requires a comparative study of the environmental impact of coal fly ash and selected mine tailings on water resources and land pollution.

This research aims to investigate and compare leachability, metal release, oxidation effects, and environmental pollution between coal fly ash and gold tailings. By contrasting these aspects, the study seeks to enhance understanding of the potential risks associated with these materials, aiding informed decision-making for their management and regulation. Additionally, the research explores the correlation between gold tailings' acid potential generation and coal fly ash's alkaline potential generation in terms of leachability, metal release, oxidation effects, and environmental pollution.

The research employed comprehensive laboratory experiments and analytical investigations, including leaching tests under simulated weathering conditions. A total of 51 gold tailings samples and 66 coal fly ash samples were analysed through SEM and XRD for mineralogical insights and ICP-MS and XRF for geochemical analyses. Statistical analysis revealed the significant roles of pH, Fe ions, Ca^{2+}, and Mg^{2+} in metal extraction from both materials.

Notably, the study identified key factors contributing to the environmental impact of coal fly ash and gold tailings. SEM imagery highlighted heterogeneous characteristics in gold tailings, while factor analysis indicated the potential release of ferrous ionic species, contributing to acidity. Trace elements like Ni, Zn, Pb, and Cu were predominantly associated with Fe/Mn oxides during leaching experiments, facilitating their mobilization with acid-generating ions.

In conclusion, this research emphasizes the potential of tailings dams to generate Acid Mine Drainage (AMD) upon exposure to oxidation, particularly in gold tailings. The study underscores the need for mitigation strategies and sustainable

UNIVERSITY of the WESTERN CAPE

http://etd.uwc.ac.za/

management practices to address the environmental implications of these mining by-products. The presence of carbonate-associated ions in coal fly ash may hinder AMD release, while Fe/Mn oxide-associated ions in tailings dams increase the likelihood of AMD release upon oxidation.

UNIVERSITY of the
WESTERN CAPE

http://etd.uwc.ac.za/

ACKNOWLEDGEMENT

First and foremost, I would like to acknowledge the almighty God, the I am that I am, the all-sufficient God, the Alpha and Omega, and the everlasting God for seeing me through my PhD programme. No word is enough to thank you.

I would like to thank my supervisor, Prof M Opuwari, for his effort day-in and day-out, and not giving up on me. Despite his tight schedule and other engagements, he scrutinised, perused my thesis, and see to the completion of this programme. May the lord bless you and grant you an everlasting joy. You added value to me

I would like to thank Prof Emeritus Charles Okujeni, for giving me this opportunity. Knowing you was a blessing. May the lord bless you Prof. You made me a better person.

I acknowledge my co-supervisor, Dr AM Siad and Prof L Petrik for grooming and moulding me into a researcher. I also acknowledge all teaching and non-teaching staff of the department of Applied Geology, most especially Prof Kanyerere and Ms. Davids for their support.

My sincere appreciation goes to my lovely parents late Mr. H.I Abegunde and Chief Mrs E.O. Abegunde for all your efforts right from my cradle to this present time, for being the instrument God used to get me to the state I am. Many thanks also go to my one and only blood sister (Abegunde Olubunmi O nee Ajayi) for your financial support even when I was stuck. You people are blessings to me.

I would like to thank my lovely, wonderful and dearest wife, Mrs. Adeola Abegunde (Princess Adeola). Ever since you arrived in South Africa, my life has taken a great turn for good. Your smiles, encouragement, prayers and full support saw me through this study. I bless God for given you to me as an uncommon gift. I love you dear; the Lord will grant you the desires of your heart and keep us together.

I also want to thank my beautiful baby, Testimony Abegunde. You brightened this year for me and completed my joy. Thank you for coming into our lives. Daddy loves you. God bless you my beautiful Testimony

http://etd.uwc.ac.za/

I want to thank my pastor and brother Prof O Fatoba and family, for orchestrating my journey to South Africa, for the support rendered always. The Lord will continue to uphold you.

I cannot but acknowledge my research partner Iris Wu for accepting me into this research and taking care of me like her brother. May God be with you and bless you abundantly in return. I also use this medium to appreciate my cousin and friend Mr Oluwasanmi Lawal for his support and encouragement.

I want to thank my brother, friend and editor, Okeowo Timilehin, for his support, care and efforts to see me scale this hurdle. You have been a good brother that I respect so much. Thank you for all you did to make sure this thesis is properly shaped. God bless you.

My thanks go to Ameh Emmanuel, Prof Oyowe and Ndubuisi for your support. The Lord will continually bless you. Also, I appreciate my Pastor at home, Pastor Dairo for his prayers and support.

Finally, I want to thank Inkaba and NRF for their financial support towards the completion of this study.

UNIVERSITY of the
WESTERN CAPE

http://etd.uwc.ac.za/

TABLE OF CONTENTS

UNIVERSITY of the WESTERN CAPE

http://etd.uwc.ac.za/

UNIVERSITY of the WESTERN CAPE
http://etd.uwc.ac.za/

UNIVERSITY of the WESTERN CAPE
http://etd.uwc.ac.za/

UNIVERSITY of the WESTERN CAPE
http://etd.uwc.ac.za/

UNIVERSITY of the WESTERN CAPE
http://etd.uwc.ac.za/

UNIVERSITY of the WESTERN CAPE

http://etd.uwc.ac.za/

LIST OF FIGURES

UNIVERSITY of the WESTERN CAPE

http://etd.uwc.ac.za/

UNIVERSITY of the
WESTERN CAPE

http://etd.uwc.ac.za/

LIST OF TABLES

UNIVERSITY of the WESTERN CAPE

http://etd.uwc.ac.za/

ACRONYM	
AMD	Acid Mine Drainage
AP	Acidic Potential
CA	Cluster analysis
DDW	Deionised distilled water
FA	Factor analysis
FD	Fresh dump
GDP	Gross Domestic Product
GIS	Geographical Information System
GMB	Geochemical Mass Balance
GPS	Global Positioning System
ICP –MS	Inductive Coupled Plasma- Mass Spectroscopy
ICP-OES	Inductive Coupled Plasma- Optical emission spectrometry
IDW	Inverse Distance Weight
LA	Laser Ablation
MPA	Maximum potential acidity
MT	Mogale tailings dam
ND	New dump
NP	Neutralisation Potential
OD	Old dump
PCA	Principal Component Analysis
QA/QC	Quality Assurance and Quality Control
REEs	Rare earth elements
SPSS	Statistical Package for Social Science
TDS	Total Dissolved Solids
USEPA	US Environmental Protection Agency
XRD	X-ray Diffraction
XRF	X-ray Fluorescence

UNIVERSITY of the WESTERN CAPE

http://etd.uwc.ac.za/

APPENDIX

UNIVERSITY of the
WESTERN CAPE

http://etd.uwc.ac.za/

PUBLICATIONS

Abegunde, O.A., Okujeni, C., Petrik, L., Siad, A.M., Madzivire, G. and Wu, C., 2020. The use of factor analysis and acid base accounting to probe the speciation of toxic metals in gold mine waste. Environmental Earth Sciences, 79(6), pp.1-12.

Abegunde O, Siad A, Okujeni C, Petrik L; Madzivire G Application of Geostatistical tools in predicting elemental speciation in mine wastes RFG 2018 Resources for Future Generations, June 16-21, 2018 | Vancouver Convention Center, Vancouver, BC, CANADA

Abegunde O, Siad A, Okujeni C; Petrik L; Madzivire G The Use of Factor Analysis to Probe the Speciation of Toxic Metals in Gold Mine Waste (gold2018: abs:2018002430), Boston, MA, USA, from August 12th-17th, 2018

Abegunde O[1] , Siad A[1] , Okujeni C[1] , Petrik L[2] The use of chemometrics in the determination of element speciation in selected mine waste, Iphakade Conference, 2018 Bloemfontein

Abegunde, O.A., Okujeni, C.D., Wu, C. & Siad, A. 2016

Distribution patterns of contaminants in the Mogale Gold tailing dam: a case study from South Africa, Environmental Earth Sciences, vol. 75, no. 20, pp. 1365

ABEGUNDE, Oluseyi A.[1], SIAD, A.M.[1], WU, Iris[2] and PETRIK, Leslie[3]: Application of Geochemical Characterization, Geostatistics and Geological Modelling in Assessment and Prediction Studies on Selected Coal and Gold Mine Waste in South Africa; 2015 GSA Annual Meeting in Baltimore, Maryland, USA (1-4 November 2015) Paper No.207-19

O., Abegunde; C., Wu; C.D., Okujeni; and A., Siad: Application of GIS interpolation in assessment of a gold tailings dam; ESRI USER CONFERENCE2015http://proceedings.esri.com/library/userconf/proc15/abstracts/a442.html

http://etd.uwc.ac.za/

CHAPTER ONE

1. INTRODUCTION

Globally, serious environmental issues, such as acid /or alkaline mine drainage (AMD) and Neutral mine drainage (NMD) emanated as an aftermath of mining activities, and since, it has remained costly to manage (Tripathy, 2014; Petrik et al., 2017; Simate & Ndlovu, 2021). The mining activities led to the release of trace elements, including highly mobile toxic ions, into the environment because they are easily transferred through aquatics and soil capillary pathway (drainage) (Madzivire et al., 2010; Petrik et al., 2017; Simate & Ndlovu, 2021). As defined, AMD is generally characterised by one or more of the following: low pH, high total dissolved solids (TDS), high sulphates (SO_4^{2-}), and high levels of heavy metals; particularly iron (Fe), manganese (Mn), nickel (Ni) and/ or cobalt (Co) (Madzivire et al., 2010).

However, to evaluate the environmental impact of elements associated with AMD accumulated in soils, tailings etc., the chemical state in which the elements are present (easily exchangeable ions, metal carbonates, oxides, sulphides, organometallic compounds, ions in crystal lattices of minerals, etc.) needs to be studied (Guillén et al., 2012).

Notably, the oxidation of pyrite produces acid and effectively lowers the pH of the drainage, water pathway and other water bodies as it enters the ground water regime beneath the dumps (Naicker, et al., 2003). Due to this effect, the extent of acidity, mobility of elements and pH level in drainages or sulphate soils or mine waste are determined by the form and magnitude of existing sulphide minerals, reactive surface area and the acid-neutralizing (carbonate) minerals confined (Nordstrom and Alpers, 1999; Skousen, J., 2017).

This study probes the elements' mobility of selected mine waste material, based on the natural elemental speciation and other possible phenomena like natural water medium, acidic and alkaline medium using sequential extraction and multivariate

UNIVERSITY of the WESTERN CAPE
http://etd.uwc.ac.za/

analysis. Therefore, this study evaluates the state of waste, environmental condition for the release of elements, the control of mineralogy within the selected waste and identification of pattern of elements released under different environmental conditions. Geostatistical tools (such as multivariate analysis) and mineralogical evaluation were used to extract more information from the three-step modified sequential extraction procedure (SEP). This approach aids better understanding of the elemental speciation or mobility of the selected waste material. Furthermore, statistical analysis results were corroborated with other information to compare the behavior of the selected waste materials to one another in terms identified relationships that exist and establishing the efficacy of the research towards predicting peculiar Mine Drainage.

1.1 Research Background

The mining industry has become one of the sources of environmental challenges for human health, due to varying nature and extent of waste materials generated(Tempelhoff & Winde, 2019; McCarthy, 2011; Hansen, 2015; Tutu, E. Cukrowska, et al., 2003; Masindi et al., 2018; Naicker et al., 2003; Rösner & Schalkwyk, 2000). Notwithstanding, the mining industry remains a valued source of revenue, with huge contributions to several job opportunities in South Africa(Lloyd, 2000; Masindi et al., 2018; Abegunde et al., 2016; Durand, 2012a). Although, operational procedures such as raw material crushing, ore reprocessing and solid waste disposal executed in the mining industry are observed as causes of pollution within the ecosystem, (Chunhacherdchai et al., 2011a; Durand, 2012b; Kroukamp & Wepener, 2022). Relative to this, a million tonnes of coal mining waste material and gold slime tailings have been produced in South Africa over the years. These wastes have contributed over 80% environmental impacts on South Africa more than a decade.

Usually, coal and gold mining are immensely effective in South Africa. Therefore, activities performed in this sector generated waste material that posed risks to the environment. Waste material generation during coal and gold mining operations are identified as coarse coal refuse (CCR) and fine coal refuse (FCR) slurry wastes

http://etd.uwc.ac.za/

which are as a result of direct mining-coal separation, coal combustion products (CCPs) for coal mining as well as waste rocks, sand and slime tailings for gold mining wastes, which requires no combustion (Jamieson et al., 2015; Brough et al., 2013). Although, similar studies have been conducted on the potential acid mine drainage (AMD) generated from the gold and coal mining waste, especially slime tailings and CCPs, due to the volume of waste produced from these processes(Younger, 2004; Robl et al., 2017; Camden-Smith et al., 2015; Dold, 2014; Lemos et al., 2021).

The discharge of these waste material to the environment has an impact on the ecosystem due to the presence of high concentrations of tracemetals. This necessitates a comparative study of the environmental impact of coal fly-ash and mine tailings in polluting water resources and land. Established assessment and prediction studies will create a map to substantiate the remediation process.

1.2 Research Problem

The impact of AMD affects land owners and people dwelling in this area who largely depend on ground water for domestic purposes such as potable water, business and agricultural uses. This is caused by the previous and present mining activities in South Africa is precarious and requires necessary intervention (Robb & Meyer, 1995; Oelofse et al., 2007; McCarthy, 2011; Akcil & Koldas, 2006; Rösner & Schalkwyk, 2000; Nengovhela et al., 2006). Early studies demonstrated that fresh groundwater in the huge dolomitic aquifer underneath is contaminated with acidic and alkaline water (Tutu et al., 2008; Oelofse et al., 2004), therefore, poses a great risk to the natural environment. It was predicted that without active pumping, groundwater would fill mine void space due to precipitation (e.g. rainfall), which could lead to surface decanting (McCarthy, 2011; Akcil & Koldas, 2006). Despite the implementation of the remediation processes, it is understood that mine drainage trace elemental load still pose a great risk to the natural environment(Abegunde et al., 2020; Benner et al., 1997; Wuana & Okieimen, 2011; Barton et al., 2005; Johnson & Hallberg, 2005). The impact of this was thoroughly

http://etd.uwc.ac.za/

evaluated in this study with the aim of pinpointing the responsible factors causing this ripple effect.

1.3 Research Questions

Some research questions were formulated to comprehend the impact of AMD on the natural environment. These questions cover areas that contribute to the impact of these wastes on the ecosystem. The questions are enumerated as follows:

- Where do wastes leached to? And to what extent have they been actively oxidised?
- What risks do they have on the environment, surface and underground aquifer? And which waste has more risk than the other?
- Are the modes of elemental pollution and speciation similar?
- What phase plays a major role in elemental release?

1.4 Research Aim and Objectives

The aim of the research is to predict and highlight the link between the gold tailings' acid potential generation and coal fly ash alkaline potential generation on their potential to pollute the environment, metal release, and oxidation effect despite having different pH environment.

UNIVERSITY of the
WESTERN CAPE

1.4.1 Research Objectives

The objectives of this study will be:

- To evaluate the trace elements speciation and mobility using modified sequential extraction techniques for coal fly ash and gold tailings.
- To use multivariate statistical analysis tool to predict the relationship between coal fly ash and gold tailings.
- To determine the link between coal fly ash and gold tailings as it impacts water quality and propose recommendations that will enable implementation of remediation process.

http://etd.uwc.ac.za/

1.5 Significance of the Research

This research holds critical importance in advancing our understanding of the environmental impact of coal fly ash and gold mine tailings, differentiating itself through unique contributions to the existing body of knowledge. The study specifically focuses on elucidating the environmental implications of these mining by-products, emphasizing factors that set it apart from prior research.

By conducting a comprehensive comparative analysis, the research aims to reveal novel findings regarding the distinct behaviours, risks, and potential impacts of coal fly ash and gold tailings on the environment. The significance lies in the depth of insights generated through the juxtaposition of leachability data and oxidation effects, leading to a better understanding of the key factors driving their respective environmental impacts.

Furthermore, this research contributes to the development of mitigation strategies, regulatory measures, and sustainable management practices. The anticipated outcomes have the potential to inform decision-making processes for environmental management, offering valuable insights for addressing the adverse effects associated with the presence of coal fly ash and gold tailings in the environment.

In essence, the significance of this research lies in its ability to fill critical gaps in the current understanding of the environmental impact of mining by-products, thereby paving the way for more informed and effective strategies in environmental management.

UNIVERSITY of the
WESTERN CAPE

1.5 Ethical Considerations

No ethical permission is required.

1.6 Dissertation Structure

Chapter 1 Introduction

Chapter 2 Literature review

Chapter 3 Methodology

Chapter 4 Geochemical and geostatistical characterisation of coal fly ash

http://etd.uwc.ac.za/

Chapter 5 Geochemical and geostatistical characterisation of gold tailings

Chapter 6 Comparative analysis of findings

Chapter 7 Conclusions and recommendations

http://etd.uwc.ac.za/

CHAPTER TWO

2. LITERATURE REVIEW

2.1 Introduction

This chapter entails a review on areas peculiar to the study such as an overview of the relationship between mining activities and the environment impact thereof, e.g. waste composition and potential pollutant sources.

2.2 Mining and The Environment

The mining industry has become one of the sources of environmental problems for human health, as it produces waste materials of variable nature and extent known as mine waste (Chunhacherdchai et al., 2011). These waste materials are produced from mining and milling operations such as raw material grinding, ore refining and solid waste disposal (Chunhacherdchai et al., 2011; Navarro et al., 2004). And they can be a disadvantage by contaminating the environment (Chunhacherdchai et al., 2011b; Navarro et al., 2004). In addition, mining and smelting of non-ferrous metals have been reported to contribute to the cause of soil pollution, metal dust emanation, water, effluents, and seepage(Alloway, 1990). The end product residue/material from the mining industry is called "mine waste". Some mine waste materials are pumped into large surface impoundment known as waste stone, coal fly ash, "tailings dams" or "Tailings Storage Facilities" (TSF) (Chunhacherdchai et al., 2011). By exposure, surface deposition of mine waste releases pollution to the atmosphere, including precipitation and surface water (Saria et al., 2006). Sulphide or pyritiferous ores in mine waste materials have high potential to react with oxygen and water (Saria et al., 2006).

Globally, serious environmental issues, such as acid mine drainage (AMD) emanated as an aftermath of mining activities, and since it remained costly to manage. These mining activities led to the release of trace elements, including highly mobile toxic ions into the environment because they are easily transferred through aquatics and soil capillary pathway (drainage). As defined, AMD is generally characterised by one or more of the following: low pH, high total dissolved solids (TDS), high sulphates (SO_4^{2-}), and high levels of heavy metals;

http://etd.uwc.ac.za/

particularly iron (Fe), manganese (Mn), nickel (Ni) and/ or cobalt (Co)(Madzivire et al., 2010).

However, to evaluate the environmental impact of elements associated with AMD accumulated in soils, tailings etc., the chemical state in which the elements are present (easily exchangeable ions, metal carbonates, oxides, sulphides, organometallic compounds, ions in crystal lattices of minerals, etc.) needs to be studied thoroughly for better understanding (Pérez et al., 2008; Guillén et al., 2012).

Notably, the oxidation of pyrite produces acid and effectively lowers the pH of the drainage, water pathway and other water bodies as it enters the ground water regime beneath the dumps (Naicker et al., 2003). Due to this effect, the extent of acidity, mobility of elements and pH level in drainages or sulphate soils or mine waste materials are determined by the form and magnitude of existing sulphide minerals, reactive surface area and the acid-neutralizing (carbonate) minerals confined (Nordstrom & Alpers, 1999b; Skousen, 2017).

In South Africa, acid mine drainage issues posed a great threat to the ecosystem (Coetzee et. al, 2007; Ramla & Sheridan, 2015; Tempelhoff & Winde, 2019). Despite more studies on acid mine drainage generation within the Witwatersrand basin, due to the large waste deposit generated such as waste rocks, sand dumps, and slime (tailing) dumps; AMD is perpetually released from these mine waste materials.

UNIVERSITY of the
WESTERN CAPE

Gold and coal mining operation techniques have been one of the major evolvements by man, which contribute largely to the discovery of underground minerals through tilling and excavating of the earth crust (Ponomarenko et al., 2021; Lemos et al., 2021; Abegunde et al., 2016; Brough et al., 2013; Lloyd, 2002). These operations result to the extraction of minerals such as gold ore and coal ore for domestic and industrial uses, as well contribute immensely to the contamination of the ecosystem. The contamination process occurred by the oxidation reaction of sulphides in the mine waste materials.(Simate & Ndlovu, 2021; Tabelin et al., 2020; Amar et al., 2020; Tripathy, 2014; Hesketh et al., 2010; Trumm, 2010) Also, as man continues

http://etd.uwc.ac.za/

to explore his environment for valuable mineral deposits by means of different technological techniques and modern science, it is realised that these actions, someway, poses huge environmental impacts(Abegunde et al., 2016). In essence, these exploration actions executed by man could lead to environmental pollution and other hazardous conditions (Abegunde et al., 2016). The deterioration of the environment, as a result of the oxidation reaction, affects the growth and nature's sustenance of vegetation, soils, and aquatic system. The aforesaid environmental components are significant indicators of a healthy ecological system (Abegunde et al., 2016; Abegunde, 2015; Quispe et al., 2013).

Previous research has laid the foundation for understanding the impact of mining activities on the environment, emphasizing the need for detailed investigations into the emission of harmful substances resulting from anthropogenic influences (Candeias et al., 2015; Oelofse et al., 2004). However, a critical evaluation of the limitations of these studies reveals a gap in assessing and predicting the impact of AMD on the environment based on elemental speciation analysis.

In recent times, environmental pollution issues have been an increasing awareness in the scientific community, with a need to investigate the emission of potentially harmful substances from anthropogenic impact of man on nature(Candeias et al., 2015 ; Sarmiento et al., 2009; Nieto et al., 2007; Oelofse et al., 2004 ;Aykol et al., 2003). Anthropogenic or man activities have been a major threat to the nature, since it involves the modification of the natural environment through the use of technology and culture acquisition (Abegunde et al., 2016; Gómez-álvarez et al., 2011; Hannigan, 2007; Navarro et al., 2004; Rösner & Schalkwyk, 2000). This effect is generally termed as displacement syndrome (Abegunde et al., 2020). And this results in positive and negative impacts due to man's quest in making the environment (Abegunde et al., 2020; Dold, 2014) comfortable for such activities as food production, improving safety, environmental transformation, soil excavation etc.(Singh et al., 2022; Singh et al., 2017).

Among the abovementioned environmental impacts, it is observed that soils are highly affected by the negative impact of the anthropogenic actions. In this case,

http://etd.uwc.ac.za/

soils are identified as a medium of contaminant transportation (Durand, 2012a). This is as a result of the relationship between the atmosphere and meteoric waters (Guillén et al., 2012).

This dissertation aims to bridge this gap by providing a comparative analysis of various waste materials, subjecting them to identical weathering conditions. Unlike previous studies that focused on individual wastes under different conditions, this approach allows for a holistic understanding of the environmental challenges posed by mining activities.

By delving into elemental speciation analysis, this study seeks to unravel the intricate chemical states of elements associated with AMD, thereby contributing to a more nuanced comprehension of the environmental impact. Through this, the dissertation addresses the limitations of prior research and endeavours to pave the way for more effective assessments and predictions in the realm of environmental management.

Although, several studies conducted in this aspect illustrated the adverse impacts of the operational activities carried out at the mining industries (Singh et al., 2017). Pertaining to this, it is crucial to regularly monitor these environmental challenges to understand, as well determine the extent of the direct or indirect impact of anthropogenic activities (Durand, 2012a).

UNIVERSITY of the
WESTERN CAPE

This study is a comparative analysis, achieved by subjecting all wastes to the same conditions since in reality, within their space of confinement, they are subjected to similar weathering conditions. Previous researches have focus on individual wastes at different conditions.

This logical progression of the literature review aligns with the overarching objectives of the dissertation, emphasizing the importance of understanding the chemical states of elements and their impact on the environment.

2.2.1 Mine Waste Composition

http://etd.uwc.ac.za/

Mine overburden (mine waste) is the waste product generated during mining and milling operations (Parbhakar-Fox et al., 2013 ; Brough et al., 2013; Stewart et al., 2006; Sracek et al., 2004). There are different types of mine waste materials, but it depends on the type of ore mined and beneficiated. The most common ones are mine tailings, which are the fine waste products of gangue materials from the extraction processes.

In coal mining, several mine wastes are generated due to sophisticated extraction process and application used. Aside from coal tailings, coal combustion products (CCPs) are also generated along the process (Robl et al., 2017; Vassilev & Vassileva, 2007; Lloyd, 2002; Lloyd, 2000).

2.2.1.1 Mine Tailings

Mine tailings are characteristically composed of fine-sand to silt-size particles of quartz, aluminosilicates, carbonates, oxides and sulphides that are removed from the ore and dumped in impoundments (Amari et al., 2014; Parviainen, 2009; Fanfani et al., 1997). Mine tailings are deposited from the mining site by sub-aerial slurry, sub-aqueous slurry, paste, and dry deposition method, which depends on the water of the tailings (Abegunde et al., 2016; Amari et al., 2014; Parviainen, 2009). The topography and placement of the dumpsite are well considered before deposition. However, mine tailings dams are a nearly limitless source of AMD by sulphide oxidation. This signifies the key environmental challenge that affect the mining industry globally. In mine tailings, available oxygen diffusion, precipitation and large surface area, due to micro meter-sized sulphides within the fine tailings (Oldecop & Rodari, 2018), are major factors that accelerate the oxidation process (Quispe et al., 2013).

The constituent of gold and coal tailings varies from one site to another based on the extraction method applied, efficiency of the method, changing ore body geochemistry, and weathering process within the mine tailings dam (Lemos et al., 2021; Blowes et al., 2003). The South African coal-processing segment presently creates more than 12 million tons of ultrafine slurry per annum; the bulk of this waste is dumped in the slimes dams (Mamba, 2011). These coal tailings contain

http://etd.uwc.ac.za/

minerals such as kaolinite, illite, quartz, muscovite, including other specific clay mineral like montmorillonite and organic matter (coal) (OruÇ & Sabah, 2006). According to Oruç and Sabah (2006), SiO_2 accounted for 40.75% (attributed to quartz), Al_2O_3 and Fe_2O_3 accounted for 15.04% of the coal tailings.

Nevertheless, low percentages of CaO and MgO found in the tailings indicate presence of a small amount of carbonate minerals that could cause low neutralisation potential of the coal tailings. Also, Sabah, et al. (2004) reported that coal tailings contained about 26% quartz, 30% clay minerals (kaolinite, illite), 23% muscovite and 20% w/w of coal, which could be reclaimed. On the other hand, gold mine tailings contained about 70-90% of quartz, 10-30% of muscovite and other phyllosilicates, 3-4% of pyrite, 1-2% of other sulphides, 1-2% of uraniferous minerals and 1-2% other primary minerals.

Using the Witwatersrand basin as case study, the average major elements in tailings dams detected at five different sites in the East Rand as presented by (Rösner, 2001; Rösner & Schalkwyk, 2000) demonstrated a similar trend to those detected in the West Rand by (Abegunde et al., 2014). High SiO_2 values were recorded at all the sites, which also account for high quartz in the gold tailings. Al_2O_3, Fe_2O_3, LOI and K_2O (arranged in descending order) showed percentage weight concentrations greater than 1. Like coal tailings, CaO and MgO were of low percentage (less than 1), even with the addition of lime at the point of discharge.(Ineich et al., 2017)

Despite the efforts of creating paddocks, covering the tailings with stones, and applying bio-vegetative approach (planting of some certain trees) to minimise the tailing dam contamination effect, however, the risk poses can never be underestimated. Many activities, such as illegal mining, can expose underground water to contamination, and possibly causes dust pollution (another mode of transporting pollutants) by exposing tailing dams' surfaces, which contained high or low radioactive substance(Tutu, E. Cukrowska, et al., 2003; Wade & Coetzee, 2008).

Acid drainage from mine tailings, waste rocks and mine edifices are caused when the fine-grained sulphides, mainly pyrite or pyrrhotite, contain in these tailings are

http://etd.uwc.ac.za/

exposed to atmospheric oxygen. And their oxidation produces acidic water with large contents of sulphate, iron and other metalloids. The acidic solution produced from the oxidation of pyrite causes dissolution of the surrounding ore and rocks in the flooded part of the mine, rock piles, tailing dams and sand dumps, and releases the metals(Eze et al., 2013; Durand, 2012a). This results in contamination since the toxic and acidic waters generated were left untreated. And has adverse effects on the ecosystem, which could lead into severe environmental liability in the mining industry(Simate & Ndlovu, 2021; Lemos et al., 2021; Kefeni et al., 2017; Tripathy, 2014; J et al., 2002).

Although, to decrease waste materials from weathering such as mine tailings, it is necessary to usually keep it saturated with or covered by water during mining operations (Wolkersdorfer et al., 2020; Holmström et al., 1999). Nonetheless, this water layer may drain in the end, and allowing the contact of sulphide minerals to dissolve oxygen as shown in **Figure 2.1**. Afterwards, an oxidation zone of varying thickness may form instantaneously below the tailings surface as reported in previous research work (Abegunde et al., 2016). This implies that oxidation of sulphides depends on the water level, because the diffusion of oxygen in water is slow. Then, until the water level falls (occasionally or seasonally), the process of oxidation remains inhibited. The uncontrollable passage of leached tailings (seepage) has become a major environmental concern in its dissemination and distribution of exchangeable trace metals in the tailings into its environment. This drainage water is determined by precipitation and sedimentation of secondary mineral.

To date, many studies have focused on predicting the amount of AMD pollution produced by mining activities (Parbhakar-Fox & Lottermoser, 2015; Parbhakar-Fox et al., 2013; Durand, 2012a; Hobbs & Cobbing, 2007; Oelofse et al., 2007; Nengovhela et al., 2006; Naicker et al., 2003) and its remediation (Naidu et al., 2019; Rodríguez-Galán et al., 2019; García-Valero et al., 2019; B & M, 2010; Tutu et al., 2008; Akcil & Koldas, 2006). Yet, only a few studies focused on the prediction of the elemental speciation (in AMD) from mine waste material of the

http://etd.uwc.ac.za/

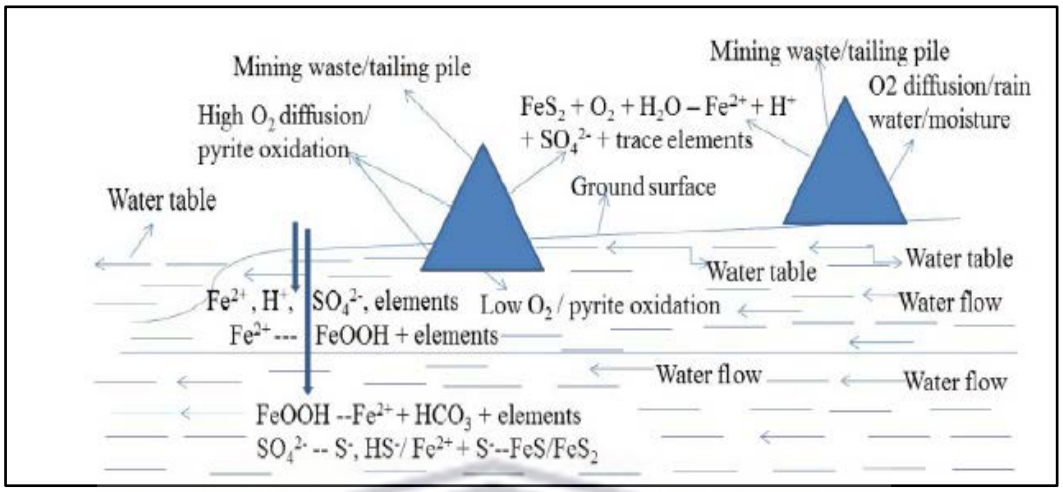

Figure 2.1: Conceptual model illustrating the pyrite oxidation from mining waste and dynamics of contaminants in surface and deeper groundwater

Diagram adapted from (Anawar, 2013)

Witwatersrand area (Abegunde et al., 2016; Sharifi et al., 2013; Nengovhela et al., 2006; Tutu, E. M. Cukrowska, et al., 2003; Grover et al., 2016). Similarly, few researchers applied sequential extraction method to probe the mobility of elements in gold tailings within South Africa (Grover et al., 2016; Camden-Smith et al., 2015; Tutu et al., 2008; Cukrowska et al., 2004). In addition, only limited studies corroborated multivariate statistics with sequential extraction procedures (Masood Khan et al., 2017; Cozzolino et al., 2017; Abollino et al., 2011; Giacomino et al., 2011; Cukrowska et al., 2004; Abegunde et al., 2020). Soils, surface water and groundwater systems around gold tailings dams have been observed to be directly polluted by the infiltration of leachates from these wastes (Camden-Smith et al., 2015; Bakatula et al., 2012; Tutu et al., 2008). Grover et al. (2016) inferred that continued leaching by rainwater could possibly be used to estimate elemental mobility in soluble mineral phase found in the material from the tailing's surface; therefore, the gold tailings have the potential to release toxic elements into the surrounding ecosystem. Hence, the use of multivariate statistics to probe the environmental and analytical data sets which has been successfully applied. Most studies have focused on certain parts of the tailings dam. Although, the whole (not only its bottom, sides, or surface) profiling of the tailings dam during sampling collection preferably would have been of great significance for constant monitoring

http://etd.uwc.ac.za/

and elemental mobility valuation (Tutu, E. M. Cukrowska, et al., 2003) as applied in this study.

2.2.1.2 Coal Fly Ash

South African coals are generally low grade with roughly 30 – 35% ash(Snyman & Botha, 1993). Due to its fairly high clay mineral and quartz content (that causes high fusion temperatures), the coal is utilised for steam raising purposes. The main coal mining areas are presently in the Witbank-Middelburg, Ermelo and Standerton-Secunda areas of the Mpumalanga Province, around Sasolburg-Vereeniging in the Free State/Gauteng and in Newcastle, Dundee, Piet-Retief, Somekele, Utrecht, Vryheid, Nongoma, Tuli, Soutpansberg and Molteno-Indwe which is in the north-western KwaZulu-Natal, where smaller operations are found(Deysel & Vermeulen, 2015; Reddick Von Blottnitz H. & Kothuis B, 2007; Cadle et al., 1993; Snyman & Botha, 1993; Falcon & Ham, 1988).

Additionally, coal emanating from geological processes contains carbon, hydrogen, oxygen, silicon, aluminium, nitrogen, sulphur and iron as major elements greater than 1wt %. The minor (1-0.1wt %) elements are potassium, calcium, titanium, magnesium, sodium, and sometimes manganese, phosphorus, strontium and barium. Other trace elements are also known to be present (Ahamed et al., 2019; Vassilev & Vassileva, 2009; Falcon & Ham, 1988).

Coal is a complex variegated blend of organic matter, with a lesser volume of inorganic substance and liquids occurring in the openings within and amongst the solid segments of the organic and inorganic matters that control its ranking. The organic matter in coal can be classified via a petrographic microscope as macerals and microlithotype groups, and lithotypes (brittle coal). Wide-ranging macerals group, nonetheless, only three major clusters of macerals are well known, which are vitrinite group, liptinite (or exinite) group, and inertinite group (Makgato et al., 2019; Hower et al., 2012; Falcon & Ham, 1988). These clusters are all defined by their overall chemical, optical, physical, and technological properties (Makgato et al., 2019; Hower et al., 2012; Falcon & Ham, 1988).

http://etd.uwc.ac.za/

Coal inorganic matter encompasses diverse solid, liquid and gaseous phases of allothigenic (made in another place other than the rock, where it originates from) or authigenic (made or produced in the rock, where it originates from) source (Eze, 2011; Vassilev & Vassileva, 2009; Guijian et al., 2006; Ward, 2002). This includes soluble salts and additional inorganic substances in the coals pore water, inorganic elements combined inside the organic composites of the coal macerals, and typical inorganic particles signifying exact mineral constituents (Eze, 2011; Vassilev & Vassileva, 2009; Guijian et al., 2006; Ward, 2002). However, studies show that normal inorganic minerals found in coal are quartz, carbonates minerals, aluminosilicate, clay minerals, feldspars, disulphide and sulphate minerals (Ahamed et al., 2019).

Actually, it is understood that the depletion of Witbank Coalfield is imminent(Cadle et al., 1993; Snyman & Botha, 1993). Therefore, additional sources for coal supply must be discovered promptly to sustain the functionality of the coal industry into twenty-first century in South Africa. Meanwhile, the Waterberg Coalfield is being considered as a fit replacement of the Witbank Coalfield, because it could potentially contain(Madzivire et al., 2014; Lloyd, 2002; Lloyd, 2000) majority of the country's virgin coal resources remain in situ. The Highveld Coalfield reserves are vital to the long-lasting of Sasol Synthetic Fuels (SSF) and Sasol Chemical Industries (SCI) (Madzivire et al., 2014).

Coal fly ash (CFAs) are fine particulate materials, with major combustion waste product (normally 60–88%) produced when burning crushed coal in thermo-electric power stations (TPSs) to produce electricity (Madzivire et al., 2014; Vassilev & Vassileva, 2007). The coal type and technological procedures used in TPSs determine the constituent and properties of these fine particulate solid products (Vassilev & Vassileva, 2009). In addition, CFAs are congregated by the cleaning equipment of flue emissions (commonly electrostatic precipitators), and then separated from the flue gas stream using either bag filters or electrostatic precipitators to inhibit discharge into the atmosphere(Eze et al., 2013; Vassilev & Vassileva, 2009). The ash is formed and generated from various inorganic and organic constituents found in feed coals from 1200-1700 ^{o}C temperature. The

UNIVERSITY of the WESTERN CAPE

http://etd.uwc.ac.za/

complex composition, fine size, varying particle morphology and properties of combustion waste products have made them the most researched areas among natural rocks and technogenic (anthropogenic) products (Vassilev & Vassileva, 2007). This results in severe problems with the identification, characterisation, specification, utilisation of CFAs and their constituents (Vassilev & Vassileva, 2007).

In South Africa, large quantities of CCPs (such as coal fly ash) are generated daily to power electricity across the country by Eskom. About 3 million tons of CFAs were produced in 2003, but nearly 1.2 million tons were used for power generation (Eze et al., 2013; Eze, 2011). While in 2009, Eskom solely produced approximately 36.7million tons of CFAs from coal combustion, however, only 5.7% was utilised to generate electricity. Therefore, this indicates that a larger portion of the FA produced were unexploited and disposed of by using dry or wet disposal technique(Madzivire et al., 2014; Madzivire et al., 2010).

The wet disposal technique is applied by blending the CFAs with brine, and then transported as slurry through pipes, with a solid to liquid ratio of 5:1. The waste material is then disposed of into an impoundment or dam, otherwise known as ash dam or pond (Eze et al., 2013; Eze, 2011; Vassilev & Vassileva, 2007). On the other hand, the dry disposal technique is applied by disposing of the CFAs from the power plants, and then transported by chute, truck or conveyor to a constructed dry dam or embankment. The ash heap formed is then dampened with brine to suppress or minimise dust pollution (Eze et al., 2013). Like other fine particulate mine wastes, CFAs dumps are linked to noticeable environmental risk like air or dust pollution, loss of land for agricultural purposes, surface and ground water contamination due to the percolating of toxic, non-degradable trace metals, and other chemical species from the ash dump(Eze et al., 2013).

Based on the industrial application, CFAs are universally classified as Class F and Class C (ASTM C 618-92a), mostly in concrete and cement production industry (Nowak, and Mirek, 2013). These two chemical classes contain oxides of aluminium, silicon and iron present. However, the first type (class F) CFA is

http://etd.uwc.ac.za/

categorised by: (i) the sum of SiO_2, Al_2O_3, Fe_2O_3 > 70%, (ii) SO_3 < 5%, (iii) moisture content <3%, (iv) loss on ignition (LOI) <6%, and (v) CaO < 20%; whereas the second type is a 50–70% aggregate of SiO_2, Al_2O_3, and Fe_2O_3 (<70%) (Eze et al., 2013; Vassilev & Vassileva, 2007).

2.3 Acid Mine Drainage (AMD) Issues Associated with Mine Wastes

Acid rock drainage (ARD), also known as acid mine drainage (AMD), is solitarily the utmost significant environmental challenge facing the mining industry. ARD is generated from tailings, waste rock, and other mine gangues(Kefeni et al., 2017; McCarthy, 2011; Verburg et al., 2009; Akcil & Koldas, 2006; Stewart et al., 2006; Blowes et al., 2003). Other human activities that could cause ARD (or AMD) are road construction waste materials, tiling and others, which are exposed to oxygen and water (Verburg et al., 2009). AMD is a major source of elements that oxidise in spontaneous reaction with the environment (nature). This reaction is associated with gold, coal and other metals ores deposits due to the presence of metallic sulphides (majorly, pyrite FeS_2) (McCarthy, 2011; Akcil & Koldas, 2006; Blowes et al., 2003).

Considering its consequence, AMD has always been seen as a major problem since the unreasonable adverse effects of the human (mining) activities became evident (Verburg et al., 2009; Tutu et al., 2008; Nengovhela et al., 2006). Due to these effects on the ecosystem, AMD is now considered as an environmental virus. It is, therefore, necessary to monitor and remediate this virus to circumvent the outbreak of highly toxic elements to the ecosystem. However, the impact of the mining activities on the surface and groundwater resources have long been assumed right after some mining operations were terminated (Kefeni et al., 2017; McCarthy, 2011).

As mentioned earlier, these acids are formed naturally when waste rocks and tailings that contain metallic sulphides are exposed to oxygen in the presence of water. In the process, the acidic solution produced from the oxidation of pyrite dissolves the surrounding ore and rocks in the flooded part of the mine, rock piles, tailing dams and sand dumps (Durand, 2012a; Naicker et al., 2003). This reaction

UNIVERSITY of the WESTERN CAPE
http://etd.uwc.ac.za/

produces metals such as aluminium Al, radium Ra, uranium U, manganese Mn, Iron Fe, Zinc Zn, Nickel Ni, Lead Pb, cobalt Co, Arsenic As, Copper Cu and Thorium Th(Durand, 2012a; Naicker et al., 2003; Alpers et al., 2003). Due to this effect, the environment is contaminated by toxic and acidic water left untreated. In effect, this can cause immense damages to the natural environment through large scale underground exploitation, which drains the surrounding areas (Brady & Brown, 2006). Therefore, there is a need to proffer adequate and reliable solution to this environmental problem to avoid any unforeseen disaster.

In addition, these elements can easily transport through aquatics and soil capillary pathway, because of their high elemental mobility(Nengovhela et al., 2006). AMD trace metals that emerge from active and inactive mines tailings requires regular assessments to circumvent massive environmental problem. In essence, an imminent response to the above illustration will aid the detection of acid generation, sulphide rich minerals, its associated trace metals. For that reason, their spatial distribution and impacts on the environment will be effectively analysed and determined. The determination of the source minerals such as pyrite and pyrrhotite in relation to their oxidation products (for example, Ferrihydrite, Copiapite, Geothite, Jarosite and Hematite) and the extent of elements released can be of immense value in identifying the effect of abandoned and active mine sites, and the potential risk involved.

UNIVERSITY of the
WESTERN CAPE

However, abandoned mine sites have been the major seat of AMD generation around the world today(Abegunde, 2015; Jacobs, 2014; Younger, 2004). Acid drainage from the mine waste rock, tailings, and mine structures such as pits and underground workings is primarily a function of the mineralogy of the rock material and the availability of water and oxygen. Due to the inconsistencies of the mineralogy and other factors that contribute to the potential of AMD from site to site, predicting the potential of AMD is difficult, costly and of questionable reliability (W. A. Price, 2009). The release of AMD and ARD from the oxidation of sulphur-rich mine waste materials, when it gets in contact with water and oxygen

http://etd.uwc.ac.za/

is highly considered as one of the main environmental challenges facing the mining industry.

The dissolved As and other elements can be immobilised with precipitation as insoluble or less soluble Fe-(oxy) hydroxides, oxides, and sulphates(Sracek et al., 2011), and by adsorption onto some materials such as clay minerals, oxides, and hydroxides(Civeira et al., 2016). This has created a great issue and threat that has remained an uncontrollable discharge of AMD to the environment. (Igarashi et al., 2020; Cukrowska et al., 2004; Benner et al., 1997).

2.3.1 Formation of AMD

AMD is generally characterised by one or more of the following: low pH, high total dissolved solids (TDS), high sulphates (SO_4), and high levels of trace metals– particularly Iron (Fe), Manganese (Mn), Nickel (Ni) and/or Cobalt (Co). According to Argane et al. (2016), there are three types of mine drainage, which are acidic, neutral and alkaline mine drainage. The chief sulphide minerals liable for AMD generation are pyrite (FeS_2) and pyrrhotite (FeS). Nonetheless, other minerals are also disposed to oxidation and successive metal discharge, such as arsenopyrite (FeAsS), chalcopyrite (CuFeS2), and sphalerite ((Zn,Fe)S) (Argane et al., 2016; Blowes et al., 2003).

Alternative form of mine drainage is referred to as contaminated neutral drainage (CND) or as neutral drainage(Argane et al., 2016). This form of mine drainage takes place when sulphide oxidation is weak, and/or when appropriate neutralisation is present in the mine tailings (Argane et al., 2016; Heikkinen et al., 2009; Benzaazoua et al., 2008). Toxic metals and metalloids, such as Ni, Zn, Co, As, and Sb are solubilised in the neutral effluents produced. Some tailings are known to possess inert properties, with no potential environmental risk. And they can be utilised as primary materials in the construction sector. These kinds of tailings are hard to find since different factors affect the speciation of trace metals within a system(Argane et al., 2016).

http://etd.uwc.ac.za/

Trace metals, being mobilised at low pH, and elevated salt levels can pose a risk to human health, as well endanger the aquatic ecosystems while also having a significant negative economic impact (Funke et al., 2022). The main cause of this AMD is metal sulphides, where the iron sulphide (pyrite or fools' gold) poses major threat. This effect is due to the reaction between pyrite, water and oxygen (McCarthy, 2011; Verburg et al., 2009; Saria et al., 2006; Akcil & Koldas, 2006; Blowes et al., 2003). Then, this reaction leads to leaching generating acid, which actually lower the pH of the drainage, water pathway and other affected water bodies (Park et al., 2019; Roychoudhury & Petersen, 2014). However, due to oxygen and water precipitation action (rainfall), the acid generated causes leaching of the surface of rocks, mine tailings and waste dump. As the water moves down the drainage, or pathway, the acidic solution dissolves in some trace metals(Roychoudhury & Petersen, 2014; Guillén et al., 2012).

In mining, this reaction occurs when the mineral deposits that containing sulphides are exposed during mining processes, such as cavern strip, sedimentary mining of numerous minerals and metals (coal, gold, zinc, lead, uranium, copper, titanium, aluminium, iron bearing minerals and silicates). In this case, after separating the acid, the waste materials (tailings) are deposited into the open pit, or sometimes, left open in the mining area. In addition, in gold mining, water and air-conditioning are required to regulate the temperature since the earth crust temperature increases by about 20 ºC/km to the ground (Masindi et al., 2018; Abegunde et al., 2016; Durand, 2012a; Tutu et al., 2008; Tutu, E. M. Cukrowska, et al., 2003). During the mining process, sulphide (FeS_2–one of the most common sulphides) containing compounds are exposed to oxygen in the air and water that surround the mine, or in the precipitation (rainfall) used in the mining process (Lemos et al., 2021; Nordstrom et al., 2015; Parbhakar-Fox et al., 2014; Blowes et al., 2003; Epa & of Wetlands, 1994).

Also, pyrite may occur in both euhedral (less reactive) or framboidal (more reactive) forms in the Witwatersrand reefs due to the presence of biogenic carbonaceous material in the area, with the presence of hydrothermally precipitated pyrite grains

http://etd.uwc.ac.za/

(Nengovhela et al., 2006). The pyrite reacts in a series of steps, where its oxidation rate determines the next step (second step). This acid proceeds into the underground water ways, and pollutes the site area covering many kilometres.

The steps are as follows:

Oxidation of pyrite in water and oxygen

1. $Fe^{2+} + 1/2O_2 + H^+ \rightarrow Fe^{3+} + 1/2H_2O$ ……..1

Oxidation of iron II to iron III. The major cause of yellow boy

2. $FeS_2 + 7/2\ O_2 + H_2O \rightarrow 2SO_4^{2-} + Fe^{2+} + 2H^+$ …….2

Conversion of ferric iron to ferric hydroxide (yellow boy)

3. $Fe^{3+} + 3H_2O \rightarrow Fe(OH)_3 + 3H^+$ ……...3

Total combination to form sulphuric acid

4. $FeS_2 + 15/4O_2 + 7/2H_2O \rightarrow 2H_2SO_4 + Fe(OH)_4$ ……4

(H+) ion is release and pH of the streams or drainage is lowered. The high acidity rate is hazardous to any object that cannot survive stronger acidity levels. However, due to carbonates, the natural buffering system of the stream may suppress the reduction effect of the pH. This effect indicates that something maybe gone wrong. The quantity of the acidity and pH value in acid drainage or acid sulphate soils are determined by the form and magnitude of existing sulphide minerals, and the acid-neutralising (carbonate) minerals confined in the intermittent tailings (Nordstrom et al., 2015; Bigham et al., 2000; Nordstrom & Alpers, 1999). Therefore, materials abounding in sulphide and deficient in carbonate generate acidic drainage and acid sulphate soils, while materials abounding in carbonate and deficient in sulphide generate alkaline systems in drainage and soils (Skousen, 2017).

It was discovered that the acid in the water neutralises the carbonate, and the bicarbonate ions initiate the formation of carbonic acid (HCO) (Skousen, 2017). This reaction weakens the natural buffering actions of the water; therefore, the

http://etd.uwc.ac.za/

buffering system is unable to reach the concentration level any longer (usually at pH of 4.2) (Skousen, 2017). During this process, the water way or drainage suddenly becomes acidic, and therefore poses a great damage late to be reversed. And due to lowered pH, there is precipitation on the surface of the water, a thin yellowish layer called yellow boy Fe $(OH)_3$ (Rezaie & Anderson, 2020a; Saria et al., 2006; Epa & of Wetlands, 1994).

2.3.2 Sources of AMD

The environmental challenge of AMD caused by mining activities has yielded many research outputs, commissioned by governments, mining industry, universities, research institutions, and other environmental groups to determine its existence, causes, prediction and best treatment approaches (Akcil & Koldas, 2006). Acid drainage challenge is concomitant with the ore mining of definite minerals that initiate prolong impairment to watercourses and biodiversity. Runoffs or seepages, during and after mining, usually contain high magnitudes of toxic materials such as toxic element which have detrimental effects on the ecosystem and wellbeing of living creatures (Kroukamp & Wepener, 2022; Akhtar et al., 2021; Srivastava et al., 2020; Hudson-Edwards et al., 2011; Heikkinen et al., 2009; Akcil & Koldas, 2006).

In addition, there are two main sources of AMD, which are primary and secondary sources. Primary sources entail waste rock dumps, tailings dams, seepages, underground and open pit mine site, impelled/natural released underground water, construction materials used (Kroukamp & Wepener, 2022; Akhtar et al., 2021; Akcil & Koldas, 2006); while the secondary sources entail treated sludge, stock piles, rock cut concentrated spills along roads, emergency ponds. However, several factors determine AMD release, namely pH, temperature, oxygen content of the gas phase (saturation less than 100%), amount of oxygen in the water phase, degree of saturation with water, chemical activity of Fe^{3+}, and surface area of exposed metal sulphide. Others are chemical activation energy essential to start acid generation, bacterial activity, and waste rock dump permeability. More so, highly permeable landfills allow easy diffusion of oxygen, which causes higher rate of chemical reaction (Lemos et al., 2021).

http://etd.uwc.ac.za/

2.3.3 Impacts of AMD

The most critical impacts of AMD are observed in aquatic environment; however, humans are only affected when they consume AMD contaminated water resource (Figure 2.2). Several river systems and past mine sites are inimical to aquatic environment except for "extremophile" bacteria. Moreover, intensified acidity lessens the capability of water bodies (such as streams) to buffer against secondary chemical changes. In this case, the water clogs diminish the light penetration, thereby impacting on photosynthesis and visibility for water organism. And once the precipitate gravitates, it covers the stream bed, choking the bottom-dwellers and their food supplies.

Acid Mine Drainage (AMD) engenders a litany of multifaceted and deleterious impacts on both aquatic and terrestrial ecosystems, with cascading consequences that extend far beyond the immediate vicinity of mining operations (McCarthy, 2011; Hobbs & Cobbing, 2007). This phenomenon is typified by its pervasive influence on water quality, soil integrity, aquatic biodiversity, and human health. The impacts of AMD, often synergistically intertwined, are characterized by their persistent and chronic nature, rendering them formidable challenges for environmental management and remediation.

UNIVERSITY of the
WESTERN CAPE

One of the hallmark repercussions of AMD is the alteration of water chemistry, manifesting as lowered pH values and elevated levels of dissolved metals. This perturbation in pH disrupts the equilibrium of aquatic systems, causing acute and chronic stress to aquatic organisms. The heightened solubility of metals like iron, aluminum, and manganese under acidic conditions results in their release into water bodies, leading to toxic effects on aquatic life. This, in turn, disrupts food chains, decreases biodiversity, and can trigger population declines of sensitive species(Lemos et al., 2021; Tabelin et al., 2020; Kefeni et al., 2017; Tripathy, 2014).

http://etd.uwc.ac.za/

The impaired water quality from AMD-tainted waters adversely affects not only aquatic organisms but also terrestrial ecosystems. Acidified waters that drain into soil can lead to soil acidification, which negatively influences nutrient availability, soil structure, and microbial activity. Consequently, the health of vegetation and the viability of terrestrial ecosystems are compromised, leading to reduced plant growth, altered species composition, and diminished ecosystem services(Simate & Ndlovu, 2021; Nleya et al., 2016; Rezaie & Anderson, 2020b; Tempelhoff & Winde, 2019).

Moreover, the pervasive metal contamination stemming from AMD carries profound implications for human health and socioeconomic activities. Downstream water bodies and groundwater resources can become contaminated, rendering them unsuitable for consumption, agriculture, and industrial processes. This contamination can pose direct health risks to communities dependent on these water sources. Additionally, the economic repercussions are notable, as contaminated water sources impact fisheries, agriculture, and tourism industries, thereby affecting local livelihoods and regional economies (Funke et al., 2022; Tempelhoff & Winde, 2019).

UNIVERSITY of the
WESTERN CAPE

The long-lasting nature of AMD impacts further exacerbates the challenge. Even after mining activities cease, the legacy of AMD persists due to the continued oxidation of sulfide minerals in abandoned mine sites. This necessitates ongoing management efforts and financial commitments for remediation.

In summation, the impacts of Acid Mine Drainage are far-reaching and encompass disruptions to aquatic and terrestrial ecosystems, impairment of water and soil quality, adverse effects on biodiversity and human health, and socioeconomic repercussions. The intricate interplay of these impacts underscores the need for

http://etd.uwc.ac.za/

comprehensive mitigation strategies, encompassing active mine management, water treatment technologies, and ecosystem restoration efforts to curtail the long-term ramifications of this pervasive environmental issue (Lemos et al., 2021).

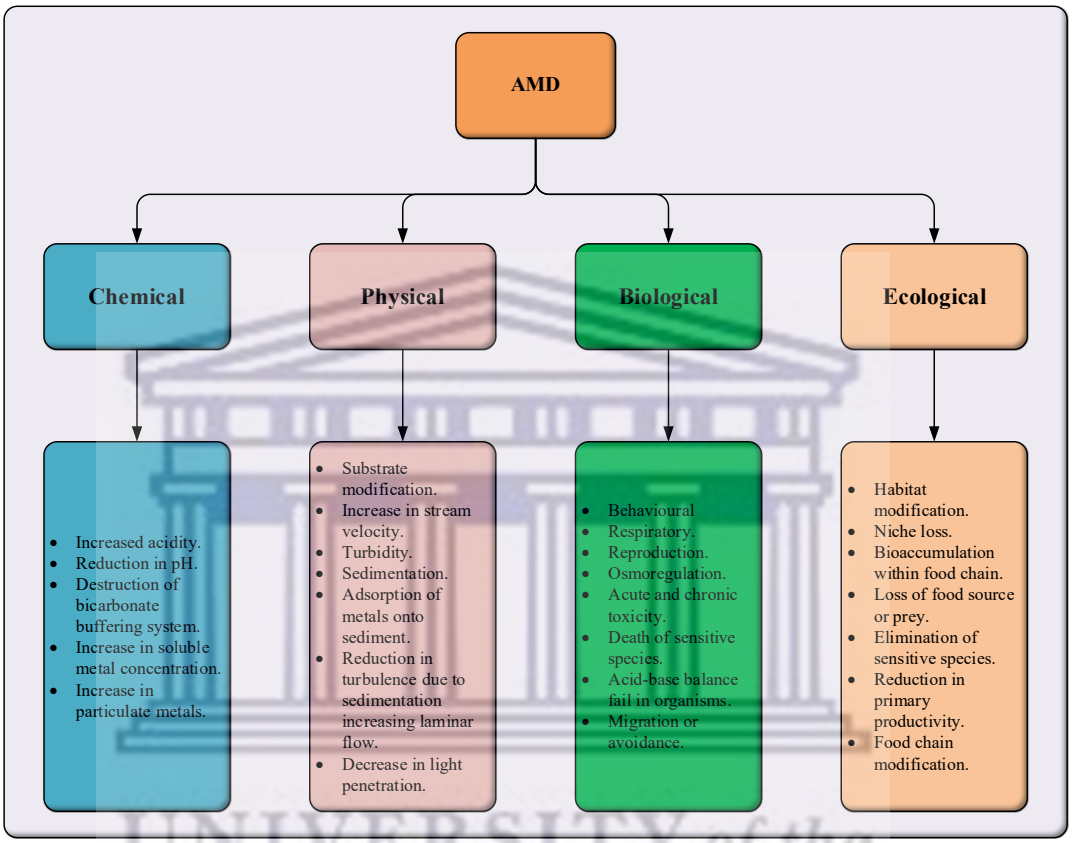

Figure 2.2: Diagram illustrating the breakdown of AMD impacts

2.3.4 Sustainability of AMD

Quality water are essential to all living organism's survival, but AMD generated from mining activities play a major role in its availability and accessibility. Assessment and prediction of AMD is used to recognize the environmental performance and the main environmental trouble spot of various robust AMD treatment techniques (Akinwekomi et al., 2020; Masindi et al., 2018), the versatility of environment to recharge and counteract with the AMD plume released into the environment.

Several approaches applied to remediate AMD are inadequate in its application due to weak performance, problematic interpretation of functionality, high costs, design

UNIVERSITY of the WESTERN CAPE
http://etd.uwc.ac.za/

flaws, diminution of natural resources, use of harmful chemicals, and the production of further waste (Moodley et al., 2018).

Numerous researches such as lime neutralisation (Igarashi et al., 2020), life cycle assessment method (Masindi et al., 2018) (an integrated process which includes lime, magnesite, soda ash and CO_2 bubbling treatment), use of natural alkaline materials (García-Valero et al., 2019), multiple conventional materials, adsorbent waste materials (Moodley et al., 2018), and utilization of sulphuric acid (Nleya et al., 2016), have been employed to sustain the effect and threat posed by AMD released into the environment.

2.3.5 Assessment and Prediction of AMD

Globally, technological evolvement in the metal extraction (mining processes) have caused drastic upsurge in mine waste production in recent times (Calas, 2017). This effect exponentially intensifies year-on-year, as its risk develops towards the safety of the ecosystem, including the humans(Calas, 2017; Wuana & Okieimen, 2011; Sarmiento et al., 2011; Bezuidenhout & Rousseau, 2006). Due to this, it is required that proper assessment and accurate prediction of the extent of risk posed by AMD is vital in alleviating the problem it could cause. This is because further sophisticated method offers low-grade ore. Hence, as the amount of mine waste increases, inaccurate prediction could become costly. Also, it is understood that the fallow/abandoned mine wastes are the seat of AMD (Rezaie & Anderson, 2020a; Parbhakar-Fox & Lottermoser, 2015; Parbhakar-Fox et al., 2014). This effect has been observed as a major problem in mining activities since human's impact in mining has become evident.

In chemistry, it is stated that there are elements present on the earth's crust; wherein elements such as H, C, N, O, Na, Mg, P, S, Cl, K and Ca constitute 99.9% of all living matter. And other elements like B, F, Cl, Si, V, Cr, Mn, Fe, Co, Cu, Sc, Mo, Sn and I are classified as essential elements, whereas some elements as Hg, Pb, Cd, As, Cr, Zn, Cu and Mn are secondary as well hazardous to the ecosystem(Akhtar et al., 2021). Explicably, elements are natural components of the environment but they become potentially harmful when their concentrations escalate above normal levels

http://etd.uwc.ac.za/

(Akhtar et al., 2021). In addition, this risk becomes higher due to rise in demand for precious elements in the manufacturing industries and continually increases global warming around the globe (Giaccio et al., 2012). More so, socio-economic development of the urban regions contributed to the physical, chemical and biological configuration changes in ecosystem in many emerging countries (des Roches et al., 2021).

Over the years, South Africa has shifted policy frameworks to address mine closure and mine water management, with the intention of changing the operational practices of the mining sector to conform to new regulations (Oelofse et al., 2007). In new and active mines, regarding the processing of mine waste material, the operators are tasked on appropriate management of waste materials to improve the release of AMD, including the transportation of elements that contaminate runoff, drainage and seepage, downstream channels during and after mine is closed down (Muniruzzaman et al., 2018). In this case, the operators are expected to provide evidence that the aforesaid task is carried out accordingly to inhibit or alleviate any cause of environmental challenges that may emerge from mining activities (Vaziri et al., 2022).

The implementation of the waste management plan could foster the characterisation of different waste and other gangue materials from current or future mining activities. In that case, this could predict the imminent behaviour of the materials once disposed of under the required environmental settings (W. Price, 2009). The possibility for mine tailings and waste to cause contamination is determined by several factors, which are ore type and its primary mineralogy, tailings pile structural pattern, remediation actions, and predominant physicochemical circumstances(Parviainen, 2009). Also, it is vital to delineate the quotient of lithogenic to anthropogenic influence, despite experiencing difficulties in assessing urbanised and industrialised zones in the areas where uncontaminated soils are nearly difficult to discover.

Although, in relation to the alleviation or evacuation of AMD, it is crucial to assess a suitable place for AMD evacuation, as well to predict what could happen if the

http://etd.uwc.ac.za/

remains of AMD are left on the ground surface (Agboola et al., 2020). In South Africa, large amount of AMD is deposited beneath and above the ground. In many cases, there are no other places to deposit the waste material after gold/coal extraction except on the ground surface (Rösner, 2001). This shows the effect of continued mining activities with lack of proper wastes management approach. As long as the extraction activities continue in the areas where mineral deposits are mined in South Africa, then there will always be a regular release of AMD into the surroundings (Rösner, 2001; Rösner & Schalkwyk, 2000).

Considering the above discussions, different assessment methods have been used over the years to ascertain the risk in the release of AMD. These methods are ABA (static and kinetic tests), sequential/selective extraction (SE), geochemical and mineralogical analyses and geostatistics (a combination of SE and statistics (chemometrics) (Giacomino et al., 2011; Abollino et al., 2011), including GIS and remote sensing tools. The above mentioned methods can be used in investigating the speciation and behaviour of elements within mine waste materials. Moreover, most prediction methods have effectively used the mineralogical composition of the ore body to deduce the amount of AMD produced, including the application of various sequential extraction (SE) methods, which were developed based on primary methods proposed by Tessier et al. (1979).

In acid generation potential, two major categorises of tests were adopted to envisage the behaviour of mine waste materials in the AMD production. The two major categories are static and kinetic tests (W. Price, 2009; Epa & of Wetlands, 1994). Static tests estimate the possibility of a sample generating an acidic environment (Hageman et al., 2015; Brough et al., 2013). Kinetic tests assess the occurrence of acidification and highlight elements leached out from the sample (Parbhakar-Fox et al., 2013), as well as forecast and speed up the reactivity of wastes so as to evaluate its long term geochemical behaviour.

http://etd.uwc.ac.za/

2.3.5.1 Application of Geostatistics

Geostatistics is applied to analyse the spatial distribution of soil parameters and spatial interpolation (Bostani et al., 2017). This geological statistical technique is a valuable tool for determining spatial uncertainty and risk assessment studies (Bostani et al., 2017). To define spatial distribution of elements and geochemical concentrations, statistical methods like probability graphs, univariate and multivariate investigations are applied (Abegunde et al., 2020; Cozzolino et al., 2017; Abollino et al., 2011; Giacomino et al., 2011; Cukrowska et al., 2004). The use of statistics to probe sequential extraction analyse large dataset thereby allowing several parameters to be considered and providing more effective visualization and interpretation of results (Giacomino et al., 2011; Abollino et al., 2011). Several researchers have employed this method of analysis (Abollino et al., 2011; Giacomino et al., 2011) and has gained a better prospect into the future of elemental speciation(Abegunde et al., 2020), transport, mobility (Cukrowska et al., 2004) and adsorption as well as AMD prediction studies (Cozzolino et al., 2017) and rare earth element characterisation (Masood Khan et al., 2017; Abegunde et al., 2016).

The assessment and prediction of Acid Mine Drainage (AMD) demand rigorous statistical methodologies to comprehend intricate relationships within datasets, prognosticate future trends, and inform strategic interventions. A suite of advanced statistical tools is imperative for the comprehensive analysis of multifaceted AMD datasets, unraveling latent patterns, and substantiating informed decision-making in AMD abatement endeavors. The application of these statistical methods in the AMD context is imperative for enhancing empirical understanding, devising predictive models, and substantiating remediation strategies.

- Descriptive and Inferential Statistics: The rigorous application of descriptive statistics facilitates the succinct characterization of essential features within the AMD dataset, thereby offering foundational insights into the central tendencies and variabilities of pertinent parameters such as pH levels and metal concentrations. Inferential statistical tests, encompassing t-

http://etd.uwc.ac.za/

tests and analysis of variance (ANOVA), are quintessential for deciphering significant variations among distinct AMD groups or phases.

- Correlation and Regression Analysis: The discernment of intricate associations within the AMD context necessitates correlation analysis, wherein Pearson's or Spearman's correlation coefficients are aptly deployed to elucidate the intensity and directionality of inter-variable relationships. Regression analysis, both linear and multivariate, avails the quantification of predictive relationships amidst variables, facilitating the forecasting of AMD parameters based on compositional or environmental attributes.
- Principal Component Analysis (PCA) and Factor Analysis: The application of dimensionality-reducing techniques such as PCA allows the condensation of complex AMD datasets into interpretable components. Factor analysis ascertains latent variables influencing AMD parameters, thereby expounding underlying causal relationships that might govern AMD dynamics.
- Time Series and Spatial Analysis: Temporal assessments within the AMD realm necessitate time series analysis to unravel chronological trends, cyclical patterns, and potential anomalies. Spatially explicit AMD datasets demand geostatistical methodologies, like kriging, for interpolating parameter distributions, leading to spatially delineated depictions of AMD propagation.
- Machine Learning and Artificial Intelligence: Advanced techniques including machine learning algorithms—random forests, support vector machines, neural networks—are employed for prognosticating AMD behavior. By assimilating intricate interdependencies within datasets, these tools proffer robust predictive models, particularly relevant when tackling AMD's multifaceted dynamics.
- Cross-Validation and Model Assessment: In the academic context, validation procedures like k-fold cross-validation are indispensable for rigorously assessing model performance and ascertaining predictive efficacy. Furthermore, sophisticated model evaluation metrics, including

UNIVERSITY of the WESTERN CAPE
http://etd.uwc.ac.za/

Root Mean Square Error (RMSE) and coefficient of determination (R^2), validate the predictive robustness of formulated models.

In summary, the systematic application of these advanced statistical methodologies bolsters the comprehension of AMD complexities. By leveraging the intrinsic relationships embedded within datasets, these tools empower researchers to delineate causal associations, prognosticate future trends, and devise holistic strategies for AMD management and environmental stewardship.

2.3.5.2 Application of GIS

Geographic Information Systems (GIS) have emerged as invaluable tools for the assessment, prediction, and management of Acid Mine Drainage (AMD) due to their capacity to integrate spatial data, visualize patterns, and facilitate informed decision-making. The application of GIS in the context of AMD encompasses diverse aspects, ranging from spatial data collection and analysis to the development of predictive models and the design of mitigation strategies.

The use of GIS has developed into a contemporary way of carrying out spatial analysis of data in a geographical area, permitting the user to store, edit, analyse and exhibit geographically referenced data. Its application permits user to execute specific spatial analysis such as multi-layer analysis, distance measurement and sophisticated geostatistical analysis (Mutanga et al., 2017).

In monitoring or assessing the impact of mining waste on the environment, researchers and decision makers often probe the occurrence and sources of the environmental pollution, as well as its extent and principal distribution and/or transportation mechanisms (Khalil et al., 2014).

Sadly, nearly all the environmental studies performed to use conventional methods such as ground surveys are proven to be costly and time consuming (Khalil et al., 2014; Khalil et al., 2013). Nonetheless, the constant advances in GIS have improved its prospects for environmental data analysis (Khalil et al., 2014; Gu & Liu, 2012). GIS methods have been gradually utilized to examine or assess the distribution of trace metals in environmental pollution(Khalil et al., 2014).

UNIVERSITY of the WESTERN CAPE
http://etd.uwc.ac.za/

An effective management of environmental issues in mine waste materials always needs a substantial amount of data associated to various field of environment, which can be incorporated into a GIS. Therefore, GIS has become a useful tool in monitoring AMD pollution as well as mapping its geographical impact

The following overview presents the multifaceted utility of GIS in AMD research and management, supported by academic references where available:

- Spatial Data Integration and Visualization: GIS enables the integration of diverse spatial datasets, including geological, hydrological, topographical, and land use information. This holistic approach aids in the visualization of spatial patterns, assisting researchers and practitioners in identifying potential AMD sources, pathways, and areas of susceptibility.
- Spatial Analysis for Source Identification: GIS facilitates the overlay and analysis of spatial layers to pinpoint areas with a high likelihood of AMD occurrence. By incorporating factors such as geology, hydrology, and proximity to mining activities, GIS aids in identifying potential pollution sources and prioritizing monitoring efforts.
- Predictive Modeling: GIS-based predictive models employ spatial analysis techniques to forecast areas susceptible to AMD development based on key environmental parameters. This aids in identifying areas where mitigation measures are most urgently required.
- Hydrological Modeling: GIS is instrumental in hydrological modelling, which assesses how water flows across landscapes. This is vital for understanding potential pathways of contaminated runoff and the subsequent dispersion of AMD pollutants.
- Decision Support Systems: GIS-based decision support systems provide stakeholders with a platform for evaluating different scenarios and mitigation strategies. This aids in making informed decisions by considering various spatial and environmental variables.
- Environmental Impact Assessment: GIS contributes to environmental impact assessments by visualizing potential AMD impacts on ecosystems,

UNIVERSITY of the WESTERN CAPE
http://etd.uwc.ac.za/

water bodies, and surrounding communities. This aids in regulatory compliance and public communication (Hay et al., 2005).

In summary, the integration of GIS technology in AMD research and management underscores its pivotal role in elucidating spatial patterns, modelling potential impacts, and guiding mitigation efforts. The references cited provide insight into the academic exploration of GIS applications within the realm of AMD assessment and prediction. In summary, the use of GIS in the assessment and prediction of Acid Mine Drainage has significantly enhanced our ability to comprehend the spatial intricacies of AMD dynamics. Academic research underscores the value of GIS in integrating diverse datasets, conducting spatial analyses, developing predictive models, and aiding decision-making processes for effective AMD management.

2.3.5.3 Application of Biokinetics

The utilization of biokinetics in the assessment and prediction of Acid Mine Drainage (AMD) entails an intricate exploration of biological processes within affected ecosystems, providing insights into the interactions between microorganisms and the chemical constituents of AMD. This approach plays a pivotal role in understanding the dynamics of microbial activities that influence the formation, mitigation, and remediation of AMD. Biokinetics contributes to elucidating the roles of microorganisms in elemental transformations, pH regulation, and the overall fate of metals within AMD-impacted environments.

AMD is produced by the microbially (Acidithiobacillus) catalysed oxidation of sulphide minerals in contact with to moisture and air which leads to continuing pollution of water bodies with acidity, sulphate and metal ions in solution, constraining successive consumption of the water without its remediation (Hesketh et al., 2010).

The use of biokinetics helps in determining the possibility and probability of acidification upon microbial colonisation, involving the relative kinetics of the acid-producing and acid-consuming effects (Hesketh et al., 2010). Present laboratory scale AMD prediction assessments are normally fast chemical tests, called static

http://etd.uwc.ac.za/

tests, or lengthy kinetic tests, for example, the humidity cell. Static tests comprise acid–base accounting (ABA) and net acid generation (NAG) studies(Oh et al., 2017).

The shortfall is that both the static nor kinetic tests did not account for the presence of microbes, therefore, biokinetics test offers more significant data than static tests, within a sufficient timeframe. Results generated often also offer further kinetic information that could assist to advise management plans (Hesketh et al., 2010).

Microbial Mediation of Elemental Transformations: Biokinetics focuses on the enzymatic activities of microorganisms that drive elemental transformations within AMD-affected systems. Microbes participate in oxidation-reduction reactions that influence the oxidation of sulfide minerals, a crucial step in AMD initiation. Biokinetic studies reveal the kinetics of microbial interactions with sulfur compounds and provide insights into the efficiency and rates of these reactions(Johnson & Hallberg, 2003).

Bioleaching and Metal Mobilization: Biokinetics investigates the phenomenon of bioleaching, where microorganisms aid in the solubilization of metals from minerals. This process influences the release of metals into solution, contributing to the elevated metal concentrations observed in AMD-affected waters. Understanding the kinetics of bioleaching reactions provides valuable data for predicting metal mobilization (Bosecker, 1997).

Microbial pH Regulation: Biokinetic studies explore the role of microorganisms in pH regulation through processes such as microbial sulfate reduction and carbon dioxide consumption. Microbial activities impact the acid-base equilibrium within AMD-affected environments, influencing pH levels and subsequently affecting the solubility of metals (Johnson, 2012).

Bioremediation Potential: Biokinetics is instrumental in evaluating the bioremediation potential of microorganisms in AMD-affected sites. Certain microbes can facilitate the precipitation of metal sulfides or form biofilms that immobilize metals, contributing to the attenuation of AMD impacts. Biokinetic data

http://etd.uwc.ac.za/

guides the selection of appropriate microbial strains and conditions for effective bioremediation strategies (Dopson & Lindström, 1999).

Predictive Modeling: Biokinetic information can be integrated into predictive models that simulate microbial activities, elemental transformations, and their cumulative effects on AMD dynamics. These models aid in forecasting future AMD trends and assessing the efficacy of potential mitigation strategies (Huang et al., 2012).

In summary, the application of biokinetics in AMD research advances our understanding of the intricate interplay between microorganisms and chemical processes that dictate AMD formation, propagation, and potential mitigation strategies. The references cited exemplify the exploration of biokinetic aspects within the broader context of AMD studies.

2.3.5.4 Application of Selective and Sequential Extraction

Selective and sequential extraction approaches are extensively employed in mine tailings researches (Holmström et al., 1999). And the accuracy and selectivity of these approaches have been censured, since they are influenced by several factors such as chemicals used, technique parameters (temperature, time and exposure to light), and sample to volume ratio, as well as the outcomes of a comprehensive mineralogical study by X-ray diffraction (XRD) targeted at selective extractions(Dold, 2003). The result reflected that the extraction approaches present a potent tool for the study of elemental mobilisation and retaining in mine tailings.

The application of sequential extraction techniques in the assessment and prediction of Acid Mine Drainage (AMD) involves a methodical approach to fractionate metals and metalloids present in mining wastes or AMD-impacted environments. This approach helps differentiate between various forms of elements, providing insights into their potential mobility, bioavailability, and environmental impact. Sequential extraction contributes to understanding the speciation of metals, which

http://etd.uwc.ac.za/

is crucial for predicting their behaviour and developing effective mitigation strategies.

Metal Speciation Assessment: Sequential extraction involves subjecting solid samples to a series of chemical reagents that target specific metal fractions. These fractions can be operationally defined as exchangeable, carbonate-bound, Fe/Mn oxide-bound, organic matter-bound, and residual forms. This process helps elucidate the speciation of metals, revealing which fractions are potentially more mobile and bioavailable (Tessier et al., 1979) .

Mobility Prediction: By assessing the mobility of metals through sequential extraction, it becomes possible to predict which metal fractions are more likely to leach into the environment under certain conditions, such as changes in pH or redox potential. This information is vital for estimating the potential impact of AMD on water bodies and surrounding ecosystems (Quevauviller et al., 1997).

Environmental Risk Assessment: Sequential extraction data enable the assessment of environmental risk associated with different metal fractions. Fractions that are more labile and easily mobilized pose a higher risk of contamination to aquatic ecosystems and groundwater. This information aids regulatory bodies and environmental managers in prioritizing sites for remediation and monitoring efforts (Ure et al., 1993).

Mitigation Strategy Design: Sequential extraction informs the selection of appropriate mitigation strategies based on metal speciation. For example, if a substantial portion of a metal is associated with easily leachable fractions, strategies like in situ immobilization or addition of amendments can be tailored to target these fractions and reduce their mobility.

Long-Term Fate Prediction: Understanding metal speciation through sequential extraction can aid in predicting the long-term fate of metals in AMD-impacted environments. This information is valuable for assessing the persistence of

UNIVERSITY of the WESTERN CAPE
http://etd.uwc.ac.za/

contamination and the potential for gradual release of metals into the environment over extended periods (Grande et al., 2005).

In academia, the systematic use of sequential extraction techniques offers a robust framework for elucidating the distribution and speciation of metals in AMD-affected environments. The references provided exemplify the incorporation of sequential extraction methodologies within the broader context of AMD research.

2.3.5.5 Application of Acid Base Accounting

ABA evaluates the balance between acid generation processes and acid neutralising processes (W. Price, 2009; Epa & of Wetlands, 1994). Values emerging from ABA are referred to as the maximum potential acidity (MPA) and acid neutralising capacity (ANC), which are categorically denoted as static tests (Abegunde, 2015; W. Price, 2009). This is because both MPA and ANC require a single measurement at a time. On the other hand, kinetic tests (column tests) are also employed in the prediction of AMD. In addition, as kinetic tests attempt to replicate natural oxidation reactions of the field settings, it also requires the use of a larger sample volume and a much longer time for completion than static tests. They are used to determine the sulphide reactivity and weathering behaviour, including the leaching of metals and oxidation rate (Oh et al., 2017; Hageman et al., 2015; Parbhakar-Fox et al., 2013).

UNIVERSITY of the
WESTERN CAPE

Among the two types of static tests stated, ABA is considered as the most applied test. This type of static tests was originally designed to evaluate acid-producing capacity of coal-mine waters, but it is also used to evaluate other mine wastes like gold (Hageman et al., 2015; Deysel & Vermeulen, 2015; W. Price, 2009; Epa & of Wetlands, 1994). ABA measures the balance between the acid-producing potential (AP) and acid-neutralising potential (NP) of the mines (Hageman et al., 2015; Deysel & Vermeulen, 2015; W. Price, 2009; Epa & of Wetlands, 1994). Furthermore, the ABA procedure measures the acid- and alkaline-producing potential of undisturbed soil and rock (overburden) in order to determine if, after disturbance, the waste material will produce acid and subsequently leach metals.

http://etd.uwc.ac.za/

Samples of overburden are taken from borehole cores and/or from a fresh high wall to distinguish geologic layers (strata). Samples from each stratum are measured for acid-producing potential (APP or AP) and neutralisation potential (NP). The difference between NP and APP is the net neutralisation potential (NNP). If NNP is positive (NP is higher than APP), then the tailings sample is predicted to produce alkaline drainage. If NNP is negative (APP is higher than NP), then the tailings sample is predicted to produce acidic drainage (Hageman et al., 2015; Deysel & Vermeulen, 2015; W. Price, 2009; Epa & of Wetlands, 1994).

The APP of the tailings sample is calculated from the total S content found using various methods such as furnace combustion, Eschka method and X-ray diffraction (Kleinmann). For each %S contained in the material, 31.25 metric tons of calcium carbonate ($CaCO_3$) are required to neutralise the sulfuric acid produced from 1000 metric tons of the material (Hageman et al., 2015; Deysel & Vermeulen, 2015; W. Price, 2009; Epa & of Wetlands, 1994).. The NP is determined by reacting a finely ground 2-gram sample with a known quantity and strength of acid (HCl). The solution is then back-titrated with a known strength of base (NaOH) to a predetermined end point to determine the sample's neutralising component expressed in equal units of calcium carbonate as APP.

ABA is the most common basis for predicting post-mining water quality basically because of its simplicity (Amar et al., 2020). However, there has been much criticisms about the accuracy of such predictions (Kleinmann, 2000). One criticism is that the method does not account for the different reaction rates of acid- and alkaline-production in samples. Reaction rates can be determined by more complicated kinetic tests such as humidity cells or columns. In addition, determining NNP for each stratum is straightforward, when information from each stratum is integrated to assess the NNP for the entire site. But, in doing so, the accuracy of ABA can be compromised (W. Price, 2009).

The utilization of Acid-Base Accounting (ABA) plays a pivotal role in the assessment and prediction of Acid Mine Drainage (AMD) by evaluating the potential for acid generation within mining waste materials. ABA involves the

http://etd.uwc.ac.za/

quantification of acid-producing (sulfide minerals) and acid-consuming (carbonates, neutralizing minerals) components within these materials. This approach aids in understanding the acid-forming potential of mining wastes, which is crucial for predicting the occurrence of AMD and designing effective mitigation strategies.

Quantification of Acid-Forming Minerals: ABA involves the determination of sulfide minerals present in mining waste materials, particularly pyrite (FeS_2), which is a primary source of acid generation. The concentration of these minerals is quantified and expressed as a measure of potential sulfuric acid production (Nordstrom & Alpers, 1999a; Bigham et al., 2000).

Evaluation of Acid-Consuming Minerals: ABA also considers the presence of acid-consuming minerals, such as carbonates (calcite, dolomite) and neutralizing minerals (aluminum hydroxides), which can neutralize the acid produced by sulfide oxidation. The capacity of these minerals to buffer acid is assessed to understand their role in mitigating acid generation .

Net Acid-Producing Potential (NAPP): The net acid-producing potential (NAPP) is calculated by subtracting the acid-consuming potential from the acid-producing potential. This quantifies the overall potential for AMD generation within a given material. A positive NAPP value suggests the potential for acid generation, while a negative value indicates acid neutralization potential (Yucel & Baba, 2016; Akabzaa et al., 2007).

AMD Prediction and Mitigation: ABA results inform predictions about the likelihood of AMD occurrence from specific mining waste materials. This knowledge aids in designing suitable waste management and remediation strategies. Materials with high potential for acid generation can be isolated, treated, or managed to minimize AMD impacts .

Environmental Impact Assessment: ABA is a crucial tool in environmental impact assessments for mining projects. It provides insights into the long-term effects of

http://etd.uwc.ac.za/

mining activities on water quality, soil integrity, and ecosystem health. By quantifying acid-forming potential, regulators can evaluate the potential impacts on local water bodies and take appropriate measures (Wei & Wolfe, 2013).

In academia and practice, the systematic use of Acid-Base Accounting contributes to a comprehensive understanding of the acid-generating potential of mining waste materials. The references cited exemplify the application of ABA within the broader context of AMD assessment and prediction.

2.3.5.6 Application of Net Acid Generation (NAG)

Net Acid Generation (NAG) is a critical concept and method used in the assessment and prediction of Acid Mine Drainage (AMD). It quantifies the potential for acidic conditions to develop as a result of sulfide oxidation in mining waste materials.

In contrast to the ABA method, the NAG method directly measures the acid producing potential of overburden material by oxidising pyrite using 30% hydrogen peroxide. When pyrite oxidises, sulfuric acid (H_2SO_4) is produced causing AMD problems (W. Price, 2009; Epa & of Wetlands, 1994). The NAG method directly measures H2SO4 production, while the ABA method simply predicts H2SO4 production by measuring the S content associated with pyrite. The NAG method accurately determines the potential acidity of a given sample, but the procedures are more complicated and time consuming.

The following discussion describes briefly how acidity potential is determined using the modified NAG method (Stewart et al., 2006). To determine the acidity potential using the NAG method, the sample is first grounded to <149 µm. And then soaked in an HCL solution for 2 hours, in order to remove carbonate minerals from the sample. By removing carbonate minerals, total acidity potential can be determined since acid neutralisation potential of the sample is removed. Initial and residual carbonate contents of the sample are measured before and after HCL treatment. The difference between the carbonate content before and after HCL treatment yields the readily soluble acid neutralising potential of the sample. The

http://etd.uwc.ac.za/

residual HCL in the sample must be removed since the HCL can cause erroneously high potential acidity values.

To remove the HCL, the samples are washed with a $CaCl_2$ solution. Of the washed sample, 0.5 g is weighed for the hydrogen peroxide (H_2O_2) oxidation procedure. Specified volumes of 30% H_2O_2 are added to the sample in order to rapidly oxidise the pyrite and produce a sulfuric acid (H_2SO_4) solution. Once enough H_2O_2 has been added to the sample to oxidise all the pyrite, copper is added to the solution to decompose the excess H_2O_2. Residual H_2O_2 can influence the potential acidity value and therefore, should be removed. The sample is then washed with a $CaCl_2$ solution to remove any H_2SO_4 that may still remain in the sample. All H_2SO_4 leachate is then titrated with a base (i.e., NaOH) to determine the potential acidity value

NAG assessments involve analysing the mineralogy and chemistry of waste rocks, tailings, or other materials to estimate whether they have a net acid-forming potential or a net acid-consuming potential. This information is vital for predicting the occurrence of AMD and designing appropriate mitigation measures.

Here's how NAG is used in AMD assessment and prediction:

Estimation of Acid-Forming Potential: NAG assessments involve determining the concentrations of acid-forming sulfide minerals, such as pyrite (FeS2), within mining waste materials. These minerals have the potential to release sulfuric acid when exposed to air and water through oxidation. By quantifying the mass of sulfide minerals present, one can estimate the potential amount of acid that could be generated upon oxidation.

Acid-Forming and Acid-Neutralizing Reactions: NAG assessments consider both the acid-forming reactions, where sulfides are oxidized to produce sulfuric acid, and the acid-neutralizing reactions, where carbonate minerals or other alkaline materials consume acid. The balance between these reactions determines whether the material has a net acid-forming potential or a net acid-consuming potential.

UNIVERSITY of the WESTERN CAPE
http://etd.uwc.ac.za/

Calculation of Net Acid Generation: The net acid generation is calculated by subtracting the potential acid-neutralizing capacity from the potential acid-generating capacity of a material. If the result is positive, the material has a net acid generation potential, indicating that it has the potential to produce acid when exposed to air and water. If the result is negative, the material has a net acid-consuming potential, suggesting that it can neutralize acid.

Mitigation and Site Management: The results of NAG assessments guide decisions on how to manage and mitigate the environmental impact of mining waste. Materials with a high net acid generation potential may need to be isolated, treated, or covered to prevent exposure to air and water, which could trigger acid generation. Conversely, materials with a negative net acid generation potential can contribute to acid neutralization and may be strategically placed to mitigate AMD impacts.

Regulatory Compliance and Long-Term Monitoring: NAG assessments are often required by regulatory agencies for permitting and environmental impact assessments associated with mining activities. These assessments provide valuable information about the potential long-term effects of mining waste materials on water quality, soil quality, and ecosystem health.

In academia and environmental management, NAG assessments are essential tools for understanding the potential for acid generation and predicting the occurrence of AMD. They guide the design of waste management strategies and help minimize the environmental impact of mining operations.

2.3.6 Remediation of AMD

Economically, there are benefits in the mining of mineral deposits, also there are environmental challenges that result from the mining activities (Xavier et al., 2021; Ponomarenko et al., 2021). Due to this, surface water found within the areas with regular mining activities are found to be extremely affected. The quality of the surface water deteriorates when exposed to AMD, thereby signifies the inability to sustain the biodiversity relationship among living organisms and ecosystems due to poor handling of mine waste materials. Even soils become structurally variable and

UNIVERSITY of the WESTERN CAPE

http://etd.uwc.ac.za/

extremely susceptible to attrition. Typically, AMD formation is attributed to the oxidation of pyrite (FeS_2) in the presence of oxygen and water, thereby oxidising pyrite to generate Fe^{2+}, SO^{2-} and H^+ ions (Roychoudhury & Petersen, 2014).

Several studies were carried out to assess the degree of pollution caused by previous mining activities in the Witwatersrand Basin/area, ever since the report of water contamination in the vicinity, as caused by high concentration of heavy and trace metal. Ata Akcil et al. (2006) emphasised on the increase in research and interest in AMD from all sector involved over the years. This group of researchers further highlighted that AMD problem can be mitigated by deploying preventive measures and treatment of affluent acid drainage migration. Also, the production of AMD usually, but not exclusively, occurs in iron sulphide–aggregated rock. The mineralogy and other factors affecting AMD can be exceedingly challenging and costly (Epa & of Wetlands, 1994).

According to the evaluations performed at the mine sites, primary factors such as pH, temperature, oxygen content of gas phase, oxygen concentration of water phase, degree of water saturation, surface area of exposed metal sulphide determine the rate of acid generation. Other factors are chemical activation energy (required to initiate acid generation), bacterial activity, stating chemical importance, biological and physical factors that also determine the rate of acid generation. Dumps with high permeability have high oxygen ingress or intake increase of chemical reaction rate by convection and water, which are the basic transport mediums for contamination; and it is a function of the control of water flow (Akcil & Koldas, 2006).

Most tailing dams often contain elevated levels of radioactive and chemo-toxic soft, and intermediate metals. However, through seepage, dissolved Uranium (U) and other metals migrate from tailing deposit via ground surface water into adjacent fluvial systems and the biosphere. Co-precipitation of U with calcium carbonate and iron /manganese compounds are the main reason for higher immobilisation rate in the flowing water system (Winde & Walt, 2004).

http://etd.uwc.ac.za/

During the formation, the mobility of the elements in acidic environments increases extensively (Tabelin et al., 2020). Meanwhile, acidic pH, together with elements toxicity can induce austere effects on aquatic biodiversity (RoyChowdhury, 2015). Clearly, abandoned mine sites catalyse the development of AMD (RoyChowdhury, 2015). Categorical, the vast development of AMD will take many years of proper management systems to achieve appropriate reclamation (RoyChowdhury, 2015). And if this prolongs, the harmful environmental consequences of AMD will be difficult to tackle.

In tackling this, two main techniques of AMD management are considered, namely:

1) Prevention (source control) technique, and
2) Remediation technique.

Prevention (source control) technique accentuates the prevention of AMD production and transport by monitoring the source, whereas remediation technique emphasises the mitigation appraisal of generated AMD. Two classified remediation technologies of AMD are discussed below.

2.3.6.1 Active Treatment Technology

Active treatment technology is the first of the two classified AMD remediation technologies. This treatment technology is applied for the treatment of both abandoned and active mine sites. Moreover, the obligation to clean-up abandoned mine sites is handled by private and government agencies(Vaziri et al., 2022; García-Valero et al., 2020; Agboola et al., 2020; Hudson-Edwards et al., 2011). The addition of several acid-neutralising and element-precipitating biochemical agents into AMD water is a common tradition used to attain the effluent discharge thresholds in a short period of time.

Generally, a broad array of chemical agents, such as hydrated lime ($Ca(OH)_2$), limestone ($CaCO_3$), soda ash (Na_2CO_3), caustic soda (NaOH), anhydrous ammonia (NH_3), calcium oxide (CaO), magnesium hydroxide ($Mg(OH)_2$) and magnesium oxide (MgO) are used in active treatment of AMD water. The potential of these chemicals are defined by factors such as site specificity (seasonal variation), day-

http://etd.uwc.ac.za/

to-day AMD load released and element concentration. Although, the choice of suitable chemical agent is crucial in realising the treatment development.

Moreover, active treatment technology is also used for active mine sites with inadequate land space accessible for remediation schemes, altering drainage chemistry and flow rate, constant electricity and workforce to supervise the treatment scheme (Table 2.1) (Trumm, 2010). Advantages in active treatment method are highlighted as:

- No extra space or construction,
- Fast and effective acidity and toxic elements elimination procedure, and
- Cost effective in terms of handling and disposal of sludge in comparison to passive treatment techniques.

Additional advantages in active treatment method, in contrast to passive treatment facilities, is that it does not require any extra space or construction as well as being a fast and effective method in eliminating acidity and toxic elements. And it is an

UNIVERSITY of the
WESTERN CAPE

http://etd.uwc.ac.za/

Table 2.1: Characteristics and benefits of chemicals used to neutralise AMD in active treatment systems

Chemical	Maximum pH attainable	Conversion factor[1]	Neutralisation efficiency (%)[2]	Dispensing mechanism	Key benefits	Key limitations
Soda ash or Sodium Carbonate (Na_2CO_3)	11.6	1.06	95−100 (in powdery form) 60 (in briquettes form)	Briquettes or powder are put into wooden box or large drum/reactor in AMD stream/ water flow	High efficiency in powder form, most elements precipitate, with low volume of sludge	Health and safety problems, poor sludge settling rates, potential sodium toxicity.
Hydrated lime or calcium hydroxide ($Ca(OH)_2$)	12.4–12.5	0.74	90-95	Silo or hopper with mechanical feed screw to dispense powder. Batching tank to mix powder with water. Can use aqueous slurry.	High efficiency, most elements precipitate, low cost, widely available.	Health and safety problems, reagent saturation can lower efficiency. Poor maintenance can result in plugged dispensing mechanism and complete failure.
Quicklime or calcium oxide (CaO)	12.4−12.5	0.56	90-95	Silo or hopper with mechanical feed screw to dispense powder. Batching tank to mix powder with water. Can use aqueous slurry. Mechanical feed screw to dispense powder or water. wheel feeder with 1 tonne	High efficiency, most elements precipitate, low cost, widely available.	Health and safety problems, reagent saturation can lower efficiency. Poor maintenance can result in plugged dispensing mechanism and complete failure. Lower efficiency, possible armouring of pebbles. Poor maintenance can result in plugged dispensing mechanism and complete failure. Must be watertight or will hydrate and form calcium hydroxide and plug dispensing mechanism.
Ammonia (NH_3 or NH_4OH)	9.2	0.34	100	Compressed and stored as liquid in tank, gas injected near bottom of pond or water inlet to a pond. No mixing required.	Very high efficiency, most elements precipitate, low sludge volumes.	Health and safety problems, poor sludge settling rates, can be toxic to aquatic life, high cost.
Caustic soda or sodium hydroxide (NaOH)	14	1063 (liquid, 50%)	100	Stored as a liquid in tank, dispense through metering pump or valve and feeder hose near top of pond or water inlet. No mixing required.	Very high efficiency, most elements precipitate, low sludge volumes. Elements precipitate, low sludge volumes.	Health and safety problems, poor sludge settling rates, can be lethal to aquatic life, high cost. highest cost of all chemicals, low freezing point
Magnesium oxide or hydroxide (MgO or $Mg(OH)_2$)	9−9.5	0.40 or 0.58	90-95	Silo or hopper with mechanical feed screw to dole out powder. Batching tank to mix powder with water. Mixing suggested.	Very high efficiency, most elements precipitate, low sludge volumes, low cost.	Some health and safety problems, not widely available, lower reaction rate than calcium hydroxide.
Limestone ($CaCO_3$)	6-7.5	1	approx. 90	Silo or hopper with mechanical feed screw to dole out powder. Batching tank to mix powder with water. Mixing suggested.	Harmless to use, lowest cost of all chemicals, readily accessible, cannot over treat.	Low efficiency, not all elements removed (unproductive for Mn), armouring.

The contents in the table are culled from Trumm (2010)

http://etd.uwc.ac.za/

expensive treatment method. While disadvantages in active treatment method are enumerated as:

- Require incessant chemicals resources and energy,
- Expensive chemicals,
- High maintenance cost, and
- High labour cost needs more manpower to sustain the system (RoyChowdhury, 2015; Trumm, 2010).

In addition, there are a range of approaches that are deemed active, but ODAS (O=oxidation, DA=dosing with alkali, and S=sedimentation), is known to be the most common and preponderant (Trumm, 2010). Other active treatment techniques seldomly used for AMD comprise biosedimentation, sulfidation, ion exchange, sorption and membrane processes such as reverse osmosis and filtration (Table 2.1) (Trumm, 2010).

The efficacy of these methods depends solely on maintenance consistency and chemical resource availability(Skousen, 2017; Trumm, 2010). With these methods, proficiency and application cost differ with the type of neutralising agent used. Due to this, methods modification becomes challenging for nearly all remotely abandoned mine sites. Chemicals, for instance, hydrated lime are also low-cost but ineffectual if higher pH (~9) is requisite for precipitation of elements, such as Mn. Even though, NaOH is nearly 1.5 times more efficient than lime, it is nearly nine times expensive. Owing to their harmful nature, chemical agents like NaOH and anhydrous NH_3 require extraordinary handling. Similarly, the usage of excess ammonia can generate problems like nitrification and denitrification in receiving water bodies(Thakur & Medhi, 2019; Trumm, 2010).

2.3.6.2 Passive Treatment Technology

Unlike active treatment technology, passive treatment technology depends on natural physical, biological and geochemical procedures, which could easily collapse if not cautiously chosen and designed (Trumm, 2010). Passive systems are generally built as per lifecycle (25 years) of neutralising substance, where no supplementary materials are required (Skousen, 2017; Trumm, 2010). Almost all

http://etd.uwc.ac.za/

passive treatment schemes depend on dissolving a neutralising substance (commonly limestone) to neutralise the acidity in AMD (Skousen, 2017; Trumm, 2010). Though adequate inhabiting period in the systems is crucial for improved dissolution rate. Limestone is economical and less soluble in water; therefore, less active than the other chemical agents (Skousen, 2017; Trumm, 2010)..

Characteristically, passive techniques are greatly suitable for supplement active techniques or abandoned mine sites, as well require huge areas of land. Also, these techniques have been the most cost effective among the two types technological techniques, particularly following mine closure (J et al., 2002; Williams et al., 2006). AMD remediation, through passive remediation techniques, can be classified into two distinct groups given as:

- Reducing and oxidising methods(Trumm, 2010), and
- Conventional and emerging technologies (RoyChowdhury, 2015).

AMD is produced through an oxidation procedure that generates high principal contaminant (Fe), which exists in two forms known as ferrous (Fe^{2+}) and ferric (Fe^{3+}) (Singer & Stumm, 1970). Oxidising methods eliminate Fe from the AMD by persistent oxidation process, in a way that all Fe^{2+} is oxidised to Fe^{3+} once the pH has been elevated adequately by precipitating out of the AMD as ferric hydroxide ($Fe(OH)_3$) (yellow boy)(Tabelin et al., 2020; Igarashi et al., 2020; Doulati Ardejani et al., 2011). The employment of oxidizing methods within the context of Acid Mine Drainage (AMD) mitigation is characterized by a sustained oxidative process aimed at the removal of iron (Fe) from the AMD solution. This process entails the complete conversion of ferrous iron (Fe^{2+}) species into ferric iron (Fe^{3+}) under conditions wherein the pH has been elevated to a requisite level. Subsequent to this oxidation, the resulting ferric ions undergo precipitation in the form of ferric hydroxide ($Fe(OH)_3$), colloquially referred to as "yellow boy." This phenomenon corresponds to the physical separation of ferric hydroxide from the aqueous phase, effectively eliminating iron from the AMD solution and thereby contributing to its remediation (Tabelin et al., 2020; Igarashi et al., 2020; Doulati Ardejani et al., 2011). In reducing methods, unlike oxidising methods, AMD oxidation procedure

http://etd.uwc.ac.za/

is reversed, thereby reducing Fe and sulphate by generating FeS_2, FeS, and H_2S. Then, dissolved Fe and sulphate were eliminated from the AMD. Passive treatment methods for AMD remediation do not usually need regular human interference (Skousen, 2017; Trumm, 2010).

Biological passive treatment methods utilised for AMD remediation typically make use of the device of dissimilatory sulphate reduction (DSR) for sulphate elimination produced by sulphate-reducing bacteria (SRB) (McCauley et al., 2008). SRB are heterotrophic bacteria that operate in anaerobic environs. They need organic carbon to act as an electron donor to induce sulphate-reducing activity(Johnson & Hallberg, 2005). It is understood that direct connection exists between the rate of sulphate reduction by SRB and the extent of carbon obtainable. Therefore, organic carbon adjustments are frequently used in biological passive treatment methods for AMD (McCauley et al., 2008). Biological remediation of AMD emerged in full-scale from passive treatment methods by constructed wetlands and compost bioreactors(Trumm, 2010; McCauley et al., 2008; Younger et al., 2003).

On the other hand, conventional passive treatment methods are being utilised over a long time(RoyChowdhury, 2015; Trumm, 2010) while emerging technologies are being probed for proficient AMD remediation results (Trumm, 2010). Some examples of conventional passive treatment methods are enumerated below:

i. Constructed wetlands (CW): – this example of conventional passive treatment methods is classified among the widely used passive AMD treatment technologies. Under CW, only aerobic and anaerobic are recognised. Among the two, aerobic wetlands are superficial water bodies (within <30 cm in depth) that offer adequate retention period to oxidise and precipitate successive element hydroxides (Trumm, 2010).

ii. Anaerobic sulphate-reducing bioreactors: – involve the use of sulphate-reducing bacteria to remediate AMD. They entail dense layer of organic-rich materials variegated with limestone. An extra thin layer of limestone lies beneath the organic layer, which thereby offers the extra alkalinity and maintain the primary drainage channels. Sulphate-reducing bacteria used the

http://etd.uwc.ac.za/

energy generated in the reduction of SO_4^{2-} to H_2S and oxidisation of organic matter (CH_2O) to bicarbonate ions (HCO^{3-}), for growth and expansion (RoyChowdhury, 2015; Trumm, 2010).

iii. Anoxic limestone drains (ALD): – these are characteristically 30 m in length, 1.5 m breath, and 0.6–20 m width underground structures packed with limestone. In ALD, CO_2 is generated when limestone reacts with AMD water, which cannot leak out from the structure and therefore increases the general alkalinity (RoyChowdhury, 2015; Trumm, 2010).

iv. Vertical flow wetlands (VFW): – these AMD passive treatment methods are also known as permeable reactive barriers (PRB), in which water runs through an organic-rich layer lined with a limestone bed, prior to its discharge through a drainage system. These methods decrease ferric to ferrous iron, as well the amount of dissolved oxygen (RoyChowdhury, 2015; Trumm, 2010).

v. Limestone leach beds (LSB): – slag leach beds (SLB) and open limestone channels (OLC) are important AMD passive treatment methods. LSBs are ponds constructed to receive waters with little or no alkalinity and dissolved metals. In SLB ponds, a bed of steel slag fines is used to remediate AMD water requires to be devoid of metals like Fe, Al and Mn (RoyChowdhury, 2015; Trumm, 2010).

2.4 Elemental Mobility and Speciation

The speciation and mobility of elements within coal ash and gold tailings significantly influence the extent of Acid Mine Drainage (AMD) impact within the surrounding environment. AMD is a deleterious phenomenon resulting from the oxidative dissolution of metal sulfides present in mine wastes, characterized by low pH values and elevated concentrations of various heavy metals. The intricate interplay between element speciation and mobility exerts a profound control over the potential for pollutant release, transport, and subsequent ecological repercussions.

http://etd.uwc.ac.za/

Element speciation refers to the chemical forms in which elements exist within a given matrix. In the context of coal ash and gold tailings, the speciation of elements, particularly sulfur-bearing compounds, dictates their susceptibility to oxidation and subsequent dissolution. Sulfur speciation, such as pyrite (FeS_2), plays a pivotal role due to its high reactivity under oxidative conditions. The extent to which pyrite or other sulfide minerals are present and accessible influences the quantity of sulfide oxidation, consequently impacting the volume of acid generation and metal release.

Moreover, the mobility of elements pertains to their propensity to migrate through environmental media, notably water and air. The mobility of metals is contingent upon factors such as solubility, complexation with organic and inorganic ligands, and adsorption onto mineral surfaces. In the case of coal ash and gold tailings, the release of soluble metal ions, particularly iron (Fe) and aluminum (Al), from oxidized minerals can facilitate the formation of secondary minerals or precipitates downstream. These secondary phases can act as carriers for other metals, either adsorbing onto their surfaces or incorporating them into their lattice structures. This can greatly influence the transport and fate of elements within the affected ecosystem.

The intricate interplay between speciation and mobility becomes evident when considering the potential pathways and mechanisms that facilitate AMD. If elements remain sequestered within relatively insoluble mineral phases or are strongly adsorbed onto stable surfaces, their mobility is limited, and the overall AMD impact may be attenuated. Conversely, if elements exist in labile forms or as soluble species due to specific speciation, their mobility increases, resulting in elevated concentrations within leachates, surface waters, and groundwater. This elevated mobility enhances the potential for long-range transport and dispersion of contaminants, exacerbating the AMD impact by contaminating aquatic ecosystems, harming aquatic life, and degrading water quality.

The intricate relationship between element speciation and mobility in coal ash and gold tailings plays a pivotal role in determining the extent of AMD impact in the environment. The speciation of sulfur-bearing compounds and the mobility of

http://etd.uwc.ac.za/

various metal ions collectively dictate the rate of acid generation, the release of heavy metals, and their subsequent transport through environmental media. A comprehensive understanding of these factors is essential for formulating effective mitigation strategies and sustainable management practices to minimize the adverse environmental consequences associated with AMD.

Appropriate study of mineralogy effect, geochemistry, drainage system in elemental mobility and speciation offers awareness on the parameters influencing AMD formation, with the development of appropriate and effective prevention methods. However, there has been little or no awareness in the mineralogical and geochemical interactions occurring in the tailing dams (Camden-Smith et al., 2015; Lindsay et al., 2015; Hansen, 2015; Sracek et al., 2014; Parviainen, 2009). The exploration of this aspect proffers the toxicity and mobility of trace metals in soils (Abegunde, 2015; Heikkinen et al., 2009). These parameters depend on elemental concentrations, associations, chemical properties, environmental conditions (pH, redox potential, biological action of the roots, and chelates formation) (Guillén et al., 2012).

Additionally, it is denoted those substances from clays and organic matter have impact on the behaviour of metals (Guillén et al., 2012). This drives the need for the assessment and identification of the speciation of metals in different fractions of soil, including other substances as tailings and sediments to determine the degree of mobility, availability and persistence in the environment (Lindsay et al., 2015; Camden-Smith et al., 2015; Guillén et al., 2012). Soil contamination, with tracemetals, and metalloids such as As, Cd, Cr, Cu, Ni, Pb and Zn poses a potential threat to the ecosystem equilibrium, humans' health and other living things (Guillén et al., 2012; Nagajyoti et al., 2010).

Impacts of elevated metals concentration on the declining ecosystem quality, as observed from abandoned/fallow mines, heighten the phytotoxicity in sediments, waterbodies and soils (A.k & Sarah, 2014). The acidity and alkalinity of the metals were also observed to ascertain their impacts on the environment. Relatively, it is mentioned that acidity increases the mobility/speciation of trace metals, and pollute

http://etd.uwc.ac.za/

the waterbodies, land and atmosphere when released into the environment. On the other hand, alkalinity increases elements associated with oxyanions (Dold, 2014; Myneni et al., 1997) (SO_4^{2-}, AsO_4^{3-}, MoO_4^{2-} and CrO_4^{2-}). As these elements are released, they aid environmental nutritional deficiencies, which thereby result in deteriorating natural vegetation and biological diversity, and ultimately lead to an ecological menace to the ecosystem (Guillén et al., 2012; Heikkinen et al., 2009).

Therefore, this necessitates a study on the chemical state wherein the elements are present (easily exchangeable ions, metal carbonates, oxides, sulphides, organometallic compounds, ions in crystal lattices of minerals, etc.) in order to evaluate environmental impact of tracemetals accumulated in the soils found in the affected areas (Guillén et al., 2012; Pérez et al., 2008). Due to high mobility of many AMD trace elements, the topmost layers of the tailings have been leached of these trace metals from the overlying materials.

High LOI and unswervingly low total oxides are indication of the existence of sulphides, carbonates, phyllosilicates and/or hydrated minerals (W. Price, 2009). Mineralogical studies using XRD technique sanctions the occurrence of all four of these categories of mineral phases. OH^- from muscovite, clinochlore and kaolinite; CO_2 from organics, dolomite, calcite and/or siderite; H_2O from gypsum; and SO_x from sulphides.

In this case, additional hindrance is the uncontrollable passage of leached tailings (seepage). This hindrance is termed as a major environmental concern in distributing exchangeable trace metals mine wastes. However, fewer studies are done on geochemical characteristics of seepages of the tailing impoundment. This decreases the chance of accessing adequate knowledges on geochemical characteristics of seepage of tailing impoundment (Edraki et al., 2019; Heikkinen et al., 2009). Seepage water is a water derived, or collected from the outflow point at the base of the tailings dams (Heikkinen et al., 2009). Seepage aids development of AMD in the soil. This effect is aided by the transportation of drainage water away from the tailing dams. A drainage water is a type of water with equilibrant surficial conditions. The quality of drainage water is determined by precipitation and

UNIVERSITY of the WESTERN CAPE
http://etd.uwc.ac.za/

sedimentation of secondary mineral, adsorption by suspended–in materials such as clay, organic matter and the mixing and dilution with other surficial material and water bodies along its pathway (Nordstrom et al., 2015; Heikkinen et al., 2009).

In relation to above illustration, the mineralogy of the mine waste materials and the chemical reaction occurring within, is reflected by the geochemistry of the tailings' pore and seepage water. In other words, the total geochemistry of the tailing is directly proportional to the mineralogical composition of tailings solids. Also, the pH of seepage and pore waters will determine the balance and correlation between acid producing and neutralizing minerals in the tailing dam (Edraki et al., 2019; Nordstrom et al., 2015; Heikkinen et al., 2009).

The pH – Eh relationship is a major factor that controls adsorption-co precipitation and dissolution-precipitation in the tailings, despite that the distribution and concentration of even though trace metals, and metalloids in seepage and pore waters highly dependent on the deposit geology (Plumlee, 1999). The seepage from these tailings is generally characterised by low pH values, high sulphate loads and elevated concentrations of toxic substances (radionuclides) (Nordstrom et al., 2015).

Notably, the oxidation of pyrite produces acid and effectively lowers the pH of the drainage, water pathway and other water bodies as it enters the ground water regime beneath the dumps (Naicker, et al., 2003). Due to this effect, the extent of acidity, mobility of elements and pH level in drainages or sulfate soils or mine waste are determined by the form and magnitude of existing sulphide minerals, reactive surface area and the acid-neutralizing (carbonate) minerals confined (Skousen, J., 2017; Nordstrom and Alpers, 1999). Waste materials or mine tailings rich in sulfides and depleted in carbonates generate acidic mine drainage (Argane et al.,2016) and acid sulfate soils, while materials rich in carbonate and depleted in sulfide generate alkaline systems in drainage and soils (Skousen, J., 2017). Therefore, acidity increases mobility/speciation of elements, which upon release into the environment pollutes water bodies, land, and the atmosphere, while alkalinity increases the elements associated with oxyanions such as SO_4^{2-}, AsO_4

UNIVERSITY of the WESTERN CAPE
http://etd.uwc.ac.za/

$^{3-}$, MoO_4^{2-}, CrO_4^{2-}. However, toxic metals pollution has been the focus of many studies over the years, in terms of speciation, economic and futuristic impact and the threat posed to man (Demkova, et al., 2017).

2.5 Study Area and Geology of Secunda/Coal Fly Ash Source

2.5.1 Study area and Geology of Secunda

The Karoo Supergroup is made of the overlying Ecca and basal Dwyka Groups placed over a basement unconventionality at 300-180 Ma(Cadle et al., 1993). The secunda complex in Secunda, Mpumulanga, South Africa, is characterised by the Ecca Group which is symbolized by the sand- and siltstone sequences Vryheid Formation episodic by five coal seams. The study area is located in Secunda, Mpumulanga Province, South Africa as showed in Figure 2.3.

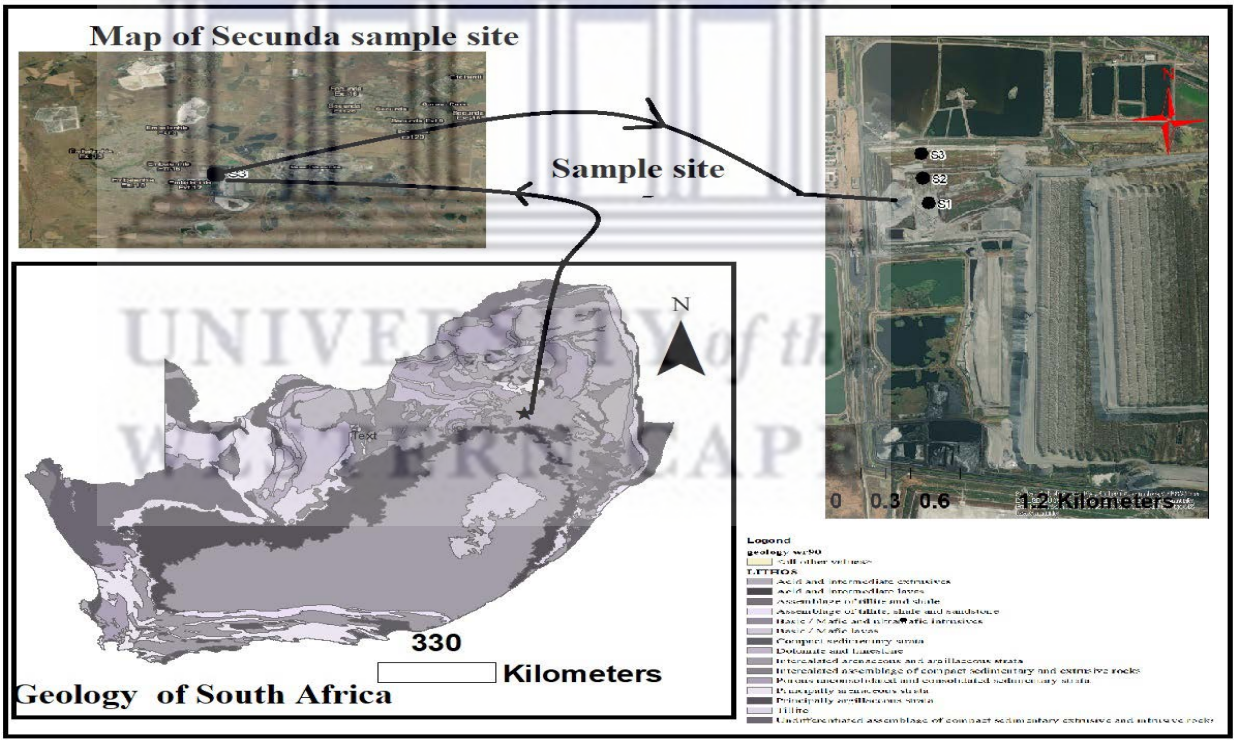

Figure 2.3: Map of the study area for coal fly ash

The sub-outcropping basement strata drift towards east-west and dips at around 15º to the north of the Transvaal. Basement strata contains lithologies affiliated with the southern lobe of the Transvaal, the Bushveld Complex, Witwatersrand and

http://etd.uwc.ac.za/

Ventersdorp (Evander Basin) Supergroup along with Meso-Archaean TTG gneisses(Hancox & Götz, 2014; Cadle et al., 1993).

The Karoo igneous occurrence initiate the emplacement of numerous networks of dykes and interconnected saucer complexes in the Secunda Complex (Svensen et al., 2012; Duncan et al., 1997).

Some originations of dolerite saucers can be separated in the zone, specifically a unique plagio-phyric saucer represent the no 8 sill and two aphyric saucers dubbed as the no. 4 and 7 sills. No. 4 sill is a dark green, fine grained dolerite rock that with the exemption of a limited localised zones happens near the current day topographic level, remain the oldest saucer types (Coetzee, 2016). No. 7 sill has an akin texture to no. 4 sill, on the other hand, occurs in remote areas solely down the length of the basement-Karoo Supergroup contact.

On the contrary, no. 8 sill has a porphyritic texture outlined by needle-like plagioclase phenocrysts, which epitomizes a particular emplacement event the Secunda Complex, besides, contains several interconnected saucers that often lapse and dislodge the Karoo stratigraphy(Coetzee, 2016; Cadle et al., 1993).

About 83 % of weathered coal fly ash from Secunda utilised in this research encompasses coal fly ash generated from pulverised coal combustion process (to generate steam and electricity), and as well as 17 % of fine ash from the gasification method and fine bottom ash. The coal fly ash has a particle size of <250 μm (Mahlaba et al., 2011). The ash was expelled as slurry of 5:1 brine/ash ratio utilising the high saline stream that was produced from the water management process in the plant.

2.6 Study Area and Geology of Randfontein

The Witwatersrand Basin is situated about 15km west of Johannesburg, Gauteng Province, South Africa. The basin encompasses the Witwatersrand Supergroup, characterized by the lower West Rand Group and the upper Central Rand Group.

http://etd.uwc.ac.za/

The West Rand Group is primarily composed of shale with some quartzite, while the Central Rand Group contains the main gold-bearing conglomerates. The focus of mining activities in the initial stage is expected to be on the Kimberley Reefs within the Central Rand Group.

The West Rand District Municipality is situated in the western part of the Gauteng Province, South Africa. It shares borders with the Bojanala District Municipality to the north, the City of Tshwane Metropolitan Municipality to the north-east, the City of Johannesburg to the east, and the Sedibeng District Municipality to the north-east. The West Rand District is comprised of three local municipalities: Mogale City, Merafong City, and Rand West City. Positioned on the southwestern edge of the Gauteng Province, it is notable for being the location of the Cradle of Humankind World Heritage Site. The West Rand of the Witwatersrand basin has experienced a lot of geological exploration, industrialization, mining activities and as well as urban settlement movement over the years. Over 90 minerals have been discovered around the gold mines, according to the South Africa mining reports (Abegunde et al., 2016; Robb & Meyer, 1995). The gold – bearing conglomerate mined in the Witwatersrand reefs has a unique mineralogical composition of quartz (70 -90%), phyllosilicates (10 – 30%), other minor minerals including base metal sulphides and U- bearing minerals in pyrite is most prominent (about 3-5%)(Abegunde et al., 2016; Nengovhela et al., 2006; Bezuidenhout & Rousseau, 2006). The mining activities in this area has exposed it to Acid Mine Drainage pollution and there is need for the evaluation of the abandoned and active mines in the West Rand because of the threat posed by Acid Mine Drainage on its surroundings such as farms, water bodies and residential areas.

The study area is located along the Randfontein and Krugersdorp (R28) road in the Gauteng province (see Figure 2.4).

http://etd.uwc.ac.za/

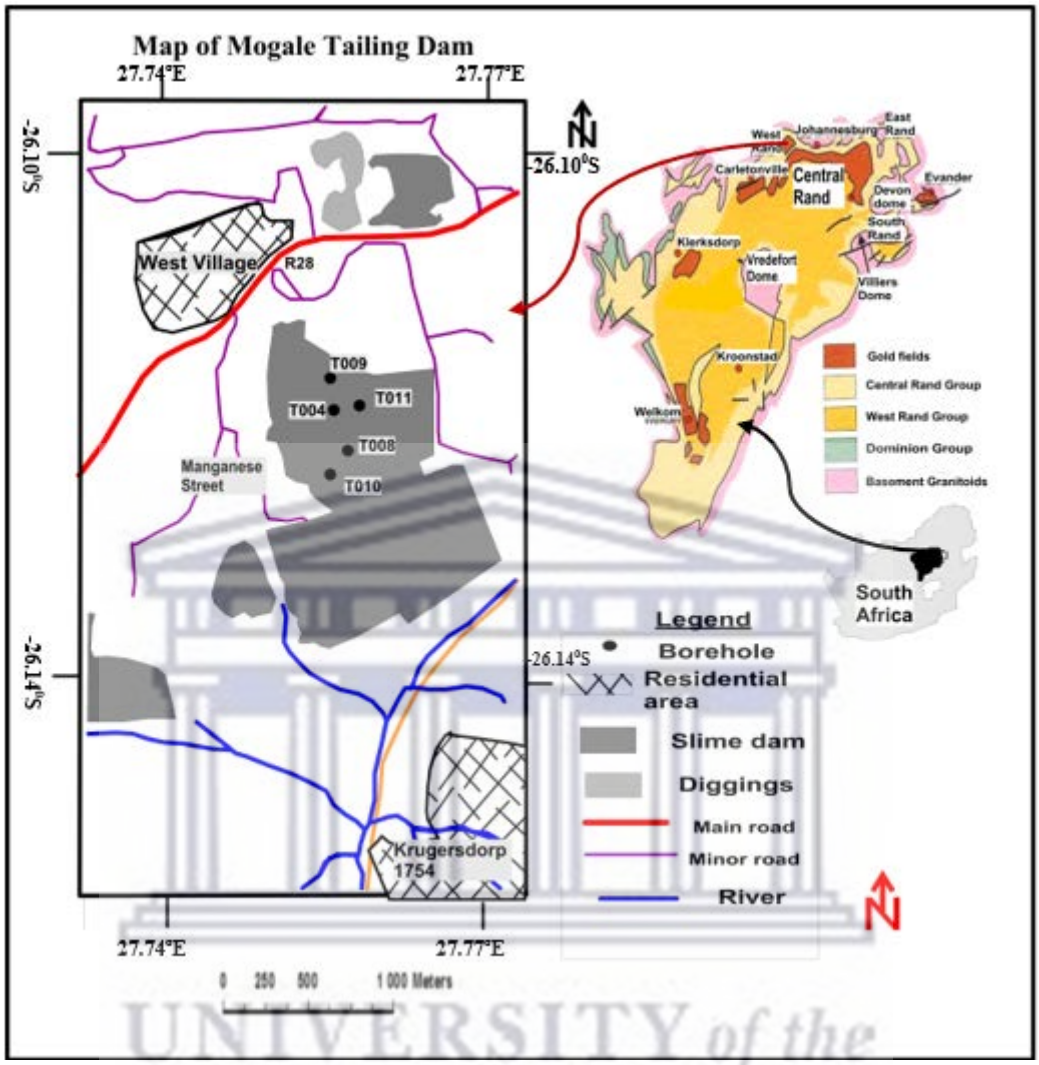

Figure 2.4: Map of the study area (Image culled from Abegunde et al. (2016))

Gold was discovered in 1886 on the southern slopes of the Witwatersrand, leading to the naming of the sedimentary succession containing gold-rich conglomerates as the "Witwatersrand Series" by Penning in 1888. Mellor's classification, proposed in 1917, became the foundational framework for subsequent investigations. Mellor divided the Witwatersrand succession into Lower and Upper Witwatersrand Systems, further subdivided into Hospital Hill, Government Reef, Jeppestown, Main-Bird, and Kimberley-Elsburg Series.

http://etd.uwc.ac.za/

Over the years, Mellor's classification proved applicable to various Witwatersrand exposures, and in 1980, the South African Committee for Stratigraphy revised the nomenclature to create the "Witwatersrand Supergroup." This supergroup is further divided into the lower "West Rand Group" and the overlying "Central Rand Group," each with specific subgroups and formations. In the current study area, only rocks correlated with the West Rand Group are exposed, consisting of quartzite, minor conglomerate, and ferruginous shale. The stratigraphy and sedimentology of the West Rand Group are well-documented, and distinctive marker beds are used for correlation. The dissertation follows the stratigraphic divisions of the West Rand Group as outlined by the Central Rand area convention.

The Witwatersrand region is a significant hub of gold mining activity in South Africa, and faces environmental challenges stemming from the vast tailing dams formed over 30 years of mining operations. These dams, covering over 700 and spanning 400 km², are integral to the Witwatersrand goldfields.

The Witwatersrand goldfields can be grouped into seven major goldfields; they are Free State goldfields, West Rand goldfields, Kosh goldfields, Far West Rand goldfields, East Rand goldfield and Central Rand goldfields, and Evander goldfields. These are indicated in the Figure 1 below, showing the central rand group strata. These areas (goldfields) have been extensively mined over the years and the consequences are now getting more prominent after it was discovered as a site for Acid Mine Drainage, which has become a second to global warming in terms of global environmental impact.

The Witwatersrand Basin, forming over 360 million years (Ma) from 3074 to 2714 Ma, experienced episodic pulses of sedimentation during distinct periods: Dominion Group (3086-3074 Ma), West Rand Group (2970-2914 Ma), and Central Rand Group (2894-2714 Ma). Detritus originated from two distinct age groups of a granite-greenstone source. Basin evolution coincided with episodic granitoid plutonism and responded to processes within a Wilson cycle related to the interaction of the Zimbabwe and Kaapvaal cratons.

http://etd.uwc.ac.za/

Metamorphism events at approximately 2500, 2300, and 2000 Ma were linked to basin loading by Ventersdorp and Transvaal cover sequences and intrusion of the Bushveld Complex or Vredefort catastrophism. Mineralization, concentrated in the Central Rand Group conglomerates, underwent a complex paragenetic sequence. Early accumulation of detrital heavy minerals was followed by three stages of remobilization due to metamorphic fluid circulation. Authigenic pyrite formation at 2500 Ma, maturation of organic material at 2300 Ma, and peak metamorphism around 2000 Ma led to gold redistribution and secondary sulphide formation. Post-depositional fluid conditions favoured effective precipitation mechanisms, resulting in the superimposition of both primary and secondary mineralization.

The Kaapvaal Craton represents an ancient continental crust segment that formed in southern Africa between 3.7 to 2.7 billion years ago (Ga). Much of this continental nucleus developed before 3.1 Ga through the formation of an extensive granitoid basement and amalgamation with arc-like oceanic terranes, including mafic/ultramafic volcanics and associated sediments. The subsequent growth of the craton involved additional continental magmatic activity, possible Cordilleran-style accretion of composite terranes along the proto-continent's margins, and the deposition of sedimentary basins. By 2.7 Ga, or shortly thereafter, the Kaapvaal Craton had achieved cratonic rigidity, marking the cessation of major orogenic processes. The Witwatersrand Basin, a terrigenous sequence about 7000 meters thick, primarily consists of arenaceous and argillaceous rocks

The West Rand Group represents key features of the Upper Witwatersrand beds and the subsequent Ventersdorp and Transvaal Systems. The Upper Witwatersrand beds exhibit a gradual thickening in a south-westerly direction from East Champ d'Or to the central part of Randfontein Estates, followed by a gradual thinning. A stratigraphical section of the Randfontein area is illustrated below.

http://etd.uwc.ac.za/

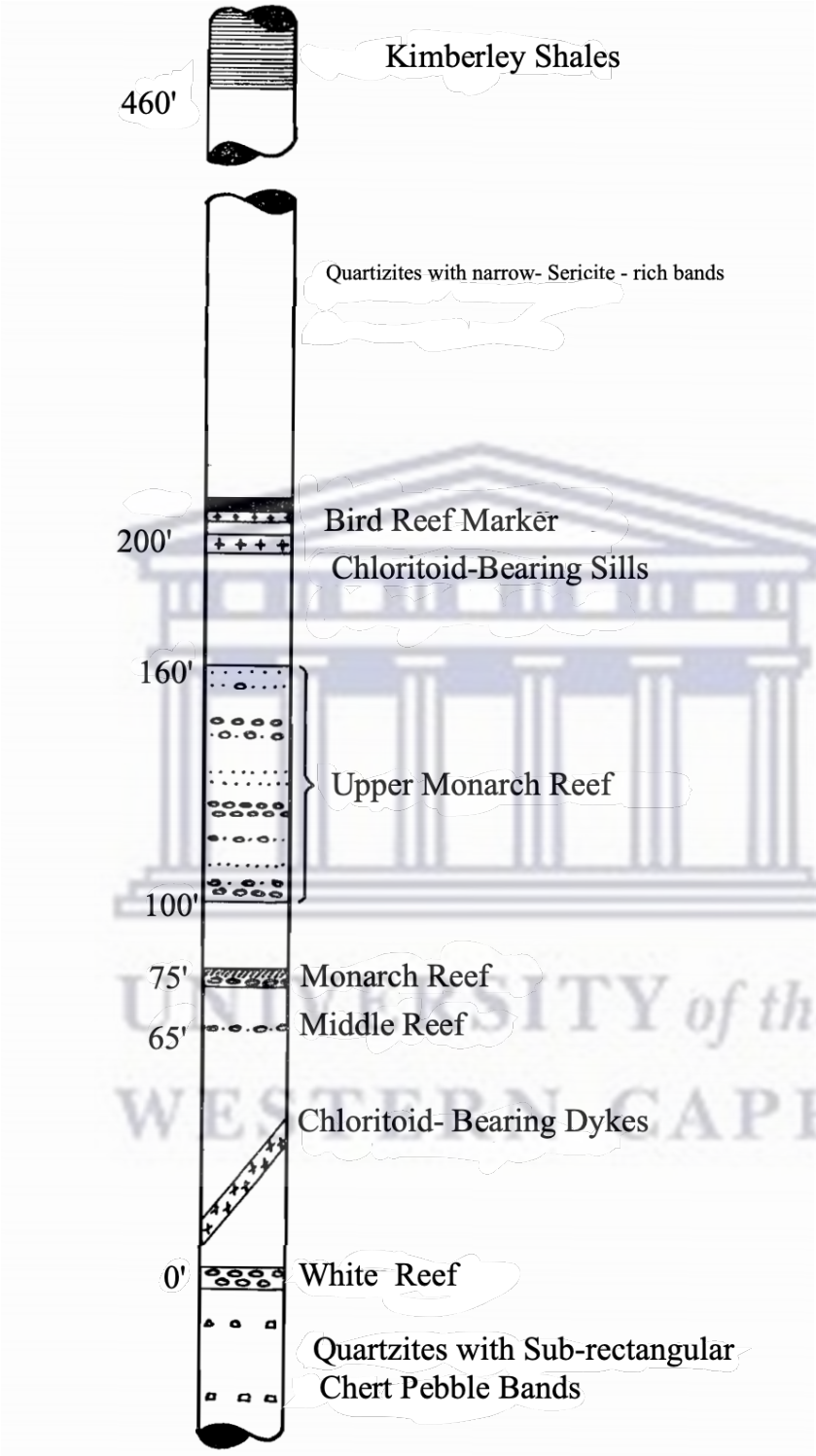

Figure 2.5 : Stratigraphy of the West Rand group, Witwatersrand Basin

(a) Footwall Beds of the Main Reef Group: Overlying the Jeppestown Shales, these beds consist of light to dark green chloritic quartzites, with thickness varying from

http://etd.uwc.ac.za/

200 feet at East Champ d'Or to around 400 feet in the central part of Randfontein Estates. Notably, the Boulder Marker, a band of irregularly shaped chert boulders, occurs in the middle of this zone. The upper section is characterized by sub-rectangular chert pebbles, leading to the Square Pebble Reef near the top. The upper contact with the Main Reef Group is distinct, suggesting no gradual transition.

(b) Main Reef Group: This group encompasses five economically significant conglomerates, including the North Reef, Main (West) Reef, South Reef, and New and Wide Reefs. The North Reef parts from the Main Reef south of Krugersdorp, gradually increasing in thickness from 80 feet in Randfontein Estates to 65 feet in the southern section. The Main Reef, second only to the South Reef in gold yield, varies in character across locations. The Black Bar, a chloritoid-rich shale, overlies the Main Reef.

The South Reef is a primary source of gold in the West Rand area, with varying thicknesses of quartzites between the Main and South Reefs. The New and Wide Reefs, occurring 80 and 140 feet above the South Reef, respectively, are locally important but diminish in gold content away from the northern section of Randfontein Estates.

(c) Livingstone Reefs: These conglomerates between the Main and Bird Reef Groups show variability in width and pebble size, with decreasing gold content away from the northern section of Randfontein Estates. The conglomerates are divided into Lower and Upper Livingstone Reefs, with the Upper Middle Reef being a significant gold-bearing conglomerate.

(d) Bird Reef Series: This group contains economically valuable reefs like the White and Monarch, with Upper Monarch Reefs carrying minimal gold. The White Reef, the main economic horizon, is characterized by a large pebbled conglomerate. The Monarch Reef is a narrow conglomerate, and the Upper Monarch Reefs show lenticular characteristics with minimal gold content.

(e) Kimberley Shales: This argillaceous horizon, with a thickness ranging from 300 to 500 feet, exhibits dolomitic features and micaceous zones.

UNIVERSITY of the WESTERN CAPE
http://etd.uwc.ac.za/

(f) Kimberley Reefs: Economically important reefs include the Lindum and Horsham, with the latter having upper reefs with insignificant gold values. The "Blue Bar Zone," composed of hard siliceous quartzites, occurs above the Upper Horsham Reefs.

(g) Elsburg Series: These conglomerates are absent in the West Rand area, possibly due to erosion before Ventersdorp lava deposition.

(h) Ventersdorp Contact Reef: Occurring just below the Ventersdorp lavas, this conglomerate is mined at various locations, such as Luipaardsvlei Estates.

(i) Black Reef: Unconformably overlying the Witwatersrand System and Ventersdorp lavas, the Black Reef is the basal conglomerate of the Transvaal System. Mining is focused on Randfontein Estates, where the reef occurs in depressions in the pre-Transvaal surface. The Black Reef is overlain by the "Upperstone" and alternating bands of quartzite and shale before the Transvaal dolomites.

2.6.1.1 Gold Mining within the Witwatersrand and its tailings

South Africa has one of the largest gold reefs in world, sitting in the Witwatersrand. It has been a major treasure and source of income to the country. Gold mining continues to be an extremely important economic activity in South Africa. South African gold mines currently account for nearly 12% of worldwide gold production each year (Abegunde et al., 2016; Durand, 2012a; Tutu et al., 2008). However, as recently as the mid-1990s, South Africa produced nearly 30% of the world's gold on the export market. Despite this decline in gold production over the last decade, the nation is still home to an estimated 50% for the world's gold reserves. Gold mining is a huge industry in South Africa and provides employment for a large proportion of the population. Nearly 500,000 people are employed in South Africa's gold mines. The gold industry accounts for roughly 18% of South Africa's annual Gross Domestic Product, or GDP (Norman, 2013; Harington McGlashan ND & Chelkowska EZ, 2004; Feinstein, 2005). In 2005, South Africa's gold exports were valued at $3.8 billion. South Africa is also home to the two deepest gold mines in

http://etd.uwc.ac.za/

the world. The East Rand Mine in Boksburg, and the TuaTona in Carletonville are both nearly 3600 meters deep. The rock is so hot at this depth that specialized cooling technology had to be developed to protect the workers (Norman, 2013)

Despite that, the gold mining has started over a century ago, the Witwatersrand as remain active and a force in gold economy and new gold mining industries have been founded and remain the actual financial block of South Africa. In respect to the gold present, 5 to 10 parts of gold are found and recovered for every million parts of rocks and due to the very efficient and well-planned techniques developed in South Africa, because this low quantity are economically extracted from great depth.

The historical timeline of gold discovery in the region includes significant events such as the founding of the Witwatersrand gold mining company in 1875, the Anglo Boer war, and the introduction of cyanide solution for metallurgical purposes. Over the years, challenges like metallurgical difficulties and labour shortages were addressed, contributing to the resilience and longevity of gold mining in the Witwatersrand.

Despite over a century of mining activities, the Witwatersrand basin remains active, hosting around 120 active mines. The basin's extensive mining history has extracted large quantities of gold and uranium, making it a crucial economic and resource centre. The presence of mine tailings dams, approximately 400 km², poses environmental concerns, particularly in relation to acid mine drainage and the presence of low-grade uranium.

In conclusion, the Witwatersrand's rich mining history, economic significance, and environmental challenges make it a focal point for research. The study seeks to address gaps in understanding the impact of mining activities, especially the comprehensive analysis of tailing zones, to inform effective reclamation strategies and environmental management practices.

http://etd.uwc.ac.za/

The tailing dams remain a major source of the acid mine drainage generation, consisting of crushed ores remnant, in fine grain size and are disposed of through some hydraulic pipe to store in a specific area of land called dam. Most of the tailing dams in the Witwatersrand are over 30 years of formation and the tailing dams are over 700 covering over 400 km^2 land. The tailing dams has been a major source of contamination and a lot of studies (Abegunde et al., 2016; Hansen, 2015; Dold, 2014)has been made on the surface or top layer of the tailings (between 0 to 3.5m, extensively on the oxidised zone), but few studies have been conducted on the interaction of the oxidised zone, transition zone and the unoxidized zone (Nengovhela et al., 2006) and the geological characteristics of tailings and link between these zones have not been extensively studied. Gold mining company, owners of the tailing dams in the Witwatersrand have started reclaiming it because of the discovered economic value of gold present in the tailings. However, the tailing dams reclaimed by these owners were not adequately reclaimed because the surface of the soil underneath still affects the area. And this study is not limited to that.

In the West Rand, the vegetation density can classify the tailing dam. Some are highly dense with trees and well covered vegetation, some a lightly dense with some part still exposed and the others are completely exposed. The surface of the tailing dams is completely oxidised and contain very fine particles that can be easily blown away by wind and precipitation.

2.7 Summary of the Chapter

This chapter serves as a foundational exploration into the intricate relationship between mining activities and their environmental consequences, with a specific focus on the composition of mine waste and the generation of acid mine drainage (AMD). Detailing the various types of mine waste materials produced during mining and milling operations, the chapter underscores the environmental challenges posed by AMD, characterized by low pH and elevated levels of dissolved solids and trace metals. The discussion delves into the sustainability of

http://etd.uwc.ac.za/

quality water in the face of AMD, emphasizing the need for thorough assessment and prediction techniques, including geostatistics, GIS, biokinetics, selective and sequential extraction, acid base accounting, and net acid generation. Additionally, the chapter touches on remediation strategies, particularly the application of passive treatment technology. The elemental mobility and speciation within coal ash and gold tailings are highlighted for their significant influence on AMD impact. The study areas, Secunda and Randfontein, are introduced, providing a geographical context for the subsequent analyses. Overall, this chapter sets the stage for the dissertation by comprehensively outlining the environmental implications of mining activities and the imperative for effective assessment and mitigation approaches.

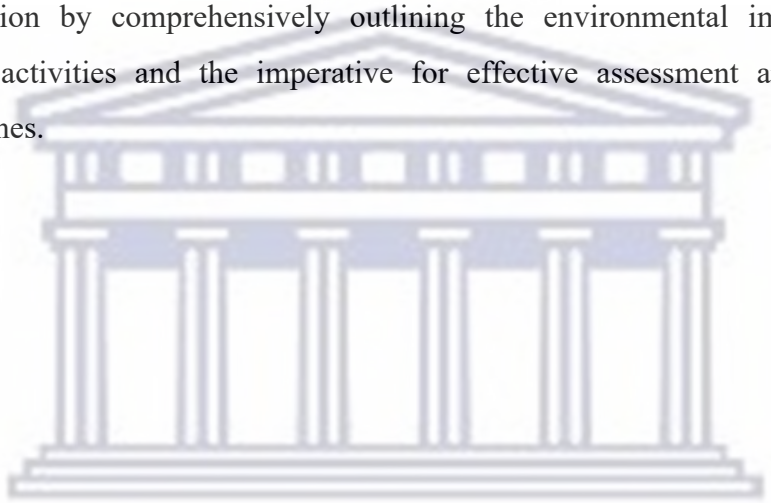

UNIVERSITY of the
WESTERN CAPE

http://etd.uwc.ac.za/

CHAPTER THREE

3. METHODOLOGY

3.1 Introduction

The chapter entails the methodology used, vary from sampling methods, chemical, geochemical analyses, sequential extraction as well as multivariate analysis used.

3.2 Coal Fly Ash Sampling Method

Over a period of 20 years, between 1989 to 2009, coal fly ash from coal gasification and power production from Sasol Secunda power station was dumped in dams (known as ash dam).

The samples of the coal fly ash used in this research were taken from the three cores S1, S2 and S3 drilled to a depth of 22.5 m at the ash dam using air flush coring and standard percussion drilling as earlier described in Figure 3.1.

The coal fly ash samples used in this study were taken using a drill (Figure 3.1) in which three cores S1, S2 and S3 were drilled to a depth of 22.5m. A mixture of air flush coring and standard percussion drilling was utilised to drill the cores at the ash dam.

UNIVERSITY of the
CAPE

Figure 3.1: Drilling process at SASOL Secunda ash dam

http://etd.uwc.ac.za/

An initial starter hole was bored (215 mm diameter) with air percussion drilling via the top cover of the ash dam. The air flush coring method was then utilised to drill to the foot of the ash dam. Large diameter vertical boreholes were bored in the ash dam to take samples for assessment. The coal fly ash samples were removed from the core and placed in zip-lock plastic bags to marmalade before analysis. The drilled holes were finished with small concrete rings as well as shallow (30 cm) sanitary seals and fortified with superior tall standing lockable caps. All the finished drilled holes were obviously numbered. Afterwards, the coal fly ash samples were then kept in airtight taped up containers to inhibit moisture loss and contact with CO_2 and O_2 from the atmosphere Figure 3.2. The sample bottles were stockpiled in a dark cool cupboard to prevent temperature variations. The coal fly ash samples were then pulverised into a homogeneous fraction before analysis (see Figure 3.2).

Figure 3.2: Sample storage and milling

Left image: Storage in air tight containers. Right image: Milled samples ready for analysis.

The fresh coal fly ash samples utilised in this study were taken from the hoppers inside the ash assortment system at Sasol Secunda power station and preserve under the same condition as the drilled coal fly ash.

The mineralogical compositions of the Secunda fly ash samples (Secunda fresh fly ash and weathered Secunda fly ash core) were studied through the application of the X-Ray Diffractometries (XRD) technique. One sample of fresh fly ash and 10

http://etd.uwc.ac.za/

samples of the weathered fly ash samples were taken from different holes at certain depths intervals of 1m for each core or borehole of the Secunda ash dam and mineralogically analysed APPENDIX A. All the ash samples were dried at 105 ^{o}C for 12 hours to remove absorbed moisture and milled to a fine powder with the aid of Dickie and Stockler milling machine before conducting analysis. The analysis procedure was conducted using Nova NanoSEM 230 series as mentioned earlier in section 3.8. 10 grams of each sample was used for this experimental procedure. A Philips Analytical instrument with a pw1480 X-ray fluorescence (XRF) spectrometer, operated at 40 kV and 25 mA, using a rhodium tube was used. The samples were step-scanned from 5 to 85 degrees 2 theta scale at intervals of 0.02 degrees and counted for 0.5 seconds per step.

With the procedural application of XRF and inductively coupled plasma–mass spectrometry (ICP-MS) following a lithium metaborate fusion (sample digestion method), all major oxides and trace elements were carefully analysed and documented from the 51 tailing samples collected from the investigated site. Total sulphur and carbon were determined by Leco analysis using Leco method Group 2A. A small amount (0.1g) of each sample were ignited in an induction furnace to about 1350^{o}C, while a stream of oxygen was passed through the samples. In addition, an estimated sample of milled tailings and water were mixed to form a paste in a specific quantity in order to measure the paste pH and EC. These measurements were obtained using a multi-meter pH-EC Electrode at Earth Science department laboratory, University of the Western Cape Bellville.

3.3 Sampling Method for Gold Tailing

Before embarking on this research, literature study was done to get ample information about and be acquainted with the gold tailing dam environments in Witwatersrand. Site investigation was done for a week to help in choosing the tailing dam of interest. The criteria used was based on its location, accessibility, proximity to residential area, the physical state of the dam (some dams are being or totally reclaimed), and how long it has been constructed. The site chosen was also within one kilometre away from the residential area.

http://etd.uwc.ac.za/

In that respect, this study probes the element mobility of the gold tailings with regard to various zone identified, based on the natural and other possible phenomena like natural water medium, acidic and alkaline medium using sequential extraction and multivariate analysis. Also, the study evaluates the state of tailings, environmental condition for the release of element, the control of mineralogy within tailings and the pattern of elements released under different environmental condition. Geostatistical tools (such as multivariate analysis) and mineralogical evaluation were used to extract more information from three step modified sequential extraction procedure (SEP) method. This approach aids better understanding of the elemental speciation or mobility from Mogale tailing dam in Randfontein area, Witwatersrand Basin, South Africa. The use of acidic potential determination of the tailings and its bulk chemistry in predicting the AMD loads discharged into the environment over time was done. Furthermore, statistical analysis results were corroborated with acid generation potential to identify various relationships that exist and establish the efficacy of the research towards predicting AMD generation potential.

Five boreholes were drilled to a depth of 10.2m and samples collected from every metre down hole and from layers with distinct appearance. After a week of site investigation, Mogale Tailing dam MT became a site of interest because of its proximity to residential areas, farms and major road and the present state of the dam. Samples were taken from the tailing dams at an interval of 1m each down hole using a hand auger Figure 3.3 Figure 3.2. All drill holes' location coordinates were recorded using a GPS (Global Positioning System). Five holes were drilled with the use of a hand auger to a depth of 10.2 meters measured constantly (as auger moved down) with a strong metallic meter rule. The drill holes were marked as T004, T008, T009, T010, and T011, respectively.

http://etd.uwc.ac.za/

Figure 3.3: Drilling process at Mogale tailings dam

Each hole drilled was carefully examined, logged to show the variation in colour, grain size and mineralogy. Since there is much similarity in the texture and size of gold tailing dams, only the colour difference and moisture were prominent. Samples collected were place in an airtight and properly sealed polythene bag and kept in dark container to minimise further oxidation. Afterwards, the samples were transported to the Earth Science Department laboratory of University of the Western Cape for sample preparation and analyses.

Prior to geochemical analysis, all tailing samples were dried at 40 ^{o}C for 16 hours and afterwards pulverised by Dickie and Stockler milling machine (TS-250mill) into powdery form without sieving for elemental analysis. The milling machine was properly cleaned with soapy water and acetone before and after milling each sample. Samples were sent to Itemba Labs and Acme Analytical Laboratories (Vancouver) Ltd for XRD and geochemical analyses (XRF and LA-ICP-MS), respectively.

http://etd.uwc.ac.za/

3.4 Characterization Techniques

3.4.1 Material and Methods

3.4.1.1 Chemicals

Highlighted below is the list of the chemicals used in extraction process. All these chemicals were supplied by Kimix South Africa.

- 99.8% Acetic acid (CH_3COOH)
- 98% Ammonium acetate (CH_3COONH_4)
- 99 % Hydroxylamine hydrochloride ($H_3NO.HCl$)
- 25 % Ammonia solution ($NH_3(aq)$)

3.4.1.2 Mineralogical Analysis Procedure of XRD

The mineralogical composition of the 37 gold tailing and 33 coal fly ash samples were analysed using the BRUKER AXS D8 Advance X-ray diffraction spectrometry (XRD) machine of ϑ-ϑ scan in locked coupled mode at the Itemba labs. These samples were selected based on the colour, texture, and mineralogical variations down hole.

The X-ray Tube Cu-Kα radiation ($\lambda K\alpha_1$=1.5406Å) and the Detectors are Position Sensitive Detector Vantec-1 appropriate for mineralogical studies.

Exactly 1.2 g of the powder sample was deposited in the centre of the sample holder, which consists of a 20mm, by 20mm corning glass (Tube voltage: 40kV, Tube current: 40mA, Slit system: V20 variable slit). The heap of powder was smoothly flattened into a disc shape of 15mm diameter and 1mm thickness by means of circular motion of a microscope glass slide until the zero level for a correct sample height was achieved.

A portion of the coal fly ash sample was oven-dried at 105 °C for 12 hours to remove adsorbed water prior to XRD analysis. Two grams of each of the samples mentioned above were pressed into rectangular aluminium sample holders using an alcohol wiped spatula and then clipped into the instrument sample holder. A Philips Analytical instrument with a pw3830 X-ray generator operated at 40 kV and 25 mA

http://etd.uwc.ac.za/

was used. The samples were step-scanned from 5 to 85 degrees 2 theta scale at intervals of 0.02 degrees and counted for 0.5 seconds per step.

Similarly, the mineralogical configuration of the fresh fly ash and the weathered fly ash was investigated using XRD.

3.4.2 Scanning Electron Microscopy (SEM)

Scanning electron microscopy was conducted to understand the changing morphology of the coal fly ash samples as the age increased. The samples were analysed using Zeiss Gemini Auriga high resolution scanning electron micro-analyser (HR-SEM) furnished with a CDU-lead detector at 25kV and a tungsten filament. The current and illumination was fixed at 5kV and 0.1mrad, whereas the magnification, working distance and resolution was captured on each sample micrograph. The qualitative elemental composition for each analysed sample focus spot was analysed by energy dispersive spectroscopic (EDS).

Before analysis, the ash samples were oven-dried at 105 °C for 12 hours to remove any adsorbed moisture. A portion of each of the four dry samples was then spread onto specimen holders using special glue mixed with carbon graphite. The analysis was carried out with a Nova NanoSEM 230 series, equipped with an Oxford X-max detector, at low voltage and high contrast mode using the backscattered electrons detector.

UNIVERSITY of the WESTERN CAPE

3.4.3 Geochemical Analyses

The geochemical analyses were conducted in the Acme Analytical Laboratories (Vancouver) Ltd (Table 3.1). Fifty one tailing samples were analysed, spanning over the 5 boreholes drilled. Sixty six samples of Coal fly ash spanning over 3 boreholes were analysed in the analytical laboratory of the Department of Chemistry, University of the Western Cape using ICP-OES.

Five grams of each sample was analysed by $Li_2B_4O_7$/ $LiBO_2$ fusion analysis by X-ray Fluorescence (XRF). The $Li_2B_4O_7$/ $LiBO_2$ fusion analysis by X- ray

http://etd.uwc.ac.za/

Fluorescence (XRF) was used to analyse the percentage concentration of the major elements and the loss of ignition.

Likewise, portion of the weathered fly ash samples were oven-dried at 105 °C for 12 hours to remove adsorbed water and then milled to a fine powder. Ten grams of each of the samples mentioned above were used for this procedure. A Phillips PANalytical pw1480 X-ray fluorescence spectrometer using a rhodium tube as the X-ray source was used. The technique reports concentration as % oxides for major elements and ppm for minor elements which was analysed by ICP MS. Elements reported as % oxides were converted to % elements by dividing the molecular weight of the element with that of its respective oxide, then multiplying the result by the reported % oxide value as shown below:

$$\text{Elemental concentration (weight \%)} = \frac{\text{Molecular weight of the element}}{\text{Molecular weight of the oxide}} \times \text{Reported value} \quad \ldots\ldots 5$$

Table 3.1: Sample preparation and analytical procedures in acmelabs

Method Code	Code Description	Test Wgt (g)	Standard used
4X	Li2B4O7/LiBO2 fusion, analysis by XRF	5	STD OREAS72A/ STD SY-4(D)
2A Leco	Analysis by Leco	0.1	STD GS311-1/ STD GS910-4
4B02	LiBO2/Li2B4O7 fusion ICP-MS analysis	0.2	STD SO-18
1DX	Aqua regia /ICP-MS analysis	2	STD OREAS45EA/ STD DS9

A measure of 0.1 g of each sample was analysed for the total percentage of carbon and sulphur present using analysis by Leco analysis. Leco analysis uses infrared absorption and thermal conductivity to determine combustion gases such as carbon,

http://etd.uwc.ac.za/

sulphur, oxygen etc. within samples that contains metallic elements. Selected grams of samples are heated and combusted in a flow of pure oxygen.

Using Aqua-regia / ICP-MS method, ultra- trace element determination was performed for Laser Ablation Inductively Coupled Plasma Mass Spectroscopy (LA ICP –MS) coupled with LiBO2/Li2B4O7 fusion analysis was used to analyse the rare earth elements for gold tailings samples, while ICP OES was used to analyse the coal fly ash.

Standard quality control was used during geochemical analysis (such as standards, blank samples and pulp duplicates) and reference materials.

A "pulp duplicate" refers to a duplicated sample created by splitting a larger sample of material, often mineral or soil samples, into two identical subsamples. The purpose of creating pulp duplicates is to assess the precision and accuracy of analytical measurements. This practice is particularly common in mining, geology, and environmental sciences where accurate and representative sample analysis is crucial.

In mining and geology, pulp duplicates are an essential part of ensuring accurate and reliable data for decision-making processes. They help researchers and professionals identify potential errors or inconsistencies in their analytical methods and make informed interpretations about the properties of the sampled material.

UNIVERSITY of the WESTERN CAPE

3.4.4 Lithium Borate Fusion Method/XRF

Samples from the investigated site were analysed by lithium -borate fusion (sample digestion method) with X- ray Fluorescence (XRF) spectrometry at the acme labs, Vancouver, Canada. A predetermined amount of sample was roasted at 950 °C to determine the loss on ignition (LOI) which is calculated as a function of weight loss after roasting (Loss on ignition (LOI) is determined by igniting a sample split then measuring the weight loss). Five grams of sample pulp was roasted at 1050 °C and the roasted sample was then fused in a platinum-gold crucible with a commercial lithium tetraborate flux. The molten material was cast in a platinum mould. Fused discs are analysed by XRF spectrometer, which was calibrated using certified

http://etd.uwc.ac.za/

reference materials. For XRF analysis, the creation of a homogenous glass disk decreases the effects linked with particle size, mineralogy and matrix to attain better accuracy However, for the preparation of a glass disk, 35% Lithium tetraborate /65% Lithium metaborate instead of 100% Lithium metaborate was used to avoid crystallization.

3.4.5 Leco Analysis for Total sulphur and carbon content

Leco analysis was done to determine the total sulphur and total carbon present in the sample using Leco method Group 2A. All the samples were prepared for analysis by igniting 0.1 g of each sample in an induction furnace to about 1350 °C while a stream of oxygen was passed through the samples.

Total sulphur was determined using a Leco sulphur analyser. The amount of sulphur dioxide released from the sample is defined by an IR detection system (that is, infrared spectroscopic analysis), which is used to generate the Total Sulphur result. Whilst, the Total carbon was determined using a Leco carbon analyser. The total carbon was calculated from the infrared spectroscopic analysis of the carbon dioxide generated.

3.4.6 Aqua-Regia Digestion

Aqua regia digestion is a multi-element analysis and requires two acids (hydrochloric acid and nitric acid) in a 3:1 ratio, forming nitrosol chloride for ultra-trace element analysis (1DX). This digests the mineral matrix and helps to release the metals present in solution and assisted by gentle heating. According to the method discussed by (Chen and Ma, 2001; Kisser, 2005), the nitric acid reacts with concentrated hydrochloric acid to form aqua regia:

$$3HCl + HNO_3 \rightarrow 2H_2O + NOCl + Cl_2 \quad \text{…..……6}$$

The aqua regia digestion was performed in 250-mL glass beakers covered with watch glasses. A thoroughly mixed sample of 0.5000 g was digested in 12 mL of aqua regia on a hotplate for 3 hours at 110°C to evaporate. After evaporation to near dryness, the sample was diluted with 20 mL of 2% (v/v with H_2O) nitric acid.

UNIVERSITY of the WESTERN CAPE

http://etd.uwc.ac.za/

Afterwards, it was taken into a 100-mL volumetric flask by filtering through Whatman no. 42 paper. Then, it was diluted to 100 mL with deionised, distilled water (DDW) which is then analysed in ICP-MS. The standards STD OREAS45EA and STD DS9 were used in the analysis. The samples were analysed for Mo, Cu, Pb, Zn, Ag, Ni, As, Au, Cd, Sb, Bi, Hg, Ti, and Se using this method (1DX).

3.4.7 Paste pH and EC

Paste pH and EC test was done by dissolving a 1-part portion of the tailing sample to 2.5 part of water, after shaken properly, and then the values are measured using a multi-meter pH- EC Electrode (TMH, 1990; MEND, 2009; INAP, 2009). Paste pH remains a modest and economical method that assist to indicate the presence of reactive carbonates or relative extent of acidity. In this study, milled tailings samples and water were mixed to form a paste in a specific proportion. The pH was first calibrated using buffer solution of pH 4 and pH 7 and the EC. Five grams of tailing samples was measured into the test tube and 15ml of distilled water was added and mixed thoroughly. The sticky solution was then measured for paste pH and EC.

3.4.8 Quality Assurance and Quality Control (QA/QC)

QA/QC is a major and important aspect of modern analytical geochemistry. A well-monitored QA/QC method gives a way of establishing confidence level in the analytical data and evaluating the limitation of the analytical data, thus, detecting the origin of analytical error. The method includes the determination of the precision, accuracy and potential contamination load from sampling to analysis. The advancement of instrumentation technology over the years has resulted in high demand for high precision and accuracy of litho-geochemical data in research, and mineralisation studies and development. Due to the tendency of uncertainty that can seldom surrounds the quality of litho-geochemical data, proper record of QA/QC is required before the data can be publicly reported and accepted. This has led to the requirement from research community suggesting the availability of standardised information about all analytical data, including a well-known QA/QC procedure.

UNIVERSITY of the WESTERN CAPE
http://etd.uwc.ac.za/

3.4.9 Precision

Precision is the measure of the reproducibility of a specific measurement performed. Precision is determined using systematic introduction of sample, pulp duplicates, and sometimes reference materials. Evaluation of data is done using scatter plots, statistical test, Thompson-Howarth plots and average coefficient of variation.

In this study, pulp duplicates of some selected samples will be used to calculate precision with the use of scatter plot. It should be noted that reference or standard materials have recognised values but limited ranges of values for a given element; and as such, do not give the true measure of precision. That is why duplicates samples are used.

Scatter plots in Figure 3.4, 3.5, and 3.6 provide a means of visualizing the pulp duplicate result from data collected by plotting the duplicate sample results on the y-axis and the initial results plots on the X-axis with control lines that depicts a specified level of precision (i.e., 5%, 10%, 20%, etc.). If all data falls within the control line, then the data is said to be precise based on the set precision, if outside, it indicates that the data is not precise at the set precision.

3.4.9.1 Precision Results for Major Elements

From the scatterplot, the LOI, SiO_2, Al_2O_3, Fe_2O_3, and CaO data fall within the control line of 5%, indicating that it is <or =5% precise, and MgO, K_2O, and TiO_2 fall within the control line of 10%.

http://etd.uwc.ac.za/

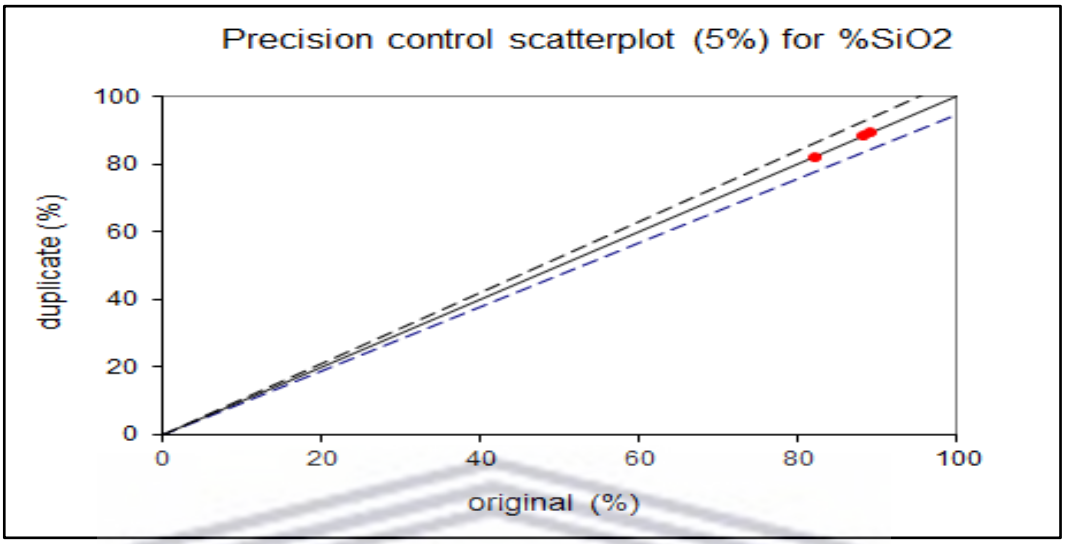

Figure 3.4: Precision results showing precision control scatterplot of 5% for Si_2O

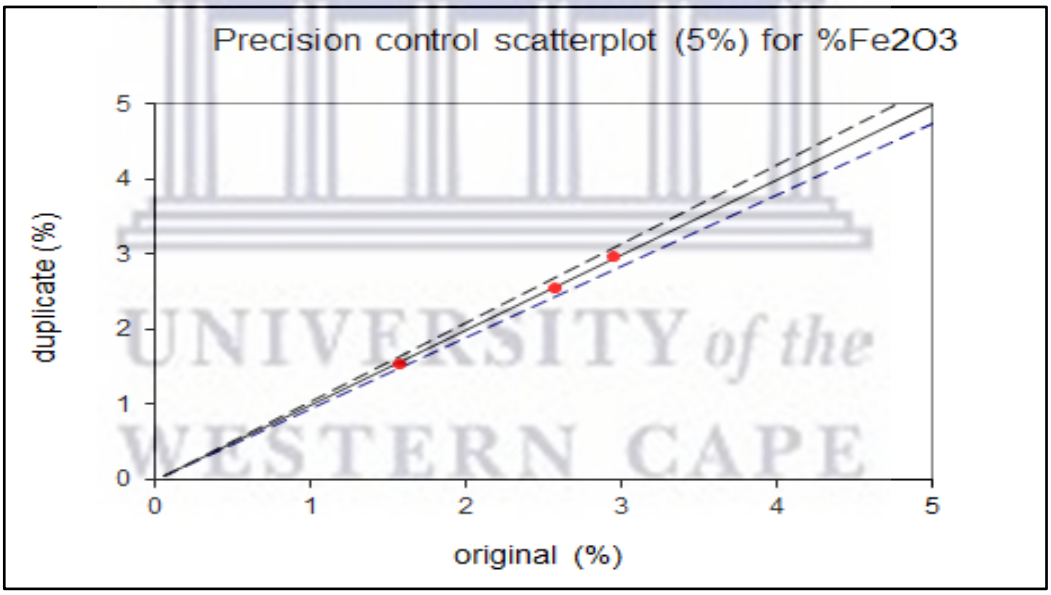

Figure 3.5: Precision results showing precision control scatterplot of 5% for Fe_2O_3

3.4.9.2 Precision Results for Trace Elements

Most trace elements data in this study fall within the control line of 10%, indicating a less or equal 10% precision Figure 3.6

http://etd.uwc.ac.za/

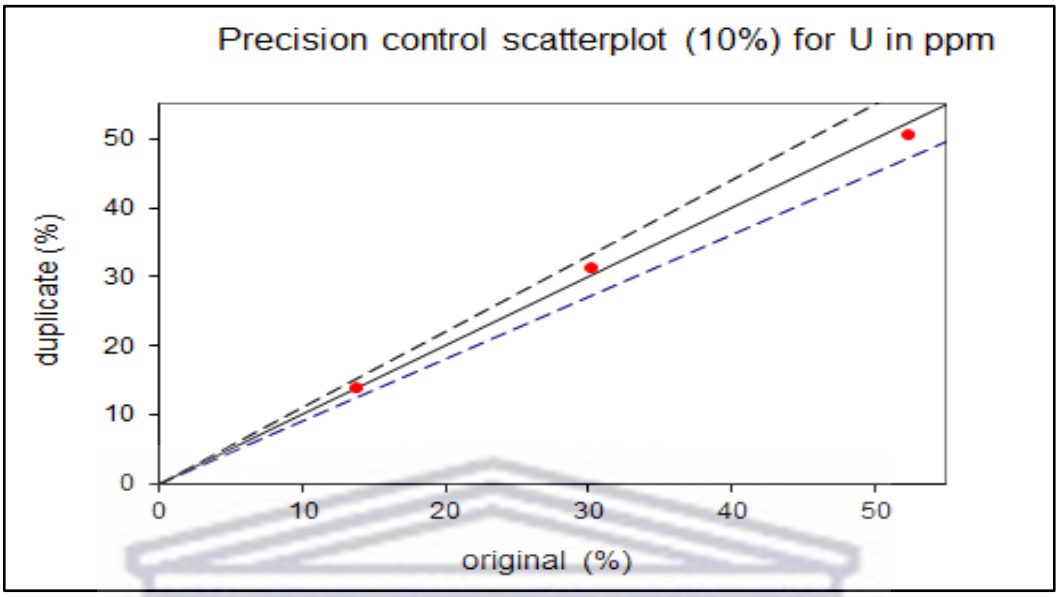

Figure 3.6: Precision results showing precision control scatterplot of 10% for U

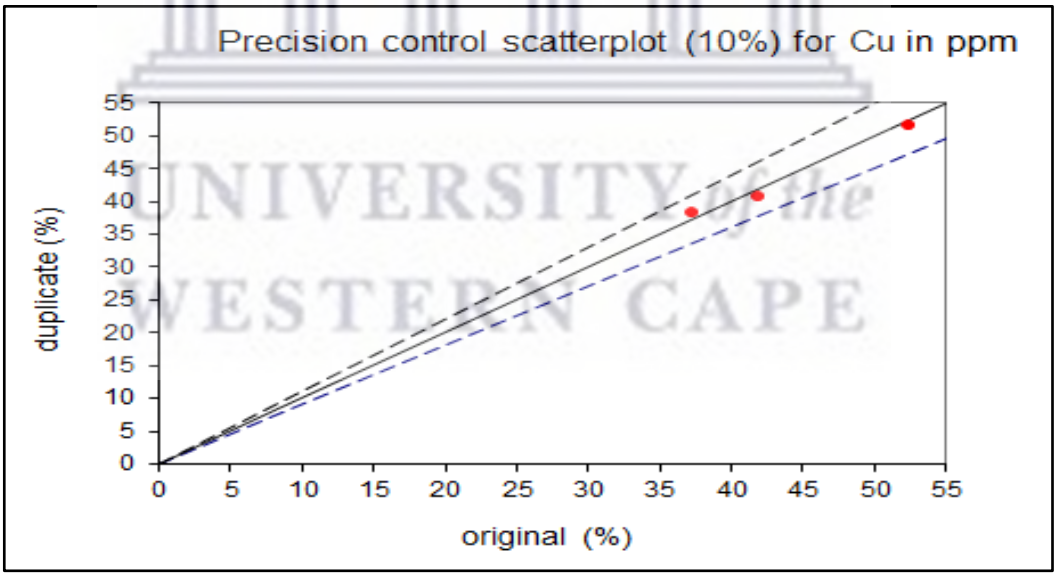

Figure 3.7: Precision results showing precision control scatterplot of 10% for Cu

3.4.10 Accuracy

Accuracy is defined as the determination of the degree of closeness of a calculated or measured value to its known and accepted value. This is determined using the

http://etd.uwc.ac.za/

analysis of reference or standard materials such as formulae, statistical test and shewart control charts. In this study, the percentage relative difference used is the percentage difference of the expected or known reference material and the measured or analysed reference material. This is calculated from the replicates analyses of reference materials as follows.

Percentage relative difference $\mathbf{(\%RD) = 100 \times \frac{(Me - STDe)}{STDe}}$ ……..……7

Where Me = mean value of element e in the standard over a number of replicates analyses results of the reference or standard material.

STDe = the certified or known value of element e for the standard or reference materials used

% RD can be negative or positive, that is <0 or >0. Generally, when %RD values are +3% or -3%, the data accuracy is considered excellent, if between 3-7%, it is termed very good, 7-10%, it is termed good, if above 10%, it is not accurate.

Some elements such Au could have an accuracy over 10% because of its nugget nature; therefore, a standard accuracy is given for this element. The results for % accuracy for major and trace elements is shown in appendix A.

3.4.11 Sequential Extraction

Gold tailings and coal fly ash samples were selected and subjected to a 3-step modified sequential extraction (Eze, et al., 2013). Multi-elemental analysis of each sequential leach phase was analysed by inductively coupled plasma- optical emission spectrometry (ICP-OES) technique.

Following the 3-step sequential extraction, the results generated in each phase were analysed using multi-variate statistics (such as cluster analysis, discriminant function analysis and factor analysis). The cluster analysis was used to probe the relationship and source pattern within each phase to help understand the mobility of elements.

UNIVERSITY of the WESTERN CAPE

http://etd.uwc.ac.za/

Water leach (step 1): The water-leach phase targeted the most labile species present in the wastes. Hence, the most labile and bio-available for the environment represents the effect of rain water on the waste. A 3 g of selected sample was measured into a 50 mL centrifuge tube and 45mL of ultra-pure water (H_2O) was added at 25 ^oC. The samples were then placed in a mechanical shaker for two hours. The process was repeated to produce duplicate samples. The solution was made to stand for one hour. Afterwards, each sample was placed in a centrifuge at 5000 rpm for 20minutes and the supernatant filtered through a 42 μm filter paper. The remaining solid portion was carefully decanted into a 100mL plastic clear bottle to decrease weight loss. The filtered supernatant solution obtained was prepared for analysis of major and trace species using a dilution factor of 10 for ICP-MS analysis. The solid residue remaining after the extraction of each sample was quantitatively recovered and kept in a refrigerated condition for the next extraction method.

Ammonium acetate leach (Extraction at pH 5): Ammonium acetate leach targeted the exchangeable metals and/or those decipherable in slightly acidic conditions. 45 mL of 1 M ammonium acetate buffer solution at pH 5 was added to the solid-remains recovered from step 1 at 25°C. The centrifuging and recovery procedure given in Step 1 was followed again.

Hydroxylamine hydrochloride leach: Hydroxylamine hydrochloride leach identified metals associated with Fe and Mn oxides that can be leached out if conditions alter from oxic to anoxic state (Favas et al. 2011; Eze, et al., 2013). 45 mL of hydroxylamine hydrochloride (0.25 M) in nitric acid (0.025 M) solution was added to each sample of the solid residue recovered from step 3. The solution was shaken for one hour at room temperature. The same process given in Step 1 was followed.

For each leach, multivariate statistics such as cluster analysis and discriminant function analysis were carried out to probe, identify and predict the speciation based on relationships. Complete statistical analysis of sequential extraction procedure results (each phase analysed differently) was performed by using IBM SPSS 20®

http://etd.uwc.ac.za/

software (Wang, 2016). In the aspect of clustering analysis (CA), Ward's method was applied to assemble objects or units present in each phase into categories (known as cluster) depending on their similarities (Santos, et al., 2005; Alkarkhi, et al., 2009; Wang, 2016). Also, discriminant analysis (DA) was used to envisage the other variables that describe each cluster; thus, elucidating the dissimilarities between groups (clusters) and defining the least number of proportions needed to describe these dissimilarities (Poulsen and French, 2004).

3.5 Data Evaluation

Statistical analysis was used to evaluate the data from the mineralogical and geochemical analyses.

3.5.1 Statistical Analysis

Bivariate and multivariate analysis was performed using SPSS 21® software. Correlation coefficient, Hierarchal-clustering and factor analysis was performed based on the method described by (Chaosheng and Olle, 1998; Abbas, et al., 2009).

3.5.1.1 Correlation Coefficient Analysis

Correlation coefficient analysis was performed for elements occurring in the samples from all the five boreholes to identify bivariate trends between two variables using Pearson's correlation method. The correlation coefficient r ranges from -1 to +1 (that is r = -1 or r = +1) representing a perfect linear relationship between two variables, showing a direct or indirect relationship with each other. When r is negative, it shows that there is a negative trend (correlation), if r is positive, there is positive correlation and if r is 0, it shows no trend at all.

Correlation coefficient r can be defined as:

$$r = \frac{n(\Sigma xy) - (\Sigma x)(\Sigma y)}{\sqrt{\left[n\Sigma x^2 - (\Sigma x)^2\right]\left[n\Sigma y^2 - (\Sigma y)^2\right]}} \quad \ldots\ldots\ldots\ldots 8$$

Where x and y are the two selected variables correlated.

http://etd.uwc.ac.za/

3.5.1.2 Cluster Analysis

In cluster analysis, geochemical data for the major oxide was analysed using hierarchical cluster analysis with a statistical agglomeration schedule under an initial none cluster membership. Cluster analysis was used to generate the prominent clusters present at r= 0.05(dendrogram) in which hierarchical cluster analysis was done using nearest neighbour linkage and Euclidean distance as a measure of proximity between samples. The ward method under the Euclidean distance interval was used and a dendrogram was plotted. Cases were labelled based on the sample no and sample ID. Box plots was used see the variation of a specific element in each group (cluster).

3.5.1.3 Factor Analysis

Factor analysis on the other hand, narrows down to the elements playing major role in the composition of the samples and helps to enhance group based elemental relationship. Factor analysis was done using principal component analysis extraction method to find and estimate the relationships among variables. This will make the interpretation of the analytical results more explicit by decreasing the number of variables that are the determinant factor, thus, narrowing the interpretation of variables distribution as a function of its geochemical and sedimentological activities and common origin. Therefore, Principal component analysis (PCA) was done to create possible factors that are responsible and determinant of the metal concentrations and source allotment. All dataset was subjected to factor analysis (FA). The number of significant principal components (PC) was selected based on varimax orthogonal rotation with Kaiser normalisation with eigenvalue greater than 1. This implies that factors with eigenvalues greater than 1 was considered and varimax orthogonal rotation was used to transform the matrix and decrease the no of variables loaded in each factor.

3.6 Summary of the Chapter

The methodology chapter outlines the systematic approach employed in the research, covering various aspects such as sampling methods, characterization techniques, and data evaluation procedures. For coal fly ash, samples were collected

UNIVERSITY of the WESTERN CAPE
http://etd.uwc.ac.za/

from Sasol Secunda power station's ash dam, specifically from three cores (S1, S2, and S3). Gold tailing samples were obtained from five boreholes drilled to a depth of 10.2m. Characterization techniques included mineralogical analysis using X-ray diffraction (XRD) and scanning electron microscopy (SEM) to understand morphological changes. Geochemical analyses involved utilizing ICP-OES, XRF, and Leco analysis for total sulfur and carbon content. Sequential extraction and statistical analyses, including correlation coefficient, hierarchical clustering, and factor analysis, were applied to interpret the data. Quality assurance and control (QA/QC) measures were implemented for precision and accuracy evaluation, ensuring the reliability of the analytical data. The comprehensive methodology ensures a robust foundation for the subsequent analyses and interpretations in the research.

UNIVERSITY of the
WESTERN CAPE

http://etd.uwc.ac.za/

CHAPTER FOUR

4. GEOCHEMICAL AND GEOSTATISTICAL CHARACTERISATION OF COAL FLY ASH

4.1 Introduction

This chapter discusses the coal fly ash results obtained in this study. The chapter encompasses the mineralogy, chemical composition, morphology and physical characteristics of Secunda fly ash core S1, S2, and S3 samples obtained from the Secunda ash dam. The analytical procedures and techniques applied include scanning electron microscopy (SEM), X-ray diffraction (XRD), X-ray fluorescence (XRF) and ICP OES. These sample were later subjected to sequential extraction procedure and analysed with ICP-OES.

4.2 Mineralogical Composition

The XRD technique was used to investigate the mineralogical composition of the Secunda fresh fly ash and the weathered Secunda fly ash core. The XRD patterns for the fresh Secunda ash and the weathered core S1, S2 and S3 samples are presented below.

From the XRD results (Figure 4.1), three prominent mineral phases quartz, mullite and lime were mainly detected in the fresh fly ash samples, however in the weathered fly ash samples, the three prominent mineral phases detected were quartz, mullite and calcite. For core S1 and S3, more minerals phases were observed as compared to core S2. Lime and calcite ($CaCO_3$) were detected but as minor peaks as well as minor phases of kaolinite ($Al_2(Si_2O_5)(OH)_4$) and nitratine ($NaNO_3$) were also detected. Nitratine is a tertiary mineral that may have produced by the interaction of brine with the coal fly ash or because of the drying procedure in the sample preparation before analysis. The kaolinite could have resulted from the alteration of the glass phase

http://etd.uwc.ac.za/

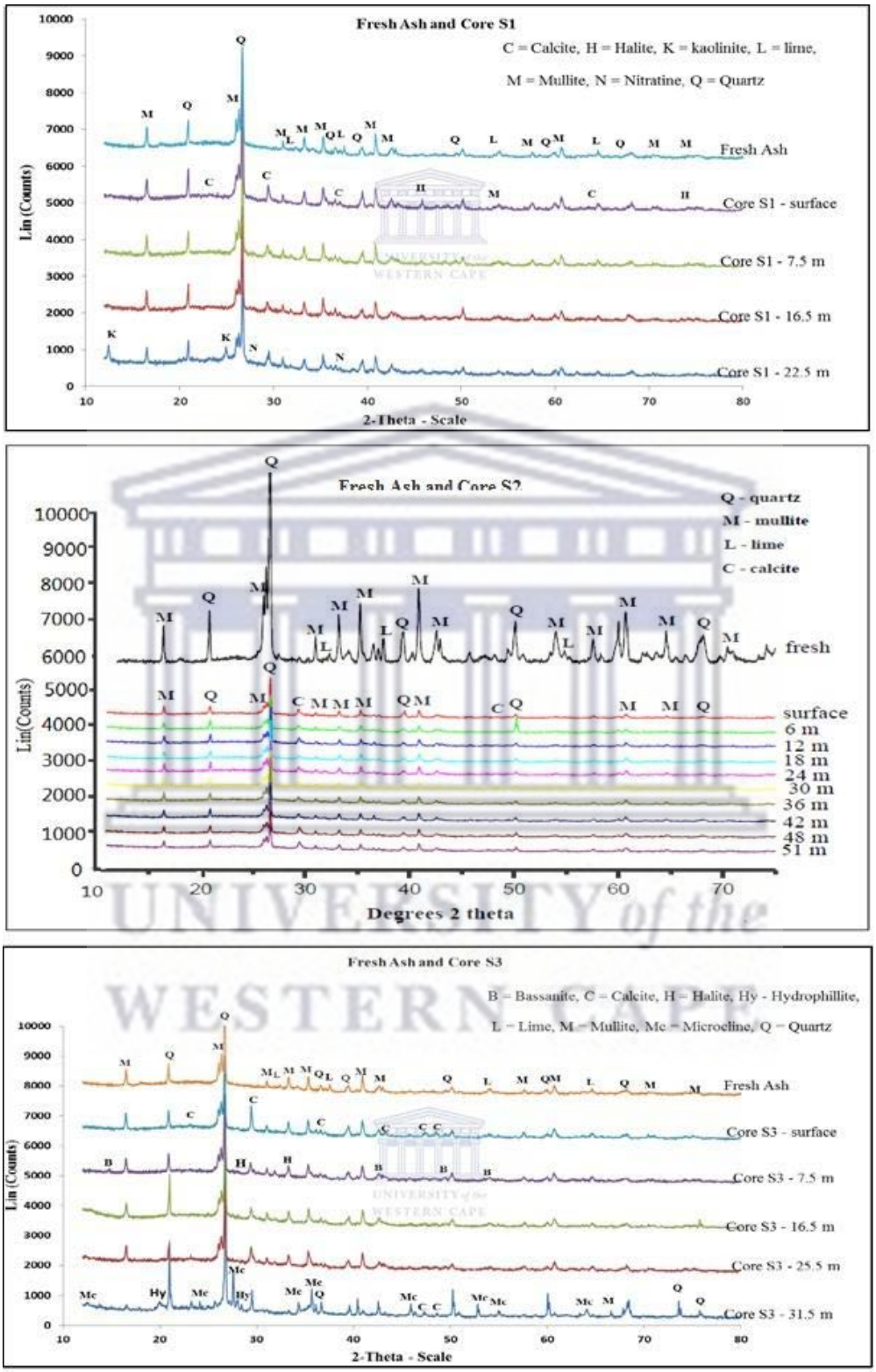

Figure 4.1: Coal fly ash XRD results

http://etd.uwc.ac.za/

or weathering of the ash in the dump (Ward et al., 2009). Halite, bassanite, nitratine, hydrophitte, microline and albite are relatively in low concentrations, and therefore considered as transient mineral produced because of interaction of brine with the coal fly ash. The XRD results revealed a similar trend from the topmost sample downhole to the bottom. According to mullite ($3Al_2O_32SiO_2$ or $Si_2Al_6O_{13}$) is produced when kaolinite [$Al_2Si_2O_5(OH)_4$] present in the parent coal goes through phase alteration under the high temperatures (1200 - 1400 °C) as presented in the equations below.

Formation of disordered metakaolin from kaolinite:

(a) $2Al_2Si_2O_5(OH)_4 \xrightarrow{Heat} 2Al_2Si_2O_7 + 4H_2O$ ..…9

(b) oxolation of the metakaolin into aluminium-silicon spinel

$2Al_2Si_2O_7 \xrightarrow{Heat} Si_3Al_4O_{12} + SiO_2$ …….10

(c) formation of mullite from aluminium-silicon spinel.

$3Si_3Al_4O_{12} \xrightarrow{Heat} 2\ Si_2Al_6O_{13} + 5SiO_2$ ..…11

Quartz (SiO_2) from parent coal endures the combustion conditions therefore, it is found unaffected in coal fly ash (Bandyopadhyay et al., 2010). The presence of lime (CaO) in the fresh fly ash could be from the thermal decomposition of calcite ($CaCO_3$) (Rausis, K et al., 2021) confined in the parent coal during coal combustion as shown in the equation below:

$CaCO_3(s) \xrightarrow{Heat} CaO(s) + CO_2(g)$ ……..12

Also, the calcite ($CaCO_3$) found in the weathered fly ash could be a result of the aqueous carbonation process involving reaction of fresh fly ash lime (CaO) with percolated CO_2 and water present in the ash dam (Nyambura et al., 2011) as shown in the equations below:

(a) Hydration of lime into calcium hydroxide suspension

$CaO + H_2O \rightarrow Ca(OH)_2$ …….13

(b) Carbonation of calcium hydroxide suspension to form calcite

$Ca(OH)_2 + CO_2 \rightarrow CaCO_3 + H_2O$ ……..14

http://etd.uwc.ac.za/

All the mineral phases detected by XRD paralleled to the significant levels of Si, Al and Ca found in the fresh fly ash and the weathered fly ash as reported by XRF analysis. While much lower concentrations of elements like Fe and Mg, for instance, may have made it challenging to be detected by XRD but a mineral phase associated with them such as hematite (Fe2O3) and enstatite (Mg2Si2O6). On the other hand, other mineral phases in the ash dam that were not detected by XRD, may be because they were in a transition/amorphous state, or found in very low thus below detectable levels.

In conclusion, it can be observed from the XRD analysis that the weathered fly ash samples obtained from the cores, in a wet ash handling system-encompassing disposal of the coal fly ash with brine as a slurry, did not display mineralogical inhomogeneity. However, it somewhat gave a constant trend from the top of the ash dam, down to the bottom of each core. The mineralogical constancy shown by XRD however probably points to the constraint of XRD as an analytical tool in that it can only detect comparatively copious crystalline mineral phases, and not identify amorphous material or minerals existing in low concentration.

4.3 Geochemical Characterization

This section presents a data geochemistry assessment of major and trace elements to illustrate the distribution of data across the selected elements. The data is described in Table 4.1in terms of the mean, range and standard deviation. The whole data geochemistry is available at APPENDIX A. The mean is estimated in arithmetic mean (A. mean) and geometric mean (Geo. mean)(Lopez-Sanchez, 2020) because the datasets are large and not normally distributed. The standard deviation values arrayed in this table denotes the degree of dispersion (variance distribution) as they reflect the activities of the investigated constituents in the evaluated environment (Lopez-Sanchez, 2020).

From the results given in Table 4.1, the concentration range of major elements observed are SiO_2 (32.87 – 58.86%), Al_2O_3 (11.87 – 25.70%), Fe_2O_3 (2.19 - 10.41%), CaO (6.15 – 11.24%), MgO (1.78 – 3.31%), Na_2O (2.18 – 3.17%), K_2O (0.75 – 4.41%), MnO (0.05 – 0.12%), TiO_2 (1.44 -2.12%), P2O5 (0.36 – 0.95%),

http://etd.uwc.ac.za/

SO_3 (0.01 – 0%) and the LOI (3.18 – 33.15%). Also, from the same dataset, the chemical analysis conducted determines the concentration of major oxides [SiO_2 (50.91 %), Al_2O_3 (25.49%), CaO (8.10 %), Fe_2O_3 (2.27%), MgO (1.87%), Na_2O (2.21 %), TiO2 (1.87 %), K_2O (0.95%), P_2O_5 (0.71%), SO3 (0.03%) and MnO (0.05 %) that are contained in the fresh Secunda fly ash samples APPENDIX A. On the other hand, further observation indicates that the concentration of the trace elements in the fresh Secunda ash samples were identified as Sr (4160 ppm), Ba (2749 ppm), Th (1922 ppm), Zr (664 ppm), Y (156 ppm), Ce (117 ppm), Nb (109 ppm), As (61 ppm), Co (32 ppm), Ni (23 ppm), Pb (28 ppm), Rb (16 ppm) and V (15 ppm)APPENDIX A. Note, all fresh samples show similar concentration, imply that values are approximately the same.

From the same table, the Geo. mean results for the concentration range of the major elements are given as SiO_2 (44.44 - 46.98 %), Al_2O_3 (22.34 -23.49%), CaO (8.1-8.98%), and LOI (7.91- 10.1%). These estimates accounted for about 82.79 – 89.4% of all the samples estimated. For the trace element, observation shows that the concentrations of Ni, Nb, Cu, Co, Ce, Ba, Th, Zr, Y, V, Sr, Rb and Pb have maximum values of 60.55 ppm, 169.40 ppm, 3758.71 ppm, 51.19 ppm, 248.08 ppm, 3476.33 ppm, 2718.17 ppm, 832.81 ppm, 205.14 ppm, 121.50 ppm, 5742.02 ppm, 134.54 ppm and 48.08 ppm, respectively. And the maximum concentration of As in all dried cores exceeded 100 ppm.

Considering the results of the analysis of each sample collected from the drilled Secunda ash core, the geometric mean concentrations of the major elements in the S1 sample were identified as SiO_2 (44.44%), Al_2O_3 (23.49 %), CaO (8.10 %), Fe_2O_3 (3.48%), MgO (2.43%), Na_2O (2.47%), TiO_2 (1.72%), K_2O (0.97 %), P_2O_5 (0.68%), SO_3 (0.09 %) and MnO (0.06 %). The geometric mean concentrations of the trace elements were determined as Sr (4382.46 ppm), Ba (2667.46 ppm), Th (2036.73 ppm), Zr (666.21 ppm), Y (164.44 ppm), Ce (180.64 ppm), Nb (123.01 ppm), As (78.61 ppm), Co (31.28 ppm), Ni (28.62 ppm), Pb, (36.28 ppm), V (67.18 ppm) and Rb (12.96 ppm).

UNIVERSITY of the WESTERN CAPE
http://etd.uwc.ac.za/

Similarly, samples collected from S2, a second drilled Secunda ash core, was analysed to obtain the geometric mean concentrations of the major elements and trace elements. The geometric mean concentrations of the major elements in the S2 samples were identified as SiO_2 (46.98 %), Al_2O_3 (22.98%), CaO (8.94%), Fe_2O_3 (3.37%), MgO (2.77%), Na_2O (2.70%), TiO_2 (1.92 %), K_2O (1.14%), P_2O_5 (0.79%), SO_3 (0.09 %) and MnO (0.07 %). In addition, the geometric mean concentrations of the trace elements in the samples were determined as Sr (4991.90 ppm), Ba (3055.83 ppm), Th (2343.95 ppm), Zr (736.21 ppm), Y (176.06 ppm), Ce (203.69 ppm), Nb (143.01 ppm), As (83.96 ppm), Co (32.87 ppm), Ni (30.19 ppm), Pb, (33.16 ppm), V (64.31 ppm) and Rb (16.19 ppm).

The last of the three drilled Secunda ash core samples, S3, was also analysed to derive the geometric mean concentrations of both major elements and trace elements. The geometric mean concentrations of the major elements in the S3 samples were identified as SiO_2 (46.68 %), Al_2O_3 (22.34 %), CaO (8.89 %), Fe_2O_3 (3.55 %), MgO (2.77 %), Na_2O (2.72 %), TiO_2 (1.89 %), K_2O (1.19 %), P_2O_5 (0.76 %), SO_3 (0.09 %) and MnO (0.07 %). Also, the geometric mean concentrations of the trace elements in the samples were determined as Sr (4638.50 ppm), Ba (2976.98 ppm), Th (2158.69 ppm), Zr (704.36 ppm), Y (164.81 ppm), Ce (198.78 ppm), Nb (133.49 ppm), As (85.86 ppm), Co (32.61 ppm), Ni (31.13 ppm), Pb (33.64 ppm), V (62.94 ppm) and Rb (16.32 ppm).

Relatively, further observation indicates that the mean concentrations of some major elements in the fresh Secunda fly ash are higher than the concentration in all the drilled Secunda ash cores S1, S2 and S3 as illustrated in Table 4.1. For example, the mean concentration of Si (50.91%) and Al (25.49%), as reported as oxides, in the fresh Secunda fly ash are higher than the mean concentrations generated for Si and Al in drilled Secunda ash cores S1, S2 and S3. Thus, the decrease in Si concentrations in core samples of S1(12.71%), S2 (7.72%) and S3 (8.31), respectively, which causes leaching of Si from the core samples as time passes (Parbhakar-Fox et al., 2013; Parbhakar-Fox & Lottermoser, 2015; Vaziri et al., 2022). Equally, related cause is applicable to the decrease in Al

http://etd.uwc.ac.za/

Table 4.1: Summary data for coal fly ash geochemical data

BHID	Major Element (%)											
	S1				S2				S3			
	Max	Min	A. mean	Geo_mean	Max	Min	A. mean	Geo_mean	Max	Min	A. mean	Geo_mean
SiO_2	50.91	32.87	43.93	44.44	58.86	41.44	47.08	46.98	**58.86**	40.65	46.80	46.68
Al_2O_3	25.57	17.58	23.21	23.49	25.70	11.87	23.04	22.98	25.70	11.87	22.57	22.34
CaO	9.87	6.15	8.07	8.10	11.24	6.69	8.98	8.94	11.24	6.69	8.94	8.89
Fe_2O_3	6.60	2.27	3.58	3.48	10.41	2.19	3.61	3.37	10.41	2.19	3.83	3.55
Na_2O	2.70	2.18	2.45	2.47	3.16	2.21	2.71	2.70	3.17	2.21	2.73	2.72
MgO	2.88	1.78	2.41	2.43	3.31	1.87	2.79	2.77	3.31	1.87	2.79	2.77
TiO_2	1.87	1.44	1.70	1.72	2.12	1.51	1.92	1.92	2.12	1.51	1.90	1.89
K_2O	1.08	0.75	0.97	0.97	1.39	0.88	1.15	1.14	4.41	0.88	1.28	1.19
P_2O_5	0.82	0.52	0.67	0.68	0.95	0.36	0.79	0.79	0.95	0.36	0.77	0.76
MnO	0.08	0.05	0.06	0.06	0.10	0.05	0.07	0.07	0.12	0.05	0.08	0.07
SO_3	0.12	0.03	0.10	0.09	0.12	0.03	0.09	0.09	0.12	0.03	0.09	0.09
%S	0.05	0.01	0.04	0.04	0.05	0.01	0.04	0.04	0.05	0.01	0.04	0.03
LOI	33.15	4.78	12.91	10.10	10.34	3.18	8.27	8.14	10.90	3.18	8.16	7.91
Total	**100.76**	**99.94**	**100.07**	**100.02**	**100.00**	**99.84**	**99.94**	**99.94**	**100.00**	**99.84**	**99.94**	**99.94**
BHID	**Trace Element (ppm)**											
	S1				S2				S3			
As	184.81	49.10	88.86	78.61	111.66	60.78	84.94	83.96	152.90	60.78	87.56	85.86
Ba	3059.38	2088.80	2686.00	2667.46	3476.33	1674.09	3063.38	3055.83	3476.33	1674.09	3002.72	2976.98
Ce	242.86	146.13	183.83	180.64	248.08	141.82	205.33	203.69	248.08	141.82	200.90	198.78
Co	49.99	20.20	32.84	31.28	51.19	23.34	33.49	32.87	51.19	18.28	33.51	32.61
Cu	3513.14	3115.86	3327.54	3316.28	3758.71	3046.69	3472.26	3469.08	N/A	N/A	N/A	N/A
Pb	48.08	26.49	36.14	36.28	44.62	23.82	33.63	33.16	46.92	23.82	34.16	33.64
Rb	36.13	4.34	16.25	12.96	33.01	1.69	18.96	16.19	134.54	1.69	24.45	16.32
Sr	4933.25	3352.11	4437.93	4382.46	5742.02	919.48	5011.04	4991.90	5742.02	919.48	4832.96	4638.50
V	110.49	15.20	72.68	67.18	121.50	15.20	69.76	64.31	121.50	15.20	68.68	62.94
Y	173.39	150.18	164.91	164.44	205.14	38.70	176.61	176.06	205.14	38.70	170.56	164.81
Zr	713.34	581.99	666.93	666.21	832.81	265.87	737.72	736.21	832.81	265.87	717.18	704.36
Th	2314.21	1527.17	2065.49	2036.73	2718.17	351.08	2354.55	2343.95	2718.17	351.08	2267.47	2158.69
Nb	148.52	103.51	125.22	123.01	169.40	26.75	144.07	143.01	169.40	26.75	139.52	133.49
Ni	35.45	22.57	28.78	28.62	39.30	22.57	30.46	30.19	60.55	22.57	31.77	31.13

http://etd.uwc.ac.za/

On the contrary, the concentrations of Mn, Fe, Na, Mg and S were higher in Secunda core samples compared to the fresh Secunda fly ash samples.

The overall increase in the concentrations of Na (10.53 % in core S1, 18.15 % in S2 and 18.75 % in core S3); Mg (23,05 % in core S1, 32.49 9 in S2 and 32.49 % in core S3) and S (66.67 % in core S1, 66.67 % in S2 and 66.67 % in core S3) in the drilled Secunda ash core sample compared to the fresh Secunda fly ash could be as a result of its contact with brine, while the increase in the concentration of Fe (53.30 % in core S1, 48.46 % in S2 and 56.39 % in core S3) could be attributed to the disposal of the spent Fe-catalyst on the ash dump where the drilled core samples were collected (Eze et al. 2013). Nyamhingura (2009) reported high concentrations of Na, Cl, Ca, K and Mg in brine samples collected from the Secunda power stations. Therefore, the slight overall increase in the concentrations of these species in the drilled core samples could be attributed to the coal fly ash and brine interaction at the dump. Although considering the high volumes of brine disposed over 20 years of operation, one would have expected higher salt content than what was found.

The loss on ignition (LOI), which indicates unburned carbon or organic content was 4.78 %, 10.10 %, 8.14 % and 8.32 % for the fresh ash, drilled ash cores S1, S2 and S3, respectively. The high LOI values for the drilled ash cores could indicate high hydrocarbon content in the ash dump because of co-disposal practices, involving the disposal of both hydrocarbon wastes and brine stream on the ash.

4.3.1 Coal fly ash classification

The sum of the mean values of SiO_2, Al_2O_3 and Fe_2O_3 was 78.67 %, 71.41 %, 73.33 and 72.57 % for the fresh fly ash, core S1, S2 and S3, respectively (Table 4.1). Thus, the fresh fly ash and drilled cores (S1, S2 and S3) can be classified as Class F. According to the American Society for Testing and Materials (ASTM C 618-92a), coal fly ash can be classified as class F or C based on the sum of the oxides of aluminium, silicon and iron in the coal fly ash. Class F fly ash are characterised by (i) the sum of SiO_2, Al_2O_3, Fe_2O_3 >70 %, (ii) SO_3 <5 %, (iii) moisture content

http://etd.uwc.ac.za/

Table 4.2: Correlation analysis of the coal fly ash whole data

	SiO_2	Al_2O_3	CaO	Fe_2O_3	Na2O	MgO	TiO_2	K_2O	P_2O_5	MnO	%S	LOI	As	Ba	Ce	Co	Nb	Ni	Pb	Sr	V	Y	Zr	Th
SiO_2	1																							
Al_2O_3	-0.085	1																						
CaO	-0.129	0.091	1																					
Fe_2O_3	-0.066	**-.401****	-0.082	1																				
Na_2O	.319*	**-.502****	.485**	0.039	1																			
MgO	.295*	-0.174	.448**	-0.046	.738**	1																		
TiO_2	0.181	0.155	.698**	-.404**	.585**	.665**	1																	
K_2O	**.625****	**-.723****	**-.344****	.322*	**.422****	0.184	-0.237	1																
P_2O_5	-0.152	.413**	.744**	**-.465****	**.333****	**.533****	.837**	-.556**	1															
MnO	0.221	-.705**	.264*	.605**	.672**	.521**	0.026	.638**	-0.162	1														
%S	**-.513****	0.154	0.224	-0.07	0.169	0.139	0.177	-.375**	.332**	-0.083	1													
LOI	-.846**	-.258*	-0.196	-0.049	-.298*	-.407**	-.365**	-.284*	-0.157	-0.203	.320*	1												
As	-.323*	-.786**	-0.212	.343**	0.136	-0.108	-.359**	.449**	-.427**	.433**	-0.039	.606**	1											
Ba	-.292*	.335**	.657**	-.503**	.287*	.424**	.769**	-.547**	.942**	-0.235	.399**	0.048	-0.239	1										
Ce	**-.456****	-0.175	.527**	0.145	.276*	0.193	.444**	-.317*	.448**	0.161	0.197	.293*	.259*	.479**	1									
Co	0.149	-.497**	-0.204	0.095	0.2	0.047	-0.112	.409**	-0.214	.262*	-0.23	0.112	.339**	-0.189	0.106	1								
Nb	**-.450****	.369**	.515**	-.518**	0.167	.318*	.679**	-.663**	.846**	-.350**	.462**	0.228	-0.18	.922**	.562**	-0.196	1							
Ni	.342**	-.775**	-0.002	.311*	.659**	.389**	-0.1	.794**	-.304*	.801**	-0.137	-0.108	.541**	-.305*	-0.02	.315*	-.380**	1						
Pb	.324*	-0.175	-0.19	-0.037	.369**	0.179	-0.018	.390**	-0.122	0.197	0.123	-0.199	-0.046	-0.172	-0.248	.391**	-0.194	.354**	1					
Sr	-.573**	.416**	.639**	-.347**	0.087	0.213	.605**	-.767**	.846**	-.301*	.490**	0.248	-0.195	.893**	.637**	-0.252	.934**	-.448**	-.300*	1				
V	-0.18	0.168	-0.15	-0.202	0.157	0.112	0.22	-0.207	0.18	-.261*	.459**	0.146	-0.079	.259*	0.003	-0.074	.429**	-0.168	0.217	.302*	1			
Y	**-.513****	**.503****	.584**	-.491**	0.041	0.219	.636**	-.836**	.853**	-.421**	.475**	0.219	-.342**	.865**	.532**	-.262*	.929**	-.545**	-.258*	.957**	.324*	1		
Zr	**-.477****	**.430****	.699**	-.361**	0.113	.279*	.706**	-.782**	.880**	-.287*	.428**	0.144	-.318*	.878**	.622**	-.300*	.899**	-.501**	-.340**	.961**	0.243	.966**	1	
Th	**-.564****	**.407****	.640**	-.360**	0.104	0.226	.615**	-.756**	.851**	-.296*	.490**	0.246	-0.19	.899**	.636**	-0.245	.940**	-.435**	-.289*	1.000**	.310*	.957**	.959**	1

UNIVERSITY of the
WESTERN CAPE

http://etd.uwc.ac.za/

<3% and (iv) loss on ignition (LOI) <6 %. (v) CaO <20 %. The fresh fly ash contained 8.95 % CaO while cores S1, S2 and S3 contained 8.10 %, 8.94 and 8.89 % CaO, respectively. These values of CaO are in the midrange among Class F fly ashes that usually have low calcium content (Vassilev & Vassileva, 2007; Vassilev & Vassileva, 2009).

Apart from the ASTM classification which showed that the coal fly ash is class F, the fresh fly ash and drilled cores can be classified as silico-aluminate ash based on the SiO_2/Al_2O_3 ratio. The fresh fly ash and drilled cores (S1, S2 and S3) samples have SiO_2/Al_2O_3 ratios of 2.0, 1.89, 2.04 and 2.09 respectively (Table 4.3). According to the United Nations subcommittee of Fly Ash Utilization, coal fly ash is classified as silico-aluminate fly ash when the SiO_2/Al_2O ratio is $\geq$ 2 and CaO content is < 15 % (Vassilev & Vassileva, 2007; Vassilev & Vassileva, 2009).

There are seven main categories of coal fly ash namely; sialic, ferric, calcic, ferrocalsialic, ferrosialic, calsialic and ferrocalsic based on a taxonomic system recommended by (Roy & Griffin, 1982)

4.3.1.1 Correlation Analysis

The correlation data reported below is based on 99% Confidence Interval (*. *Correlation is significant at the 0.05 level (2-tailed). **. Correlation is significant at the 0.01 level (2-tailed))*. As Table 4.2 shows, the concentration of SiO_2 was negatively correlated with S, LOI, Ce, Nb, Sr, Y, Zr and Th at a confidence level of 99%, whereas the concentration of SiO_2 was positively correlated to the concentration of Ni. It means that the concentrations of S, Ce, Nb, Sr, Y, Zr and Th as well as the LOI decrease as the concentration of SiO_2 increases, while the reverse is true in relation to Ni. The concentration of Al_2O_3 was negatively correlated with Fe_2O_3, Na_2O, K_2O, MnO, As, Co and Ni, but the concentration of Al_2O_3 was positively correlated to the concentrations of P_2O_5, Ba, Sr, Y, Zr and Th. It suggests that the concentrations of Fe_2O_3, Na_2O, K_2O, MnO, As, Co and Ni decrease as the concentration of Al_2O_3 increases, whereas the concentrations of P_2O_5, Ba, Sr, Y, Zr and Th increase with Al_2O_3.

http://etd.uwc.ac.za/

The concentration of CaO was negatively correlated with only the concentration of K_2O, whereas the concentration of CaO was positively correlated to the concentrations of Na_2O, MgO, TiO_2, P_2O_5, Ba, Ce, Nb, Sr, Y, Zr and Th. This shows that the concentration of K_2O decreases as the concentration of CaO increases, while the opposite holds in relation to Na_2O, MgO, TiO_2, P_2O_5, Ba, Ce, Nb, Sr, Y, Zr and Th. The concentration of Fe_2O_3 was negatively correlated with only the concentration of Al_2O_3, TiO_2, P_2O_5, Ba, Nb, Sr, and Y, whereas the concentration of Fe_2O_3 was positively correlated to the concentration of MnO and As. This reveals that the concentrations of Al_2O_3, TiO_2, P_2O_5, Ba, Nb, Sr, and Y decrease as the concentration of Fe_2O_3 increases, while the concentrations of MnO and As increase with Fe_2O_3.

The concentration of Na_2O was negatively correlated with the concentration of Al_2O_3 and the LOI, whereas the concentration of Na_2O was positively correlated to the concentrations of MgO, TiO_2, MnO, Ni and Pb. It indicates that the concentrations of Al_2O_3 and the LOI decrease as the concentration of Na_2O increases, while the reverse is true in relation to MgO, TiO_2, MnO, Ni and Pb. The concentration of MgO was negatively correlated with only the LOI, whereas the concentration of MgO was positively correlated to the concentrations of CaO, TiO_2, P_2O_5, MnO, Ba and Ni. It means that the LOI decreases as the concentration of MgO increases, while the reverse is true in relation to CaO, TiO_2, P_2O_5, MnO, Ba and Ni.

The concentration of TiO_2 was negatively correlated with the concentrations of Fe_2O_3, As and the LOI, whereas the concentration of TiO2 was positively correlated to the concentrations of CaO, Na_2O, MgO, P_2O_5, Ba, Ce, Nb, Sr, Y, Zr and Th. It means that the concentrations of Fe_2O_3, As and the LOI decrease as the concentration of TiO_2 increases, while the reverse is true in relation to CaO, Na_2O, MgO, P_2O_5, Ba, Ce, Nb, Sr, Y, Zr and Th. The concentration of K_2O was negatively correlated with the concentrations of Al_2O_3, CaO, P_2O_5, S, Ba, Nb, Sr, Y, Zr and Th, whereas the concentration of TiO_2 was positively correlated to the concentrations of Na_2O, MnO, As, Co, Ni and Pb. It means that the concentrations of Al_2O_3, CaO, P_2O_5, S, Ba, Nb, Sr, Y, Zr and Th decrease as the concentration of

UNIVERSITY of the WESTERN CAPE
http://etd.uwc.ac.za/

K_2O increases, while the reverse is true in relation to Na_2O, MnO, As, Co, Ni and Pb.

The concentration of P_2O_5 was negatively correlated with the concentrations of Fe_2O_3, K_2O and As, whereas the concentration of P_2O_5 was positively correlated to the concentrations of Al_2O_3, CaO, Na_2O, MgO, TiO_2, S, Ba, Ce, Nb, Sr, Y, Zr and Th. It means that the concentrations of Fe_2O_3, K_2O and As decrease as the concentration of P_2O_5 increases, while the reverse is true in relation to Al_2O_3, CaO, Na_2O, MgO, TiO_2, S, Ba, Ce, Nb, Sr, Y, Zr and Th. The concentration of MnO was negatively correlated with the concentrations of Al_2O_3, Nb and Y, whereas the concentration of MnO was positively correlated to the concentrations of Fe_2O_3, Na_2O, MgO, K_2O, As and Ni. It means that the concentrations of Al_2O_3, Nb and Y decrease as the concentration of MnO increases, while the reverse is true in relation to Fe_2O_3, Na_2O, MgO, K_2O, As and Ni.

The concentration of S was negatively correlated with the concentrations of SiO_2 and K_2O, whereas the concentration of S was positively correlated to the concentrations of P_2O_5, Sr, V, Y, Zr and Th. It means that the concentrations of SiO_2 and K_2O decrease as the concentration of S increases, while the reverse is true in relation to P_2O_5, Sr, V, Y, Zr and Th. The LOI was negatively correlated with the concentrations of SiO_2, MgO and TiO_2, whereas the LOI was positively correlated to the concentrations of As. It means that the concentrations of SiO_2, MgO and TiO_2 decrease as the concentration of S increases, while the reverse is true in relation to As.

The concentration of As was negatively correlated with the concentrations of Al_2O_3, TiO_2, P_2O_5 and Y, whereas the As was positively correlated to the concentrations of Fe_2O_3, K_2O, MnO, LOI, Co and Ni. It means that the concentrations of SiO_2, MgO and TiO_2 decrease as the concentration of S increases, while the reverse is true in relation to Fe_2O_3, K_2O, MnO, LOI, Co and Ni. The concentration of Ba was negatively correlated with the concentrations of Fe_2O_3, whereas the As was positively correlated to the concentrations of Al_2O_3, CaO, MgO, TiO_2, P_2O_5, S, Ce, Nb, Sr, Y, Zr and Th. It means that the concentration of Fe_2O_3 decreases as the

http://etd.uwc.ac.za/

concentration of S increases, while the reverse is true in relation to Al_2O_3, CaO, MgO, TiO_2, P_2O_5, S, Ce, Nb, Sr, Y, Zr and Th.

The concentration of Ce was negatively correlated with the concentrations of SiO_2, whereas the As was positively correlated to the concentrations of CaO, TiO_2, P_2O_5, Ba, Nb, Sr, Y, Zr and Th. It means that the concentration of SiO_2 decreases as the concentration of Ce increases, while the reverse is true in relation to CaO, TiO_2, P_2O_5, Ba, Nb, Sr, Y, Zr and Th. The concentration of Co was negatively correlated with the concentrations of Al_2O_3. It means that the concentration of Al_2O_3 decreases as the concentration of Co increases. The concentration of Nb was negatively correlated with the concentrations of SiO_2, Fe_2O_3, K_2O, MnO and Ni, whereas the As was positively correlated to the concentrations of Al_2O_3, CaO, TiO_2, P_2O_5, S, Ba, Ce, Sr, V, Y, Zr and Th. It means that the concentrations of SiO_2, Fe_2O_3, K_2O, MnO and Ni decrease as the concentration of Nb increases, while the reverse is true in relation to Al_2O_3, CaO, TiO_2, P_2O_5, S, Ba, Ce, Sr, V, Y, Zr and Th.

The concentration of Ni was negatively correlated with the concentrations of Al_2O_3, Nb, Sr, Y, Zr and Th, whereas As was positively correlated to the concentrations of SiO_2, Na_2O, MgO, K_2O, MnO, As and Pb. It means that the concentrations of Al_2O_3, Nb, Sr, Y, Zr and Th decrease as the concentration of Nb increases, while the reverse is true in relation to SiO_2, Na_2O, MgO, K_2O, MnO, As and Pb. The concentration of Pb was negatively correlated with the concentrations of Zr, whereas the Pb was positively correlated to the concentrations of Na_2O, K_2O, Co and Ni. It means that the concentration of Zr decreases as the concentration of Pb increases, while the reverse is true in relation to Na_2O, K_2O, Co and Ni. The concentration of Sr was negatively correlated with the concentrations of SiO_2, Fe_2O_3, K_2O and Ni, whereas the Sr was positively correlated to the concentrations of Al_2O_3, CaO, TiO_2, P_2O_5, S, Ba, Ce, Nb, Y, Zr and Th. It means that the concentrations of SiO_2, Fe_2O_3, K_2O and Ni decrease as the concentration of Sr increases, while the reverse is true in relation to Al_2O_3, CaO, TiO_2, P_2O_5, S, Ba, Ce, Nb, Y, Zr and Th.

http://etd.uwc.ac.za/

The concentration of Y was negatively correlated with the concentrations of SiO_2, Fe_2O_3, K_2O, MnO, As and Ni, whereas the Y was positively correlated to the concentrations of Al_2O_3, CaO, TiO_2, P_2O_5, S, Ba, Ce, Nb, Sr, Zr and Th. It means that the concentrations of SiO_2, Fe_2O_3, K_2O, MnO, As and Ni decrease as the concentration of Y increases, while the reverse is true in relation to Al_2O_3, CaO, TiO_2, P_2O_5, S, Ba, Ce, Nb, Sr, Zr and Th. The concentration of Zr was negatively correlated with the concentrations of SiO_2, Fe_2O_3, K_2O, Ni and Pb, whereas the Zr was positively correlated to the concentrations of Al_2O_3, CaO, TiO_2, P_2O_5, S, Ba, Ce, Nb, Sr, Y and Th. It means that the concentrations of SiO_2, Fe_2O_3, K_2O, Ni and Pb decrease as the concentration of Zr increases, while the reverse is true in relation to Al_2O_3, CaO, TiO_2, P_2O_5, S, Ba, Ce, Nb, Sr, Y and Th. The concentration of Th was negatively correlated with the concentrations of SiO_2, Fe_2O_3, K_2O and Ni, whereas the Th was positively correlated to the concentrations of Al_2O_3, CaO, TiO_2, P_2O_5, S, Ba, Ce, Nb, Sr, Y and Zr. It means that the concentrations of SiO_2, Fe_2O_3, K_2O and Ni decrease as the concentration of Th increases, while the reverse is true in relation to Al_2O_3, CaO, TiO_2, P_2O_5, S, Ba, Ce, Nb, Sr, Y and Zr. V was positively correlated with both S and Nb.

4.4 Sequential Extraction Results

4.4.1 Cluster Analysis of the Sequential Extraction Results

This section presents the sequential extraction results derived from the cluster analysis performed on the coal fly ash data as illustrated in Table 4.3 below. The hierarchical clustering analyses produced for water fraction, carbonate fraction and hydroxylamine fraction are represented on dendrogram (Figure 4.2, Figure 4.3 and Figure 4.4). The water-leach was classified into two main clusters and six sub clusters, and carbonate fraction was classified into two main clusters and five sub clusters, while hydroxylamine fraction was classified into two main clusters and seven sub clusters. The two major clusters of the coal fly ash samples are characterised by their variable contents in SiO_2, Fe_2O_3, CaO, LOI and Al_2O_3.

http://etd.uwc.ac.za/

Table 4.3: Tabularised illustration of water fraction, carbonate fraction and hydroxylamine fraction clusters for elements in coal fly ash

Elements	Water Fraction						Carbonate Fraction					Hydroxylamine Fraction						
	WF1	**WF2**	**WF3**	**WF4**	**WF5**	**WF6**	**CF1**	**CF2**	**CF3**	**CF4**	**CF5**	**HF1**	**HF2**	**HF3**	**HF4**	**HF5**	**HF6**	**HF7**
Si (ppm)	1484.98	3900.61	1935.31	172.03	1048.68	3441.19	14725.97	15488.47	6225.60	24666.83	9232.50	14571.82	20313.19	1574.30	9276.55	19633.49	30034.39	7844.30
Al (ppm)	475.10	620.60	312.61	239.62	258.46	333.55	10558.18	3128.40	2890.46	4712.16	7715.14	8548.97	5297.03	398.52	4171.17	12952.25	11756.01	9288.61
Ca (ppm)	935.56	537.89	447.86	1031.40	2705.71	1980.07	2278.39	2374.41	1683.20	2868.56	1942.11	1843.97	2706.74	3967.00	1713.53	3100.37	1852.19	1035.00
Fe (ppm)	6.93	31.90	10.15	14.33	17.66	20.68	223.99	68.84	82.77	75.99	152.85	2239.38	3273.55	1139.36	3558.09	4946.79	4862.71	1181.61
Na (ppm)	1599.07	1095.01	1084.67	554.82	1542.47	1046.44	179.73	141.01	159.74	254.00	196.01	271.67	186.28	112.89	373.57	144.05	849.13	50.67
K (ppm)	438.27	500.96	81.13	72.80	576.31	422.86	106.06	49.20	74.11	101.89	89.43	86.64	173.86	246.68	107.74	35.54	162.24	45.53
Mg (ppm)	20.80	43.14	155.56	21.21	17.97	23.19	277.47	296.22	349.22	318.74	311.19	747.27	691.00	26.94	748.55	824.04	705.39	669.63
Sr (ppm)	50.62	70.58	40.18	106.51	35.65	64.36	244.99	175.84	290.14	463.44	293.20	228.15	325.18	411.23	263.33	205.26	323.56	112.45
Ba (ppm)	6.88	11.33	4.14	31.23	3.01	8.31	219.68	160.02	236.67	463.90	260.19	102.61	170.31	220.55	89.36	112.61	123.91	53.73
Mn (ppm)	0.76	0.01	0.74	0.16	0.13	0.74	24.24	11.80	12.91	11.71	23.84	69.22	110.88	7.44	90.96	97.37	76.92	26.08
As (ppm)	1.02	10.39	0.77	0.97	2.40	22.60	1.56	1.90	3.71	1.65	0.26	1.48	1.00	1.13	1.39	0.89	1.38	1.69
Pb (ppm)	1.17	6.91	0.20	0.28	2.21	2.56	1.59	1.37	0.80	0.13	1.23	0.27	0.58	0.17	1.26	0.19	0.37	0.08
Zn (ppm)	1.14	0.92	0.18	0.97	2.88	0.45	0.38	0.25	0.45	0.68	0.96	1.14	1.36	1.68	0.41	0.51	0.02	1.65
Ni (ppm)	0.24	0.79	0.05	0.21	0.01	1.32	0.63	1.25	0.77	1.23	0.46	0.91	1.09	0.99	0.50	0.72	0.74	0.59
Mo (ppm)	0.49	0.22	0.03	0.08	0.20	0.03	1.57	0.24	0.36	0.99	0.78	1.31	0.45	0.26	0.22	0.49	0.14	1.67
Cu (ppm)	0.33	0.24	0.06	0.10	0.96	0.17	0.36	0.11	0.22	0.28	0.30	0.30	0.48	0.76	0.36	0.12	0.29	0.14
Cr (ppm)	0.19	0.40	0.13	0.13	0.25	0.56	0.46	0.68	0.70	0.63	0.34	0.47	0.14	0.02	0.33	0.40	0.28	0.38

http://etd.uwc.ac.za/

4.4.2 Water Fraction for Coal Fly Ash

The sequential extraction results of the water leach for coal fly ash are contained in the first section of Table 4.3. Observation indicates that elements such as Si, Al, Ca, Na and K showed high concentrations in water leach, while Fe, Mg, Sr and other elements demonstrated low concentrations. From the results, Si leaching ranges approximately from 172 ppm – 3000 ppm, with Al leaching ranges approximately from 230 ppm and 630 ppm and Fe leaching ranges approximately from 6 ppm – 32 ppm.

As part of the observations, concentrations of elements in the increasing pattern of sub-clusters were denoted to reveal the quantity of elemental concentrations in different samples water leached. In the table, it is observed that the concentration of Si followed an increasing value pattern for sub-cluster 4> 5> 1> 3> 6> 2, with Al and Ca concentrations following increasing value patterns for sub-cluster 4> 5> 3> 6> 1> 2 and 3> 2> 1> 4> 6> 5, respectively. Further observation indicates that elements such as Si, Al, Na and K, with high concentrations in water leaching exhibited lowest concentration at sub-cluster 4 except Ca whereas elements such as Mg and Sr, with low concentrations in water leach exhibited lowest concentration at sub-cluster 5 unlike Fe with lowest concentration at sub-cluster 1. Despite this observation, it is noted that none of these elements exhibited similar concentration characters in each subgroup while conducting extraction process in an aqueous matrix.

UNIVERSITY of the
WESTERN CAPE

4.4.3 Carbonate Fraction for Coal Fly Ash

The second section of Table 4.3 contains the sequential extraction results for carbonate fraction for coal fly ash. The section of the table displays array of five sub-clustering results relative to the concentration of different elements within samples. Similar to water fraction, it is noted that elements such as Si, Al, Ca demonstrated high concentrations, but Na and K have low concentrations along with other elements like Fe, Mg, Sr, etc. Although, there are some elements with lower concentrations in each sub-cluster. From the results, leaching ranges for Si, Al and Ca appeared greater than in water fraction. Si leaching ranges approximately

http://etd.uwc.ac.za/

from 6000 ppm – 24700 ppm, with Al leaching ranges approximately from 2700 ppm – 10600 ppm and Fe leaching ranges approximately from 70 ppm – 230 ppm. Low concentration elements in the carbonate fraction have no significant impact in neutralising the acidity caused by some elements with higher concentrations.

The concentrations of elements in carbonate fraction were also discussed in terms of the increasing pattern of sub-clusters as conducted for water fraction. The process established that the concentration of Si, as the element with largest leaching ranges, followed an increasing value pattern for sub-cluster 3> 5> 1> 2> 4, with Al and Ca concentrations following increasing value pattern for sub-cluster 3> 2> 4> 5> 1 and 3> 5> 1> 2> 4, respectively. Unlike in water fraction, elements with high concentrations in carbonate fraction exhibited lowest concentration at sub-cluster 3. Fe indicated lowest concentration at sub-cluster 2 and highest concentration at sub-cluster 1, with Mg indicating lowest concentration at sub-cluster 1 and highest concentration at sub-cluster 3. Unlike these two elements, Sr, Na and Br equally demonstrated lowest concentration at sub-cluster 2 and highest concentration at sub-cluster 4, which indicates that they have similar concentration characteristics in each subgroup during extraction process in an aqueous matrix.

4.4.4 Hydroxylamine (FeMn) Fraction for Coal Fly Ash

The last section of Table 4.3 presents the sequential extraction results for hydroxylamine fraction for coal fly ash. This section arrays seven sub-cluster results containing the concentration of different elements in samples. Elements such as Si, Al, Ca and Fe demonstrated high concentrations in hydroxylamine fraction, whereas other listed elements in the table indicated low concentrations. Elements with higher leaching concentration such as Si ranges approximately from 1500 ppm – 30100 ppm, with Al leaching ranges approximately from 380 ppm – 13000 ppm, followed by Ca leaching ranges from 1000 ppm – 4000 ppm and Fe leaching ranges from 1100 ppm – 5000 ppm. Unlike water leaching and carbonate fractions, the concentration of Fe in the hydroxylamine fraction is higher in quantity.

In addition, the concentration increasing value patterns for the elements were carefully observed. Results indicate that Si concentration follows an increasing

http://etd.uwc.ac.za/

value pattern for sub-cluster 3> 7> 4> 1> 5> 2> 6, while Al concentration follows an increasing value pattern for sub-cluster 3> 4> 2> 1> 7> 6> 5, Ca concentration follows an increasing value pattern for sub-cluster 7> 4> 1> 6> 2> 5> 3 and Fe concentration follows an increasing value pattern for sub-cluster 3> 7> 1> 2> 4> 6> 5. From the pattern, observation specifies that Si, Al and Fe indicated lowest concentration at sub-cluster 3, while only Ca exhibited lowest concentration at sub-cluster 7. Further observation establishes that Al and Fe showed highest concentration at sub-cluster 5, while Si and Ca showed highest concentration at sub-clusters 6 and 3, respectively. The above illustration signifies some similarities in concentration characters in each subgroup, where some elements demonstrated increase in concentration at the same sub-cluster. For instance, Si and Fe indicated increase in concentration at sub-cluster 7, while Al and Ca indicated increase in concentration at sub-cluster 4.

4.4.5 Correlation analysis for different coal fly ash phases (SEP)

4.4.5.1 Water Phase

As Table 4.4 shows, the concentration of Si was negatively correlated with Ba and Sr at a confidence level of 99%, whereas the concentration of Si was positively correlated to the concentration of Al, Na, K, As, Pb and Ni at a confidence level of 99%. It means that the concentrations of Ba and Sr decrease as the concentration of Si increases, while the reverse is true in relation to Al, Na, K, As, Pb and Ni. The concentration of Al was positively correlated with Si, Na and Ni at a confidence level of 99% in the water-soluble fraction. It means that the concentrations of Si, Na and Ni increase as the concentration of Al increases in the fraction. The concentration of Ca was negatively correlated with Mg at a confidence level of 99%, whereas the concentration of Ca was positively correlated to the concentration of K, Zn and Cu at a confidence level of 99%. It means that the concentration of Mg decreases as the concentration of Ca increases, while the reverse is true in relation to K, Zn and Cu.

The concentration of Fe was positively correlated with Ba at confidence level of 99% in the water-soluble fraction. It means that the concentration of Ba increases

http://etd.uwc.ac.za/

as the concentration of Fe increases in the fraction. The concentration of Na was negatively correlated with Sr and Ba at a confidence level of 99%, whereas the concentration of Na was positively correlated to the concentration of Si, Al, K, Mn and Mo at a confidence level of 99%. It means that the concentration of Sr and Ba decreased as the concentration of Na increased, while the reverse is true in relation to Si, Al, K, Mn and Mo. The concentration of K was negatively correlated with Mg, Sr and Ba at a confidence level of 99%, whereas the concentration of K was positively correlated to the concentration of Si, Ca, Na, Pb, Mo and Cu at a confidence level of 99%. It means that the concentration of Mg, Sr and Ba decreased as the concentration of K increases, while the reverse is true in relation to Si, Ca, Na, Pb, Mo and Cu.

The concentration of Mg was negatively correlated with Ca, K, Sr, Ba and Zn at a confidence level of 99%, whereas the concentration of Mg did not display any positive correlation to the concentration of other elements at a confidence level of 99%. It means that the concentration of Ca, K, Sr, Ba and Zn decreased as the concentration of Mg increases. The concentration of Sr was negatively correlated with Si, Na, K, Mg and Mn at a confidence level of 99%, whereas the concentration of Sr was positively correlated to the concentration of Ba at a confidence level of 99%. It means that the concentration of Si, Na, K, Mg and Mn decreased as the concentration of Sr increases, while the reverse is true in relation to Ba. The concentration of Ba was negatively correlated with Si, Na, K, Mg and Mn at a confidence level of 99%, whereas the concentration of Ba was positively correlated to the concentration of Fe and Sr at a confidence level of 99%. It means that the concentration of Si, Na, K, Mg and Mn decrease as the concentration of Ba increases, while the reverse is true in relation to Fe and Sr.

The concentration of Mn was negatively correlated with Sr and Ba at a confidence level of 99%, whereas the concentration of Mn was positively correlated to the concentration of Na at a confidence level of 99%. It means that the concentration of Sr and Ba decreased as the concentration of Mn increases, while the reverse is true in relation to Na. The concentration of As was positively correlated with Si, K and Pb at confidence level of 99%. It means that the concentration of Si, K and Pb

http://etd.uwc.ac.za/

Table 4.4: Correlation analysis of the coal fly ash extract in the water fraction phase

Correlations for water fraction																		
		Si	Al	Ca	Fe	Na	K	Mg	Sr	Ba	Mn	As	Pb	Zn	Ni	Mo	Cu	Cr
Si		1	**.370****	-.209	.227	**.429****	.466**	.255	-.441**	-.575**	.264	.586**	.496**	-.219	.342*	.122	.026	.244
Al			1	-.155	.160	.488**	.239	-.082	-.107	-.134	.095	.036	.038	-.016	.265	.126	.159	.025
Ca				1	.124	.007	.369**	-.474**	.185	.172	-.224	.307*	.132	.616**	.155	.238	.479**	.114
Fe					1	-.061	.227	-.089	.108	.177	-.067	.396**	.381**	.230	.040	-.063	.232	-.169
Na						1	.583**	.030	-.528**	-.565**	.438**	.069	.048	.089	.032	.206	.443**	.053
K							1	-.387**	-.388**	-.412**	.200	.496**	.564**	.504**	.232	.460**	.658**	.130
Mg								1	-.395**	-.404**	.128	-.225	-.184	-.436**	-.208	-.250	-.167	-.115
Sr									1	.802**	-.501**	-.047	-.138	.114	.083	-.113	-.376**	.048
Ba										1	-.448**	-.114	-.119	.107	.095	-.180	-.297*	-.078
Mn											1	.141	.023	-.145	.008	.086	.080	-.232
As												1	.725**	.019	.540**	.084	.168	-.008
Pb													1	.216	.421**	.408**	.255	-.249
Zn														1	-.089	.343*	.578**	.004
Ni															1	.066	-.073	.080
Mo																1	.226	-.030
Cu																	1	-.166
Cr																		1
****. Correlation is significant at the 0.01 level (2-tailed). Water fraction**																		
***. Correlation is significant at the 0.05 level (2-tailed).**																		

UNIVERSITY of the WESTERN CAPE

http://etd.uwc.ac.za/

increase as the concentration of As increases. The concentration of Pb was positively correlated with Si, K, As, Ni and Mo at confidence level of 99%. It means that the concentration of Si, K, As, Ni and Mo increase as the concentration of Pb increases. The concentration of Zn was positively correlated with Ca, K and Cu at confidence level of 99%., whereas Zn was negatively correlated with the concentration of Mg at confidence level of 99%. It means that the concentration of Ca, K and Cu increase as the concentration of Zn increases, while the concentration of Mg decreased with the concentration of Zn.

The concentration of Ni was positively correlated with Si, Al, As and Pb at confidence level of 99%. It means that the concentration of Si, Al, As and Pb increased as the concentration of Ni increased. The concentration of Mo was positively correlated with Na, K and Pb at confidence level of 99%. It means that the concentration of Na, K and Pb increased as the concentration of Mo increased. The concentration of Cu was positively correlated with Ca, K and Zn at confidence level of 99%. It means that the concentration of Ca, K and Zn increased as the concentration of Mo increased.

4.4.5.2 Correlation results for the Carbonate fraction

As Table 4.5 shows, the concentration of Al was negatively correlated with Ni at confidence level of 99%, whereas the concentration of Al was positively correlated to the concentration of Mn and Mo at confidence level of 99%. It means that the concentrations of Ni decreased as the concentration of Al increased, while the reverse is true in relation to Mn and Mo. The concentration of Ca was negatively correlated with Mn and Mo at confidence level of 99%, whereas the concentration of Ca was positively correlated to the concentration of Na, K, Mg, Sr, Ba and Zn at confidence level of 99%. It means that the concentrations of Mn and Mo decreased as the concentration of Ca increased, while the reverse is true in relation to Na, K, Mg, Sr, Ba and Zn. The concentration of Fe was positively correlated with Mn at confidence level of 99% in the carbonate fraction. It means that the concentrations of Mn increased as the concentration of Fe increased in the fraction.

The concentration of Na was negatively correlated with Mn and Cr at confidence level of 99%, whereas the concentration of Na was positively correlated to the concentration of Ca, K, Mg, Sr, Ba, Zn and Cu at confidence level of 99%. It means that the concentrations of Mn and Cr decreased as the concentration of Na increased, while the reverse is true in

http://etd.uwc.ac.za/

relation to Ca, K, Mg, Sr, Ba, Zn and Cu. The concentration of K was negatively correlated with Mn and Cr at a confidence level of 99%, whereas the concentration of K was positively correlated to the concentration of Ca, Na, Mg, Sr, Ba and Zn at confidence level of 99%. It means that the concentrations of Mn and Cr decreased as the concentration of K increased, while the reverse is true in relation to Ca, Na, Mg, Sr, Ba and Zn. The concentration of Mg was negatively correlated with Mn and Mo at a confidence level of 99%, whereas the concentration of Mg was positively correlated to the concentration of Ca, Na, K, Sr, Ba and Zn at confidence level of 99%. It means that the concentrations of Mn and Mo decreased as the concentration of Mg increased, while the reverse is true in relation to Ca, Na, K, Sr, Ba and Zn.

The concentration of Sr was negatively correlated with Mn and Cr at a confidence level of 99%, whereas the concentration of Sr was positively correlated to the concentration of Ca, Na, K, Mg, Ba and Zn at confidence level of 99%. It means that the concentrations of Mn and Cr decreased as the concentration of Sr increased, while the reverse is true in relation to Ca, Na, K, Mg, Ba and Zn. The concentration of Ba was negatively correlated with Mn and Cr at a confidence level of 99%, whereas the concentration of Ba was positively correlated to the concentration of Ca, Na, K, Mg, Sr and Zn at confidence level of 99%. It means that the concentrations of Mn and Cr decreased as the concentration of Ba increased, while the reverse is true in relation to Ca, Na, K, Mg, Sr and Zn. The concentration of Mn was negatively correlated with Ca, Na, K, Mg, Sr, Ba and Zn at a confidence level of 99%, whereas the concentration of Mn was positively correlated to the concentration of Al, Fe, and Mo at confidence level of 99%. It means that the concentrations of Ca, Na, K, Mg, Sr, Ba and Zn decreased as the concentration of Mn increased, while the reverse is true in relation to Al, Fe, and Mo.

The concentration of As was positively correlated with Ni at confidence level of 99% in the carbonate fraction. It means that the concentration of Ni increased as the concentration of As increased in the fraction. The concentration of Zn was negatively correlated with Mn, Mo and Cr at a confidence level of 99%, whereas the concentration of Zn was positively correlated to the concentration of Ca, Na, Mg, Sr, Ba, and Cu at confidence level of 99%. It

http://etd.uwc.ac.za/

Table 4.5: Correlation analysis of the coal fly ash extract in the carbonate fraction phase

Correlations for carbonate fraction																
	Si	Al	Ca	Fe	Na	K	Mg	Sr	Ba	Mn	As	Pb	Zn	Ni	Mo	Cu
Si	1															
Al	.183	1														
Ca	.185	.013	1													
Fe	.024	.480**	-.209	1												
Na	-.076	.004	.623**	-.270	1											
K	-.069	.138	.605**	-.060	.891**	1										
Mg	-.148	-.231	.180	-.210	.365**	.275	1									
Sr	-.050	-.068	.556**	-.224	.865**	.779**	.500**	1								
Ba	.056	-.043	.549**	-.189	.845**	.760**	.466**	.976**	1							
Mn	.096	.567**	-.448**	.551**	-.622**	-.455**	-.207	-.510**	-.495**	1						
As	-.019	-.174	-.058	-.115	-.111	-.142	.283*	-.093	-.123	.004	1					
Pb	-.138	.205	.081	.204	-.305*	-.217	-.364**	-.445**	-.428**	.177	.052	1				
Zn	-.236	.079	.444**	-.251	.732**	.653**	.224	.660**	.653**	-.297*	-.147	-.098	1			
Ni	.164	-.312*	.197	-.253	.096	-.008	.179	.040	.057	-.227	.608**	.035	.073	1		
Mo	.187	.376**	-.334*	.644**	-.393**	-.281*	-.328*	-.261	-.223	.479**	-.060	.063	-.450**	-.083	1	
Cu	-.079	.323*	.238	.032	.378**	.412**	-.131	.310*	.315*	.010	-.143	.160	.618**	.128	-.030	1
Cr	.032	-.291*	.155	.114	-.292*	-.298*	-.119	-.296*	-.314*	-.106	.079	.185	-.387**	.080	.142	-.330*

UNIVERSITY of the WESTERN CAPE

http://etd.uwc.ac.za/

means that the concentrations of Mn, Mo and Cr decreased as the concentration of Zn increased, while the reverse is true in relation to Ca, Na, Mg, Sr, Ba, and Cu. The concentration of Ni was negatively correlated with Al at a confidence level of 99%, whereas the concentration of Ni was positively correlated to the concentration of As at confidence level of 99%. It means that the concentrations of Al decreased as the concentration of Ni increased, while the reverse is true in relation to As.

The concentration of Mo was negatively correlated with Ca, Na, Mg and Zn at a confidence level of 99%, whereas the concentration of Mo was positively correlated to the concentration of Al and Mn at confidence level of 99%. It means that the concentrations of Ca, Na, Mg and Zn decreased as the concentration of Mo increased, while the reverse is true in relation to Al and Mn. The concentration of Cu was negatively correlated with Cr at a confidence level of 99%, whereas the concentration of Cu was positively correlated to the concentration of Na and Zn at confidence level of 99%. It means that the concentration of Cr decreased as the concentration of Cu increased, while the reverse is true in relation to Na and Zn. The concentration of Cr was negatively correlated with Na, K, Sr, Ba, Zn and Cu at confidence level of 99% in the carbonate fraction. It means that the concentrations of Na, K, Sr, Ba, Zn and Cu decreased as the concentration of Cr increased in the fraction.

4.4.5.3 Correlation results for the Fe/Mn fraction

As Table 4.6 shows, the concentration of Si, in the Fe/ Mn fraction was negatively correlated with Zn at confidence level of 99%, whereas the concentration of Si was positively correlated to the concentration of Al, Fe, Na and Sr at confidence level of 99%. It means that the concentrations of Zn decreased as the concentration of Si increased, while the reverse is true in relation to Al, Fe, Na and Sr. The concentration of Al was negatively correlated with K, Zn and Cu at confidence level of 99%, whereas the concentration of Al was positively correlated to the concentration of Si at confidence level of 99%. It means that the concentrations of K, Zn and Cu decreased as the concentration of Al increased, while the reverse is true in relation to Si. The concentration of Ca was negatively correlated with Mo at confidence level of 99%, whereas the concentration of Ca was positively correlated to the concentration of Sr, Ba and Mn at confidence level of 99%. It means that the

http://etd.uwc.ac.za/

concentrations of Mo decreased as the concentration of Ca increased, while the reverse is true in relation to Sr, Ba and Mn.

The concentration of Fe was negatively correlated with Zn and Mo at confidence level of 99%, whereas the concentration of Fe was positively correlated to the concentration of Si, Na, Mn and Pb at confidence level of 99%. It means that the concentrations of Zn and Mo decreased as the concentration of Fe increased, while the reverse is true in relation to Si, Na, Mn and Pb. The concentration of Na was negatively correlated with Zn and Mo at confidence level of 99%, whereas the concentration of Na was positively correlated to the concentration of Si, Fe and Pb at confidence level of 99%. It means that the concentrations of Zn and Mo decreased as the concentration of Na increased, while the reverse is true in relation to Si, Fe and Pb. The concentration of K was negatively correlated with Al and Mg at confidence level of 99%, whereas the concentration of K was positively correlated to the concentration of Cu at confidence level of 99%. It means that the concentrations of Al and Mg decreased as the concentration of K increased, while the reverse is true in relation to Cu.

The concentration of Mg was negatively correlated with K and Cu at confidence level of 99%, whereas the concentration of Mg was positively correlated to the concentration of Mn at confidence level of 99%. It means that the concentrations of K and Cu decreased as the concentration of Mg increased, while the reverse is true in relation to Mn. The concentration of Sr was positively correlated with Si, Ca, Ba and Cu at confidence level of 99% in the carbonate fraction. It means that the concentrations of Si, Ca, Ba and Cu increased as the concentration of Sr increased in the fraction. The concentration of Ba was negatively correlated with Cr at confidence level of 99%, whereas the concentration of Ba was positively correlated to the concentration of Ca, Sr, and Cu at confidence level of 99%. It means that the concentrations of Cr decreased as the concentration of Ba increased, while the reverse is true in relation to Ca, Sr, and Cu. The concentration of Mn was negatively correlated with As at confidence level of 99%, whereas the concentration of Mn was positively correlated to the concentration of Ca, Fe and Mg at confidence level of 99%. It means that the concentrations of As decreased as the concentration of Mn increased, while the reverse is true in relation to Ca, Fe and Mg.

http://etd.uwc.ac.za/

Table 4.6: Correlation analysis of the coal fly ash extract in the Fe/Mn fraction phase

Correlations for HF																	
	Si	Al	Ca	Fe	Na	K	Mg	Sr	Ba	Mn	As	Pb	Zn	Ni	Mo	Cu	Cr
Si	1																
Al	.439**	1															
Ca	0.11	-.296*	1														
Fe	.583**	0.247	0.144	1													
Na	.532**	0.186	-0.057	.416**	1												
K	0.136	-.411**	0.151	0.071	.301*	1											
Mg	0.213	.358*	-0.009	.351*	0.008	-.364**	1										
Sr	.339*	-.334*	.360*	0.27	0.179	.360*	-0.218	1									
Ba	0.278	-.403**	.529**	.287*	-0.028	.295*	-0.254	.885**	1								
Mn	.321*	-0.053	.382**	.416**	-0.064	-0.12	.661**	0.175	0.219	1							
As	-0.144	0.068	-0.26	-0.264	0.128	0.028	-0.251	-0.109	-0.166	-.562**	1						
Pb	0.075	-0.224	-0.103	.365**	.339*	0.013	0.142	-0.098	-0.105	0.125	0.099	1					
Zn	-.434**	-0.271	0.039	-.425**	-.661**	-0.147	-0.15	-0.007	0.254	-0.077	0.137	-.308*	1				
Ni	0.185	-0.013	0.252	-0.128	-0.064	-0.189	-0.207	0.147	0.176	0.023	-0.076	-0.004	0.01	1			
Mo	-0.238	0.187	-.351*	-.322*	-.367**	-0.253	-0.055	-.291*	-0.275	-0.275	.309*	-0.212	.431**	-0.058	1		
Cu	0.013	-.572**	0.207	0.051	0.096	.488**	-.592**	.407**	.556**	-0.252	0.083	0.134	0.169	-0.078	-0.18	1	
Cr	-0.053	.364**	-0.272	-0.044	0.09	-0.246	0.169	-.349*	-.393**	-0.183	0.198	0.087	-0.107	-0.037	0.125	-.282*	1

http://etd.uwc.ac.za/

The concentration of As was negatively correlated with Mn at confidence level of 99%, whereas the concentration of As was positively correlated to the concentration of Mo at confidence level of 99%. It means that the concentrations of Mn decreased as the concentration of As increased, while the reverse is true in relation to Mo. The concentration of Pb was positively correlated with Fe and Na at confidence level of 99% in the carbonate fraction. It means that the concentrations of Fe and Na increased as the concentration of Pb increased in the fraction. The concentration of Zn was negatively correlated with Si, Al, Fe and Na at confidence level of 99%, whereas the concentration of Zn was positively correlated to the concentration of Mo at confidence level of 99%. It means that the concentrations of Si, Al, Fe and Na decreased as the concentration of Zn increased, while the reverse is true In relation to Mo.

Mo was negatively correlated with Ca, Fe and Na at confidence level of 99%, whereas the concentration of Mo was positively correlated to the concentration of As and Zn at confidence level of 99%. It means that the concentrations of Ca, Fe and Na decreased as the concentration of Mo increased, while the reverse is true in relation to As and Zn. The concentration of Cu was negatively correlated with Al and Mg at confidence level of 99%, whereas the concentration of Cu was positively correlated to the concentration of K, Sr and Ba at confidence level of 99%. It means that the concentrations of Al and Mg decreased as the concentration of Cu increased, while the reverse is true in relation to K, Sr and Ba. The concentration of Cr was negatively correlated with Ba at confidence level of 99% in the fraction. It means that the concentrations of Ba decreased as the concentration of Cr increased in the fraction.

4.4.6 Analysis of Dendrogram

4.4.6.1 Water Fraction Dendrogram for Coal Fly Ash

The appearance of samples of greater depths as represented in Figure 4.2 illustrates that samples like S1_19m, 22.5 m S2, S1_18m in sub-Cluster 1 of Main Cluster 1; 19.5mS2, 21mS2, 18mS2 in sub-Cluster 3 of Main Cluster 1; and S1_10.5m, S1_16.5m and S1_12m in sub-Clusters 6 and 2 of Main Cluster 1 with larger concentrations may be attributed to the presence of iron catalysts that are usually co-disposed with mine wastes.

http://etd.uwc.ac.za/

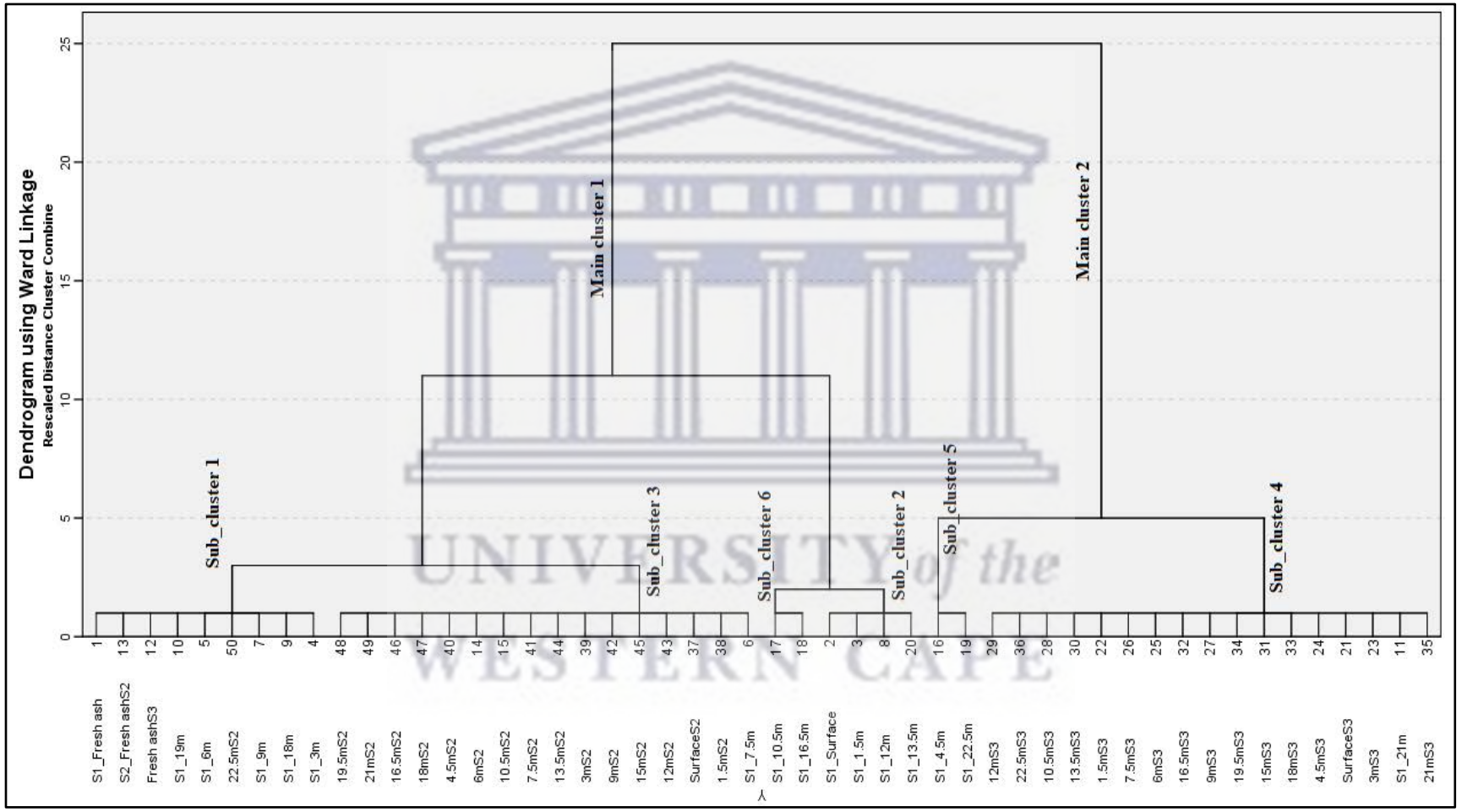

Figure 4.2: Dendrogram for coal fly ash water leach fraction (fraction 1) clusters

UNIVERSITY of the WESTERN CAPE
http://etd.uwc.ac.za/

Samples in groups 4 and 5 (in cluster two) are mostly from the upper grey (d1), ferruginous, and lower grey layers, respectively, and are characterised by a high content of Al_2O_3 and Fe_2O_3. It is noteworthy that samples S1_4.5m (sub-Cluster 5) and 1.5mS3, 6mS3, 4.5mS3, SurfaceS3 and 3mS3 (sub-Cluster 4) appeared in Main Cluster 2, which mainly comprises Al_2O_3 and Fe_2O_3. The appearance of these samples in Main cluster 2 may be attributed to the leaching of components typically associated with the oxidised and transition zones under harsh environmental conditions.

The infiltration of brine waste, usually co-disposed with other mine wastes, could be responsible for the leaching of various chemical species including Ca, Mg, Na, K, Br, Fe, SiO_2, Cl^-, NH_3, CO_3^{2-}, NO_3, SO_4, Fl^- as well as organic compounds (Nyamhingura, 2009). Thus, the existence of components typically linked to the oxidised and transition zones in greater depths.

4.4.6.2 Carbonate Fraction Dendrogram for Coal Fly Ash

The dendrogram given in Figure 4.3 illustrates the hierarchical clustering analysis with two major clusters of the tailing dam samples characterised by their variable contents in SiO_2, Fe_2O_3 and Al_2O_3. The cluster groups of the samples can be further subdivided into sub-groups. Groups 1, 2 and 4 (in cluster one) contain a mixture of samples mainly from the oxidised (a), transitional (b), and some samples from the upper (d1) and lower grey (d2) layers and are mainly SiO_2.

Other oxides, especially those of Al and Fe have minimal concentrations close to the surface due to oxidation effect; however, their concentrations increase with depth. Jarosite, an oxide of iron, sometimes exists in noticeable amount in the oxidation zone, but Fe_2O_3 and hematite rarely occur in the oxidation zone (Abegunde et al. 2016). The appearance of samples typically associated with greater depths, for example 22.5mS3, 18mS2, 19.5mS2 in sub-Cluster 1 of Main Cluster 1; S1_16.5m, S1_18m in sub-Cluster 2 of Main Cluster 1; and S1_19m, and S1_13.5m in sub-Cluster 4 of Main Cluster 1 may be attributed to the presence of iron catalysts that are usually co-disposed with mine wastes.

http://etd.uwc.ac.za/

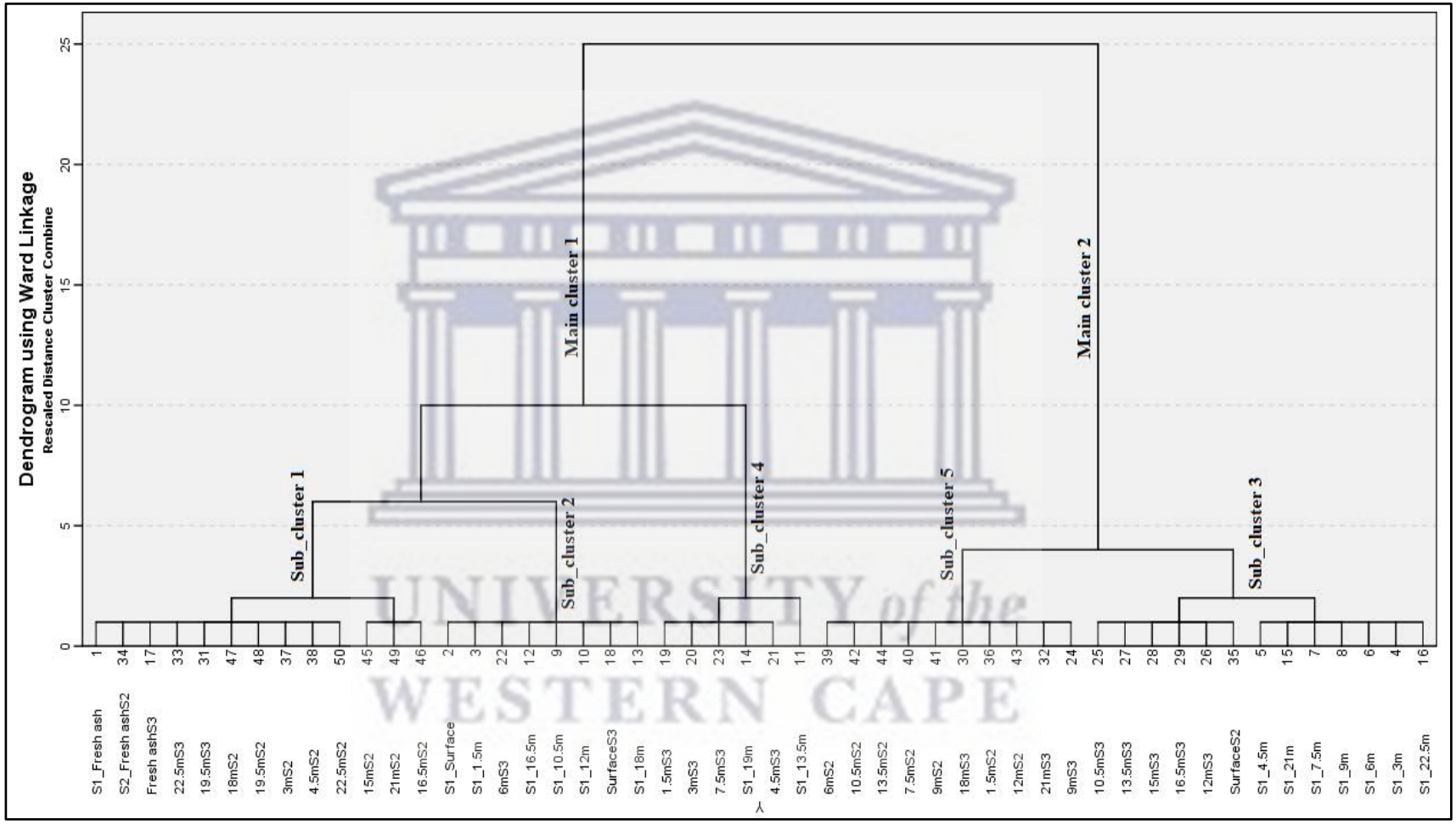

Figure 4.3: Dendrogram for coal fly ash carbonate fraction (fraction 2) clusters

http://etd.uwc.ac.za/

Samples in groups 3, and 5 (in cluster two) are mostly from the upper grey (d1), ferruginous, and lower grey layers, respectively, which are characterised by a high content of Al_2O_3 and Fe_2O_3. It is noteworthy that samples 6mS2 and 1.5mS2 (sub-Cluster 5); and SurfaceS2, S1_4.5m, S1_6m and S1_3m (sub-Cluster 3) appeared in Main Cluster 2, which mainly comprises Al_2O_3 and Fe_2O_3. The appearance of these samples in Main cluster 2 may be attributed to the leaching of components typically associated with the oxidised and transition zones under harsh environmental conditions.

4.4.6.3 Hydroxylamine Fraction for Coal Fly Ash

The hierarchical clustering analysis presented in Figure 4.4 represents a dendrogram illustrating the richness of SiO_2 in the samples like S1_Fresh ash, S2_Fresh ash, Fresh ash S3, S1_3m and SurfaceS3 and others. This group of samples were found in the oxidised, transition, upper grey and lower grey zones in the drilled cores. The appearance of samples typically associated with greater depths, for example S1_16.5m, 13.5mS3, 16.5mS2 and 18mS3 in sub-Cluster 1 of Main Cluster 1; S1_10.5m, S1_22.5m and 22.5mS3 in sub-Cluster 5 of Main Cluster 1; S1_12m, S1_19m and S1_13.5m in sub-Cluster 2 of Main Cluster 1; and 9mS3, 12mS3 and 15mS3 in sub-cluster 6 of main group may be attributed to the presence of iron catalysts that are usually co-disposed with mine wastes.

Samples in groups 3, 4 and 7 (in cluster two) are mostly from the upper grey (d1), ferruginous, and lower grey layers, respectively, which are characterised by a high content of Al_2O_3 and Fe_2O_3. It is noteworthy that samples S1-6m and S1_1.5m (sub-Cluster 3); and 1.5mS2, SurfaceS2, 4.5mS2, 3mS2 and 6mS2 (sub-Cluster 7); and S1_4.5m, 1.5mS3, 3mS3, 4.5mS3 and 6mS3 in sub-cluster 4 appeared in Main Cluster 2, which mainly comprises Al_2O_3 and Fe_2O_3. The appearance of these samples in Main cluster 2 may be attributed to the leaching of components typically associated with the oxidised and transition zones under harsh environmental conditions.

http://etd.uwc.ac.za/

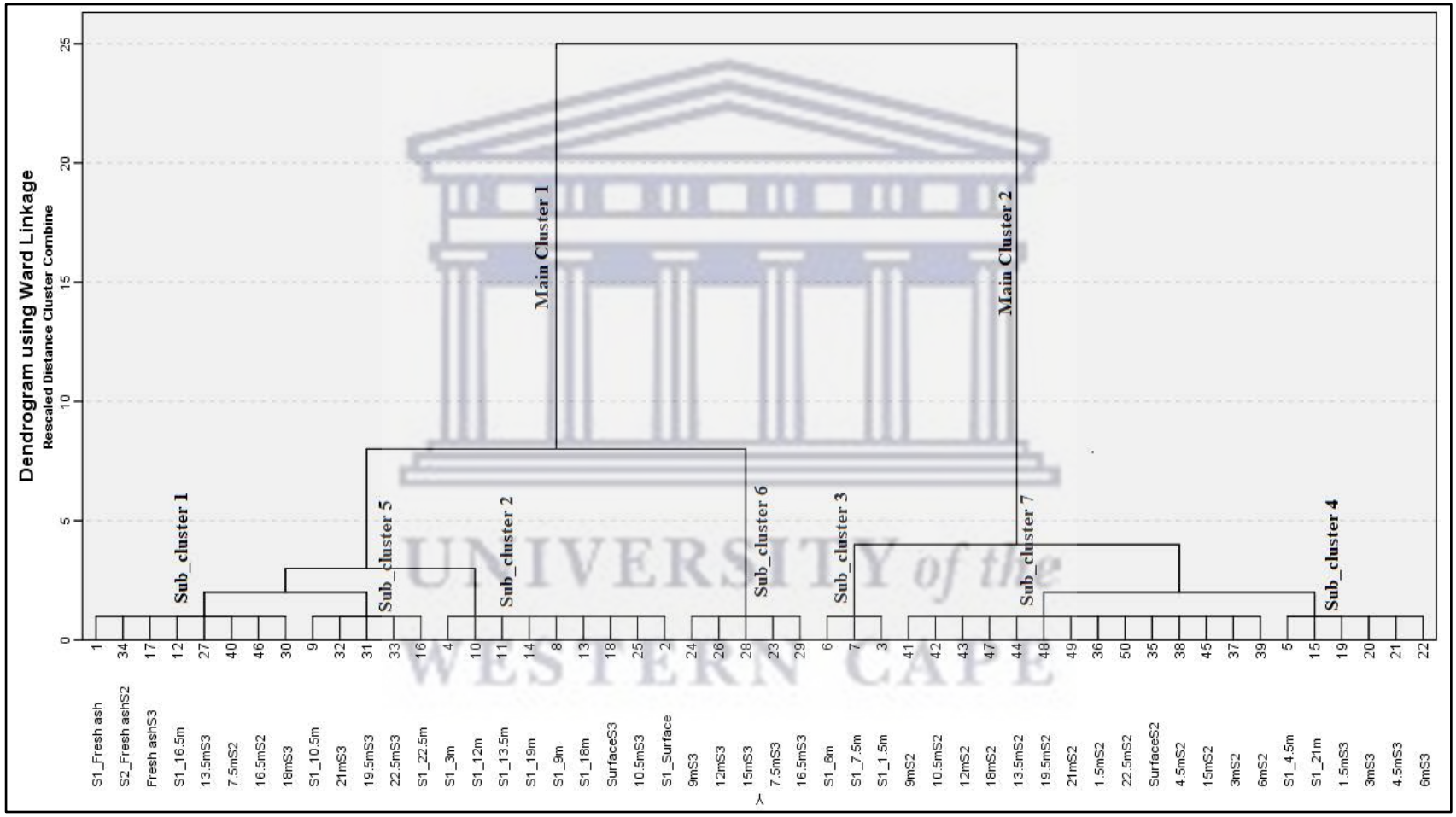

Figure 4.4: Dendrogram for coal fly ash hydroxylamine fraction (fraction 3) clusters

http://etd.uwc.ac.za/

4.4.7 Discriminant Function Analysis for Coal Fly Ash

Two discriminant function analyses were conducted to highlight the number of associations that define the system under the group functions (GFs) for coal fly ash. The two discriminant analyses are identified as the standardised canonical discriminant function coefficient (SCDFC) and the structure matrix. SCDFC illustrates the association of various groups between the variables used in terms of concentration, while the structure matrix demonstrates an absolute correlation between each variable that defines each group function. The canonical discriminant function analysis of elements in the three fractions is graphically represented in the Figure 4.5 and numerical estimates are arrayed in Table 4.7 and Table 4.8.

4.4.7.1 Water phase

The results obtained from the graphical analysis of four group functions through the use of SCDFC are given in Table 4.7. 57%, 18.6%, 16.2% and 8.2% variances were obtained for GF1, GF2, GF3 and GF4, respectively, as the positive values in the table signifying improvements or accumulations and the negative values signifying loss or release. The higher the proportion of the variance, the stronger the impact or effect of a GF; thus, GF1> GF2> GF3> GF4. GF1 constituted 57% of the system in the tailings, as it indicated positive values for Si, Al, Ca, Fe, K, Mg, Sr, Pb, Ni, Cu and Cr based on the weathering pattern, whereas elements such as Na, Ba, Mn, As, Zn and Mo indicated negative values. Amongst these elements, only Si contributed highest impact as the most positive element under GF1. As indicated in structure matrix (Table 4.4), both Fe and Ca exhibited positive values, which stipulates that Fe element released into the acid mine tailings was neutralised by the present of Ca. In the same way, it can be neutralised by the high presence of Mg as a carbonate species. As a result, it is understood that the mine tailings have negligible hazard on their surroundings.

The results in the GF2 (18.6%) indicated that a few numbers of elements exhibited positive values, unlike in the GF1. Al, Ca, Na, Mg, Sr, Mn and Pb indicated positive

http://etd.uwc.ac.za/

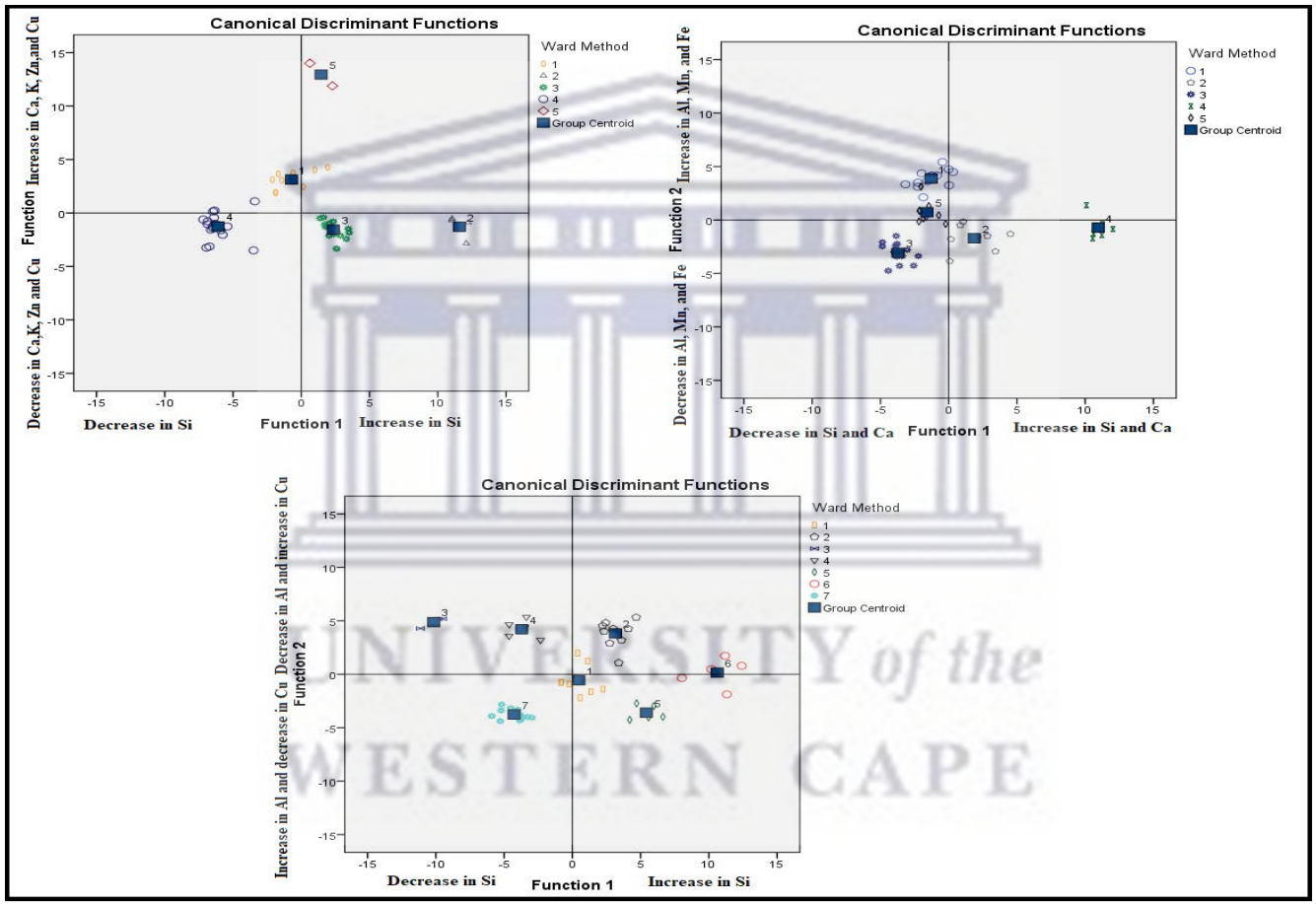

Figure 4.5: Canonical Discriminant function analysis of coal fly ash elements in water fraction, carbonate fraction and hydroxylamine fraction

http://etd.uwc.ac.za/

Table 4.7 Standardised canonical discriminant function coefficients for the three fractions for elements concentration

Standardized Canonical Discriminant Function Coefficients WF					Standardized Canonical Discriminant Function Coefficients CF					Standardized Canonical Discriminant Function Coefficients HF						
	Function					Function					Function					
	1	2	3	4		1	2	3	4		1	2	3	4	5	6
Si	1.218	-0.009	-0.177	-0.407	**Si**	1.618	0.208	-0.067	-0.185	**Si**	1.260	0.322	0.255	-0.269	0.168	-0.381
Al	0.538	0.210	0.527	0.154	**Al**	-0.458	0.861	-0.108	0.197	**Al**	0.250	-1.310	-0.459	0.229	-0.029	0.346
Ca	0.567	1.957	-0.462	-1.297	**Ca**	0.707	0.357	-0.009	-0.486	**Ca**	0.168	0.069	-0.710	0.377	0.192	-0.163
Fe	0.133	-0.056	0.141	-0.091	**Fe**	0.050	0.014	-0.320	-0.492	**Fe**	0.162	0.236	0.072	0.531	0.240	-0.517
Na	-0.260	0.619	-0.664	0.466	**Na**	-1.388	0.403	-0.712	-1.485	**Na**	0.032	0.287	0.240	-0.292	-1.144	0.328
K	0.259	0.798	0.907	0.904	**K**	-0.649	0.650	0.127	1.130	**K**	0.009	-0.295	-0.360	-0.502	0.166	0.326
Mg	0.382	0.047	-0.292	0.186	**Mg**	-0.069	0.055	0.077	0.064	**Mg**	-0.076	-0.074	0.675	-0.588	0.360	0.775
Sr	0.041	0.224	0.211	0.023	**Sr**	-3.227	1.078	-2.021	-2.279	**Sr**	-0.989	0.205	1.317	1.535	0.430	-0.436
Ba	-0.435	-0.406	0.466	0.219	**Ba**	3.633	-1.495	1.639	3.312	**Ba**	0.282	0.054	-2.124	-1.514	-0.828	1.099
Mn	-0.062	0.240	-0.822	-0.210	**Mn**	-0.989	0.364	0.416	-0.166	**Mn**	1.101	0.149	0.237	0.620	-0.035	0.721
As	-0.323	-2.251	1.319	1.499	**As**	0.242	-0.158	0.319	0.673	**As**	0.467	-0.103	0.380	0.249	0.069	0.095
Pb	0.386	1.610	-0.873	-1.793	**Pb**	-0.200	0.362	-0.193	-0.454	**Pb**	-0.600	0.355	-0.237	0.346	0.360	-0.193
Zn	-0.196	-0.334	0.155	0.029	**Zn**	2.147	-0.360	2.317	-0.784	**Zn**	-0.552	-0.470	0.726	-0.538	0.107	-0.755
Ni	0.102	-0.272	0.450	0.200	**Ni**	-0.379	0.253	-0.551	-0.479	**Ni**	-0.037	0.379	0.215	-0.498	0.159	0.753
Mo	-0.754	-0.533	0.215	1.577	**Mo**	0.921	0.420	0.797	-0.035	**Mo**	0.044	0.242	-0.149	-0.083	-0.176	0.662
Cu	0.011	-0.535	0.215	-0.448	**Cu**	-0.404	0.068	-0.679	1.053	**Cu**	0.559	-0.068	0.493	0.356	0.300	1.052
Cr	0.620	-0.101	0.509	-0.103	**Cr**	-0.056	-0.422	0.050	0.829	**Cr**	0.175	0.063	0.108	0.179	0.144	0.535

UNIVERSITY of the
WESTERN CAPE

http://etd.uwc.ac.za/

Table 4.8: Structure matrix illustration of the three fractions for elements concentration and discriminant function (group functions)

Structure Matrix WF					Structure Matrix CF					Structure Matrix HF						
	Function					Function					Function					
	1	2	3	4		1	2	3	4		1	2	3	4	5	6
Si	.678*	-0.080	-0.026	0.226	**Si**	.465*	0.275	-0.382	-0.067	**Si**	.642*	0.118	0.059	-0.209	-0.144	-0.210
Ca	-0.037	.359*	0.252	-0.240	**Ca**	.076*	0.049	-0.064	-0.046	**Al**	0.270	-.624*	0.024	0.267	-0.130	0.057
K	0.152	.342*	0.202	0.262	**Al**	-0.053	.757*	0.215	0.126	**Cu**	-0.015	.176*	-0.124	-0.145	-0.123	0.080
Zn	-0.046	.270*	0.162	-0.057	**Mn**	-0.053	.217*	0.184	-0.041	**Ca**	0.034	0.145	-.499*	-0.037	0.158	0.159
Cu	0.019	.237*	0.044	-0.023	**Fe**	-0.036	.189*	0.017	0.062	**Ba**	0.038	0.198	-.333*	-0.227	-0.021	0.073
Mg	0.080	-0.143	-.349*	-0.122	**Zn**	0.012	0.012	.427*	0.002	**Zn**	-0.115	-0.057	-0.016	-.519*	0.274	-0.013
Ba	-0.182	-0.135	.287*	-0.134	**Cr**	0.014	-0.108	-.182*	0.077	**Fe**	0.150	0.075	-0.111	.357*	0.110	-0.157
Sr	-0.114	-0.103	.242*	-0.077	**Ni**	0.054	-0.060	-.143*	-0.066	**Pb**	0.006	0.155	0.177	.297*	0.166	-0.114
As	0.138	-0.028	.213*	-0.030	**Ba**	0.076	-0.009	0.155	.256*	**Na**	0.129	0.094	0.159	0.225	-.774*	0.002
Mn	0.039	0.005	-.187*	0.176	**Cu**	-0.007	0.132	0.121	.241*	**Mn**	0.082	0.093	0.033	0.102	.408*	0.090
Ni	0.070	-0.030	.173*	0.041	**Sr**	0.044	-0.017	0.124	.218*	**Mg**	0.066	-0.066	0.231	0.170	.382*	0.131
Pb	0.083	0.027	.127*	0.007	**Pb**	-0.049	0.094	-0.081	-.217*	**K**	0.013	0.129	-0.079	-0.135	-.195*	-0.084
Fe	0.043	-0.019	.119*	-0.097	**K**	0.010	0.078	0.063	.173*	**As**	-0.031	-0.055	0.152	-0.011	-.189*	0.019
Cr	0.063	0.020	.095*	0.012	**Mo**	0.012	0.159	-0.008	.160*	**Sr**	0.042	0.183	-0.159	-0.053	-.186*	0.065
Na	0.129	0.284	-0.164	.343*	**Mg**	-0.010	-0.086	0.057	.113*	**Cr**	0.003	-0.109	0.128	0.156	0.038	.432*
Mo	0.003	0.152	0.045	.305*	**As**	-0.012	-0.047	-0.081	.107*	**Ni**	0.022	0.059	-0.086	-0.220	0.094	.236*
Al	0.073	0.033	0.043	.172*	**Na**	0.026	0.016	0.068	.070*	**Mo**	-0.047	-0.124	0.119	-0.151	0.057	.193*

Pooled within-groups correlations between discriminating variables and standardized canonical discriminant functions
Variables ordered by absolute size of correlation within function. * Largest absolute correlation between each variable and any discriminant function

UNIVERSITY of the
WESTERN CAPE

http://etd.uwc.ac.za/

values, while Si, Fe, Ba, As, Zn, Ni, Mo, Cu and Cr showed negative values. In the GF2, Ca contributed greatest impact as the most positive element, while As is considered the most negative element. According to the illustration in the structure matrix, the negative value for Fe suggests that the element was insignificantly leached into the acid mine tailings, which suggests that the mobility and acidity occurrence at the tailings would be negligible. Notwithstanding, the huge presence of Ca will neutralise any strong presence of Fe in the tailings since it is considerably effective, whereas presence of As and Mg were inconsiderably released from the coal fly ash.

Equal number of elements exhibited positive values in the GF3 (16.2%) like in GF1, with a few of them different. Al, Fe, K, Sr, Ba, As, Zn, Ni, Mo, Cu and Cr indicated positive values, while other elements such as Si, Ca, Na, Mg, Mn, Pb were recorded as negative values. Further observation indicates that As is the most positive element, while Pb is determined as the most negative element. Additionally, the results displayed in the structure matrix showed an absolute correlation between elements and discriminant function. And the positive value for Fe and As signify that they were discharged into the acid tailings and they could degenerate, but the presence of Ca in the mine tailings is adequate to neutralise their acidic effects. However, Mg (a carbonate species) is considered inadequate based on its negative values. This signifies that concentration of Mg is inconsiderable to enhance the presence of any carbonate species in neutralising acidity in the mine tailings.

The last group function (GF4) for water fraction presented a high number of elements with positive values like GF1 and GF3. In GF4, Al, Na, K, Mg, Sr, Ba, As, Zn, Ni and Mo showed positive values, with elements such as Si, Ca, Fe, Mn, Pb, Cu and Cr exhibiting negative values. Among these elements, Mo is the most positive element followed by As, while Fe is considered most negative element. The data arrayed in the structure matrix for GF4 showed an absolute correlation between some elements and the discriminant function, such as Na, Mo and Al. From the structure matrix, the negative values derived for Fe and As indicated insignificant discharge of these elements into the mine tailings, but they do not pose

http://etd.uwc.ac.za/

any hazard on the environment. And neutralising elements such as Ca and Mg also have negative values, which indicates that they have no neutralisation effect on any presence of acidity in the tailings.

4.4.7.2 Carbonate phase

In the carbonate phase, similar observation process to water phase was followed to ascertain the concentration impact of each element on the acid mine tailings. Four main group functions (GFs) were identified through the application of SCDFC. The percentage estimates of variance for GF1, GF2, GF3 and GF4 in the second section of Table 4.8 are given as 67.3%, 24.2%, 5.6% and 3.0%, respectively, which resulted in the decreasing order of the GFs as thus; GF1> GF2> GF3> GF4. In GF1 (67.3%), some elements exhibited positive values while negative values were shown by other elements. Elements with positive values demonstrate substantial impact on the mine tailings, while the elements with negative values specifies insubstantial effect on the tailings. In that case, based on the results displayed in the carbonate phase, a fewer number of elements indicated positive values such as Si, Ca, Fe, Ba, As, Zn and Mo, while other elements indicated negative values (Al, Na, K, Mg, Sr, Mn, Pb, Ni, Cu and Cr). In addition, Ba contributed greatest impact as the most positive element followed by the substantial amounts of Zn and Si, while Na is considered the most negative element among other elements. Considering the data given in the structure matrix (Table 4.8), it is observed that Fe and As discharged into the mine tailings have no considerable impact on the environment, even with the considerable presence of Ca in the tailings as Mg indicated negligible amount. However, there is no positive correlation between Ca and Mg, which suggests that these carbonate species originated from different mines.

In the GF2 (24.2%), there are more elements with positive values than the number of elements with negative values, which signifies that more elements have impact on the tailings. Si, Al, Ca, Fe, Na, K, Mg, Sr, Mn, Pb, Ni, Mo and Cu exhibited positive values, while only four elements (Ba, As, Zn and Cr) exhibited negative values. According to the data displayed in the structure matrix, Al, Mn and Fe yielded strong positive correlation, which specifies that they emanate from the same

http://etd.uwc.ac.za/

source. Although, there is a high presence of Fe, with an insignificant amount of As. It is understood that strong presence of Fe is considered highly impactful on the environment. This effect is predicted to be neutralised with the amount of carbonate species.

SCDFC results derived for GF3 (5.6%) in carbonate phase contained almost equal number of positive values elements and negative values elements. Elements such as K, Mg, Ba, Mn, As, Zn, Mo and Cr exhibited positive values, while Si, Al, Ca, Fe, Na, Sr, Pb, Ni and Cu exhibited negative values. Amongst these elements, Zn is the most positive value element, followed by Ba while Sr is determined as the most negative value element, followed by Na. This signifies that there is higher concentration of Zn than other elements, with Sr having the lowest concentration. Additionally, the results obtained from the structure matrix showed an absolute correlation between elements and discriminant function in opposite direction. According to the results, the large amount of Zn (positive value) released stipulates that the element have considerable impact on the tailing environment. The amount might be aided by the presence of Fe in the tailing environment. It is observed that presence of Ca in the tailing is inconsiderable to neutralise any effect of Fe and Zn, even with the small amount Mg detected in the tailing.

GF4 (3.0%) yielded few numbers of positive value elements (Al, K, Mg, Ba, As, Cu and Cr) in SCDFC, with Ba identified as the most positive elements, followed by K and Cu. The negative value elements are Si, Ca, Fe, Na, Sr, Mn, Pb, Zn, Ni and Mo. Sr is identified as the most negative element, followed by Na. The illustration shows that higher amount of Ba was detected, while lowest amount of Sr was detected. The structure matrix data shows a strong absolute correlation between elements varying in the same direction. Ba has the strongest absolute correlation with Cu and Sr, which signifies their impact level on the tailing environment. These elements were released into the tailing environment in higher concentrations. However, the release of Fe into the environment could aid the mobility of these elements as well increases their environment impact. It is predicted that the presence of any carbonate species could neutralise the impact of

http://etd.uwc.ac.za/

these elements on the environment: though the amount of Ca present in the environment is negligible.

4.4.7.3 Hydroxylamine phase

In the hydroxylamine phase, the following observation to ascertain the concentration impact of each element on the acid mine tailings surfaced. Six main group functions (GFs) were identified through the application of SCDFC. The percentage estimates of variance for GF1, GF2, GF3, GF4, GF5 and GF6 in the second section of Table 4.8 are given as 64.2%, 25.5%, 4.7%, 3.4%, 1.4% and 0.7%, respectively, which resulted in the decreasing order of the GFs as thus; GF1> GF2> GF3> GF4> GF5>GF6>GF7. GF1 and GF2 are more significant and accounted for 89.7% of the sample.

GF1 represented (64.2%), with few numbers of negative value elements (Mg, Sr, Pb, Sn and Ni). From the results, Si is classified as the most positive element, followed by Mn while Sr is identified as the most negative element, followed by Pb. This signifies that Si has the highest concentration than other elements. The structure matrix results indicated only one absolute correlation. Sr has strongest impact on the environment with a large amount of it released into the tailing environment. Large amount of Al, Fe and Na released into the environment could increase the environmental hazard around the tailing area, with negligible amount of Ca and Mg.

In GF1 (64.2%), based on the structure matrix, only Si showed a positively significant value, indicating a release in Si which is the main constituent of the coal fly ash. Despite exposing the coal fly to a harsher condition, non-reactivity could be observed. In GF2 (25.5%), a depletion in Ca and increase in Cu was observed. Only Cu release was significant as the Ca decrease which could be used as buffer. This implies that there are less easily released mobile phase in the coal fly ash, In the carbonate fraction, Ca was released, as the Ca is released, this could create a buffer, increasing the pH, and available Ca increases the neutralisation potential of the coal fly ash.

UNIVERSITY of the WESTERN CAPE
http://etd.uwc.ac.za/

GF2 (%) results indicated that fewer numbers of elements (Al, K, Mg, As, Zn and Cu) have negative values, which indicates their level of concentration. The other elements (Si, Ca, Fe, Na, Sr, Ba, Mn, Pb, Ni, Mo and Cr) have positive values. Among these elements, Ni is identified as the most positive elements, while Al is considered as the most negative element. The structure matrix shows few absolute correlations between elements and discriminant function. The observation indicates that presence of Ba, Cu, Pb and Si could cause more harm on the environment, with minimal content Fe detected which could intensify the impact of the toxic metals on the tailing environment. Although, there is a significant quantity of Ca that can neutralise the presence of acidic element. Other group function showed negligible effects, but confirmed possibility of an ineffective Fe.

4.4.8 Factor Analysis for Coal Fly Ash

Factor analysis was used to establish the origin, controls, and behaviour of elements in the coal fly ash samples and layers.

Factors were extracted by the Principal Component Analysis (PCA) based on the Varimax with the Kaiser normalisation rotation method Table 4.9, with eigenvalue > 1. Values below ±0.3 were not included due to their significance. Factors gave an effective description of the water-soluble fraction. Based on eigen values greater than one, Factor 1, 2, 3, 4, 5 and 6 represent 25.868%, 19.257%, 12.822%, 8.664%, 6.996% and 6.429% of the sample respectively. These estimates denote the order of relevance of the four factors. Clearly, this accounts for a cumulative sum of 80.036% of the sample.

Factor 1 indicates positive components for Si, Na, Mn, K and Zn, whereas negative components were recorded for Ba and Sr; factor 2 indicates positive components for Ca, K, Zn, Cu and Mo whereas negative components were recorded for Ba and Sr; factor 3 shows positive components for Si, K, Pb, As and Ni while factor 4 shows a positive component for Al and Na: factor 5 shows a positive component for Cr: factor 6 shows a positive component for Fe but negative component for Mo

http://etd.uwc.ac.za/

In the effect, factor 1 represents the most labile elements that can be easily leached Mg shows no correlation with Ca. And factor 2 shows Ca carbonates, which play a prominent role as it is responsible for trace such as Zn and Cu. Fe didn't really play a major role and could require a stronger solution or environment to release it. The fact that it is not associated with mobile element shows it could have been introduced.

In the case of the ammonium acetate fraction, six factors were identified. Based on eigen values greater than one, Factor 1, 2, 3, 4, 5 and 6 represent 34.263%, 15.897%, 9.317%, 8.817%, 8.268% and 6.253% of the sample respectively. These estimates denote the order of relevance of the factors. This accounts for a cumulative sum of 82.815% of the sample. Factor 1 indicates positive values for Ca, Mg, Na, Zn, Ba, Sr and K, but negative values for Mn, Mo and Fe; factor 2 indicates positive values for Mn, Mo, Al, Fe and Cu but negative values for As and Ni; and factor 3 indicates positive values for Cu, As and Fe.

Factor 3 indicates positive values for Cu, Ni, and Pb: factor 4 indicates positive values for Mo, As, Ni and Si: and factor 5 indicates positive values for Ca, and Cr, but negative values for As; and factor 6 indicates positive values for Cr and Fe, but negative values for Si. In factor 1, the effect of the carbonates present on the acidity was observed when Ca associated with Mg and shows negative relationship with Fe. And this denotes that the coal fly ash contained a considerable amount of neutralising potential. Therefore, as leaching conditions become stronger, there is a tendency for an increase in alkalinity within the tailings.

For the hydroxylamine phase, there were a greater number of factors of more complexity. Six factors were identified. Based on eigen values greater than one, Factor 1, 2, 3, 4, 5 and 6 represent 34.263%, 15.897%, 9.317%, 8.817%, 8.268% and 6.253% of the sample respectively. These estimates denote the order of relevance of the factors. This accounts for a cumulative sum of 78.24% of the coal fly ash. More so, factor 1 indicates positive values for Ba, Ca, Pb, Cu, Sr, and K but

http://etd.uwc.ac.za/

Table 4.9 : Rotated component matrix illustration of the three fractions for elements concentration (factors)

WF Rotated Component Matrix[a]							CF Rotated Component Matrix[a]							HF Rotated Component Matrix[a]						
	Component							Component							Component					
	1	2	3	4	5	6		1	2	3	4	5	6		1	2	3	4	5	6
Ba	-0.925						**Na**	0.918						**Ba**	0.889					
Sr	-0.907						**K**	0.899						**Sr**	0.795					
Na	0.620			0.592			**Sr**	0.890						**Cu**	0.770					
Mn	0.553						**Ba**	0.884						**Al**	-0.650		0.609			
Zn		0.878					**Ca**	0.770						**K**	0.578			0.465		
Cu		0.791					**Zn**	0.712				0.453		**Cr**	-0.559					
Ca		0.766					**Fe**		0.890					**Ca**	0.495	0.434				
K	0.402	0.673	0.459				**Mo**		0.783					**Mn**		0.889				
Mg	0.514	-0.529					**Al**		0.680			0.412		**As**		-0.753				
As			0.903				**Mn**	-0.516	0.655					**Mg**	-0.459	0.670				
Pb			0.836				**Pb**			0.824				**Si**			0.837			
Ni			0.712				**Mg**			-0.599				**Fe**			0.687			
Si	0.552		0.648				**As**				0.891			**Zn**				-0.825		
Al				0.936			**Ni**				0.859			**Na**			0.472	0.699		
Cr					0.945		**Cr**					-0.878		**Mo**				-0.666		
Fe						0.741	**Cu**	0.450		0.488		0.540		**Pb**					0.934	
Mo		0.414				-0.571	**Si**						0.946	**Ni**						0.946
Extraction Method: Principal Component Analysis. Rotation Method: Varimax with Kaiser Normalization.[a]																				
a. Rotation converged in 8 iterations							a. Rotation converged in 6 iterations							a. Rotation converged in 17 iterations						

UNIVERSITY of the
WESTERN CAPE

http://etd.uwc.ac.za/

negative values for Mg, Cr, Al; factor 2 indicates positive values for Ca, Mg and Mn but negative values for As; factor 3 indicates positive values for Al Si, Fe and Na; followed by factor 4 which indicates a positive value for K and Na, but negative values for Zn and Mo; factor 5 which indicates a positive value for Pb, and lastly factor 6 showed a positive value for Ni. This means that most trace elements such as Ni, Zn, Pb, and Cu are not associated with the Fe/Mn oxides. Ca played a major role which could be as a result of added lime to the coal fly ash and factor indicated the presence of carbonates form as a result of weathering that created secondary product.

Factor 4 showed that Fe is associated to Si, a non-reactive element, a pointer that they might have been released during processing and pulverising of those fine wastes.

4.5 Summary

Note both the gold tailings and coal fly ash samples used in this study were subjected to a similar condition. It could be observed when coal fly ash samples were exposed to leaching conditions, it could take time for elements to be released, and the presence of Ca showed a more neutralisation potential presence in the coal fly ash.

In this study, the statistical analysis was able to establish that Ca^{2+} and Mg^{2+} played a major role in the released metals. Out of the six associations identified in cluster analysis results for Water fraction (WF), A more prominent Si and Ca effect showed positive neutralisation potential. For the water phase, the release of Ca ions into the surroundings can be associated with the gradual neutralisation of any acidity release, therefore showing a tendency of an alkaline mine drainage could be responsible for the release of toxic metals.

In the case of the Ammonium acetate fraction (AMF), cluster analysis and discriminant analysis confirmed that elements associated with the carbonates are also relatively release in this phase but there were no association with Mg associated

http://etd.uwc.ac.za/

compound. Fe presence showed no relative effect, which could imply that a harsher condition might be needed.

For HF, association observed in-group function tends to slight release of elements associated with the Fe/Mn phase, with Ca negatively impacted but nonreactive elements Si are released which could be as a result of high silicate materials in the coal fly ash.

As the leaching environment becomes harsh (AMF) and more carbonates are released, then more Ca ions are released. In the end, the available Fe ions react to produce slight acidity (HF), which then suppressed but the notable presence of Carbonates. The trends observed in the carbonate phase showed that despite the level of acidity, the coal fly ash contained enough neutralising agent to serve as a buffer and therefore create an alkaline mine drainage.

Out of the six factors identified in factor analysis results for Water fraction (WF), Ca contributed more significantly with Fe showing insignificantly, without any association with toxic elements. For the water phase, the release of Ca ions into the surroundings can be associated with the gradual mobility or releases of toxic metals within an alkaline medium.

In the case of the ammonium acetate fraction (AMF) (also known as carbonate fraction), factor analysis indicated that Ca was no associated with Fe. This demonstrates the effect of the carbonates found alkalinity, and the coal fly ash contain a considerable amount of neutralising potential with less or without the presence of Fe ions. Therefore, as leaching conditions become stronger, there is a tendency for an increase in alkalinity within the coal fly ash but there is possibility mobile Fe ions are not present in abundance.

There is great possibility that more Fe element present were released during the coal fly ash processing.

http://etd.uwc.ac.za/

CHAPTER FIVE

5. GEOCHEMICAL AND GEOSTATISTICAL CHARACTERISATION OF ELEMENT SPECIATION IN GOLD TAILINGS

5.1 Introduction

This chapter entails the results of the complete geochemistry analysis, sequential extraction and as well as the statistical analysis performed on the gold tailings.

5.2 Complete Gold Tailing Data Geochemistry

Table 5.1 and APPENDIX E lists selected major and trace elements for the whole composite dataset and SEP phase analysis of samples from the Mogale tailings dam. An appraisal of APPENDIX L shows that SiO_2 (84.24%), Al_2O_3 (6.25%), Fe_2O_3 (2.64%) and LOI (3.28%) defines about 97.05% of the whole composition of the samples while concentrations of U, Au, Ni, As, Cu, and Zn have maximum values of 655.5 ppm, 1417.7ppb, 274.1ppm, 471.4 ppm, 308.8 ppm, and 817 ppm. The average arsenic contents are also well above 100 ppm.

Based on the selected elements, Table 5.1 compares the whole sample data with their corresponding leached values for each SEP leached phase. For the major elements, their equivalent values in % oxide for the whole sample were converted to ppm to allow proper comparison. Except for Ca, Mn, Cu, Zn, Co and Ni, all other elements' maximum concentration is lower than the minimum concentration of their corresponding whole composite value. The percentage leached for each selected element was calculated based on their average values.

http://etd.uwc.ac.za/

Table 5.1: Selected major and trace elements contents for all composite data and each SEP fraction (% leach of element) in the Mogale tailings dam

Major Element	Composite Oxide %			Composite ppm value			Water fraction				Ammonium Acetate Fraction				Hydroxylamine fraction			
	Min	Max	Ave	Min	Max	Ave	Min	Max	Ave	%Leach	Min	Max	Ave	%Leach	Min	Max	Ave	%Leach
Ca	0.06	2.75	0.53	429.00	19654.00	3788.00	13.01	1105.91	370.39	9.78	34.61	1280.83	370.90	9.79	1.95	235.67	82.93	2.19
Mg	0.09	0.86	0.40	543.00	5188.00	2413.00	0.49	259.13	77.02	3.19	9.21	96.67	29.53	1.22	3.15	74.14	23.54	0.98
Na	0.02	0.28	0.09	148.00	2077.00	668.00	0.01	27.44	5.76	0.86	0.43	10.84	3.94	0.59	5.72	377.58	117.86	17.64
K	0.17	0.65	0.34	1411.00	5396.00	2823.00	21.15	108.50	53.28	1.89	10.09	546.98	157.11	5.57	1.54	81.14	29.39	1.04
Mn	0.01	0.65	0.06	77.00	5034.00	465.00	0.00	133.77	15.40	3.31	0.00	174.93	12.95	2.78	0.12	148.13	4.94	1.06
Fe	0.86	9.31	3.03	6015.00	65114.00	21192.00	0.02	1238.84	255.09	1.20	2.19	268.74	36.91	0.17	4.62	531.42	213.86	1.01
Trace Elements	**Composite Oxide %**			**Composite ppm value**			**Water fraction**				**Ammonium Acetate Fraction**				**Hydroxylamine fraction**			
	Min	**Max**	**Ave**	**Min**	**Max**	**Ave**	**Min**	**Max**	**Ave**	**%Leach**	**Min**	**Max**	**Ave**	**%Leach**	**Min**	**Max**	**Ave**	**%Leach**
Pb	Nil	Nil	Nil	15.40	150.20	49.66	0.00	1.40	0.25	0.50	0.01	2.33	0.61	1.23	0.12	6.20	0.83	1.67
Cu	Nil	Nil	Nil	3.80	308.80	51.29	0.01	11.34	2.15	4.19	0.00	2.15	0.28	0.55	0.13	4.37	0.76	1.48
As	Nil	Nil	Nil	15.30	471.40	123.12	0.00	6.16	0.59	0.48	0.51	2.67	1.41	1.15	0.11	6.66	1.08	0.88
Zn	Nil	Nil	Nil	4.00	817.00	129.31	0.01	86.43	13.52	10.46	0.01	3.58	0.72	0.56	0.13	19.75	2.15	1.66
Co	Nil	Nil	Nil	0.90	125.90	38.06	0.00	13.35	3.22	8.46	0.01	1.55	0.46	1.21	0.11	3.14	0.61	1.60
Ni	Nil	Nil	Nil	3.80	274.10	99.79	0.00	54.93	10.87	10.89	0.06	7.32	1.56	1.56	0.11	12.93	1.27	1.27

Leco	Composite Oxide %			Composite ppm value			Static test	Composite		
	Min	Max	Ave	Min	Max	Ave		Min	Max	Ave
TOT/C	0.01	0.22	0.07	100.00	2200.00	700.00	Paste pH	2.61	8.69	4.50
TOT/S	0.26	2.19	1.14	2600.00	21900.00	11400.00	EC (mS/cm)	0.43	3.99	1.27
Sulphide	0.15	2.11	0.84	1508.53	21100.00	8394.03				

http://etd.uwc.ac.za/

However, subject to the mean, Ca, Mg, Fe, K and Na are generally the prevalent concentration (see Table 5.1) of the bulk composition of the samples in each sequential extraction phase. Except for Zn and Ni in the water phase and Na in the hydroxylamine phase, the percentage of each element leached from the whole sample was less than 10% (majority are also less than 5%) of the composite concentration. For water phase, the mean leaching of the major elements such as Ca (13.01-1105.91 ppm), Mg (0.49-259.13 ppm), K (21.15-108.5 ppm), Na (0.006-27.44 ppm), Mn (0.003-133.77 ppm), and Fe (0.017-1238.84 ppm) are 370.39, 77.02, 5.76, 53.28, 15.40, and 255.09 ppm respectively. Trace elements Pb (0.25 ppm), Cu (2.15 ppm), As (0.59 ppm), Zn (13.52 ppm), Co (3.22 ppm), Ni (10.87 ppm) were leached out in a considerable amount in the water phase (WF). Percentage leached for Ca, Mg, K, Na, Mn, Fe, Pb, Cu, As, Zn, Co, and Ni are 9.78%, 3.19%, 1.89%, 0.86%, 3.31%, 1.20%, 0.5%, 4.19%, 10.46%, 8.46% and 10.89%, respectively.

For the ammonium acetate leach (AMF), where the average sample concentration for Ca (34.61-1280.83ppm), Mg (9.21-96.67ppm), Na (0.43-10.84 ppm), K (10.09-546.98 ppm), Mn (0.004-174.93 ppm), and Fe (2.19- 268.74 ppm) 370.9ppm, 29.53ppm, 3.94ppm, 157.11ppm, 12.95ppm, 36.91 ppm. For the hydroxylamine leach (HF), Ca (1.95-235.67 ppm), Mg (3.15-74.14 ppm), Na (5.72-377.58ppm), K (1.54-81.14ppm), Mn (0.12-148.13ppm), and Fe (4.62-531.42ppm) their average concentrations are 82.93, 23.54, 117.86, 29.39, 4.94, 213.86 ppm respectively. The Water leach (WF) showed highest leaching values for most elements as compared to other phase. Trace elements Pb (0.61 ppm), Cu (0.28 ppm), As (1.41 ppm), Zn (0.72 ppm), Co (0.46 ppm), Ni (1.56 ppm) were leached out in the AMF, while in the HF Pb (0.83 ppm), Cu (0.76 ppm), As (1.08 ppm), Zn (2.15 ppm), Co (0.61 ppm), Ni (1.27 ppm) were leached out. The average total sulphur of the composite samples (11400 ppm) was greater than the sulphide_sulphur (8394.03 ppm) present, indicating that the tailings have considerable amount of oxidisable sulphide. The average total carbon was 700ppm. The average pH of 4.5 showed that the mine tailings were generally acidic. An average EC value of 1.27 mS/cm showed a considerable presence of leachable elements (Abegunde et al., 2016).

http://etd.uwc.ac.za/

5.3 Morphology

Morphology of a few randomly selected tailing samples were studied using SEM-EDS based on the specific horizons in the cores (Figure 5.1). The SEM image measured at 25 μm shows non-spherical shapes of varying particle sizes. Sample MT020 (1 m depth) showed inhomogeneity that did not distinguish the grains properly. The high presence of Si, Al, and low S in EDS indicated possible oxidised zones. The EDS result for Sample MT005 (5 m depth) showed a flake-like shape with sharp edges with a high value of Si, S, and Fe, yet demonstrated low Al levels compared to MT001 that indicated a more enrich zone, which were altered and contained some sulphides. Sample MT007 (about 7.8m in depth) showed smaller round shapes, flake-like shapes, and bigger particles. A low Si but high Fe and S content in this sample compared to others indicated the presence of a Fe mineral, associated with sulphides. For sample MT025 (6 m depth), the image is characterised by varying particle shapes that show high Fe and other elements. Additionally, more elements were identified in the EDS analysis. In general, the EDS analysis showed inhomogeneous distribution of particles and metals for all samples.

UNIVERSITY of the
WESTERN CAPE

http://etd.uwc.ac.za/

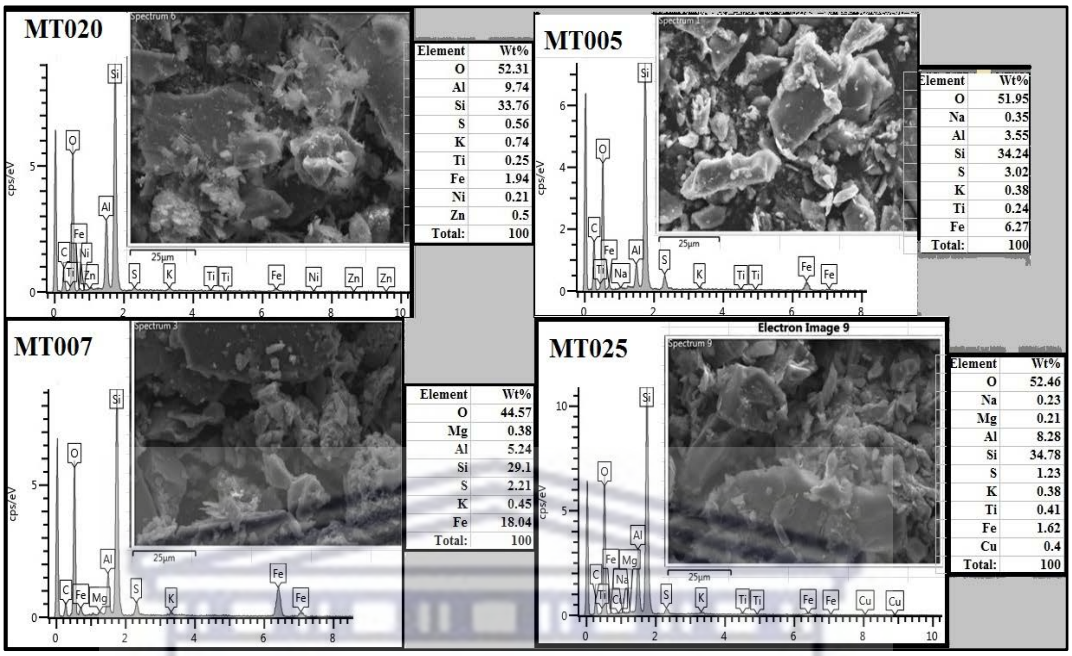

Figure 5.1: SEM-EDX analysis of selected samples representing peculiar horizon within Mogale tailings dam

5.4 Downhole Description of The SEP Results

Samples from boreholes T008 and T009 were further analysed by using SEP coupled with statistical analysis as presented in Figure 5.2 and Figure 5.3, the choice of borehole was based on the general . NB: Boreholes T008 and T009 are strategically positioned within the exploration area to capture variations in geology and potential mineralization. They are spaced in a manner that helps in understanding the lateral extent and vertical continuity of mineralization, providing valuable insights into the deposit's geometry. All the values in Figure 5.2 and Figure 5.3 were presented in mg/L and selected to have an overview of the gold tailings downhole. Generally, the water

http://etd.uwc.ac.za/

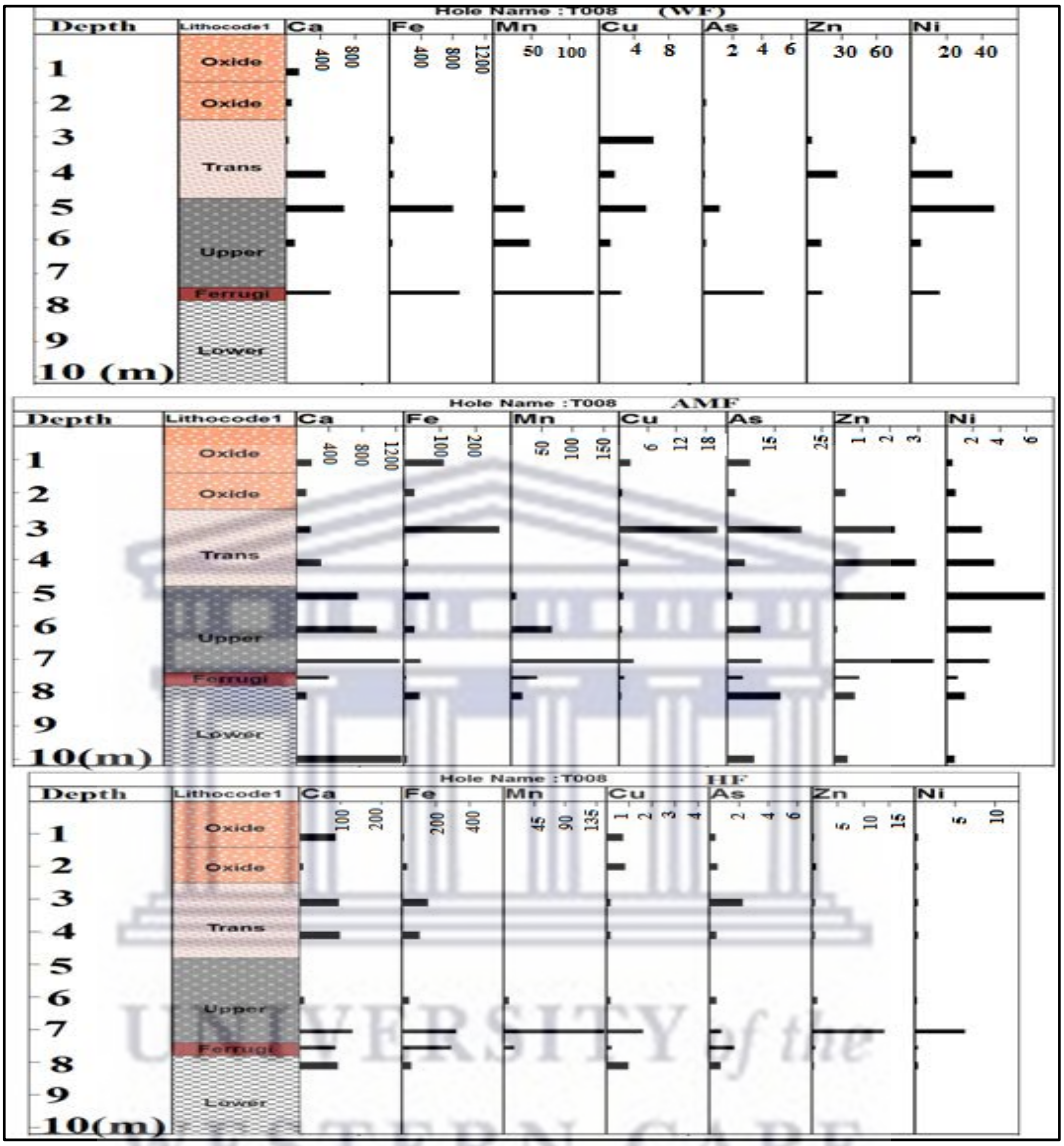

Figure 5.2: Downhole plots of selected elements from each SEP fraction in borehole T008 (measured in mg/L)

WF = Water fraction; AMF = Ammonium acetate Fraction; HF = Hydroxylamine Fraction

leach showed that more trace elements such as Zn, Cu, As and Ni were leached out by water compared to the other leachants showing their high solubility and mobility. For the major elements (Fe, Ca, and Mn), the concentration leached out in the water-leach phase increased downhole. This could be due to the available leachable material and initial elemental concentration of the tailings which increases downhole. However, a considerable amount of calcium was leached out in the water phase. This could be attributed to the presence of secondary minerals, which are the

http://etd.uwc.ac.za/

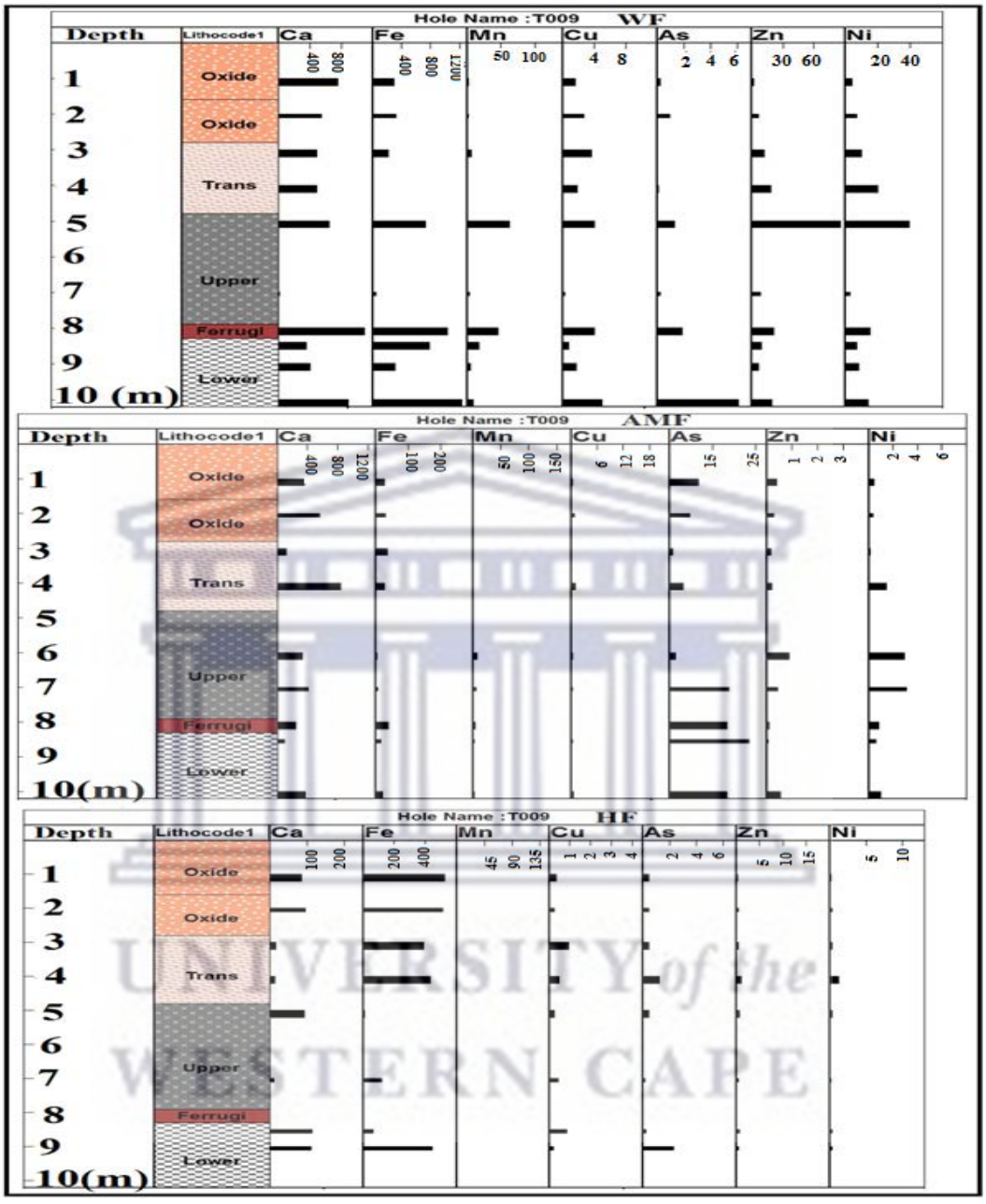

Figure 5.3: Downhole plots of selected elements from each SEP fraction in borehole T009 (measured in mg/L)

product of redox reduction derived from the oxidation and weathering of overlaying layers.

Further observations deduced showed that a general increase in leached content downhole was observed in the water phase, while more Ca was released in the ammonium acetate leachant compared to other phase(s).

http://etd.uwc.ac.za/

For T008, the concentration of Ca increased downhole but was more prominent at the base of the upper zone. Whereas for T009, it increased downhole and later decreased by demonstrating uneven weathering. The presence of high Ca in AMF indicated the presence of carbonate materials or neutralising minerals. No specific trend was observed for other major elements, except for a very low amount leached out in all samples' concentration of Mn from T009 compare to borehole T008. For the trace elements (Cu, Zn, As, Ni), there was no particular trend downhole. Although the topmost layer showed low concentrations indicating extreme download. Among the toxic trace elements, As leaching was most prominent from the two boreholes.

For the hydroxylamine fraction (HF), Fe was prominently leached compared to other major elements. Low values were observed for Mn and Ca in both boreholes. There is no particular downhole trend in the concentration of the trace elements as shown in Figure 5.2 and Figure 5.3. In borehole T009, Fe showed a high concentration between oxidised - transition zone.

Generally, sample mineralogy as shown in Figure 5.4 (XRD chromatogram) comprised of variable amounts of quartz, muscovite, pyrophyllite, gypsum, jarosite/hydronian, delhayelite, hematite, pyrite and clinochlore. Quartz, muscovite, and pyrophyllite were more prominent minerals in the sample. Samples at the upper depth or horizon demonstrated a high quantity of quartz, thereby accounted for high silica present. In the process, this demonstrates significant weathering. As part of the observations, the secondary products of oxidation of sulphide minerals, such as Jarosite and gypsum, were found mostly at the upper layers. More so, hematite was found in the samples derived from the ferruginised layer, and pyrite was found mainly from the second layer to the base layer.

http://etd.uwc.ac.za/

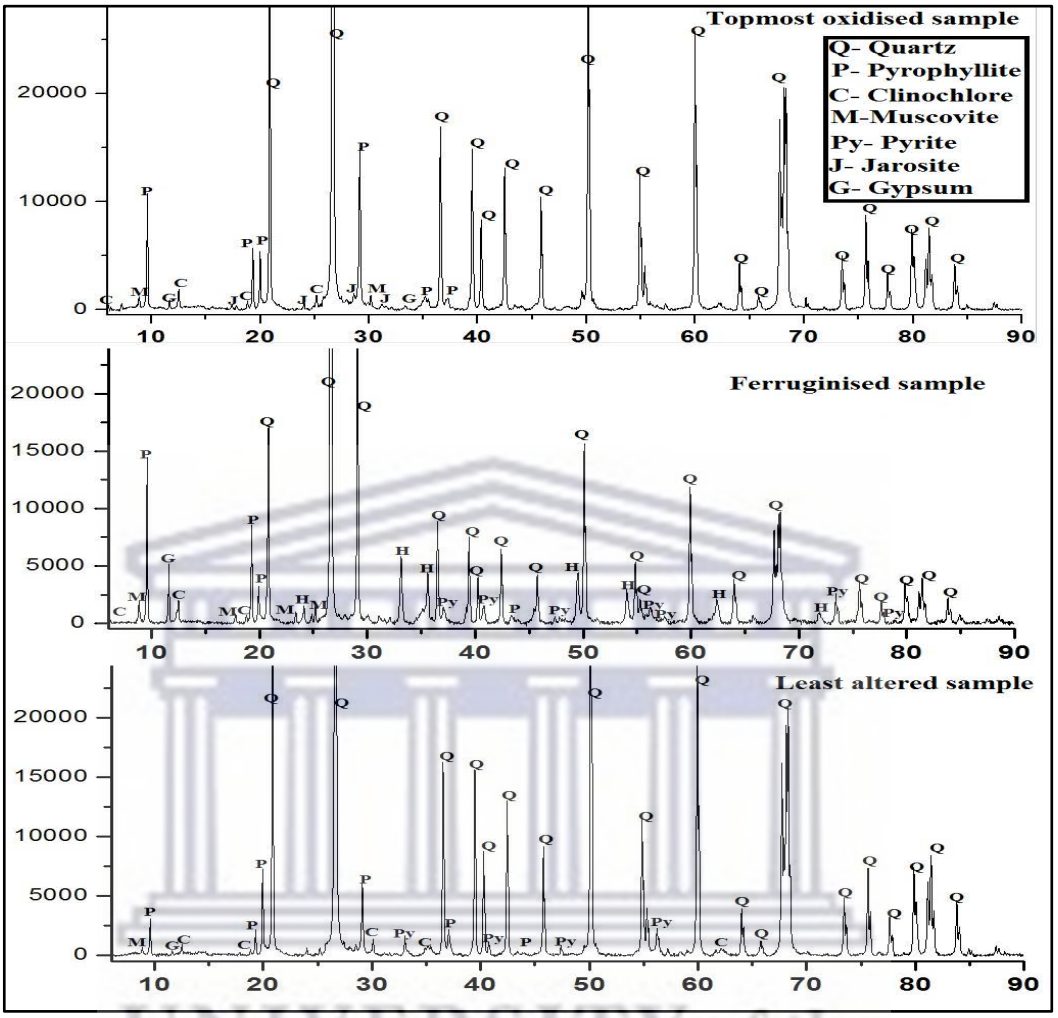

Figure 5.4: XRD results for selected representative core samples to have an overview of the mineralogy of the Mogale tailings dam

5.5 Sequential Extraction of Tailing Data

5.5.1 Water Fraction

The water-leach was classified into 5 clusters, the AMC was classified into 3 clusters, and HF was classified into 4 clusters. This was due to the number of substantial characteristics identified which defined each phase.

For the water-leached phase, leaching was observed to correspond to depth illustrated in Figure 5.4 and Figure 5.3. Trending downhole, the amount of elements

UNIVERSITY of the WESTERN CAPE
http://etd.uwc.ac.za/

Table 5.2: Tabularised illustration of gold tailing water fraction, ammonium acetate fraction and hydroxylamine fraction clusters

Sample No	Water Fraction					Ammonium Fraction			Hydroxylamine Fraction			
	WF1_AVE	WF2_AVE	WF3_AVE	WF4_AVE	WF5_AVE	AMF1	AMF2	AMF3	HF1	HF2	HF3	HF4
Ca (ppm)	68.94	365.24	507.76	534.72	1006.1	116.04	389.77	1025.35	79	108.74	68.09	81.59
Mg (ppm)	9.5	55.66	185.41	94.42	205.27	18.42	33.5	53.84	18.39	22.74	22.88	30.41
Na (ppm)	0.28	12.23	2.79	2.76	3.38	2.32	4.97	6.91	49.88	281.09	63.27	138.93
K (ppm)	32.5	55.99	71.57	61.59	62.62	91.89	166.72	318.23	32.84	29.53	26.94	26.3
Pb (ppm)	0.07	0.22	0.59	0.12	0.66	0.54	0.48	0.95	0.39	0.56	1.39	1.22
Cu (ppm)	2.15	1.38	3.31	2.02	4.54	0.46	0.06	0.1	0.52	0.56	0.98	1.03
As (ppm)	0.21	0.03	1.58	0.24	4.03	1.7	1.16	0.97	0.78	1.01	2.19	0.87
Zn (ppm)	3.02	12.65	46.65	5.47	20.34	0.38	0.9	1.37	0.45	0.32	4.95	3.62
Co (ppm)	0.85	3.08	7.68	1.7	7.49	0.27	0.59	0.81	0.4	0.42	0.88	0.82
Ni (ppm)	1.62	9.71	33.44	6.38	14.9	0.88	1.74	3.15	0.31	0.45	2.46	2.19
Mn (ppm)	6.01	5.07	67.15	2.64	27.29	1.67	8.04	49.59	0.7	0.37	27.35	0.22
Fe (ppm)	29.22	33.47	857.68	281.34	1140.02	49.17	14.03	34.74	54.79	98.13	265.67	436.73

WF- Water leach fraction cluster; AMF- Ammonium acetate fraction cluster; HF- Hydroxylamine Fraction Cluster

http://etd.uwc.ac.za/

leached increased from cluster 1 to 5 (see Table 5.2). This illustrates that leaching (clusters) is a function of concentration of elements, caused by weathering since topmost layers of the tailings dam contained low concentrations of most labile elements (Abegunde et al., 2016). Table 6.2 shows that Ca leaching range from 68.943 - 1006.1 ppm while Fe ranged from 29.215 - 1140.02 ppm from cluster 1-5. From Figure 5.5, most surface samples are found in cluster 1, while cluster 5 is mainly bottom samples. Downhole, most of the topmost layers yielded lower concentration compare to others as shown in Table 5.2.

The concentration of Ca followed a pattern of increasing value for sub-cluster 1< 2< 3< 4 < 5, for Mg and Fe concentrations sub-cluster 1< 2< 4< 3 < 5, for Zn, Co and Ni sub-cluster 1< 4< 2< 5 < 3, for As sub-cluster 2< 1< 4< 3 < 5 for Mn sub-cluster 4< 2< 1< 5 < 3. According to observations derived, high concentrations of elements were observed within clusters 3 and 5, while sub-cluster 1, 2, 4 showed lower concentrations of elements analysed for. Most samples that fell within sub-cluster 3 and 5 were samples from the enriched (Ferrugi) zones and least oxidised zone of the tailings (see Figure 5.2 and Figure 5.3). Samples from sub-cluster 1 fall within the topmost (oxide zone) layer of the tailings. This is ascribed to the weathered nature of the oxidised layer (see Figure 5.5). Hence, the water-leach phase demonstrated a definite progression of upsurge release of elements.

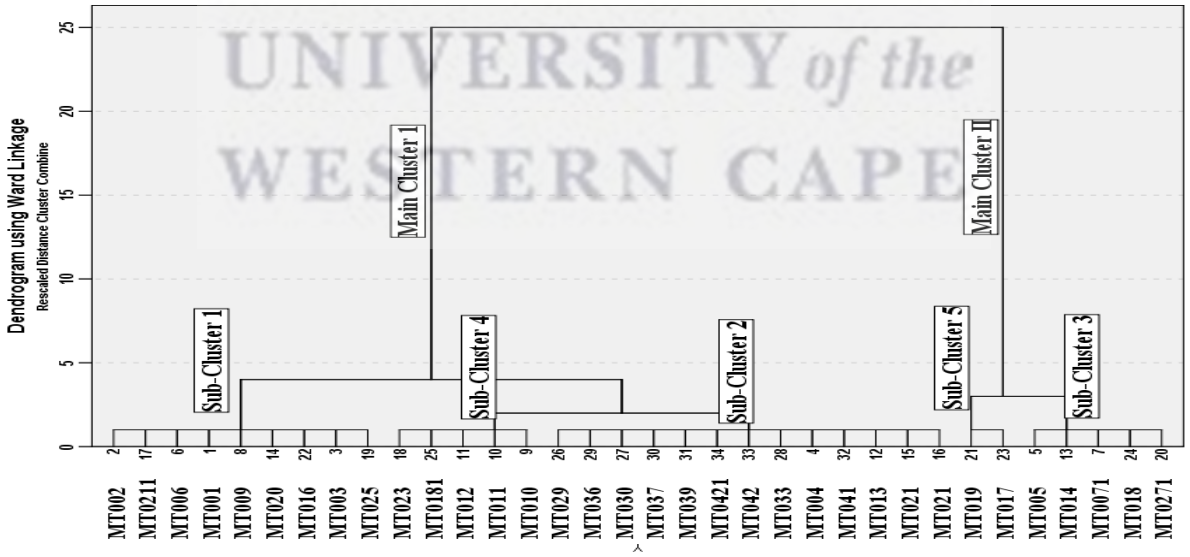

Figure 5.5: Dendrogram for water leach fraction (Fraction 1) Clustering

http://etd.uwc.ac.za/

5.5.2 Ammonium Fraction

For the ammonium acetate pH 5, the dendrogram results showed three prominent clustering relating to peculiarity in relationships within samples (see Figure 5.6).

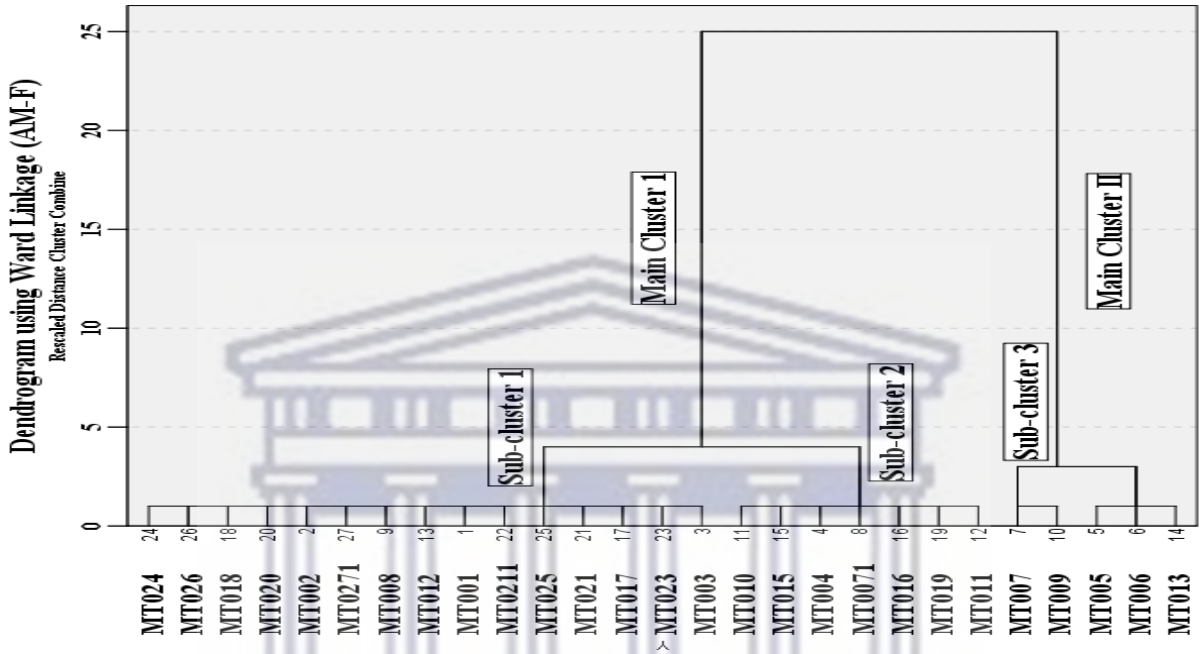

Figure 5.6: Dendrogram for Ammonium Acetate fraction (Fraction 2) Clustering

According to the illustrations in Figure 5.6, cluster 1 was defined by high leaching of Fe and As; cluster 2 was defined by high leaching of Ca and Mg compare to other elements; and cluster 3 shows high leaching of other toxic elements such as Ni and Zn. Most of the major elements except Fe showed a trend in which their concentration varied from sub-cluster 3>2>1 (see Figure 5.6). For Fe, the concentration decreases from sub-cluster 1>3>2. The average concentration of Ca for sub-cluster 3 showed the highest value of 1025.35 ppm compare to the lowest concentration in sub-cluster 1 of 116.038 ppm. The high concentration of Ca leached could be due to its association with carbonates. A considerable concentration of trace elements such as Pb, As, Ni, and Zn was leached out (see Table 5.2), while K showed a considerably high concentration (91.888- 318.232ppm).

However, the bulk of the samples fall within sub-cluster 1 and 2 (see Figure 5.6) and, does not show any correlation with depth compare to the water-leached phase (see Figure 5.2 and Figure 5.3). Only Zn and Ni demonstrated the same concentration trend as Ca in terms of the clustering pattern identified (see Figure 5.2 and Figure 5.3).

UNIVERSITY of the WESTERN CAPE
http://etd.uwc.ac.za/

5.5.3 Hydroxylamine Fraction

For the hydroxylamine phase (Mn and Fe Phase), four sub-clusters were derived (see Figure 5.7). From Table 5.2, Ca concentration ranged from 68.945 -108.74 ppm and was completely lower than the other phase. Fe showed higher concentration ranging from 54.794 - 436.725 ppm. Cluster 3 and 4 (see Table 5.2 and Figure 5.7) shows a high concentration of element except for Ca, K, Na. But cluster 4 stood out from the rest. However, cluster 3 (see Table 5.2) shows the highest trace elemental concentration release in this phase. However, each cluster has their own trend.

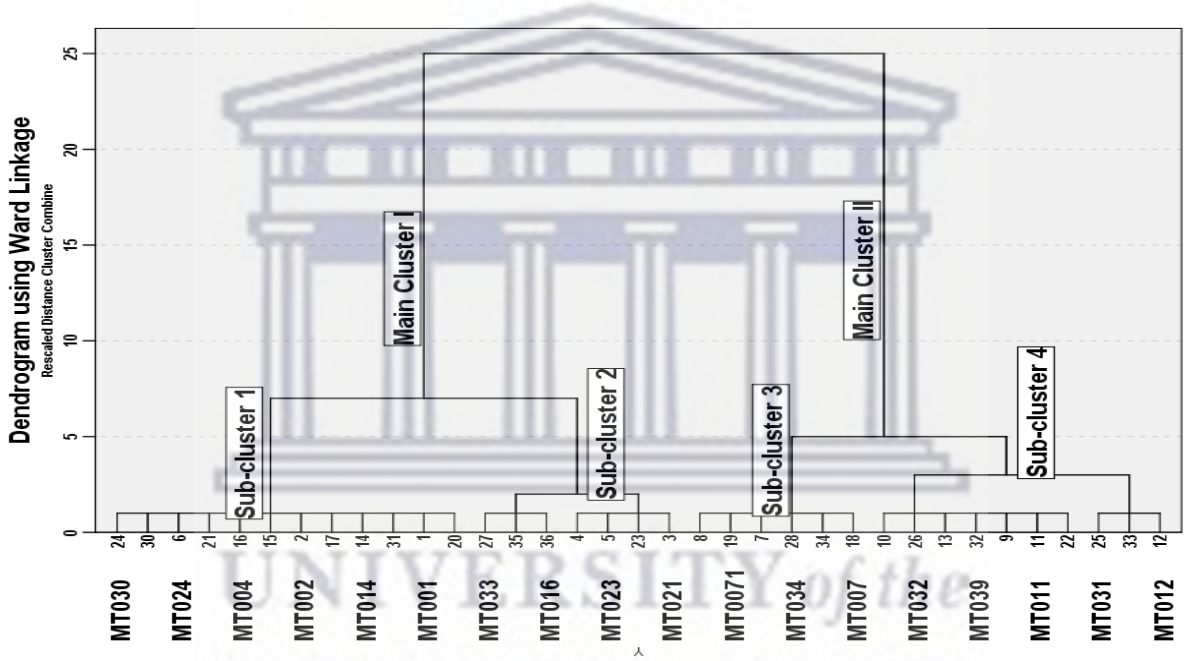

Figure 5.7: Dendrogram for Hydroxylamine fraction (Fraction 3) Clustering

From Table 5.2, it could be observed that the concentration of elements followed a pattern. For Ca Sub-cluster 2>4>1>3, for Mg sub-cluster 4> 3>2>1, for Na Sub-cluster 2>4>3>1, for Fe and Cu sub-cluster 4>3>2>1, for K sub-cluster 1>2>3>4, for Pb, Co and Ni sub-cluster 3>4>2>1, for As sub-cluster 3>2>4>1, for Mn sub-cluster 3>1>2>4. However, it can be inferred that the most element analysed plays a role in the leaching of mine tailing and proportional to the fineness of the waste materials. The cluster analysis was able to show that not until we have a harsh condition does leaching takes place and leaching in water fraction is proportional to depth. Therefore, the need to further probe the cluster analysis is inevitable.

http://etd.uwc.ac.za/

5.6 Discriminant function analysis

Using discriminant function, several functions were observed based on the variable used in the analysis. Group functions highlight the number of associations that defined the system. In this case, two-discriminant analysis were performed which are:

1. the standardised canonical discriminant function coefficient (SCDFC), which shows the various group association between variables used in terms of concentration, and

2. the structure matrix which shows an absolute correlation between each variable used including any discriminant function, which shows the variable that defines each group function.

For the water phase, four group functions (GFs) were identified that use the SCDFC (see Table 5.3). The percentage estimates of variance for GF 1, GF 2, GF 3, and GF 4 are 92.7, 4.6, 2.1 and 0.5 respectively. These values are obtained based on the effect or impact, group function 1>2>3>4. Notably, positive values indicate enrichment or accumulation while negative values indicate loss or release in terms of weathering pattern. Group function 1 (account for 92.7% of the system within the tailings) shows positive values for Fe, K, and Ca, and negative values for As and Ni. Group function 2 shows positive values for Ca, Mg, K, Na and Ni, but negative value for Zn. Group function 3 shows positive values for Mn, Na and Pb, but negative values for Ca, Ni, Zn and Cu. Group function 4 shows positive values for Ca, Ni, and Cu, and negative values for Mn and Mg. From these results, we can infer that Ca, Fe, and K are present in considerable quantity in the mine tailing. Also, play a major role in leaching and mostly associated. Since Fe presence relates to acidity, it could be inferred that as Fe ions are released, Ca ions are released to neutralise the acidity leading to the formation of secondary oxidation minerals such as gypsum and jarosite (see Figure 5.7). For Zn, As and Ni, instead of forming complexes, they are easily leached out of the tailings by acidic rain.

The structure matrix gave more clarity by indicating positive values for Fe and Mg in group function 1, with positive value for Ca in group function 2, followed by positive values for Mn, Ni, Zn, K and Cu in group function 3, and positive values for Na, Pb and As in group function 4. These four group functions define the leach.

UNIVERSITY of the WESTERN CAPE
http://etd.uwc.ac.za/

Table 5.3: Discriminant function analysis results for all SEP fractions

Structure Matrix (WF)					Standardized Canonical Discriminant Function Coefficients (WF)					Structure Matrix (AMF)			Standardized Canonical Discriminant Function Coefficients AM-F			Structure Matrix HF					Standardized Canonical Discriminant Function Coefficients HF			
	Function					Function					Function			Function			Function					Function		
	1	2	3	4		1	2	3	4		1	2		1	2		1	2	3		1	2	3
Fe	***.570****	-0.271	-0.1	0.183	**Ca**	***0.617***	***0.852***	***-0.624***	0.363	**Ca**	***.464****	-0.249	**Ca**	***1.398***	***-0.944***	**Fe**	***.697****	0.07	0.235	**Ca**	***-0.608***	-0.127	-0.071
Mg	***.148****	0.088	0.106	0.011	**Mg**	0.009	***0.798***	0.052	***-1.011***	**K**	***.122****	-0.046	**Mg**	***0.539***	***2.688***	**Na**	0.019	***-.631****	0.437	**Mg**	***1.027***	-0.063	0.069
Ca	0.158	***.337****	-0.231	-0.151	**Na**	0.422	***1.054***	0.188	***0.65***	**Na**	***.119****	0.105	**Na**	***0.999***	***1.867***	**Ca**	-0.01	***-.173****	0.018	**Na**	0.088	***-1.233***	0.445
Mn	0.091	-0.152	***.379****	0.277	**K**	***0.864***	***0.592***	**1.263**	***-0.886***	**Mg**	***.107****	0.013	**K**	***0.702***	***1.7***	**Mg**	0.059	***-.071****	0.014	**Pb**	***-1.743***	0.005	***-0.78***
Ni	0.074	0.007	***.355****	0.291	**Pb**	-0.102	-0.3	***-0.599***	***0.599***	**Ni**	***.099****	-0.013	**Pb**	***0.545***	-0.159	**Mn**	0.005	0.165	***.490****	**Cu**	0.149	0.178	***-0.59***
Zn	0.065	-0.029	***.326****	0.314	**Cu**	-0.236	-0.336	***-0.545***	0.129	**Zn**	***.066****	0.041	**Cu**	0.278	-0.242	**As**	0.011	0.118	***.484****	**As**	***-0.572***	-0.192	***0.511***
K	0.064	0.153	***.248****	-0.072	**As**	***-0.665***	0.211	-0.453	0.273	**Fe**	-0.023	***-.176****	**As**	-0.331	0.135	**Zn**	0.061	0.102	***.241****	**Zn**	***-1.913***	***-1.959***	0.368
Cu	0.027	-0.042	***-.101****	0.008	**Zn**	0.189	***-2.671***	***-0.91***	***1.521***	**Pb**	0.042	***-.137****	**Zn**	-0.367	***1.559***	**Pb**	0.055	0.059	***.238****	**Co**	-0.024	***-0.661***	***-0.57***
Na	-0.019	0.27	0.182	***.537****	**Ni**	***-0.87***	***2.329***	***1.157***	-0.437	**Cu**	-0.04	***-.128****	**Ni**	***1.264***	***-1.763***	**Co**	0.052	0.054	***.208****	**Ni**	***2.767***	***2.548***	***1.287***
Pb	0.059	0.022	0.038	***.324****	**Mn**	0.176	-0.491	***0.624***	0.057	**Mn**	0.084	***-.125****	**Mn**	***-1.176***	***-2.279***	**Ni**	0.064	0.07	***.203****	**Mn**	0.245	***0.776***	***0.839***
As	0.113	-0.061	-0.276	***.310****	**Fe**	***1.716***	-0.393	0.056	0.035	**As**	-0.073	***-.119****	**Fe**	***-1.136***	***-1.364***	**Cu**	0.057	0.035	***.109****	**Fe**	***1.371***	-0.033	-0.04

For structure matrix analysis, pooled within-groups correlations between discriminating variables and standardized canonical discriminant functions; Variables ordered by absolute size of correlation within function. *. Largest absolute correlation between each variable and any discriminant function.

http://etd.uwc.ac.za/

The elements that determined the system within the tailing are Fe, Mg and Ca. In this case, a more prominent Fe effect shows positive acidic potential despite the presence of Mg and Ca. The release of Fe ions into the surroundings can be associated with the gradual mobility or releases of toxic elements.

For the ammonium acetate pH 5 phase, two group functions were identified. The percentage estimates of variance for GF 1 and GF 2 are 95.5 and 4.5 respectively. This implies that group function 1 accounted for 95.5% of the system within the tailings Table 5.3. In group function 1, the SCDFC indicates positive values for Ca, Mg, Na, K, Pb and Ni, but negative values for Mn and Fe. Similarly, in group function 2, positive values are indicated for K, Na, Mg, Zn but negative values are indicated for Ni, Mn, and Fe. The structure matrix gave a more detailed or defined relationship. In group function 1, positive values are indicated for Ca, K, Na, Mg, Ni, Cu and Zn while group function 2 indicates negative values for Fe, Pb, Cu, Mg and As. This means that elements in group function 1 are associated with the carbonates and readily leached out in this phase as compared to group function 2.

For the hydroxylamine phase, three group functions were identified. The percentage estimates of variance for GF 1, GF 2, and GF 3 are 92.2, 6.4, and 1.3 respectively. Group function 1 accounted for 92.2% of the system within the tailings. The SCDFC indicates that Mg, Ni and Fe values are positive in group function 1, but negative values are Ca, Pb, Zn, and As. In group function 2, positive values for Ni, P, Mn were obtained, meanwhile negative values were obtained for Co, Zn and Na. In group function 3, positive values Mn, Ni, and As were obtained with negative values for Pb, Cu, Co.

The structure matrix indicates positive value for Fe in group function 1, negative values for Na, Ca, Mg in group function 2, and positive values for Mn, As, P, Cu, n, Pb, Co, and Ni in group function 3. The association observed in-group function 3 tends towards the release of elements associated with the Mn phase. This could denote that the concentration of hydroxylamine used target elements associated with the Mn Phase. Nevertheless, the positive value of Fe in GF 1 demonstrated a

http://etd.uwc.ac.za/

potential release of Fe ionic species into the environment, which has the attribute to increase the acidity of the tailings.

5.7 Factor Analysis

Principal component analysis was used to extract factors based on varimax with the Kaiser Normalisation rotation method, with eigen value >1. Values lower than ±0.3 were not considered because of their significance. In water phase, four factors were extracted (Table 5.4) : factor 1 indicates positive components for Ni, Zn, Mn, Mg, Pb, Fe, and K; factor 2 indicates positive components for Mn, Mg, As, P and Fe, but negative component for Na; also, factor 3 shows positive components for Mg, Pb, Ca, Fe and K, while factor 4 indicates positive component for Cu.

Based on eigen values greater than one, factor 1, 2, 3 and 4 represent 32.685%, 18.087%, 16.037% and 13.976% of the sample respectively. These estimates denote the order of relevance of the four factors. Clearly, this accounts for a cumulative sum of 80.786% of the sample. Out of the four factors, Fe contributed to 3 factors that indicate presence of Fe ions (assuming Fe^{2+} and Fe^{3+}) responsible for the acidity increase of the tailings.

In the effect, factor 1 represents the most labile elements that can be easily leached. And factor 3 neutralizing agents such as Ca and Mg carbonates, which do not play an integral role than Fe and thereby provided insufficient neutralisation potential.

In the case of ammonium acetate phase, three factors were identified. Based on eigen values greater than one, Factor 1, 2 and 3 represent 33.130%, 20.055% and 16.897% of the sample respectively. These estimates denote the order of relevance of the factors. This accounts for a cumulative sum of 70.082% of the sample. Factor 1 indicates positive values for Ca, Mg, Na, Zn, Ni, Mn and Fe, but negative values for As; factor 2 indicates positive values for Ca, K, Pb and Mn; and factor 3 indicates positive values for Cu, As and Fe. In factor 1, the effect of the carbonates present on the acidity was observed when Ca associate with Fe. And this denotes that the tailings contained a considerable amount of neutralising potential. Therefore, as leaching conditions become stronger, there is a tendency for an increase in alkalinity within the tailings.

UNIVERSITY of the WESTERN CAPE
http://etd.uwc.ac.za/

Table 5.4: Factor analysis result for all SEP fraction (Extraction Method: Principal Component Analysis. Rotation Method: Varimax with Kaiser Normalization

Rotated Component Matrix[a] (WF)					Rotated Component Matrix[a] AM-F				Rotated Component Matrix[a] HH-F					
	Component					**Component**				**Component**				
	1	**2**	**3**	**4**		**1**	**2**	**3**		**1**	**2**	**3**	**4**	**5**
Ni	**0.931**				**Ca**	**0.61**	**0.618**		**Ni**	**0.976**				
Zn	**0.929**				**Mg**	**0.797**			**Zn**	**0.951**				
Mn	**0.691**	**0.55**			**Na**	**0.756**			**Pb**	**0.946**				
Mg	**0.668**	**0.341**	**0.437**		**K**		**0.904**		**Cu**	**0.925**				
Pb	**0.53**		**0.525**		**Pb**		**0.732**		**As**		**0.914**			
As		**0.804**	**0.337**		**Cu**		**,**	**0.85**	**Ca**			**0.908**		
Fe	**0.469**	**0.7**	**0.394**		**As**	**-0.472**		**0.69**	**Mg**	***0.517***		**0.587**		
Na		**-0.543**			**Zn**	**0.835**			**K**				**0.878**	
Ca			**0.884**		**Ni**	**0.814**			**Fe**	***0.357***	***0.353***		**-0.502**	
K	**0.405**		**0.772**		**Mn**	**0.581**	**0.581**		**Na**					**0.813**
Cu				**0.957**	**Fe**	***0.304***		**0.659**	**Mn**	***0.363***				**-0.61**

a. Rotation converged in 5 iterations

http://etd.uwc.ac.za/

http://etd.uwc.ac.za/

For the hydroxylamine phase, there were a greater number of factors of more complexity. In this case, only five factors were identified. Based on eigen values greater than 1, factor 1, 2, 3, 4 and 5 represents 38.788%, 14.620%, 10.542%, 8.794%, 8.475% of the sample respectively. More so, factor 1 indicates positive values for Ni, Zn, Pb, Cu, Mg, Fe and Mn; factor 2 indicates positive values for As and Fe; factor 3 indicates positive values for Ca and Mg; followed by factor 4 which indicate positive value for K and negative value for Fe; and lastly factor 5 showed positive value for Na and negative value for Mn. This means that most trace elements such as Ni, Zn, Pb, and Cu are associated with the Fe/Mn oxides, and easily transport with the acid generating ions.

5.8 Summary

The inhomogeneous characteristics of the mine tailings particles from the SEM image were revealed, while surface samples show the presence of reactivity. However, the statistical analysis was able to establish that pH or acidity, Fe ions, Ca^{2+} and Mg^{2+} played a major role in the released metals. Out of the five associations identified in cluster analysis results for Water fraction (WF), A more prominent Fe effect showed positive acidic potential despite the presence of Mg and Ca. For the water phase, the release of Fe ions into the surroundings can be associated with the gradual mobility or releases of toxic metals.

In the case of the Ammonium acetate fraction (AMF), cluster analysis and discriminant analysis confirmed that elements associated with the carbonates are also relatively leached out in this phase.

For HF, association observed in-group function tends towards the release of elements associated with the Fe/Mn phase, which could imply that increase in acidity is proportional to elements mobility. Most trace elements such as Ni, Zn, Pb, and Cu are associated to the Fe/Mn oxides are loss, thus easily transport with the acid generating ions.

As the leaching environment becomes harsh (AMF) and more carbonates are released, then more Ca ions are released. In the end, the available Fe ions react to

http://etd.uwc.ac.za/

produce more acidity (HF), which then caused more trace elements to be released. That is why zones of accumulation showed increased pH compare to the topmost and the bottommost layers. The trends observed in the carbonate phase showed that despite the posit of acidity, the tailings contain a considerable amount of neutralising agent to serve as a buffer. The trend observed in the Mn and Fe phase showed that in the long-run, the Fe ions released will overcome the buffer system within the tailings and more acidity are produced. And thereby release toxic metals.

Out of the four factors identified in factor analysis results for Water fraction (WF), Fe contributed to 3 factors which showed the presence of Fe ions (assuming Fe^{2+} and Fe^{3+}) responsible for the increased acidity of the tailings. A more prominent Fe effect showed positive acidic potential despite the presence of Mg and Ca. For the water phase, the release of Fe ions into the surroundings can be associated with the gradual mobility or releases of toxic metals. Factor 1 represent the most labile elements that can be easily leached while factor 3 represented the presence of neutralizing agents such as Ca and Mg carbonates but did not play a more integral role than Fe, thereby could not provide enough neutralisation potential.

In the case of the Ammonium acetate fraction (AMF), Factor analysis indicated that Ca was associated with Fe. This demonstrates the effect of the carbonates found on the acidity, and the tailings contain a considerable amount of neutralising potential. Therefore, as leaching conditions become stronger, there is a tendency for an increase in alkalinity within the tailings.

The factor analysis showed that the positive value of Fe reflected the potential release of Fe ionic species into the environment, which can increase the acidity of the tailings. Most trace elements such as Ni, Zn, Pb, and Cu are associated to the Fe/Mn oxides are loss, thus easily transport with the acid generating ions.

http://etd.uwc.ac.za/

CHAPTER SIX

6 COMPARATIVE ANALYSIS OF FINDINGS

6.1 Discussion

This chapter discussed the results from chapter 4 and 5 in conformation with the aims and objectives of the study. The analysis of the composition of major oxides and heavy metals present in the tailing dam and coal fly ash, and the use of statistical techniques to make notable inference in relation to the objectives:

6.2 Mineral and Elemental Composition of The Mogale Tailing Dam and Coal fly ash

The five drilled holes (T004, T008, T009, T010, and T011) were sampled and classified into four distinct layers. (Nengovhela et al., 2006) classified the tailing dam into three zones, which are the oxidized, transition and decreased zone (otherwise known as un-oxidized zone) (Abegunde et al., 2016). Except for the third layer (which is a distinct reddish layer) (table), the other three layers describe indicating that the third layer is peculiar to Mogale tailing dam (Nengovhela et al., 2006; Abegunde et al., 2016). Based on the fact that, slime (tailing) dam oxidized to the depth 2m by (Oelofse et al., 2007) while the oxidized zone (saturated) is said to be between the 0m to 3.5m by (Nengovhela et al., 2006; Abegunde et al., 2016) and the transition zone between the oxidized and un-oxidized zone. The oxidised layer varied from 2.4m to 3.2m from the results within all five boreholes.

For the coal fly ash, three drilled holes (S1, S2 and S3) were sampled and could only be classified as fresh sample 0-0.5m (Eze et al., 2013; Madzivire et al., 2014), weathered sample and non-weathered samples (Eze et al., 2013; Madzivire et al., 2014). No transition zone was found.

6.2.1 Mineralogy

In the gold tailings, Quartz have dominantly been found and contained about 70 to 90% (table), other minerals such as pyrophyllite, and muscovite, chlorite (Rösner, 2001; Winde & Walt, 2004; Bezuidenhout & Rousseau, 2006; Nengovhela et al.,

http://etd.uwc.ac.za/

2006; Abegunde et al., 2016). In the coal fly ash, Quartz have dominantly been found and contained about 45 to 55%. Three prominent mineral phases quartz, mullite and lime were mainly detected in the fresh fly ash, however in the weathered fly ash the three prominent mineral phases detected were quartz, mullite and calcite(Behera & Mohapatra, 2018; Eze et al., 2013; Ayanda et al., 2012; Eze, 2011; Vassilev & Vassileva, 2007). For core S1 and S3, more minerals phases were identified as compared to core S2. Lime and calcite ($CaCO_3$) were detected but as minor peaks as well as minor phases of kaolinite ($Al_2(Si_2O_5)(OH)_4$) and nitratine ($NaNO_3$) were also detected. Nitratine is a tertiary mineral that may have produced by the interaction of brine with the coal fly ash or because of the drying procedure in the sample preparation before analysis (Eze et al., 2013).

The kaolinite could have resulted from the alteration of the glass phase. No prominent Fe oxides was found as compared to the gold tailings. Halite, bassanite, nitratine, hydrophitte, microline and albite are relatively low concentrations, and therefore considered as transient mineral produced because of interaction of brine with the coal fly ash(Eze et al., 2013). The XRD results revealed a similar trend from the topmost sample downhole to the bottom. Mullite ($3Al_2O_32SiO_2$ or $Si_2Al_6O_{13}$) is produced when kaolinite [$Al_2Si_2O_5(OH)_4$] present in the parent coal goes through phase alteration under the high temperatures (1200 - 1400 °C)(Zhang et al., 2022). It can be observed from the XRD analysis that the weathered fly ash samples obtained from the cores did not display mineralogical inhomogeneity. However, it somewhat gave a constant trend from the top of the ash dam, down to the bottom of each core. This mineralogical constancy shown by XRD however probably points to the constraint of XRD as an analytical tool in that it can only detect comparatively copious crystalline mineral phases, and not identify amorphous material or minerals existing in low concentration (Luhar & Luhar, 2022).

The mineralogy of the gold tailings has a similar mineralogy with Witwatersrand geology (Abegunde et al., 2016) because no special process was done as compared to coal fly ash that goes through combustion. This shows that the gold tailings are gangue materials after gold has been extracted. The XRD was able to detect a total

http://etd.uwc.ac.za/

number of nine different minerals (quartz, muscovite, pyropyllite, gypsum, jarosite, Delhayelite, hematite, pyrite and clinochor are present). Quartz is by far the most dominant mineral in all the samples (Abegunde et al., 2016; Camden-Smith et al., 2015; Nengovhela et al., 2006; Bezuidenhout & Rousseau, 2006), while pyropyllite was the second in abundance (Rösner, 2001; Nengovhela et al., 2006), there is variation in the amount of jarosite, gypsum, and pyrite present in the samples, and these are the indicators of oxidized tailings and extent of generated AMD (Hobbs & Cobbing, 2007; Oelofse et al., 2007).

From these results, the actual percentage of minerals present is not known, but major, minor and trace minerals can be known through the peaks present. This could not confirm the percentage of minerals in the tailings dam as compared to literature (Rösner, 2001; Bezuidenhout & Rousseau, 2006). The results show the presence of quartz in abundance in every sample result. Samples at the top are unique because of the absence of pyrite, indicating that the first and second meter might have been completely oxidized.

The presence of delhayellite has not been observed in any mineralogical of the Witwatersrand gold ore and tailings, except for this study and therefore questionable. Delhayellite could be traced to have been present ever since the start of the tailing dam and because of its unreactive nature. Delhayelite is known to be an aluminosilicate that can be found within the framework of rhodesite meroplesiotype series (Pushcharovsky et al., 2011).

Primarily, the oxidation of sulphide minerals results in the production of secondary minerals such as jarosite and gypsum (Abegunde et al.,2016; Vermeulen, 2001; Rösner & Schalkwyk, 2000). There is a variation in jarosite in respect to pyrite because its peaks become more prominent at the absence of pyrite. It was observed that jarosite is dominant only in samples on or closely beneath the tailing dam surface where there is no or slight trace of pyrite. As we move down the tailings, pyrite surfaced (transition) and at a depth of an average 5m below, it became prominent (un-oxidized).

http://etd.uwc.ac.za/

The reddish samples contain hematite, which accounted for their coloration. The reddish layer found around 7.4m to 8.3m does not represent oxidation but rather might have been deposited from the onset formation of the tailing dam showing the richness of the tailing dam in Fe, S and its associated elements. Alternatively, it could be because of oxidation of Fe_2S to form its oxide as the slime drained downward and settled down on this layer. No literature obtained highlighted the presence of this reddish layer (Figure 5.2) . This could be peculiar to Mogale tailing dam.

In addition, most of the samples contain gypsum, a secondary mineral that can be suspected to have its origin from dolomitic compound (responsible for the neutralization with sulphuric acid generated). Its presence is more prominent on surfaced samples than beneath. Gypsum was found throughout the sample but was more profound in the first 2 to 3 meters.

6.2.2 Geochemistry

For coal fly ash the major element shows a range of SiO_2 (32.87 – 58.86%) >Al_2O_3 (11.87 – 25.70%) > LOI (3.18 – 33.15%) >CaO (6.15 – 11.24%) >Fe_2O_3 (2.19 - 10.41%) > K_2O (0.75 – 4.41%) > MgO (1.78 – 3.31%) > Na_2O (2.18 – 3.17%) > TiO_2 (1.44 -2.12%) > P_2O_5 (0.36 – 0.95%) > MnO (0.05 – 0.12%) > SO_3 (0.01 – 0.04%) Table 4.1. High LOI indicates high presence of organic content with very negligible presence of sulphides increasing the mechanical properties of the coal fly ash. Ca and Fe are present in a considerable high quantity but Fe-rich minerals was not detected (could be in amorphous phase) by XRD while Ca-rich minerals were discovered. A considerable high presence of LOI as compared to the gold tailings. Results showed likely tendency of an alkaline environment.

The chemical analysis conducted determines the concentration of major oxides SiO_2 (50.91 %), Al_2O_3 (25.49 %), CaO (8.10%), Fe_2O_3 (2.27%), MgO (1.87 %), Na_2O (2.21 %), TiO2 (1.87 %), K_2O (0.95 %), P_2O_5 (0.71 %), SO3 (0.03%) and MnO (0.05 %) that are contained in the fresh Secunda fly ash samples, with considerable

http://etd.uwc.ac.za/

presence of minor elements such Sr (4160 ppm), Ba (2749 ppm), Th (1922 ppm), Zr (664 ppm), Y (156 ppm), Ce (117 ppm), Nb (109 ppm), As (61 ppm), Co (32 ppm), Ni (23 ppm), Pb (28 ppm), Rb (16 ppm) and V (15 ppm) Table 4.1 (Table 4.1).

The Geo. mean results for the concentration range and its average of the following major elements SiO_2 (44.44 - 46.98 %, =45,71%), Al_2O_3 (22.34 -23.49%, =22,915%), CaO (8.1-8.98%, = 8,54%), and LOI (7.91- 10.1%, =9.005%), accounted for about 82.79 – 89.4% (average = 86.095%) of all the samples estimated. Therefore, the total percentage of SiO_2, Al_2O_3, and Fe_2O_3 (3.47%) exceeded 70% of the total sample (72,095%), which is peculiar to class F type of coal fly ash (Vassilev & Vassileva, 2007). For the trace element, observation shows that the concentrations of Ni, Nb, Cu, Co, Ce, Ba, Th, Zr, Y, V, Sr, Rb and Pb have maximum values of 60.55 ppm, 169.40 ppm, 3758.71 ppm, 51.19 ppm, 248.08 ppm, 3476.33 ppm, 2718.17 ppm, 832.81 ppm, 205.14 ppm, 121.50 ppm, 5742.02 ppm, 134.54 ppm and 48.08 ppm, respectively. And the maximum concentration of As in all dried cores exceeded 100 ppm.

For gold tailings, The major elements show a trend of SiO_2(84.24%)> Al_2O_3(6.25%)>LOI(3.28%)>Fe_2O_3(2.64%)>CaO(0.43%)>MgO(0.35%)>K_2O(0.32%)>TiO_2(0.24%)>Na_2O(0.07)>Cr_2O_3(0.04%)>MnO(0.02%) ≈ P_2O_5(0.02%) Table 5.1(Table 5.1) in terms of its relative abundance. This trend generally characterised the properties of gold tailings as compared to the other tailing dams in the Witwatersrand (Rösner & Schalkwyk, 2000; Rösner, 2001).

The most prominent major oxides present in the tailing dam are SiO_2, Al_2O_3, Fe_2O_3 and volatiles (LOI). The total carbon content of up to 0.2 % wt is indicative of a significant content of organic matter in the mine tailings (Rösner & Schalkwyk, 2000; Rösner, 2001).

SiO_2 is the most abundant major element and reflects the high presence of quartz revealed by the mineralogy (Figure 5.4). There is variation for Fe_2O_3 present, which could be because of the method of gold extraction. Also, CaO and MgO could be said to be responsible for the presence of carbonates that neutralise the acid

http://etd.uwc.ac.za/

generated within the tailings (Rösner & Schalkwyk, 2000; Bezuidenhout & Rousseau, 2006)

Tailing dams in Witwatersrand basin often contain elevated levels of radioactive and chemo-toxic heavy metals as presented in (Winde & Walt, 2004) which was not seen in the coal fly ash. The contents of U, Hg As, Co, Cu, Pb, Zn, Ni in (Table 5.1) are however significantly higher than is permissible in mine waste (Hobbs & Cobbing, 2007).

The presence of total sulphur ranges from 0.26-2.19%: and points to a significant potential acid generating capacity of the tailings dam (Nengovhela et al., 2006). Low total sulphur in the uppermost layer suggests an extensive depletion in sulphides in the horizon.

In terms of the trace elements, As, Co, Cu, Pb, Zn, Ni of pyritic association are highly correlated with total S and Fe_2O_3 and show considerably high mean concentration, and that is why they are correlated with total S and Fe_2O_3. In addition, U shows a considerable high concentration and therefore, a possible source of radioactive transport into the environment. As observed, the surface layer of the tailings shows depletion, this might imply that possible transportation or leaching away of Uranium. Zr is also present in considerable amount. Therefore, the tailing dam could be said to be uraniferous-gold tailing. The concentration of Au indicates that tailings could still be reprocessed for gold.

Since the results shows that the tailing dam is generally acidic in pH, this implies that the tailings generate acid mine drainage and these related heavy metals will percolate into the underlying layers under normal condition, and negatively decreases the pH down hole (thus, responsible for the low pH of the tailings).

It should be noted that the acidity of the tailings is because of the presence of and oxidation of pyrite and other mineral sulphides. Related heavy metals present accompanied depositional oxidation of tailings and vary in the tailing dam. However, there is presence of buffer reactions, within the tailings but its acid potential is greater than the neutralisation potential.

UNIVERSITY of the WESTERN CAPE
http://etd.uwc.ac.za/

It should be noted that the gold tailings contained high concentrations of SiO_2 as compared to coal fly ash, but the presence of sulphides accounted for a possible acid generation potential. Both wastes showed the presence of Ca, which could be as a result of added lime acting as a neutralising agent, while the brine present in coal fly ash could activate more salt formation.

6.2.3 Cluster Analysis

The hierarchical clustering analyses produced for water fraction, carbonate fraction and hydroxylamine fraction are represented on dendrogram (Figure 5.2, Figure 5.3 and Figure 5.4). The water-leach was classified into two main clusters and six sub clusters, and carbonate fraction was classified into two main clusters and five sub clusters, while hydroxylamine fraction was classified into two main clusters and seven sub clusters. The two major clusters (Table 4.3) of the coal fly ash samples are characterised by their variable contents in SiO_2, Fe_2O_3, CaO, LOI and Al_2O_3. Observation from water phase leachates indicated that elements such as Si, Al, Ca, Na and K showed high concentrations in water leach, while Fe, Mg, Sr and other elements demonstrated low concentrations.

However, elements with low concentrations in the water fraction have no significant impact on the acidity of the coal fly ash, which implies that most toxic elements are mostly inert. Therefore, elements such as Fe has no significant impact on the acidity of the tailings. On the other hand, the elements with high concentrations in the water fraction have significant impact on the acidity of the coal fly ash, which specifies that they are active. Thus, elements such as Ca has high significant impact, with active carbonate groups that can neutralise any presence of Fe species in the water fraction. However, many of these elements were detected due to the mining activities undertaken around the wastes.

Similar to water fraction, In the carbonate leachates (Table 4.3), it is noted that elements such as Si, Al, Ca demonstrated high concentrations, but Na and K have low concentrations along with other elements like Fe, Mg, Sr, etc. Although, there are some elements with lower concentrations in each sub-cluster. From the results,

http://etd.uwc.ac.za/

leaching ranges for Si, Al and Ca appeared greater than in water fraction. High concentration of Calcium indicated that as the leaching condition becomes harsher, more Ca ions are released to neutralised any potential release of acid, buffering a more like alkaline environment. Fe plays no major role, which pointed to the its in-reactivity.

The Hydroxylamine fraction showed seven sub-cluster containing the concentration of different elements in samples (Table 4.3). Elements such as Si, Al, Ca and Fe demonstrated high concentrations in hydroxylamine fraction, whereas other listed elements in the table indicated low concentrations. Elements with higher leaching concentration such as Si ranges approximately from 1500 ppm – 30100 ppm, with Al leaching ranges approximately from 380 ppm – 13000 ppm, followed by Ca leaching ranges from 1000 ppm – 4000 ppm and Fe leaching ranges from 1100 ppm – 5000 ppm. Unlike water leaching and carbonate fractions, the concentration of Fe in the hydroxylamine fraction is higher in quantity. This indicated that as the leaching condition become harsher, Fe ions were released.

For the sequential extraction result of the gold tailings, the water-leach was classified into two main clusters and five sub clusters, and carbonate fraction was classified into two main clusters and three sub clusters, while hydroxylamine fraction was classified into two main clusters and four sub clusters. The two major clusters of the coal fly ash samples are characterised by their variable contents in Fe_2O_3, CaO and Al_2O_3.

For the water-leached phase, leaching was observed to correspond to depth illustrated in Figure Figure 5.2 and Figure 5.3. Trending downhole, the number of elements leached increased from cluster 1 to 5 (Table 5.2). Table 5.2 shows that Ca leaching range from 68.943 - 1006.1 ppm while Fe ranged from 29.215 - 1140.02 ppm from cluster 1-5. From Figure 5.6, most surface samples are found in cluster 1, while cluster 5 is mainly bottom samples. Downhole, most of the topmost layers yielded lower concentration compare to others as shown in Table 5.2. More Fe ions leached out during this phase indicating a more mobile Fe ions which could be responsible for the release of toxic elements.

http://etd.uwc.ac.za/

For the ammonium acetate phase, high leaching of Fe and As; cluster 2 was defined by high leaching of Ca and Mg compare to other elements; and cluster 3 shows high leaching of other toxic elements such as Ni and Zn. Most of the major elements except Fe showed a trend in which their concentration varied from sub-cluster 3>2>1 (see Figure 5.6 and Table 5.3). More minor elements were leached out as compared to coal fly ash.

For hydroxylamine fraction, Ca and Fe showed high concentrations and the discriminant function show association of the release of trace elements to be association with Fe and Ca (Table 5.3).

However, it can be inferred that the most element analysed plays a role in the leaching of mine tailing and proportional to the fineness of the waste materials. The cluster analysis was able to show that not until we have a harsh condition does leaching takes place and leaching in water fraction is proportional to depth. Therefore, the need to further probe the cluster analysis is inevitable.

6.3 Factor Analysis

For the water Phase in coal fly ash Table 4.9, factor 1 represents the most labile elements that can be easily leached Mg shows no correlation with Ca. And factor 2 shows Ca carbonates, which play a prominent role as it is responsible for trace such as Zn and Cu. Fe didn't really play a major role and could require a stronger solution or environment to release it. The fact that it is not associated with mobile element shows it could have been introduced.

In gold tailings water phase, out of the four factors, Fe contributed to 3 factors that indicate presence of Fe ions (assuming Fe^{2+} and Fe^{3+}) responsible for the acidity increase of the tailings Table 5.4. Factor 1 represents the most labile elements that can be easily leached with Fe playing a major role. And factor 3 neutralizing agents such as Ca and Mg carbonates, which do not play an integral role than Fe and thereby provided insufficient neutralisation potential.

For coal fly ash ammonium phase Table 4.8 and Table 4.9, the effect of the carbonates present on the acidity was observed when Ca associated with Mg and

UNIVERSITY of the WESTERN CAPE
http://etd.uwc.ac.za/

shows negative relationship with Fe. And this denotes that the coal fly ash contained a considerable amount of neutralising potential. Therefore, as leaching conditions become stronger, there is a tendency for an increase in alkalinity within the tailings

For gold tailing ammonium phase, the effect of the carbonates present on the acidity was observed when Ca associate with Fe. And this denotes that the tailings contained a considerable amount of neutralising potential.

For the coal hydroxylamine fraction Table 4.8 and Table 4.9, there were several factors playing a role as compared to gold tailing, most trace elements such as Ni, Zn, Pb, and Cu are not associated with the Fe/Mn oxides. Ca played a major role which could be as a result of added lime to the coal fly ash and factor indicated the presence of carbonates form as a result of weathering that created secondary product. Factor analysis indicated that Ca was no associated with Fe. This demonstrates the effect of the carbonates found alkalinity, and the coal fly ash contain a considerable amount of neutralising potential with less or without the presence of Fe ions. Therefore, as leaching conditions become stronger, there is a tendency for an increase in alkalinity within the coal fly ash but there is possibility mobile Fe ions are not present in abundance. There is great possibility that more Fe element present were released during the coal fly ash processing.

For gold tailing hydroxylamine phase Table 5.4, factor 1 indicates positive values for Ni, Zn, Pb, Cu, Mg, Fe and Mn; factor 2 indicates positive values for As and Fe; factor 3 indicates positive values for Ca and Mg; followed by factor 4 which indicate positive value for K and negative value for Fe; and lastly factor 5 showed positive value for Na and negative value for Mn. This means that most trace elements such as Ni, Zn, Pb, and Cu are associated with the Fe/Mn oxides, and easily transport with the acid generating ions. As the leaching environment becomes harsh (AMF) and more carbonates are released, then more Ca ions are released. In the end, the available Fe ions react to produce more acidity (HF), which then caused more trace elements to be released. That is why zones of accumulation showed increased pH compare to the topmost and the bottommost layers. The trends observed in the carbonate phase showed that despite the posit of acidity, the tailings

http://etd.uwc.ac.za/

contain a considerable amount of neutralising agent to serve as a buffer. The trend observed in the Mn and Fe phase showed that in the long-run, the Fe ions released will overcome the buffer system within the tailings and more acidity are produced. And thereby release toxic metals.

UNIVERSITY of the
WESTERN CAPE

http://etd.uwc.ac.za/

CHAPTER SEVEN

7 CONCLUSIONS AND RECOMMENDATIONS

Summary of the mineralogy of Coal Fly Ash and Gold Tailings

Coal Fly Ash:

- **Source:** By-product of coal combustion in power plants.
- **Mineralogical Composition:** Primarily quartz, mullite, lime, with additional phases like kaolinite and nitratine.
- **Weathering:** Subjected to weathering in dump areas, leading to the formation of new minerals.
- **Interactions:** Interaction with brine may lead to nitratine formation.

Gold Tailings:

- **Source:** Residue from gold ore processing, stored in tailings ponds.
- **Mineralogical Composition:** Mainly quartz, muscovite, pyrophyllite, gypsum, jarosite, delhayelite, hematite, pyrite, clinochlore.
- **Weathering:** Shows signs of weathering over time in tailings .
- **Interactions:** Oxidation of sulphide minerals results in secondary products like jarosite and gypsum.

Commonalities:

- **Quartz Presence:** Both contain a significant amount of quartz.
- **Weathering Effects:** Both materials exhibit signs of weathering and alteration over time.

Differences:

http://etd.uwc.ac.za/

- **Source and Composition:** Coal fly ash is a by-product of coal combustion, while gold tailings result from ore processing.
- **Mineral Phases:** Specific mineralogical composition varies between coal fly ash and gold tailings.
- **Formation Conditions:** Conditions for mineral formation (e.g., mullite) differ.
- **Interactions:** Coal fly ash may interact with brine, leading to nitratine formation, which is not observed in gold tailings.

In summary, while both coal fly ash and gold tailings share commonalities such as the presence of quartz and signs of weathering, their distinct sources, compositions, and mineralogical characteristics set them apart. Understanding these differences is crucial for assessing their environmental implications and potential impacts.

Summary of comparison between Coal Fly Ash and Gold Tailings Geochemistry:

1. **Composition:**
    - **Coal Fly Ash:**
        - **Major Elements:** SiO2 (32.87 – 58.86%), Al2O3 (11.87 – 25.70%), CaO (6.15 – 11.24%), Fe_2O_3 (2.19 -10.41%).
            - **Geo. Mean (Major Elements):** SiO_2 (45.71%), Al2O3 (22.915%), CaO (8.54%).
            - **LOI (Loss on Ignition):** High LOI (3.18 – 33.15%) indicating organic content.
            - **Trace Elements:** Sr, Ba, Th, Zr, Y, Ce, Nb, As, Co, Ni, Pb, Rb, V.
    - **Gold Tailings:**

http://etd.uwc.ac.za/

- **Major Elements:** SiO_2 (84.24%), Al_2O_3 (6.25%), CaO (0.43%), Fe_2O_3 (2.64%).
- **Carbon Content:** Up to 0.2% wt, indicating organic matter.
- **Trace Elements:** Elevated levels of U, Hg, As, Co, Cu, Pb, Zn, Ni, Zr.
- **Sulphur Content:** 0.26-2.19%, suggesting potential acid generation.

2. **Acid Generation Potential:**
   - **Coal Fly Ash:**
     - **LOI Significance:** High LOI indicates organic content, enhancing mechanical properties.
     - **Environment:** Likely tendency of an alkaline environment.
   - **Gold Tailings:**
     - **Sulphur Content:** Significant sulphides suggest potential acid generation.
     - **pH:** Generally acidic, indicative of acid mine drainage.
     - **Heavy Metal Correlation:** As, Co, Cu, Pb, Zn, Ni correlate with total S and Fe_2O_3.
3. **Environmental Implications:**
   - **Coal Fly Ash:**
     - **Trace Elements:** Presence of various elements, possibly influenced by brine interaction.
     - **Neutralization:** Presence of Ca may act as a neutralizing agent.
   - **Gold Tailings:**

UNIVERSITY of the WESTERN CAPE
http://etd.uwc.ac.za/

- **Heavy Metals:** Elevated levels of U, Hg, and other heavy metals raise environmental concerns.
- **Uranium Presence:** Possible uraniferous-gold tailing.
- **Acid Mine Drainage:** Presence of sulphides indicates potential for acid mine drainage.

4. **Reprocessing Potential:**
    - **Coal Fly Ash:**
        - **Composition:** Suitable for certain applications due to its mineral composition.
    - **Gold Tailings:**
        - **Gold Concentration:** Indicates potential for reprocessing.
5. **Overall Implications:**
    - **Coal Fly Ash:**
        - **Brine Interaction:** Presence of brine may influence mineral composition.
        - **Alkaline Environment:** Tends towards an alkaline environment.
    - **Gold Tailings:**
        - **Environmental Risks:** Elevated heavy metal levels pose environmental risks.
        - **Acidity:** Potential for acid mine drainage with a notable presence of sulphides.

In summary, while both materials share commonalities in terms of containing SiO_2 and other elements, their differences lie in acidity potential, heavy metal concentrations, and environmental implications. Coal fly ash leans towards an alkaline environment, while gold tailings raise concerns about acid mine drainage

UNIVERSITY of the WESTERN CAPE
http://etd.uwc.ac.za/

and elevated heavy metal content, emphasizing the need for proper environmental management in gold tailings disposal.

Summary of Hierarchical Clustering Analyses for Coal Fly Ash and Gold Tailings:

1. **Coal Fly Ash:**
    - **Water Fraction:**
        - Classified into two main clusters and six sub-clusters.
        - Elements like Si, Al, Ca, Na, and K showed high concentrations.
        - Fe, Mg, Sr, and other elements had low concentrations in water leach, indicating inactivity.
        - Ca demonstrated a significant impact on acidity neutralization.
    - **Carbonate Fraction:**
        - Classified into two main clusters and five sub-clusters.
        - Si, Al, and Ca had high concentrations.
        - Fe played a minor role, suggesting inactivity.
        - Increasing Ca concentrations indicated a buffering effect towards an alkaline environment.
    - **Hydroxylamine Fraction:**
        - Classified into two main clusters and seven sub-clusters.
        - Si, Al, Ca, and Fe showed high concentrations.
        - Fe concentrations increased with harsher leaching conditions.
2. **Gold Tailings:**
    - **Water Fraction:**

UNIVERSITY of the WESTERN CAPE

http://etd.uwc.ac.za/

- Classified into two main clusters and five sub-clusters.
- Fe, Ca, and Al contents varied with depth.
- More Fe ions leached out at greater depths.

- **Carbonate Fraction:**
  - Classified into two main clusters and three sub-clusters.
  - High leaching of Fe and As in cluster 1, Ca and Mg in cluster 2, and other toxic elements in cluster 3.
  - Minor elements were leached out compared to coal fly ash.
- **Hydroxylamine Fraction:**
  - Classified into two main clusters and four sub-clusters.
  - Ca and Fe showed high concentrations.
  - Discriminant function associated the release of trace elements with Fe and Ca.

3. **Comparative Observations:**
   - **Coal Fly Ash vs. Gold Tailings:**
     - Both materials exhibited clustering patterns indicating leaching.
     - Proportional leaching to the fineness of waste materials.
     - Ca played a significant role in neutralization for both.
4. **Inference:**
   - **Cluster Analysis:**
     - Leaching occurs under harsh conditions, proportional to depth.
     - Harsher leaching conditions lead to increased Fe ion release.
     - Need for further investigation highlighted.

UNIVERSITY of the WESTERN CAPE
http://etd.uwc.ac.za/

In summary, the hierarchical clustering analyses provided insights into the leaching behavior of both coal fly ash and gold tailings. The role of elements, especially Ca and Fe, in acidity neutralization and trace element release was highlighted. The findings suggest the importance of understanding leaching patterns under different conditions and emphasize the need for further exploration in cluster analysis for comprehensive insights.

Summary of Factor Analysis for Water, Ammonium, and Hydroxylamine Phases in Coal Fly Ash and Gold Tailings:

1. **Water Phase:**
    - **Coal Fly Ash:**
        - **Factors:**
            - Factor 1: Represents labile elements easily leached.
            - Factor 2: Indicates Ca carbonates, influencing Zn and Cu.
            - Fe doesn't play a major role, requiring a stronger solution.
    - **Gold Tailings:**
        - **Factors:**
            - Factors 1 and 3: Fe plays a major role in leaching.
            - Factor 3: Inadequate neutralization potential by Ca and Mg carbonates.
2. **Ammonium Phase:**
    - **Coal Fly Ash:**
        - **Observations:**
            - Ca associated with Mg, showing a negative relationship with Fe.

UNIVERSITY of the WESTERN CAPE

http://etd.uwc.ac.za/

- Indicates a considerable amount of neutralizing potential.
- Stronger leaching conditions tend to increase alkalinity.

- **Gold Tailings:**
  - **Observations:**
    - Ca associated with Fe, indicating neutralizing potential.
    - Presence of carbonates observed in neutralization.

3. **Hydroxylamine Fraction:**

- **Coal Fly Ash:**
  - **Observations:**
    - Ca plays a major role, possibly from added lime or weathering.
    - Factors indicate the presence of carbonates creating secondary products.
    - Ca not associated with Fe, suggesting neutralizing potential.

UNIVERSITY of the
WESTERN CAPE

- **Gold Tailings:**
  - **Factors:**
    - Factor 1: Ni, Zn, Pb, Cu associated with Fe/Mn oxides, easily transported.
    - Factors 3 and 5: Ca, Mg, K, Na show positive/negative values.
    - Increasing acidity observed in the long run as Fe ions overcome buffers.

http://etd.uwc.ac.za/

4. **Comparative Observations:**
    - **Coal Fly Ash vs. Gold Tailings:**
        - Both show neutralizing potential in ammonium and hydroxylamine phases.
        - Coal fly ash may release more Fe ions during processing.
        - Gold tailings exhibit a potential for increased acidity and release of toxic metals in the long run.

In summary, the factor analysis reveals key insights into the leaching behavior and potential environmental impact of both coal fly ash and gold tailings. The role of Fe, Ca, and Mg in neutralization and the influence of carbonates on acidity and toxic metal release are highlighted. The findings underscore the importance of understanding the dynamic processes in these waste materials to manage potential environmental risks effectively.

Conclusions

From the study, the following conclusions are reached:

1. The tailing dam can be characterized into four distinct layers based on the petrographical analysis namely the oxidised layer, the transition layer, the Au-Fe rich layer and the un-oxidised layer. For coal fly ash, no real distinct layer was observed, it is either a weathered zone or un weathered zone. This formed the basis of the study.
2. The mineralogical composition is similar to previous research done except for the presence of delhayelite detected. 9 minerals were observed in the tailings and is given as follows; quartz, muscovite, pyropyllite, gypsum, jarosite, delhayelite, hematite, pyrite and clinochor but vary in each sample. In coal fly ash, three prominent mineral phases quartz, mullite and lime were mainly detected in the fresh fly ash, however in the weathered fly ash the three prominent mineral phases detected were quartz, mullite and calcite

http://etd.uwc.ac.za/

3. This study shows that the tailings dam has the potential to generate acid mine drainage if exposed to oxidation, and this could account for the general acidic pH of the tailings dam (implies that the neutralisation potential is lower than the acidic potential). The study showed that there are enough carbonates in coal fly ash that will make it difficult for acid drainage to be generated
4. Therefore, tailings dam has the potential to generate acid mine drainage if exposed to oxidation, and the neutralisation potential is lower than the acidic potential; in coal fly ash the neutralisation potential is higher than the acidic potential
5. The reddish layer (Au-Fe rich) is peculiar to the tailing dam sampled and contained gold of economic value. In coal fly ash, no enrichment zone found but there could be other beneficiation of coal fly ash to construction industrial since it contains it toxic elements.
6. Despite subject both waste to the same leaching conditions, the leaching out of trace elements is more profound in the gold tailings as compared to the coal fly ash, as elemental speciation tends towards acidic mine generation. Fe in coal fly ash show redundancy and not easily oxidisable, which could have been ingest during milling process. The role of Ca^{2+} cannot be overemphasised showing that the its presence could have as a result of added lime used to mitigate Acid Mine drainage. Both wastes had the potential to leach out toxic elements such as As, Cd, Cr, Cu, Ni, Pb and Zn though more prominent in gold tailing, the coal fly ash leaching out trace element under more harsher conditions.

Recommendations

A need to compare results of various sequential method on more types of mine waste will help understand and prediction their various acid generation potential.

The use of statistical method couple with geochemical species could give us a better understanding of the mobility of element within a mine waste dump. This research

http://etd.uwc.ac.za/

was delayed because it was difficult to get access to coal tailings, because of its intricate effect.

Research like this should be performed to assess various wastes.

UNIVERSITY of the
WESTERN CAPE

http://etd.uwc.ac.za/

REFERENCE

Abegunde, O.A. 2015. Geologic and geological assessment of Acid Mine Drainage and heavy metals contamination in the West Rand, Witwatersrand Basin, South Africa.

Abegunde, O.A., Okujeni, C., Petrik, L., Siad, A.M., Madzivire, G. & Wu, C. 2020. The use of factor analysis and acid base accounting to probe the speciation of toxic metals in gold mine waste. *Environmental Earth Sciences*, 79(6).

Abegunde, O.A., Okujeni, C.D., Wu, C. & Siad, A. 2016. Distribution patterns of contaminants in the Mogale Gold tailing dam: a case study from South Africa. *Environmental Earth Sciences*, 75(20): 1365.

Abegunde, O.A., Wu, I., Okujeni, C. & Siad, A. 2014. Distribution Patterns of Contaminants in the Mogale Gold Tailing Dam; Case Study from South Africa. In *2014 GSA Annual Meeting*.

Abollino, O., Malandrino, M., Giacomino, A. & Mentasti, E. 2011. The role of chemometrics in single and sequential extraction assays: A review Part I. Extraction procedures, uni-and bivariate techniques and multivariate variable reduction techniques for pattern recognition. *Analytica Chimica Acta*, 688: 104–121.

Agboola, O., Babatunde, D., Fayomi, O.S.I., Sadiku, R., Popoola, P., Moropeng, M., Yahaya, A. & Angela, M. 2020. A review on the impact of mining operation: Monitoring, assessment and management.

Ahamed, M.A.A., Perera, M.S.A., Matthai, S.K., Ranjith, P.G. & Dong-yin, L. 2019. Coal composition and structural variation with rank and its influence on the coal-moisture interactions under coal seam temperature conditions–A review article. *Journal of Petroleum Science and Engineering*, 180: 901–917.

A.k, A. & Sarah, A. 2014. Al-Mahaqeri, Assessment of Abandoned Mine Impacts on Concentrations and Distribution of Heavy Metals in Surface Sediments of Catchments Around Sungai Lembing Abandoned Tin Mine. *Iranica Journal of Energy & Environment*, 5: 453–460.

UNIVERSITY of the WESTERN CAPE

http://etd.uwc.ac.za/

Akabzaa, T.M., Armah, T.E.K. & Baneong-Yakubo, B.K. 2007. Prediction of acid mine drainage generation potential in selected mines in the Ashanti Metallogenic Belt using static geochemical methods. *Environmental geology*, 52: 957–964.

Akcil, A. & Koldas, S. 2006. Acid Mine Drainage (AMD): causes, treatment and case studies. *Journal of Cleaner Production*, 14(12-13 SPEC. ISS.): 1139–1145.

Akhtar, N., Syakir Ishak, M.I., Bhawani, S.A. & Umar, K. 2021. Various natural and anthropogenic factors responsible for water quality degradation: A review. *Water*, 13(19): 2660.

Akinwekomi, V., Maree, J.P., Masindi, V., Zvinowanda, C., Osman, M.S., Foteinis, S., Mpenyana-Monyatsi, L. & Chatzisymeon, E. 2020. Beneficiation of acid mine drainage (AMD): A viable option for the synthesis of goethite, hematite, magnetite, and gypsum – Gearing towards a circular economy concept. *Minerals Engineering*, 148: 106204.

Alloway, B.J. 1990. Heavy metals in soils. John Willey and Sons. *Inc. NY USA*, 2.

Alpers, C.N., Hunerlach, M.P., Hamlin, S.N. & Zierenberg, R.A. 2003. *Reconnaissance of Acid Drainage Sources and Preliminary Evaluation of Remedial Alternatives at the Copper Bluff Mine, Hoopa Valley Reservation, California*. http://ca.water.usgs.gov.

Amar, H., Benzaazoua, M., Elghali, A., Bussière, B. & Duclos, M. 2020. Upstream environmental desulphurisation and valorisation of waste rocks as a sustainable AMD management approach. *Journal of Geochemical Exploration*, 215: 106555.

el Amari, K., Valera, P., Hibti, M., Pretti, S., Marcello, A. & Essarraj, S. 2014. Impact of mine tailings on surrounding soils and ground water: Case of Kettara old mine, Morocco. *Journal of African Earth Sciences*, 100: 437–449.

http://etd.uwc.ac.za/

Anawar, H.M. 2013. Impact of climate change on acid mine drainage generation and contaminant transport in water ecosystems of semi-arid and arid mining areas. *Physics and Chemistry of the Earth*, 58(Parts A/B/C): 13–21.

Argane, R., El Adnani, M., Benzaazoua, M., Bouzahzah, H., Khalil, A., Hakkou, R. & Taha, Y. 2016. Geochemical behavior and environmental risks related to the use of abandoned base-metal tailings as construction material in the upper-Moulouya district, Morocco. *Environmental Science and Pollution Research*, 23(1): 598–611.

Ayanda, O.S., Fatoki, O.S., Adekola, F.A. & Ximba, B.J. 2012. Characterization of fly ash generated from Matla power station in Mpumalanga, South Africa. *E-Journal of Chemistry*, 9(4): 1788–1795.

Aykol, A., Budakoglu, M., Kumral, M., H Gultekin, A., Turhan, M., Esenli, V., Yavuz, F. & Orgun, Y. 2003. Heavy metal pollution and acid drainage from the abandoned Balya Pb-Zn sulfide Mine, NW Anatolia, Turkey. *Environmental Geology*, 45(2): 198–208.

B, A.O. & M, M. 2010. Remediation of heavy metals in drinking water and wastewater treatment systems: Processes and applications. *International Journal of Physical Sciences*, 5(12): 1807–1817.

Bakatula, E.N., Cukrowska, E.M., Chimuka, L. & Tutu, H. 2012. Characterization of cyanide in a natural stream impacted by gold mining activities in the Witwatersrand Basin, South Africa. *Toxicological & Environmental Chemistry*, 94(1): 7–19. http://www.tandfonline.com/doi/abs/10.1080/02772248.2011.638637 18 January 2019.

Bandyopadhyay, S., Zaeni, A., Nath, D., Yu, A., Zeng, Q., Blackburn, D. & White, C. 2010. Advanced utilization of as received and near whitened fly ash in polypropylene polymer to improve mechanical, notched impact and whiteness colour properties. *International Journal of Plastics Technology*, 14: 51–56.

UNIVERSITY of the WESTERN CAPE

http://etd.uwc.ac.za/

Barton, C., Paddock, L., Romanek, C., Maharaj, S. & Seaman, J. 2005. Metal attenuation processes in a landfill containing coal combustion waste: Implictions for remediation. *Environmental Geosciences*, 12(1): 45–55.

Behera, A. & Mohapatra, S.S. 2018. Challenges in Recovery of Valuable and Hazardous Elements from Bulk Fly Ash and Options for Increasing Fly Ash Utilization. In *Coal Fly Ash Beneficiation - Treatment of Acid Mine Drainage with Coal Fly Ash*. InTech. http://www.intechopen.com/books/coal-fly-ash-beneficiation-treatment-of-acid-mine-drainage-with-coal-fly-ash/challenges-in-recovery-of-valuable-and-hazardous-elements-from-bulk-fly-ash-and-options-for-increasi 10 December 2018.

Benner, S.G., Blowes, D.W. & Ptacek, C.J. 1997. A full-scale porous reactive wall for prevention of acid mine drainage. *Ground Water Monitoring and Remediation*, 17(4): 99–107.

Benzaazoua, M., Bussière, B., Demers, I., Aubertin, M., Fried, É. & Blier, A. 2008. Integrated mine tailings management by combining environmental desulphurization and cemented paste backfill: Application to mine Doyon, Quebec, Canada. *Minerals Engineering*, 21(4): 330–340.

Bezuidenhout, N. & Rousseau, P.D.S. 2006. Investigations into the depth and rate of weathering on witwatersrand gold tailings dam surfaces as key information for long-term ard risk assessments. In *7th International Conference on Acid Rock Drainage 2006, ICARD - Also Serves as the 23rd Annual Meetings of the American Society of Mining and Reclamation*. 128–139.

Bigham, J.M., Nordstrom, D.K., Alpers, C.N., Jambor, J.I. & Nordstrom, D.K. 2000. *Sulfate Minerals, Crystallography, Geochemistry, and Environmental Significance. Reviews in Mineralogy and Geochemistry*. null, ed.

Blowes, D.W., Ptacek, C.J., Jambor, J.L. & Weisener, C.G. 2003. 9.05 - The Geochemistry of Acid Mine Drainage. In H. D. Holland & K. K. Turekian, eds. *Treatise on Geochemistry*. Oxford: Pergamon: 149–204. https://www.sciencedirect.com/science/article/pii/B0080437516091374.

UNIVERSITY of the WESTERN CAPE
http://etd.uwc.ac.za/

Bosecker, K. 1997. Bioleaching: metal solubilization by microorganisms. *FEMS Microbiology reviews*, 20(3–4): 591–604.

Bostani, A., Salahedin, M., Rahman, M. & Davood, N.-K. 2017. Spatial Mapping of Soil Properties Using Geostatistical Methods in the Ghazvin Plains of Iran. *Modern Applied Science*, 11: 23.

Brady, B.H.G. & Brown, E.T. 2006. *Rock mechanics: for underground mining*. Springer science & business media.

Brough, C.P., Warrender, R., Bowell, R.J., Barnes, A. & Parbhakar-Fox, A. 2013. The process mineralogy of mine wastes. *Minerals Engineering*, 52: 125–135.

Cadle, A.B., Cairncross, B., Christie, A.D.M. & Roberts, D.L. 1993. The Karoo Basin of South Africa: type basin for the coal-bearing deposits of southern Africa. *International Journal of Coal Geology*, 23(1): 117–157. https://www.sciencedirect.com/science/article/pii/016651629390046D.

Calas, G. 2017. Mineral resources and sustainable development. *Elements: An International Magazine of Mineralogy, Geochemistry, and Petrology*, 13(5): 301–306.

Camden-Smith, B., Pretorius, P., Camden-Smith, P. & Tutu, H. 2015. Chemical transformations of metals leaching from gold tailings. In *10th international conference on acid rock drainage and International Mine Water Association annual conference, Chile*.

Candeias, C., Ávila, P.F., da Silva, E.F., Ferreira, A., Durães, N. & Teixeira, J.P. 2015. Water–rock interaction and geochemical processes in surface waters influenced by tailings impoundments: impact and threats to the ecosystems and human health in rural communities (panasqueira mine, central Portugal). *Water, Air, & Soil Pollution*, 226(2): 1–30.

Chevrel, S., Courant, C., Cottard, F., Coetzee, H., Bourguinon, A. & Ntsume, A. 2003. Very high resolution remote sensing coupled to GIS-based Environmental Assessment-East Rand Goldfield, South Africa Report BRGMIRP-52724-FR [Pretoria, South Africa]: Council for Geoscience.

http://etd.uwc.ac.za/

Chevrel, S., Croukamp, L., Bourguignon, A. & Cottard, F. 2008. A Remote-Sensing and GIS-Based Integrated Approach for Risk-Based Prioritization of Gold Tailings Facilities—Witwatersrand, South Africa. In *Mine Closure 2008: Proceedings of the Third International Seminar on Mine Closure*. Australian Centre for Geomechanics: 639–650.

Chunhacherdchai, L., Chotpantarat, S. & Tongcumpou, C. 2011a. Investigating of heavy metals in different depths of soil tailings from Akara Gold Mine, Thailand using three-steps modified BCR sequential extraction. In *2nd International Conference on Environmental Science and Technology*. 28–31.

Chunhacherdchai, L., Chotpantarat, S. & Tongcumpou, C. 2011b. Investigating of heavy metals in different depths of soil tailings from Akara Gold Mine, Thailand using three-steps modified BCR sequential extraction. In *2nd International Conference on Environmental Science and Technology*. 28–31.

Chunhacherdchai, L., Chotpantarat, S. & Tongcumpou, C. 2011c. Investigating of heavy metals in different depths of soil tailings from Akara Gold Mine, Thailand using three-steps modified BCR sequential extraction. In *2nd International Conference on Environmental Science and Technology, CSIT Press Singapore*. V2-28.

Civeira, M., Oliveira, M.L.S., Hower, J.C., Agudelo-Castañeda, D.M., Taffarel, S.R., Ramos, C.G., Kautzmann, R.M. & Silva, L.F.O. 2016. Modification, adsorption, and geochemistry processes on altered minerals and amorphous phases on the nanometer scale: examples from copper mining refuse, Touro, Spain. *Environmental Science and Pollution Research*, 23(7): 6535–6545.

Coetzee, A. 2016. *The geometry of Karoo dolerite dykes and saucers in the Highveld Coalfield: constraints on emplacement processes of mafic magmas in the shallow crust*. Stellenbosch: Stellenbosch University.

Cozzolino, D., Chandra, S., Roberts, J., Power, A., Rajapaksha, P., Ball, N., Gordon, R. & Chapman, J. 2017. There is gold in them hills: Predicting potential acid mine drainage events through the use of chemometrics. https://doi.org/10.1016/j.scitotenv.2017.11.063.

UNIVERSITY of the WESTERN CAPE

http://etd.uwc.ac.za/

Cukrowska, E.M., Govender, K. & Viljoen, M. 2004. Ion mobility based on column leaching of South African gold tailings dam with chemometric evaluation. *Chemosphere*, 56(1): 39–50.

Deysel, L.M. & Vermeulen, D. 2015. A Detailed ABA Study of the Coal-Bearing Formations in the Waterberg Coalfield, Limpopo Province, South Africa. In *Proceedings of the 10th International Conference on Acid Rock Drainage & IMWA Annual Conference, Santiago, Chile*. 21–24.

Dold, B. 2014. Evolution of acid mine drainage formation in sulphidic mine tailings. *Minerals*, 4(3): 621–641.

Dold, B. 2003. Speciation of the most soluble phases in a sequential extraction procedure adapted for geochemical studies of copper sulfide mine waste. *Journal of Geochemical Exploration*, 80(1): 55–68. https://www.sciencedirect.com/science/article/pii/S0375674203001821?via%3Dihub 18 January 2019.

Dopson, M. & Lindström, E.B. 1999. Potential role of Thiobacillus caldus in arsenopyrite bioleaching. *Applied and environmental microbiology*, 65(1): 36–40.

Doulati Ardejani, F., Jodieri Shokri, B., Moradzadeh, A., Shafaei, S.Z. & Kakaei, R. 2011. Geochemical characterisation of pyrite oxidation and environmental problems related to release and transport of metals from a coal washing low-grade waste dump, Shahrood, northeast Iran. *Environmental Monitoring and Assessment*, 183(1–4): 41–55.

Durand, J.F. 2012a. The impact of gold mining on the Witwatersrand on the rivers and karst system of Gauteng and North West Province, South Africa. *Journal of African Earth Sciences*, 68: 24–43.

Durand, J.F. 2012b. The impact of gold mining on the Witwatersrand on the rivers and karst system of Gauteng and North West Province, South Africa. *Journal of African Earth Sciences*, 68: 24–43. https://www.sciencedirect.com/science/article/pii/S1464343X12000593.

UNIVERSITY of the WESTERN CAPE

http://etd.uwc.ac.za/

Edraki, M., Baumgartl, T., Mulligan, D., Fegan, W. & Munawar, A. 2019. Geochemical characteristics of rehabilitated tailings and associated seepages at Kidston gold mine, Queensland, Australia. *International Journal of Mining, Reclamation and Environment*, 33(2): 133–147. https://doi.org/10.1080/17480930.2017.1362542.

Epa, U. & of Wetlands, O. 1994. *Technical Document: Acid Mine Drainage Prediction*.

Eze, C.P. 2011. Chemical, physical and morphological changes in weathered coal fly ash: a case study of brine impacted wet ash dump.

Eze, C.P., Nyale, S.M., Akinyeye, R.O., Gitari, W.M., Akinyemi, S.A., Fatoba, O.O. & Petrik, L.F. 2013. Chemical, mineralogical and morphological changes in weathered coal fly ash: A case study of a brine impacted wet ash dump. *Journal of Environmental Management*, 129: 479–492.

Falcon, R. & Ham, A. 1988. The characteristics of South African coals. *Journal of the Southern African Institute of Mining and Metallurgy*, 88(5): 145–161.

Fanfani, L., Zuddas, P. & Chessa, A. 1997. *Heavy metals speciation analysis as a tool for studying mine tailings weathering*.

Feinstein, C.H. 2005. *An economic history of South Africa: Conquest, discrimination, and development*. Cambridge University Press.

Funke, N., Huitema, D. & Petersen, A. 2022. Impending doom or unnecessary panic? The struggle for discursive hegemony in South Africa's acid mine drainage policy problem. *Critical Policy Studies*: 1–21.

García-Valero, A., Martínez-Martínez, S., Faz, A., Rivera, J. & Acosta, J.A. 2019. Environmentally sustainable acid mine drainage remediation: Use of natural alkaline material. https://doi.org/10.1016/j.jwpe.2019.101064.

García-Valero, A., Martínez-Martínez, S., Faz, A., Rivera, J. & Acosta, J.A. 2020. Environmentally sustainable acid mine drainage remediation: Use of natural alkaline material. *Journal of Water Process Engineering*, 33: 101064.

UNIVERSITY of the WESTERN CAPE

http://etd.uwc.ac.za/

Giaccio, L., Cicchella, D., de Vivo, B., Lombardi, G. & de Rosa, M. 2012. Does heavy metals pollution affects semen quality in men? A case of study in the metropolitan area of Naples (Italy). *Journal of Geochemical Exploration*, 112: 218–225.

Giacomino, A., Abollino, O., Malandrino, M. & Mentasti, E. 2011. The role of chemometrics in single and sequential extraction assays: A Review. Part II. Cluster analysis, multiple linear regression, mixture resolution, experimental design and other techniques. *Analytica Chimica Acta*, 688: 122–139.

Gómez-álvarez, A., Valenzuela-García, J.L., Meza-Figueroa, D., de la O-Villanueva, M., Ramírez-Hernández, J., Almendariz-Tapia, J. & Pérez-Segura, E. 2011. Impact of mining activities on sediments in a semi-arid environment: San Pedro River, Sonora, Mexico. *Applied Geochemistry*, 26(12): 2101–2112.

Grande, J.A., Beltrán, R., Sáinz, A., Santos, J.C., De La Torre, M.L. & Borrego, J. 2005. Acid mine drainage and acid rock drainage processes in the environment of Herrerías Mine (Iberian Pyrite Belt, Huelva-Spain) and impact on the Andevalo Dam. *Environmental Geology*, 47: 185–196.

Grover, B.P.C., Johnson, R.H. & Tutu, H. 2016. Leachability of metals from gold tailings by rainwater: An experimental and geochemical modelling approach. *Water SA*, 42(1): 38–42.

Gu, F. & Liu, W. 2012. Geo-spatial Information Science Applications of remote sensing and GIS to the assessment of riparian zones for environmental restoration in agricultural watersheds. https://www.tandfonline.com/action/journalInformation?journalCode=tgsi20.

Guijian, L., Liugen, Z., Enjiang, W. & Zicheng, P. 2006. Depositional and chemical characterization of coal from Yayu coal field. *Energy exploration & exploitation*, 24(6): 417–437.

Guillén, M.T., Delgado, J., Albanese, S., Nieto, J.M., Lima, A. & Vivo, B. de. 2012. Heavy metals fractionation and multivariate statistical techniques to evaluate

UNIVERSITY of the WESTERN CAPE

http://etd.uwc.ac.za/

the environmental risk in soils of Huelva Township (SW Iberian Peninsula). *Journal of Geochemical Exploration*, 119–120: 32–43.

Hageman, P.L., Seal, R.R., Diehl, S.F., Piatak, N.M. & Lowers, H.A. 2015. Evaluation of selected static methods used to estimate element mobility, acid-generating and acid-neutralizing potentials associated with geologically diverse mining wastes. *Applied Geochemistry*, 57: 125–139.

Hancox, P.J. & Götz, A.E. 2014. South Africa's coalfields—A 2014 perspective. *International Journal of Coal Geology*, 132: 170–254.

Hannigan, R. 2007. Chapter 1 What goes around comes around: Today's environmental geochemistry. *Developments in Environmental Science*, 5: 1–6.

Hansen, R.N. 2015. Contaminant leaching from gold mining tailings dams in the Witwatersrand Basin, South Africa: A new geochemical modelling approach. *Applied Geochemistry*, 61: 217–223.

Harington McGlashan ND** & Chelkowska EZ***, J. 2004. A century of migrant labour in the gold mines of South Africa. *Journal of the Southern African Institute of Mining and Metallurgy*, 104(2): 65–71.

Hay, G.J., Castilla, G., Wulder, M.A. & Ruiz, J.R. 2005. An automated object-based approach for the multiscale image segmentation of forest scenes. *International Journal of Applied Earth Observation and Geoinformation*, 7(4): 339–359.

Heikkinen, P.M., Räisänen, M.L. & Johnson, R.H. 2009. Geochemical characterisation of seepage and drainage water quality from two sulphide mine tailings impoundments: Acid mine drainage versus neutral mine drainage. *Mine Water and the Environment*, 28(1): 30–49.

Hesketh, A.H., Broadhurst, J.L., Bryan, C.G., Van Hille, R.P. & Harrison, S.T.L. 2010. Biokinetic test for the characterisation of AMD generation potential of sulfide mineral wastes. *Hydrometallurgy*, 104(3–4): 459–464.

Hobbs, P.J. & Cobbing, J. 2007. A Hydrogeological Assessment of Acid Mine Drainage Impacts in the West Rand Basin, Gauteng Province. *Csir.*: 59.

UNIVERSITY of the WESTERN CAPE

http://etd.uwc.ac.za/

Holmström, H., Ljungberg, J. & Öhlander, B. 1999. Role of carbonates in mitigation of metal release from mining waste. Evidence from humidity cells tests. *Environmental Geology*, 37(4): 267–280.

Hower, J.C., Wagner, N.J., O'Keefe, J.M.K., Drew, J.W., Stucker, J.D. & Richardson, A.R. 2012. Maceral types in some Permian southern African coals. *International journal of coal geology*, 100: 93–107.

Huang, L.-N., Kuang, J.-L. & Shu, W.-S. 2016. Microbial ecology and evolution in the acid mine drainage model system. *Trends in microbiology*, 24(7): 581–593.

Hudson-Edwards, K.A., Jamieson, H.E. & Lottermoser, B.G. 2011. Mine wastes: past, present, future. *Elements*, 7(6): 375–380.

Igarashi, T., Herrera, P.S., Uchiyama, H., Miyamae, H., Iyatomi, N., Hashimoto, K. & Tabelin, C.B. 2020. The two-step neutralization ferrite-formation process for sustainable acid mine drainage treatment: Removal of copper, zinc and arsenic, and the influence of coexisting ions on ferritization. *Science of The Total Environment*, 715: 136877.

Ineich, T., Degreve, C., Karamoutsos, S. & du Plessis, C. 2017. Utilization efficiency of lime consumption during magnesium sulfate precipitation. *Hydrometallurgy*, 173(January): 241–249.

J, Skousen, J, Simmons, LM, M. & P, Z. 2002. Acid-base accounting to predict post-mining drainage quality on surface mines. *Journal of environmental quality*, 31(6): 2034–2044. https://pubmed.ncbi.nlm.nih.gov/12469854/ 29 July 2021.

Jacobs, J.A. 2014. Overview of resources from acid drainage and postmining opportunities. *Acid Mine Drainage, Rock Drainage, and Acid Sulfate Soils: Causes, Assessment, Prediction, Prevention, and Remediation*: 361–375.

Jamieson, H.E., Walker, S.R. & Parsons, M.B. 2015. Mineralogical characterization of mine waste. *Applied Geochemistry*, 57: 85–105. https://www.sciencedirect.com/science/article/pii/S0883292714003278?via%3Dihub 18 January 2019.

http://etd.uwc.ac.za/

Johnson, D.B. 2012. Geomicrobiology of extremely acidic subsurface environments. *FEMS microbiology ecology*, 81(1): 2–12.

Johnson, D.B. & Hallberg, K.B. 2005. Acid mine drainage remediation options: a review. *Science of The Total Environment*, 338(1–2): 3–14.

Johnson, D.B. & Hallberg, K.B. 2003. The microbiology of acidic mine waters. *Research in microbiology*, 154(7): 466–473.

Kefeni, K.K., Msagati, T.A.M. & Mamba, B.B. 2017. Acid mine drainage: Prevention, treatment options, and resource recovery: A review. *Journal of Cleaner Production*, 151: 475–493.

Khalil, A., Hanich, L., Bannari, A., Zouhri, L., Pourret, O. & Hakkou, R. 2013. Assessment of soil contamination around an abandoned mine in a semi-arid environment using geochemistry and geostatistics: Pre-work of geochemical process modeling with numerical models. *Journal of Geochemical Exploration*, 125: 117–129.

Khalil, A., Hanich, L., Hakkou, R. & Lepage, M. 2014. GIS-based environmental database for assessing the mine pollution: A case study of an abandoned mine site in Morocco. *Journal of Geochemical Exploration*, 144(PC): 468–477.

Kleinmann, R.L.P. 2000. *Prediction of water quality at surface coal mines*. Citeseer.

Kroukamp, E. & Wepener, V. 2022. Toxic trace metals in the environment, a study of water pollution. *Environmental and Biochemical Toxicology: Concepts, Case Studies and Challenges*: 191.

Lemos, M., Valente, T., Reis, P.M., Fonseca, R., Delbem, I., Ventura, J. & Magalhães, M. 2021. Mineralogical and Geochemical Characterization of Gold Mining Tailings and Their Potential to Generate Acid Mine Drainage (Minas Gerais, Brazil). *Minerals*, 11(1). https://www.mdpi.com/2075-163X/11/1/39.

UNIVERSITY of the WESTERN CAPE

http://etd.uwc.ac.za/

Lindsay, M.B.J., Moncur, M.C., Bain, J.G., Jambor, J.L., Ptacek, C.J. & Blowes, D.W. 2015. Geochemical and mineralogical aspects of sulfide mine tailings. *Applied geochemistry*, 57: 157–177.

Lloyd, P.J. 2000. The potential of coal wastes in South Africa. *Journal of the Southern African Institute of Mining and Metallurgy*, 100(1): 69–72.

Lloyd, P.J.D. 2002. Coal mining and the environment. *Energy Research Institute*.

Lopez-Sanchez, M.A. 2020. Which average, how many grains, and how to estimate robust confidence intervals in unimodal grain size populations. *Journal of Structural Geology*, 135: 104042.

Luhar, I. & Luhar, S. 2022. A comprehensive review on fly ash-based geopolymer. *Journal of Composites Science*, 6(8): 219.

Madzivire, G., Maleka, P.P., Vadapalli, V.R.K., Gitari, W.M., Lindsay, R. & Petrik, L.F. 2014. Fate of the naturally occurring radioactive materials during treatment of acid mine drainage with coal fly ash and aluminium hydroxide. *Journal of environmental management*, 133: 12–17.

Madzivire, G., Petrik, L.F., Gitari, W.M., Ojumu, T. V & Balfour, G. 2010. Application of coal fly ash to circumneutral mine waters for the removal of sulphates as gypsum and ettringite. *Minerals Engineering*, 23(3): 252–257.

Mahlaba, J.S., Kearsley, E.P. & Kruger, R.A. 2011. Physical, chemical and mineralogical characterisation of hydraulically disposed fine coal ash from SASOL Synfuels. *Fuel*, 90(7): 2491–2500.

Makgato, S.S., Falcon, R.M.S. & Chirwa, E.M.N. 2019. Reduction in coal fines and extended coke production through the addition of carbonisation tar: environmentally clean process technology. *Journal of Cleaner Production*, 221: 684–694.

Mamba, C.K. 2011. Using froth flotation to mitigate acid rock drainage risks while recovering valuable coal from ultrafine colliery wastes. : 71.

http://etd.uwc.ac.za/

Masindi, V., Chatzisymeon, E., Kortidis, I. & Foteinis, S. 2018. Assessing the sustainability of acid mine drainage (AMD) treatment in South Africa. *Science of The Total Environment*, 635: 793–802.

Masood Khan, A., Behkami, S., Yusoff, I., Bin, S., Zain, M., Kartini, N., Bakar, A., Farid, A. & Alias, Y. 2017. Geochemical characteristics of rare earth elements in different types of soil: A chemometric approach. http://dx.doi.org/10.1016/j.chemosphere.2017.06.032.

McCarthy, T.S. 2011. The impact of acid mine drainage in South Africa. *South African Journal of Science*, 107(5/6).

McCauley, C., O'Sullivan, A., Weber, P., Trumm, D., Brough, A.K. & Milke, M.W. 2008. Research Initiatives for Developing Passive-Treatment Technologies for Ameliorating Acid Mine Drainage in New Zealand.

Moodley, I., Sheridan, C.M., Kappelmeyer, U. & Akcil, A. 2018. Environmentally sustainable acid mine drainage remediation: Research developments with a focus on waste/by-products. *Minerals Engineering*, 126: 207–220.

Muniruzzaman, M., Kauppila, P.M. & Karlsson, T. 2018. Water quality prediction of mining waste facilities based on predictive models. *Geol Surv Finl Open File Res Rep*, 16: 67.

Mutanga, S., Mujuru, M., Hlahane, K. & Moshobane, M.D. 2017. The Role of GeospatialTechnologies in Modeling Acid Mine Drainage. *Management and Mitigation of Acid Mine Drainage in South Africa: Input for Mineral Beneficiation in Africa*: 181.

Myneni, S.C.B., Traina, S.J., Logan, T.J. & Waychunas, G.A. 1997. Oxyanion Behavior in Alkaline Environments: Sorption and Desorption of Arsenate in Ettringite. *Environmental Science & Technology*, 31(6): 1761–1768. https://doi.org/10.1021/es9607594.

Nagajyoti, P.C., Lee, K.D. & Tvm, S. 2010. Heavy metals, occurrence and toxicity for plants: A review. Environmental Chemistry Letters, 8(3), 199-216. *Environmental Chemistry Letters*, 8: 199–216.

UNIVERSITY of the WESTERN CAPE

http://etd.uwc.ac.za/

Naicker, K., Cukrowska, E. & McCarthy, T.S. 2003. Acid mine drainage arising from gold mining activity in Johannesburg, South Africa and environs. *Environmental Pollution*, 122(1): 29–40.

Naidu, G., Ryu, S., Thiruvenkatachari, R., Choi, Y., Jeong, S. & Vigneswaran, S. 2019. A critical review on remediation, reuse, and resource recovery from acid mine drainage *. https://doi.org/10.1016/j.envpol.2019.01.085.

Navarro, A., Collado, D., Carbonell, M. & Sanchez, J.A. 2004. *Impact of mining activities on soils in a semi-arid environment: Sierra Almagrera district, SE Spain*.

Nengovhela, A.C., Yibas, B. & Ogola, J.S. 2006. Characterisation of gold tailings dams of the Witwatersrand Basin with reference to their acid mine drainage potential, Johannesburg, South Africa. *Water SA*, 32(4): 499–506.

Nieto, J.M., Sarmiento, A.M., Olías, M., Canovas, C.R., Riba, I., Kalman, J. & Delvalls, T.A. 2007. Acid mine drainage pollution in the Tinto and Odiel rivers (Iberian Pyrite Belt, SW Spain) and bioavailability of the transported metals to the Huelva Estuary. *Environment international*, 33(4): 445–455.

Nleya, Y., Simate, G.S. & Ndlovu, S. 2016. Sustainability assessment of the recovery and utilisation of acid from acid mine drainage. *Journal of Cleaner Production*, 113: 17–27.

Nordstrom, D.K. & Alpers, C.N. 1999a. Geochemistry of acid mine waters. *The environmental geochemistry of mineral deposits*, 6(October): 133–160.

Nordstrom, D.K. & Alpers, C.N. 1999b. Negative pH, efflorescent mineralogy, and consequences for environmental restoration at the iron mountain superfund site, California. In *Proceedings of the National Academy of Sciences of the United States of America*. 3455–3462.

Nordstrom, D.K., Blowes, D.W. & Ptacek, C.J. 2015. Hydrogeochemistry and microbiology of mine drainage: An update. *Applied Geochemistry*, 57: 3–16. https://www.sciencedirect.com/science/article/pii/S0883292715000396.

UNIVERSITY of the WESTERN CAPE

http://etd.uwc.ac.za/

Norman, N. 2013. *Geological journeys: A traveller's guide to South Africa's rocks and landforms*. Penguin Random House South Africa.

Nyamhingura, A. 2009. *Characterization and chemical speciation modelling of saline effluents at Sasol Synthetic Fuels Complex-Secunda and Tukuta power station*. University of the Western Cape.

Oelofse, S., Hobbs, P., Rascher, J. & Cobbing, J. 2007. The Pollution and Destruction Threat of Gold Mining Waste on the Witwatersrand: Rand Case Study", 10th International Symposium on Environmental Issues and Waste management in Energy and Mineral Production (SWEMP, , Bangkok, pp. 11. , 2007 SRC.

Oelofse, S.H., Hobbs, P.J., Rascher, J. & Cobbing, J.E. 2004. The pollution and destruction threat of gold mining waste on the Witwatersrand - A West Rand case study. In *CSIR, Natural Resources and the Environment*. 617–627.

Oh, C., Ji, S., Chon, C.M., Yim, G. & Cheong, Y. 2017. Reliability improvement for predicting acid-forming potential of rock samples using static tests. *Environmental Monitoring & Assessment*, 189(5). http://europepmc.org/abstract/MED/28382432 LK - link%7Chttp://europepmc.org/abstract/MED/28382432 SRC - BaiduScholar FG - 0.

Oldecop, L.A. & Rodari, G. 2018. Unsaturated soil mechanics in mining. In *PanAm Unsaturated Soils 2017*. 257–280.

OruÇ, F. & Sabah, E. 2006. Effect of mixing conditions on flocculation performance of fine coal tailings. In *IMPC 2006 - Proceedings of 23rd International Mineral Processing Congress*. 1192–1198.

Parbhakar-Fox, A., Lottermoser, B. & Bradshaw, D. 2013. Evaluating waste rock mineralogy and microtexture during kinetic testing for improved acid rock drainage prediction. *Minerals Engineering*, 52: 111–124.

http://etd.uwc.ac.za/

Parbhakar-Fox, A. & Lottermoser, B.G. 2015. A critical review of acid rock drainage prediction methods and practices. http://dx.doi.org/10.1016/j.mineng.2015.03.015 10 December 2018.

Parbhakar-Fox, A.K., Edraki, M., Hardie, K., Kadletz, O. & Hall, T. 2014. Identification of acid rock drainage sources through mesotextural classification at abandoned mines of Croydon, Australia: Implications for the rehabilitation of waste rock repositories. *Journal of Geochemical Exploration*, 137: 11–28.

Park, I., Hiroyoshi, N., Tabelin, C.B., Jeon, S., Li, X., Seno, K. & Ito, M. 2019. A review of recent strategies for acid mine drainage prevention and mine tailings recycling. *Chemosphere*, 219: 588–606.

Parviainen, A. 2009. Tailings mineralogy and geochemistry at the abandoned Haveri Au-Cu mine, SW Finland. *Mine Water and the Environment*, 28(4): 291–304.

Pérez, G., López-Mesas, M. & Valiente, M. 2008. Assessment of heavy metals remobilization by fractionation: Comparison of leaching tests applied to roadside sediments. *Environmental Science and Technology*, 42(7): 2309–2315.

Petrik, L.F., Fatoba, O.O., Missengue, R., Kalombe, R.M., Nyale, S. & Madzivire, G. 2017. Water Research Commission.

Ponomarenko, T., Nevskaya, M. & Jonek-Kowalska, I. 2021. Mineral Resource Depletion Assessment: Alternatives, Problems, Results. *Sustainability*, 13: 862.

Price, W. 2009. Prediction manual for drainage chemistry from sulphidic geologic materials. *Mend Report*, (December): 1–579. http://scholar.google.com/scholar?hl=en&btnG=Search&q=intitle:Prediction+Manual+for+Drainage+Chemistry+from+Sulphidic+Geologic+Materials#0.

UNIVERSITY of the WESTERN CAPE

http://etd.uwc.ac.za/

Price, W.A. 2009. Prediction Manual for Drainage Chemistry from Sulphidic Geologic Materials. MEND Report 1.20. 1. CANMET–Mining and Mineral Sciences Laboratories. Smithers. *British Columbia*.

Pushcharovsky, D.Y., Zubkova, N. V & Pekov, I. V. 2011. Structural and mineralogical school of NV Belov at Moscow State University: New data on silicates obtained at the Department of Crystallography and Crystal Chemistry. *Crystallography Reports*, 56(6): 986–993.

Quevauviller, P., Rauret, G., Rubio, R., López-Sánchez, J.-F., Ure, A., Bacon, J. & Muntau, H. 1997. Certified reference materials for the quality control of EDTA-and acetic acid-extractable contents of trace elements in sewage sludge amended soils (CRMs 483 and 484). *Fresenius' journal of analytical chemistry*, 357: 611–618.

Quispe, D., Pérez-López, R., Acero, P., Ayora, C. & Nieto, J.M. 2013. The role of mineralogy on element mobility in two sulfide mine tailings from the Iberian Pyrite Belt (SW Spain). *Chemical Geology*, 345: 119–129.

Ramla, B. & Sheridan, C. 2015. The potential utilisation of indigenous South African grasses for acid mine drainage remediation. *Water SA*, 41(2): 247–252.

Reddick Von Blottnitz H.** & Kothuis B***, J. 2007. A cleaner production assessment of the ultra-fine coal waste generated in South Africa. *Journal of the Southern African Institute of Mining and Metallurgy*, 107(12): 811–816.

Rezaie, B. & Anderson, A. 2020a. Sustainable resolutions for environmental threat of the acid mine drainage. *Science of the Total Environment*, 717: 137211.

Rezaie, B. & Anderson, A. 2020b. Sustainable resolutions for environmental threat of the acid mine drainage. , 717: 137211. https://www.sciencedirect.com/science/article/pii/S004896972030721X 19 July 2021.

Robb, L.J. & Meyer, F.M. 1995. The Witwatersrand Basin, South Africa: Geological framework and mineralization processes. *Ore Geology Reviews*,

UNIVERSITY of the WESTERN CAPE

http://etd.uwc.ac.za/

10(2): 67–94. http://www.sciencedirect.com/science/article/pii/0169136895000119 LK - link%7Chttp://www.sciencedirect.com/science/article/pii/0169136895000119 SRC - BaiduScholar FG - 0.

Robl, T., Oberlink, A. & Jones, R. 2017. *Coal Combustion Products (CCPs): Characteristics, Utilization and Beneficiation*. Woodhead Publishing.

des Roches, S., Brans, K.I., Lambert, M.R., Rivkin, L.R., Savage, A.M., Schell, C.J., Correa, C., de Meester, L., Diamond, S.E. & Grimm, N.B. 2021. Socio-eco-evolutionary dynamics in cities. *Evolutionary Applications*, 14(1): 248–267.

Rodríguez-Galán, M., Baena-Moreno, F.M., Vázquez, S., Arroyo-Torralvo, F., Vilches, L.F. & Zhang, Z. 2019. Remediation of acid mine drainage. *Environmental Chemistry Letters*, 17(4): 1529–1538. https://doi.org/10.1007/s10311-019-00894-w.

Rösner, T. 2001. A preliminary assessment of pollution contained in the unsaturated and saturated zone beneath reclaimed gold-mine residue deposits. *Water Research Commission*.

Rösner, T. & Schalkwyk, A. van. 2000. The environmental impact of gold mine tailings footprints in the Johannesburg region, South Africa. *Bulletin of Engineering Geology & the Environm...*, 59(2): 137–148. http://link.springer.com/article/10.1007/s100640000037 LK - link%7Chttp://link.springer.com/article/10.1007/s100640000037 SRC - BaiduScholar FG - 0.

Roy, W.R. & Griffin, R.A. 1982. A proposed classification system for coal fly ash in multidisciplinary research. *Journal of Environmental Quality*, 11(4): 563–568.

Roychoudhury, A.N. & Petersen, J. 2014. Geochemical evaluation of soils and groundwater affected by infiltrating effluent from evaporation ponds of a heavy mineral processing facility, West Coast, South Africa. *Journal of*

http://etd.uwc.ac.za/

Geochemical Exploration, 144: 478–491. https://www.sciencedirect.com/science/article/pii/S0375674214000806.

RoyChowdhury, A. 2015. *Green Remediation of Acid Mine Drainage (AMD)-Impacted Soil and Water*. https://digitalcommons.montclair.edu/etd.

Saria, L., Shimaoka, T. & Miyawaki, K. 2006. Leaching of heavy metals in acid mine drainage. *Waste Management & Research*, 24(2): 134–140.

Sarmiento, A.M., DelValls, A., Nieto, J.M., Salamanca, M.J. & Caraballo, M.A. 2011. Toxicity and potential risk assessment of a river polluted by acid mine drainage in the Iberian Pyrite Belt (SW Spain). *Science of the Total Environment*, 409(22): 4763–4771.

Sarmiento, A.M., Nieto, J.M., Olías, M. & Cánovas, C.R. 2009. Hydrochemical characteristics and seasonal influence on the pollution by acid mine drainage in the Odiel river Basin (SW Spain). *Applied Geochemistry*, 24(4): 697–714.

Sharifi, R., Moore, F. & Keshavarzi, B. 2013. Geochemical behavior and speciation modeling of rare earth elements in acid drainages at Sarcheshmeh porphyry copper deposit, Kerman Province, Iran. *Chemie der Erde*, 73(4): 509–517.

Simate, G.S. & Ndlovu, S. 2021. *Acid Mine Drainage: From Waste to Resources*. CRC Press.

Singer, P.C. & Stumm, W. 1970. Acidic mine drainage: the rate-determining step. *Science*, 167(3921): 1121–1123. http://europepmc.org/abstract/med/17829406 LK - link%7Chttp://europepmc.org/abstract/med/17829406 SRC - BaiduScholar FG - 0.

Singh, B.S.M., Singh, D. & Dhal, N.K. 2022. Enhanced phytoremediation strategy for sustainable management of heavy metals and radionuclides. *Case Studies in Chemical and Environmental Engineering*, 5: 100176.

Singh, P., Nel, A. & Durand, J.F. 2017. The use of bioassays to assess the toxicity of sediment in an acid mine drainage impacted river in Gauteng (South Africa). *Water SA*, 43(4): 673–683.

UNIVERSITY of the WESTERN CAPE

http://etd.uwc.ac.za/

Skousen, J. 2017. A methodology for geologic testing for land disturbance: Acid-Base Accounting for surface mines. *Geoderma*, 308: 302–311.

Snyman, C.P. & Botha, W.J. 1993. Coal in south Africa. *Journal of African Earth Sciences (and the Middle East)*, 16(1–2): 171–180.

Sracek, O., Choquette, M., Gélinas, P., Lefebvre, R. & Nicholson, R. v. 2004. Geochemical characterization of acid mine drainage from a waste rock pile, Mine Doyon, Québec, Canada. *Journal of Contaminant Hydrology*, 69(1–2): 45–71.

Sracek, O., Filip, J., Mihaljevič, M., Kříbek, B., Majer, V. & Veselovský, F. 2011. Attenuation of dissolved metals in neutral mine drainage in the Zambian Copperbelt. *Environmental Monitoring and Assessment*, 172(1–4): 287–299.

Sracek, O., Mihaljevič, M., Kříbek, B., Majer, V., Filip, J., Vaněk, A., Penížek, V., Ettler, V. & Mapani, B. 2014. Geochemistry and mineralogy of vanadium in mine tailings at Berg Aukas, northeastern Namibia. *Journal of African Earth Sciences*, 96: 180–189.

Srivastava, R.R., Pathak, P. & Perween, M. 2020. Environmental and health impact due to uranium mining. In *Uranium in Plants and the Environment*. Springer: 69–89.

Stewart, W., Miller, S. & Smart, R. 2006. Advances in acid rock drainage (ARD) characterisation of mine wastes. http://imwa.info/docs/imwa_2006/2098-Stewart-AU.pdf 29 July 2021.

Tabelin, C.B., Corpuz, R.D., Igarashi, T., Villacorte-Tabelin, M., Alorro, R.D., Yoo, K., Raval, S., Ito, M. & Hiroyoshi, N. 2020. Acid mine drainage formation and arsenic mobility under strongly acidic conditions: Importance of soluble phases, iron oxyhydroxides/oxides and nature of oxidation layer on pyrite. *Journal of Hazardous Materials*, 399: 122844. https://www.sciencedirect.com/science/article/pii/S0304389420308335.

UNIVERSITY of the WESTERN CAPE

http://etd.uwc.ac.za/

Tempelhoff, J.W.N. & Winde, F. 2019. Acid mine water drainage in South Africa: policy, economic issues and public concerns. *Water Services Management and Governance*: 77.

Tessier, A., Campbell, P.G.C. & Bisson, M. 1979. Sequential Extraction Procedure for the Speciation of Particulate Trace Metals. *Analytical Chemistry*, 51(7): 844–851.

Thakur, I.S. & Medhi, K. 2019. Nitrification and denitrification processes for mitigation of nitrous oxide from waste water treatment plants for biovalorization: Challenges and opportunities. *Bioresource technology*, 282: 502–513.

Tripathy, D.P. 2014. Prevention and treatment of acid mine drainage: an overview. *Recent Trends in Modelling of Environmental Contaminants*: 95–117.

Trumm, D. 2010. Selection of active and passive treatment systems for AMD - Flow charts for New Zealand conditions. *New Zealand Journal of Geology and Geophysics - N Z J GEOL GEOPHYS*, 53.

Tutu, H., Cukrowska, E., McCarthy, T., Mphephu, N. & Hart, R. 2003. Determination and modelling of geochemical speciation of uranium in gold mine polluted land in South Africa", Proceedings: International Congress on Mine Water and the Environment, pp. 137. , 2003 SRC.

Tutu, H., Cukrowska, E.M., McCarthy, T.S., Mphephu, N.F. & Hart, R. 2003. Determination and modelling of geochemical speciation of uranium in gold mine polluted land in South Africa. In *D. Armstrong, AB de Villiers, RLP Kleinmann, TS McCarthy & PJ Norton, Mine water and the environment. Proceedings of the 8th International Mine Water Association Congress, Johannesburg, South Africa*. 137–149.

Tutu, H., McCarthy, T. & Cukrowska, E. 2008. The chemical characteristics of acid mine drainage with particular reference to sources, distribution and remediation: The Witwatersrand Basin, South Africa as a case study. *Applied Geochemistry*, 23(12): 3666–3684.

http://etd.uwc.ac.za/

Ure, A.M., Quevauviller, P.H., Muntau, H. & Griepink, B. 1993. Speciation of heavy metals in soils and sediments. An account of the improvement and harmonization of extraction techniques undertaken under the auspices of the BCR of the Commission of the European Communities. *International journal of environmental analytical chemistry*, 51(1–4): 135–151.

Vassilev, S. V & Vassileva, C.G. 2007. A new approach for the classification of coal fly ashes based on their origin, composition, properties, and behaviour. *Fuel*, 86(10–11): 1490–1512.

Vassilev, S. V & Vassileva, C.G. 2009. A new approach for the combined chemical and mineral classification of the inorganic matter in coal. 1. Chemical and mineral classification systems. *Fuel*, 88(2): 235–245.

Vaziri, V., Sayadi, A.R., Parbhakar-Fox, A., Mousavi, A. & Monjezi, M.,. 2022. Improved mine waste dump planning through integration of geochemical and mineralogical data and mixed integer programming: Reducing acid rock generation from mine waste. *Journal of Environmental Management*, 309.

Verburg, Rens, Bezuidenhout, Nico & Chatwin. 2009. The Global Acid Rock Drainage Guide (GARD Guide). *Mine Water & the Environment*, 28(4): 305–310. http://link.springer.com/article/10.1007/s10230-009-0078-4 LK - link%7Chttp://link.springer.com/article/10.1007/s10230-009-0078-4 SRC - BaiduScholar FG - 0.

Vermeulen, N.J. 2001. The composition and state of gold tailings.

Wade, P. & Coetzee, H. 2008. Risk Assessment of Uranium in Selected Gold Mining Areas in South Africa" in Uranium, Mining and Hydrogeology Springer, , pp. . , 2008 SRC: 141–150.

Ward, C.R. 2002. Analysis and significance of mineral matter in coal seams. *International Journal of Coal Geology*, 50(1–4): 135–168.

Wei, X. & Wolfe, F.A. 2013. Minerals and mine drainage. *Water Environment Research*, 85(10): 1515–1547.

UNIVERSITY of the WESTERN CAPE

http://etd.uwc.ac.za/

Williams, D.J., Mulligan, D.R., Currey, N.A., Fourie, A. & Tibbett, M. 2006. *First International Seminar on Mine Closure. First International Seminar on Mine Closure*. null, ed.

Winde, F. & Walt, I. 2004. The significance of groundwater–stream interactions and fluctuating stream chemistry on waterborne uranium contamination of streams—a case study from a g... *Journal of Hydrology*, 287(1): 178–196. http://www.sciencedirect.com/science/article/pii/S0022169403004189 LK - link%7Chttp://www.sciencedirect.com/science/article/pii/S0022169403004189 SRC - BaiduScholar FG - 0.

Wolkersdorfer, C., Nordstrom, D.K., Beckie, R.D., Cicerone, D.S., Elliot, T., Edraki, M., Valente, T., França, S.C.A., Kumar, P., Lucero, R.A.O. & Soler i Gil, A. 2020. Guidance for the Integrated Use of Hydrological, Geochemical, and Isotopic Tools in Mining Operations. *Mine Water and the Environment*, 39(2): 204–228.

Wuana, R.A. & Okieimen, F.E. 2011. Heavy Metals in Contaminated Soils: A Review of Sources, Chemistry, Risks and Best Available Strategies for Remediation. *ISRN Ecology*, 2011: 1–20. https://www.hindawi.com/archive/2011/402647/ 18 January 2019.

Xavier, L.H., Giese, E.C., Ribeiro-Duthie, A.C. & Lins, F.A.F. 2021. Sustainability and the circular economy: A theoretical approach focused on e-waste urban mining. *Resources Policy*, 74: 101467. https://www.sciencedirect.com/science/article/pii/S0301420717305433.

Younger, P.L. 2004. Environmental impacts of coal mining and associated wastes: a geochemical perspective. *Geological Society, London, Special Publications*, 236(1): 169–209.

Younger, P.L., Jayaweera, A., Elliot, A., Wood, R., Amos, P., Daugherty, A.J., Martin, A., Bowden, L., Aplin, A.C. & Johnson, D.B. 2003. Passive treatment of acidic mine waters in subsurface-flow systems: Exploring RAPS and permeable reactive barriers. *Land Contamination and Reclamation*, 11(2): 127–136.

UNIVERSITY of the WESTERN CAPE

http://etd.uwc.ac.za/

Yucel, D.S. & Baba, A. 2016. Prediction of acid mine drainage generation potential of various lithologies using static tests: Etili coal mine (NW Turkey) as a case study. *Environmental monitoring and assessment*, 188: 1–16.

Zhang, J., Li, H. & Li, S. 2022. Mechanisms of Separation and Crystal Growth of Mullite Grains during Preparation of Mullite-Based Ceramics from High Alumina Coal Fly Ash. *Processes*, 10(11): 2416.

http://etd.uwc.ac.za/

APPENDIX

APPENDIX A: Coal fly ash whole data

SNo	Lon	Lat	Elevation	DepthFrom	depthTo	BHID	SiO2	Al2O3	CaO	Fe2O3	Na2O	MgO	TiO2	K2O	P2O5	MnO	SO3	S	LOI	Sum	As	Ba	Ce	Co	Cu
S1_Fresh ash	-26.56	29.12	1636.00	0.00	0.15	S1	50.91	25.49	8.96	2.27	2.21	1.87	1.78	0.95	0.71	0.05	0.03	0.01	4.78	100.00	61.32	2748.73	176.81	32.40	311
S1_Surface	-26.56	29.12	1635.70	0.30	0.50	S1	47.05	24.30	6.15	4.50	2.42	2.64	1.74	0.90	0.54	0.06	0.05	0.02	9.62	99.96	73.59	2088.80	172.49	26.19	322
S1_1.5m	-26.56	29.12	1634.70	1.30	1.50	S1	49.66	25.36	6.82	3.73	2.33	2.32	1.54	0.75	0.52	0.05	0.08	0.03	6.87	100.03	49.10	2117.76	158.07	35.19	331
S1_3m	-26.56	29.12	1633.20	2.80	3.00	S1	47.96	25.41	7.71	2.32	2.51	2.62	1.82	1.07	0.82	0.06	0.11	0.04	7.60	100.00	65.81	3059.38	175.02	31.49	332
S1_4.5m	-26.56	29.12	1631.70	4.30	4.50	S1	47.87	25.57	8.28	2.88	2.53	2.66	1.82	0.96	0.76	0.07	0.11	0.04	6.47	99.98	59.92	2850.41	158.15	35.10	319
S1_6m	-26.56	29.12	1630.20	5.80	6.00	S1	46.74	25.01	8.63	2.99	2.70	2.88	1.87	1.00	0.77	0.07	0.12	0.05	7.19	99.97	71.05	3008.75	192.92	37.81	346
S1_7.5m	-26.56	29.12	1628.70	7.30	7.50	S1	46.08	24.66	8.79	3.95	2.57	2.64	1.75	0.94	0.73	0.07	0.12	0.05	7.67	99.98	64.66	2592.50	146.13	20.20	326
S1_9m	-26.56	29.12	1627.20	8.80	9.00	S1	46.17	24.87	8.58	3.24	2.65	2.64	1.77	0.99	0.74	0.07	0.11	0.04	8.16	99.97	72.27	2658.84	158.72	39.25	332
S1_10.5m	-26.56	29.12	1625.70	10.30	10.50	S1	42.57	22.53	8.53	2.97	2.48	2.39	1.75	0.97	0.68	0.07	0.11	0.05	14.91	99.95	91.68	2770.29	197.60	29.37	328
S1_12m	-26.56	29.12	1624.20	11.80	12.00	S1	44.87	23.43	8.67	4.31	2.60	2.66	1.77	0.95	0.69	0.08	0.12	0.05	9.81	99.96	75.80	2699.57	194.45	28.30	335
S1_13.5m	-26.56	29.12	1622.70	13.30	13.50	S1	43.42	22.71	9.87	6.60	2.51	2.59	1.66	0.99	0.66	0.08	0.12	0.05	8.74	99.96	74.81	2559.92	178.38	36.20	330
S1_16.5m	-26.56	29.12	1619.70	16.30	16.50	S1	43.98	23.56	9.14	4.31	2.48	2.55	1.77	1.06	0.72	0.07	0.11	0.04	10.18	99.94	81.56	2709.95	200.16	30.77	321
S1_18m	-26.56	29.12	1618.20	17.80	18.00	S1	34.57	18.80	7.26	3.61	2.33	1.83	1.53	0.96	0.57	0.06	0.11	0.04	28.62	100.26	158.38	2684.65	242.86	34.68	351
S1_19m	-26.56	29.12	1617.20	18.80	19.00	S1	41.10	21.83	7.55	3.03	2.44	2.28	1.68	1.08	0.69	0.06	0.10	0.04	18.17	100.01	105.53	2880.44	188.87	26.16	340
S1_21m	-26.56	29.12	1615.20	20.80	21.00	S1	37.02	20.19	7.37	3.39	2.31	2.14	1.53	0.96	0.63	0.06	0.11	0.04	24.62	100.33	131.56	2791.79	189.43	32.29	346
S1_22.5m	-26.56	29.12	1613.70	22.30	22.50	S1	32.87	17.58	6.85	3.28	2.18	1.78	1.44	0.92	0.55	0.06	0.11	0.04	33.15	100.77	184.81	2754.26	211.25	49.99	347
S2_Fresh ashS2	-26.56	29.12	1635.00	0.00	0.15	S2	50.91	25.49	8.96	2.27	2.21	1.87	1.78	0.95	0.71	0.05	0.03	0.01	4.78	100.00	61.32	2748.73	176.81	32.40	311

http://etd.uwc.ac.za/

SurfaceS2	-26.56	29.12	1634.70	0.30	0.50	S2	46.16	23.43	8.45	3.18	2.36	3.31	1.91	1.14	0.83	0.07	0.06	0.02	9.05	99.95	95.41	3140.90	189.71	36.69	337
1.5mS2	-26.56	29.12	1633.70	1.30	1.50	S2	47.47	25.70	8.10	2.73	2.45	2.78	1.83	1.09	0.75	0.06	0.12	0.05	6.90	99.98	81.17	3110.10	159.97	23.80	337
3mS2	-26.56	29.12	1632.20	2.80	3.00	S2	47.52	24.71	8.14	3.12	2.56	2.56	1.92	1.22	0.71	0.07	0.09	0.04	7.33	99.94	76.55	2807.65	188.41	32.17	331
4.5mS2	-26.56	29.12	1630.70	4.30	4.50	S2	47.45	25.50	7.40	2.87	2.57	2.60	1.74	1.25	0.74	0.06	0.09	0.04	7.72	99.99	60.78	3076.57	163.15	37.15	336
6mS2	-26.56	29.12	1629.20	5.80	6.00	S2	45.43	24.43	8.89	3.50	2.79	2.58	1.90	1.24	0.78	0.07	0.10	0.04	8.22	99.93	92.52	3174.48	174.93	32.56	346
7.5mS2	-26.56	29.12	1627.70	7.30	7.50	S2	45.08	23.59	8.57	4.99	2.61	2.56	1.75	1.15	0.72	0.07	0.12	0.05	8.76	99.96	72.66	2808.59	168.96	23.34	336
9mS2	-26.56	29.12	1626.20	8.80	9.00	S2	45.75	20.69	9.90	4.30	3.00	2.77	2.10	1.29	0.81	0.08	0.11	0.04	9.04	99.85	104.42	3177.48	247.10	37.95	363
10.5mS2	-26.56	29.12	1624.70	10.30	10.50	S2	47.88	22.08	8.93	3.16	2.85	2.93	2.04	1.34	0.82	0.07	0.10	0.04	7.71	99.93	91.83	3217.71	211.03	27.32	347
12mS2	-26.56	29.12	1623.20	11.80	12.00	S2	49.65	21.27	8.51	3.39	2.90	3.00	2.08	1.40	0.83	0.07	0.11	0.04	6.73	99.94	80.01	3095.75	226.47	40.74	350
13.5mS2	-26.56	29.12	1621.70	13.30	13.50	S2	41.44	21.53	9.22	10.41	2.53	2.57	1.68	0.98	0.67	0.10	0.09	0.03	8.76	99.97	111.66	2656.86	248.08	26.31	358
15mS2	-26.56	29.12	1620.20	14.80	15.00	S2	45.89	23.59	7.75	5.10	2.38	2.44	1.74	1.15	0.71	0.07	0.08	0.03	9.07	99.97	80.29	2702.93	217.03	51.19	335
16.5mS2	-26.56	29.12	1618.70	16.30	16.50	S2	45.64	21.53	8.76	4.21	2.66	2.76	1.88	1.24	0.75	0.08	0.09	0.03	10.32	99.91	79.35	2984.96	200.16	37.68	344
18mS2	-26.56	29.12	1617.20	17.80	18.00	S2	47.77	22.32	8.69	3.33	2.88	2.90	1.98	1.27	0.84	0.07	0.09	0.04	7.80	99.94	83.98	3240.60	203.27	34.23	358
19.5mS2	-26.56	29.12	1616.20	18.80	19.00	S2	47.74	22.91	9.34	3.19	2.72	2.81	1.97	1.26	0.76	0.08	0.09	0.04	7.08	99.94	78.36	2920.14	198.83	31.62	335
21mS2	-26.56	29.12	1614.20	20.80	21.00	S2	48.13	22.51	9.60	2.94	2.80	2.91	2.08	1.21	0.81	0.08	0.09	0.04	6.78	99.93	82.44	3105.39	223.88	26.17	341
22.5mS2	-26.56	29.12	1612.70	22.30	22.50	S2	47.04	25.42	8.64	2.19	2.57	2.74	1.85	0.98	0.80	0.07	0.08	0.03	7.60	99.98	108.61	3108.29	225.37	31.18	361
24mS2	-26.56	29.12	1611.20	23.80	24.00	S2	46.62	21.21	9.98	2.47	3.02	3.10	2.11	1.10	0.84	0.08	0.10	0.04	9.28	99.90	86.66	3320.22	213.57	34.69	355
27mS2	-26.56	29.12	1608.20	26.80	27.00	S2	45.03	21.35	9.81	2.92	3.13	3.19	2.05	1.00	0.89	0.08	0.11	0.04	10.34	99.90	86.21	3319.43	231.74	42.38	375
28.5mS2	-26.56	29.12	1606.70	28.30	28.50	S2	44.74	20.08	11.24	2.90	3.16	3.31	2.12	0.88	0.95	0.09	0.09	0.04	10.27	99.84	91.83	3476.33	217.72	36.05	374
30mS2	-26.56	29.12	1605.20	29.80	30.00	S2	43.53	24.54	9.76	2.63	2.74	2.83	1.85	0.95	0.85	0.08	0.10	0.04	10.11	99.95	77.68	3137.80	225.83	27.71	353
31.5mS2	-26.56	29.12	1603.70	31.30	31.50	S2	58.86	11.87	6.69	6.81	3.17	2.91	1.51	4.41	0.36	0.12	0.04	0.02	3.18	99.93	152.90	1674.09	141.82	49.01	304

http://etd.uwc.ac.za/

Fresh ashS3	-26.56	29.12	1610.00	0.00	0.15	S3	50.91	25.49	8.96	2.27	2.21	1.87	1.78	0.95	0.71	0.05	0.03	0.01	4.78	100.00	61.32	2748.73	176.81	32.40
SurfaceS3	-26.56	29.12	1609.70	0.30	0.50	S3	46.16	23.43	8.45	3.18	2.36	3.31	1.91	1.14	0.83	0.07	0.06	0.02	9.05	99.95	95.41	3140.90	189.71	36.69
1.5mS3	-26.56	29.12	1608.70	1.30	1.50	S3	47.47	25.70	8.10	2.73	2.45	2.78	1.83	1.09	0.75	0.06	0.12	0.05	6.90	99.98	81.17	3110.10	159.97	23.80
3mS3	-26.56	29.12	1607.20	2.80	3.00	S3	47.52	24.71	8.14	3.12	2.56	2.56	1.92	1.22	0.71	0.07	0.09	0.04	7.33	99.94	76.55	2807.65	188.41	32.17
4.5mS3	-26.56	29.12	1605.70	4.30	4.50	S3	47.45	25.50	7.40	2.87	2.57	2.60	1.74	1.25	0.74	0.06	0.09	0.04	7.72	99.99	60.78	3076.57	163.15	37.15
6mS3	-26.56	29.12	1604.20	5.80	6.00	S3	45.43	24.43	8.89	3.50	2.79	2.58	1.90	1.24	0.78	0.07	0.10	0.04	8.22	99.93	92.52	3174.48	174.93	32.56
7.5mS3	-26.56	29.12	1602.70	7.30	7.50	S3	45.08	23.59	8.57	4.99	2.61	2.56	1.75	1.15	0.72	0.07	0.12	0.05	8.76	99.96	72.66	2808.59	168.96	23.34
9mS3	-26.56	29.12	1601.20	8.80	9.00	S3	45.75	20.69	9.90	4.30	3.00	2.77	2.10	1.29	0.81	0.08	0.11	0.04	9.04	99.85	104.42	3177.48	247.10	37.95
10.5mS3	-26.56	29.12	1599.70	10.30	10.50	S3	47.88	22.08	8.93	3.16	2.85	2.93	2.04	1.34	0.82	0.07	0.10	0.04	7.71	99.93	91.83	3217.71	211.03	27.32
12mS3	-26.56	29.12	1598.20	11.80	12.00	S3	49.65	21.27	8.51	3.39	2.90	3.00	2.08	1.40	0.83	0.07	0.11	0.04	6.73	99.94	80.01	3095.75	226.47	40.74
13.5mS3	-26.56	29.12	1596.70	13.30	13.50	S3	41.44	21.53	9.22	10.41	2.53	2.57	1.68	0.98	0.67	0.10	0.09	0.03	8.76	99.97	111.66	2656.86	248.08	26.31
15mS3	-26.56	29.12	1595.20	14.80	15.00	S3	45.89	23.59	7.75	5.10	2.38	2.44	1.74	1.15	0.71	0.07	0.08	0.03	9.07	99.97	80.29	2702.93	217.03	51.19
16.5mS3	-26.56	29.12	1593.70	16.30	16.50	S3	45.64	21.53	8.76	4.21	2.66	2.76	1.88	1.24	0.75	0.08	0.09	0.03	10.32	99.91	79.35	2984.96	200.16	37.68
18mS3	-26.56	29.12	1592.20	17.80	18.00	S3	47.77	22.32	8.69	3.33	2.88	2.90	1.98	1.27	0.84	0.07	0.09	0.04	7.80	99.94	83.98	3240.60	203.27	34.23
19.5mS3	-26.56	29.12	1591.20	18.80	19.00	S3	47.74	22.91	9.34	3.19	2.72	2.81	1.97	1.26	0.76	0.08	0.09	0.04	7.08	99.94	78.36	2920.14	198.83	31.62
21mS3	-26.56	29.12	1589.20	20.80	21.00	S3	48.13	22.51	9.60	2.94	2.80	2.91	2.08	1.21	0.81	0.08	0.09	0.04	6.78	99.93	82.44	3105.39	223.88	26.17
22.5mS3	-26.56	29.12	1587.70	22.30	22.50	S3	47.04	25.42	8.64	2.19	2.57	2.74	1.85	0.98	0.80	0.07	0.08	0.03	7.60	99.98	77.21	3057.52	166.83	18.28
24mS3	-26.56	29.12	1586.20	23.80	24.00	S3	46.62	21.21	9.98	2.47	3.02	3.10	2.11	1.10	0.84	0.08	0.10	0.04	9.28	99.90	86.66	3320.22	213.57	34.69
25.5MS3	-26.56	29.12	1584.70	25.30	25.50	S3	40.65	23.27	10.39	5.50	2.81	2.74	1.79	0.90	0.79	0.09	0.10	0.04	10.90	99.93	108.61	3108.29	225.37	31.18
27mS3	-26.56	29.12	1583.20	26.80	27.00	S3	45.03	21.35	9.81	2.92	3.13	3.19	2.05	1.00	0.89	0.08	0.11	0.04	10.34	99.90	86.21	3319.43	231.74	42.38
28.5mS3	-26.56	29.12	1581.50	28.50	28.50	S3	44.74	20.08	11.24	2.90	3.16	3.31	2.12	0.88	0.95	0.09	0.09	0.04	10.27	99.84	91.83	3476.33	217.72	36.05

http://etd.uwc.ac.za/

30mS3	-26.56	29.12	1580.20	29.80	30.00	S3	43.53	24.54	9.76	2.63	2.74	2.83	1.85	0.95	0.85	0.08	0.10	0.04	10.11	99.95	77.68	3137.80	225.83	27.71	
31.5mS3	-26.56	29.12	1578.70	31.30	31.50	S3	58.86	11.87	6.69	6.81	3.17	2.91	1.51	4.41	0.36	0.12	0.04	0.02	3.18	99.93	152.90	1674.09	141.82	49.01	

APPENDIX B: Coal fly ash water fraction

Sampleno	Si	Al	Ca	Fe	Na	K	Mg	Sr	Ba	Mn	As	Pb	Zn	Ni	Mo	Cu
S1_Fresh ash	1217.26	495.52	792.11	5.61	1618.3	355.22	20.34	56.72	5.59	0.8	1.51	0.23	0.59	0.34	0.47	0.
S1_3m	2041.24	439.4	1445.56	1.42	1654.92	391.86	30.55	109.15	7.67	0.01	0.01	0.01	1.83	0.2	0.88	0.
S1_6m	1216.92	153.58	828.38	6.1	1387.71	528.78	10.68	75.72	6.77	0.01	0.01	0.01	0.9	0.01	0.09	
S1_9m	1703.72	496.58	1308.6	8.44	1072.25	362.47	34.52	51.03	3.26	0.71	0.01	2.64	0.8	0.01	1.32	0.
S1_18m	1656.61	225.32	1197.86	11.17	1195.69	636.09	15.66	0.01	0.81	1.54	4.57	4.29	3	0.01	0.56	0.
S1_19m	1147.54	499.43	619.48	18.42	1818.74	620.3	34.72	0.01	1.18	1.23	0.01	2.85	1.99	0.01	0.36	
Fresh ashS3	1217.26	495.52	792.11	5.61	1618.3	355.22	20.34	56.72	5.59	0.8	1.51	0.23	0.59	0.34	0.08	0.
S2_Fresh ashS2	1217.26	495.52	792.11	5.61	1618.3	355.22	20.34	56.72	5.59	0.8	1.51	0.23	0.59	0.34	0.47	0.
22.5mS2	1947	975.03	643.81	0.01	2407.4	339.31	0.01	49.47	25.43	0.98	0.01	0.04	0.01	0.88	0.17	0.
S1_Surface	3481.31	512.7	323.01	0.01	1100.94	429.91	35.64	28.24	5.98	0.01	0.01	0.01	0.01	1.6	0.02	0.
S1_1.5m	3407.7	1056.85	361.07	42.75	1155.43	448.36	73.47	108.67	13.87	0.01	0.01	0.01	2.18	0.01	0.05	0.
S1_12m	4139.8	704.8	708.94	48.06	1523.15	422.23	49	94.23	13.91	0.01	18.45	7.6	0.24	0.01	0.01	0.
S1_13.5m	4573.63	208.06	758.53	36.76	600.53	703.34	14.46	51.18	11.54	0.01	23.08	20.03	1.25	1.52	0.78	0.
S1_7.5m	2638.17	76.88	344.73	18.2	1410.09	458.09	5.34	67.13	5.95	2.24	11.57	3.13	0.31	0.01	0.01	0.
6mS2	1843.72	646.28	381.83	16.99	1305.82	57.83	54.48	31.95	3.3	0.72	0.04	0.01	0.35	0.08	0.05	0.
10.5mS2	1966.56	305.52	454.55	21.69	1538.11	71.95	156.41	32.72	3.7	0.6	0.02	0.01	1.37	0.06	0	0.
SurfaceS2	1883.28	202.59	382.56	0.01	678.36	19.21	241.22	27.82	0.8	0.01	0.01	0.01	0.01	0.02	0.07	0.
1.5mS2	1981.59	735.07	501.31	16.16	695.78	49.41	79.23	34.3	5.88	0.47	0.06	0	0.1	0.11	0.01	0.

http://etd.uwc.ac.za/

3mS2	1845.53	331.22	442.91	9.69	880.24	48.96	177.88	36.91	4.77	1.2	0.04	0.01	0.2	0.08	0.08	0.
4.5mS2	1868.29	396.06	473.96	14.82	1073.68	58.11	78.42	42.57	1.6	1.1	0.07	0.01	0.01	0.12	0.01	0.
7.5mS2	1864.64	262.91	398.44	1.25	1145.83	57.35	273.74	36.66	4.42	0.41	0.02	0	0.08	0.01	0.03	0.
9mS2	1931.44	317.6	386.73	6	899.89	47.31	224.64	37.89	6.63	0.41	0.01	0.01	0.05	0.02	0.01	0.
12mS2	2000.18	301.92	366.05	0.01	1015.04	46.14	202.3	39.3	5.3	1	0.06	0.01	0.07	0.02	0.07	0.
13.5mS2	1841.44	176.97	488.56	40.26	1019.99	44.51	314.47	39.89	1.25	0.73	0.05	0.01	0.05	0.01	0.01	0.
15mS2	1854.39	246.23	476.62	8.71	974.8	50.97	183.38	40.95	3.76	0.4	0.06	0.01	0.09	0.12	0.01	0.
16.5mS2	1822.27	275.13	573.82	0.01	1131.36	49.43	139.36	45.12	4.99	0.78	0.08	0.01	0.06	0.01	0.03	0.
18mS2	1874.9	259.17	531.67	3.14	1072.97	95.93	114.8	44.58	5.53	0.63	0.05	0.01	0.18	0.04	0.01	0.
19.5mS2	1899.2	248.31	467.91	5.43	1233.44	71.44	85.86	43.39	4.13	0.5	0.04	0.01	0.01	0.07	0.05	0.
21mS2	1849.39	219.92	494.12	0.01	1279.26	71.36	157.43	41.77	4.16	0.67	0.07	0.01	0.01	0.03	0.03	0.
S1_21m	514.53	206.59	1050.11	19.78	1153.12	516.32	14.36	0.01	0.23	0.47	5.7	1.59	1.22	0.01	0.02	0.
SurfaceS3	38.81	233.96	989.18	9.83	291.85	31.97	23.34	71.1	27.74	0.01	0.01	0.01	0.01	0.01	0.08	0.
1.5mS3	0.01	225.84	1276.81	6.9	457.54	51.13	21.27	157.15	34.34	0.01	0.01	0.01	1.52	0.01	0.09	0.
3mS3	332.9	213.95	1007.06	0.01	572.08	56.72	42.14	113.16	33.49	0.01	0.01	0.01	1.34	0.01	0.06	0.
4.5mS3	0.01	238.48	1036.19	0.01	612.04	53.58	16.85	94.2	32.12	0.01	0.01	0.01	0.63	0.01	0.13	0.
6mS3	0.01	214.82	833.25	0.01	691.12	50.85	21.03	102.84	19.54	0.01	0.01	0.01	0.76	0.01	0.01	0.
7.5mS3	136.65	221.55	1312.29	17.98	702.61	47.34	27.16	131	65.41	0.01	0.01	0.01	1.18	0.3	0.07	0.
9mS3	46.8	216.68	991.43	12.59	550.37	47.04	18.91	120.24	23.81	0.01	0.01	0.01	1.24	0.23	0.09	0.
10.5mS3	167.71	246.43	1168.03	48.33	613.67	52.62	21.78	118.8	40.63	0.17	0.01	0.01	0.99	0.27	0.09	0.
12mS3	44.48	273.98	1131.27	0.01	548.65	40.85	15.12	126.27	21.86	0.01	0.01	0.01	0.91	0.25	0.11	0.
13.5mS3	150.83	267.98	1168.74	3.57	424.52	29.94	13.82	102.8	26.51	0.82	1.8	0.29	1.12	0.71	0.21	0.
15mS3	90.69	247.69	1017.26	8.12	455.3	42.34	23.67	147.4	30.5	0.13	1.7	1.03	0.74	0.53	0.07	0.
16.5mS3	136.15	234.11	674.96	15.44	504	51.83	31.72	115.31	36.45	0.05	0.01	0.89	1.12	0.54	0.01	0.
18mS3	54.11	243.97	953.19	4.8	425	38.69	7.53	94.19	29.14	0.01	3	0.72	1.12	0.01	0.12	0.
19.5mS3	81.63	256.75	955.5	23.6	503.67	49.74	33.95	109.57	37.92	0.01	0.27	0.12	0.64	0.68	0.01	0.

http://etd.uwc.ac.za/

21mS3	1013.06	258.1	783.34	22.75	412.97	25.27	22.5	89.23	28.5	0.7	1.54	0.01	0.79	0.01	0.13	0.
22.5mS3	116.09	272.64	1185.25	49.85	513.44	51.45	5.4	117.41	42.71	0.2	2.39	0.01	1.15	0.01	0.01	0.
S1_4.5m	1313.55	90.99	2510.36	8.25	1340.88	389.52	6.33	71.29	4.81	0.01	0.01	0.01	2.59	0.01	0.09	0.
S1_22.5m	783.81	425.93	2901.05	27.07	1744.05	763.1	29.61	0.01	1.21	0.24	4.78	4.41	3.17	0.01	0.31	1.
S1_10.5m	3554.26	649.46	2108.9	20.09	1251.81	405.19	45.15	79.77	10.82	1.04	27.36	5.1	0.6	2.62	0.01	0.
S1_16.5m	3328.12	17.64	1851.23	21.27	841.07	440.52	1.23	48.94	5.8	0.43	17.83	0.01	0.29	0.01	0.04	0.

UNIVERSITY of the
WESTERN CAPE

http://etd.uwc.ac.za/

APPENDIX C: Coal fly ash carbonate fraction

Sample_no	Si	Al	Ca	Fe	Na	K	Mg	Sr	Ba	Mn	As	Pb	Zn	Ni	Mo	Cu
S1_Fresh ash	12439	9860.47	3927.94	189.7	207.3	147.47	202.16	113.66	111.84	17.2	2.9	3.84	0.78	1.27	0.64	0.48
S1_Surface	18056.07	2713.27	3035.34	0.01	227.15	52.45	131.87	30.41	47.99	5.51	0.01	0.01	0.01	0.01	0.01	0.01
S1_1.5m	18485.11	2791.33	2522.66	295.23	237.73	101.21	266.26	49.8	67.2	14.3	4.54	2.13	0.01	2.24	0.01	0.01
S1_3m	8685.94	2367.21	1022.45	180.26	0.01	55.08	349.34	62.08	51.44	12.08	0.01	0.77	0.01	0.01	0.01	0.01
S1_4.5m	6241.21	1504.18	1269.59	152.81	0.01	53.27	442.77	57	62.7	17.04	0.01	0.01	0.08	0.01	0.01	0.01
S1_6m	8733.3	1256.72	1276.16	0.01	0.01	3.25	367.28	52.8	79.3	14.7	0.01	2.24	0.01	1.12	0.49	0.01
S1_7.5m	8680.74	1681.95	1177.38	0.01	0.01	0.01	514.17	114.76	80.68	20.32	42.06	1.2	0.01	3.94	0.22	0.01
S1_9m	9081.7	1573.83	1201.23	0.01	0.01	0.01	392.01	153.84	122.45	18.71	2.24	2	0.62	1.65	0.28	0.73
S1_10.5m	14938.76	3182.82	3077.37	108.51	0.01	0.01	262.33	104.94	120.49	11.13	1.69	5.37	0.01	0.01	0.58	0.01
S1_12m	13774.49	3299.75	3210.35	0.01	0.01	0.01	276.94	130.63	157.25	11.95	1.41	1.47	0.01	2.88	0.93	0.01
S1_13.5m	29416.95	10072.41	2668.46	0.01	0.01	0.01	321.38	107.69	147.96	17.33	2.37	0.01	0.01	0.01	0.32	0.01
S1_16.5m	16985	5746.6	1705.91	0.01	0.01	0.01	542.14	168.13	159.39	23.99	0.01	0.85	0.01	0.01	0.01	0.01
S1_18m	12788.63	557.94	1038.78	59.73	0.01	0.01	235.63	115.27	91.58	15.24	1.31	0.99	0.01	0.01	0.01	0.01
S1_19m	23873.44	1925.49	1734.39	93.53	0.01	0.01	243.94	144.1	136.74	14.87	3.63	0.01	0.01	1.83	4.39	0.01
S1_21m	6457.69	851.35	2847.22	71.42	0.01	0.01	364.68	142.27	127.16	21.67	0.01	0.01	0.01	0.91	0.01	0.01
S1_22.5m	10320.14	2551.01	31.14	84.73	0.01	114.17	247.88	153.66	152.97	15.79	0.01	0.01	0.01	0.01	0.01	0.01
Fresh ashS3	12439	9860.47	3927.94	189.7	207.3	147.47	202.16	113.66	111.84	17.2	2.9	3.84	0.78	1.27	0.48	0.78
SurfaceS3	11664.2	3173.22	2587.29	31.74	304.79	127.25	293.54	487.23	337.02	5.7	2.79	0.01	0.99	2.45	0.1	0.45

http://etd.uwc.ac.za/

1.5mS3	24051.54	3911.07	2825.58	78.81	337.16	115.78	345.88	634.39	632.13	11.61	1.08	0.64	1.01	1.9	0.18	0.49
3mS3	22801.2	3902.78	3031.27	27.31	355.47	158.58	354.67	612.3	599.43	11.67	0.01	0.07	1.03	1.12	0.07	0.24
4.5mS3	26194.41	3748	2862.67	81.65	387.13	133.31	322.82	580.94	568.58	9.34	1.52	0.06	0.99	1.7	0.46	0.57
6mS3	17215.5	3562.26	1817.54	55.48	358.4	112.65	361.06	320.29	299.21	6.61	3.43	0.16	0.97	2.38	0.28	0.34
7.5mS3	21663.42	4713.18	4088.96	174.65	444.24	203.65	323.75	701.23	698.57	5.46	1.28	0.01	1.05	0.83	0.51	0.38
9mS3	8196.06	4359.64	4547.89	75.06	571.05	260.61	474.98	998.8	751.05	5.62	0.56	0.01	1.15	0.35	0.69	0.23
10.5mS3	4710.36	4063.47	2942.86	62.1	349.66	161.62	348.03	689.13	479.11	5.88	1.94	0.01	0.98	0.34	0.01	0.39
12mS3	2989.24	3912.74	1132.12	49.07	368.15	83.91	316.16	361.94	319.81	4.25	0.01	0.31	1.03	0.75	0.57	0.53
13.5mS3	4652.22	4259.76	3240.69	42.65	448.04	167.79	380.45	706.46	547.98	9.4	1.31	0.01	1	0.39	0.01	0.39
15mS3	3733.14	3621.96	2769.47	91.36	454.19	120.67	387.04	673.42	472.35	8	0.28	0.53	0.99	0.42	0.01	0.27
16.5mS3	3127.2	3566.04	2480.67	54.79	451.98	170.68	297.66	537.69	422.97	5.95	0.29	0.83	1.04	0.39	0.01	0.42
18mS3	10510.62	6561.07	2269.89	39.15	540.11	220.83	404.88	484.54	387.75	6.87	0.18	0.24	1.01	0.37	0.01	0.26
19.5mS3	10738.44	10219.05	3143.5	99.66	644.32	271.63	551.16	636.02	557.2	8.6	1.36	0.51	1.13	0.74	0.01	0.3
21mS3	7226.7	7827.1	2382.75	45.69	399.08	94.32	438.32	455.22	422.59	10.38	0.84	0.85	1.1	1.52	0.01	0.27
22.5mS3	12891.06	11058.1	3443.9	94.63	539.66	175.37	447.02	788.31	628.67	9.85	2.07	0.81	1.09	0.46	0.01	0.22
S2_FreshashS2	12439	9860.47	3927.94	189.7	207.3	147.47	202.16	113.66	111.84	17.2	2.9	3.84	0.78	1.27	0.64	0.48
SurfaceS2	3519.95	6365.8	490.59	286.76	4.48	33	132.43	66.81	157.85	14.1	0.01	2.43	0.07	0.1	3.06	0.1
1.5mS2	6975.12	7769.31	889.82	521.07	2.95	28.98	268.11	113.13	155.44	22.51	0.14	2.15	0.45	0.09	3.21	0.27
3mS2	14394.84	10326.06	1256.51	353.67	4.53	38.16	325.09	183.57	185.4	32.79	3.42	1.48	0.14	0.17	1.73	0.33
4.5mS2	13787.7	10392.04	1668.52	585.15	3.33	63.44	384.76	238.94	214.12	41.46	2.03	0.5	0.12	0.36	3.52	0.21
6mS2	11270.87	8924.7	1468.89	351.25	3.67	46.26	329.81	194.97	197.43	42.13	0.01	1.26	0.29	0.55	3.81	0.33
7.5mS2	9101.98	7615.72	1667.48	0.01	90.42	65.75	225.63	130.2	110.64	33.5	0.01	2.32	1.33	0.46	0.01	0.45
9mS2	9776.82	8803.3	1658.08	171.07	91.44	57.88	292.01	154.68	164.75	35.11	0.81	1.4	1.13	0.22	0.01	0.18
10.5mS2	10869.83	9050.29	1750.2	146.5	90.25	59.21	278.05	132.83	134.41	38.31	0.01	0.6	1.24	0.47	0.01	0.41
12mS2	7859.45	7505.75	1395.65	75.36	88.37	44.77	209.05	133.39	162.07	23.55	0.01	2.52	0.98	0.38	0.01	0.34

http://etd.uwc.ac.za/

13.5mS2	10537.5	8734.56	1390.43	103.37	82.78	15.71	191.05	134.23	115.74	20.41	0.01	0.99	0.95	0.15	0.01	0.29
15mS2	19522.58	10610.63	1328.25	240.41	84.78	91.24	210.78	157.2	129.66	29.14	1.6	0.24	0.01	0.28	2.5	0.28
16.5mS2	20384.19	12446.88	1685.33	352.5	85.73	60.05	271.17	184.49	152.24	34.84	0.01	1.32	0.01	0.25	1.6	0.17
18mS2	13775.49	9750.33	1082.47	107.7	88.6	43.19	177.85	137.4	116.74	21.46	0.01	1.37	0.01	0.55	2.57	0.26
19.5mS2	14107.26	10035.72	1232.19	113.39	85.67	57.29	199.66	156.45	153.59	24.67	0.01	1.61	0.01	0.54	1.76	0.47
21mS2	18356.22	11542.23	1588.22	174.69	85.79	63.29	222.21	189.22	186.96	30.97	0.01	0.6	0.01	0.38	2.58	0.33
22.5mS2	16162.83	11293.92	1406.34	220.96	92.17	72.77	210.96	172.24	195.77	29.73	1.07	0.68	0.09	0.66	2.38	0.32

UNIVERSITY of the
WESTERN CAPE

http://etd.uwc.ac.za/

APPENDIX D: Coal fly ash Fe/Mn results

Sampleno	Si	Al	Ca	Fe	Na	K	Mg	Sr	Ba	Mn	As	Pb	Zn	Ni	Mo	C
S1_Fresh ash	13545.89	8328.45	2152.95	1996.23	404.45	98.03	653.33	262.53	138.72	40.51	1.96	0.41	1.65	0.97	0.55	
S1_Surface	18571.49	5082.05	687.37	3955.33	71.67	90.15	358.56	309.82	205.46	145.73	0.49	0.4	2.35	0.85	0.67	
S1_1.5m	3515.56	92.57	3178.9	3370	79.31	111.45	3.93	559.66	303	11.13	1.44	0.38	2.51	0.01	0.77	
S1_3m	17567.22	6190.17	5674.96	4063.21	0.01	0.01	1042.04	209.68	144.66	199.24	1.04	0.45	1.67	1.71	0.4	
S1_4.5m	6990.53	3706.5	3530.52	1720.28	0.01	37.83	1298.87	207.78	78.59	271.09	0.35	0.49	1.34	0.5	0.53	
S1_6m	550.71	619.56	4559.73	15.3	72.6	351.11	12.65	353.2	186.32	4.75	0.9	0.03	1.58	1.4	0.01	
S1_7.5m	656.64	483.42	4162.38	32.77	186.77	277.48	64.23	320.83	172.33	6.45	1.06	0.1	0.94	1.57	0.01	
S1_9m	20394.69	5724.28	3419.05	1860.3	0.01	0.01	645.44	347.9	168.01	144.39	0.3	0.25	1.54	2.11	0.01	
S1_10.5m	22206.44	13095.7	3712.9	4425.38	0.01	0.01	787.47	460.93	234.6	145.84	1.05	0.01	1.29	1.39	0.84	
S1_12m	17772.37	2604.28	5170.91	3741.37	169.87	335.82	915.83	449.62	247.5	81.57	1.61	0.22	1.71	0.01	0.31	
S1_13.5m	22788.55	3053.52	1705.83	4209.29	292.47	816.57	310.2	450.47	194.66	81.54	1.46	0.28	1.24	0.01	0.27	
S1_16.5m	14030.63	6547.47	2814.7	2527.04	0.01	0.01	1392.87	340.32	154.73	254.63	0.01	0.34	1.07	0.01	0.01	
S1_18m	21280.08	4827.3	2211.04	3130.88	0.01	45.42	1155.43	411.09	184.71	167.15	0.01	0.26	1.52	1.38	0.88	
S1_19m	24833.66	5057.4	2854.66	3879.3	98.36	22.55	262.33	416.13	272.48	31.21	1.91	1.03	2.13	1.79	0.9	
S1_21m	7822.76	816.41	1913.59	728.64	109.76	195.22	293.66	203.43	86.3	42.35	0.96	0.17	1.1	0.01	0.62	
S1_22.5m	15439.08	13169.63	2459.41	10251.84	0.01	11.03	1439.83	34.16	93.52	181.4	0.01	0.88	1.22	0.01	1.16	
Fresh ashS3	13545.89	8328.45	2152.95	1996.23	404.45	98.03	653.33	262.53	138.72	40.51	1.96	0.41	1.65	0.97	0.37	
SurfaceS3	19907.79	6378.53	938.78	2396.73	442.16	124.59	891.96	16.9	4	76.84	1.66	2.35	0.03	1.05	0.38	
1.5mS3	8333.15	5580.66	1264.33	4018.03	402.73	99	830.77	46.27	14.81	64.28	1.86	2.51	0.01	0.81	0.01	
3mS3	9202.16	5298.86	1448.14	4157.61	544.11	79.85	492.09	158.55	47.38	52.57	1.71	2.27	0.01	0.55	0.01	
4.5mS3	11015.38	4255.76	906.2	5151.71	559.13	117.41	786.3	300.62	126.64	55.71	1.68	1.63	0.01	0.62	0.01	

http://etd.uwc.ac.za/

6mS3	12295.33	5368.84	1218.37	5572.25	625.7	117.11	789.63	663.35	182.43	59.75	1.75	0.47	0.01	0.52	0.15	
7.5mS3	35558.62	12835.6	1446.14	5884.41	960.35	205.49	755.29	449	163.59	87.17	0.4	1.04	0.01	0.61	0.11	
9mS3	27987.43	11432.28	1444.96	2817.66	696.93	196.02	743.79	498.32	156.06	80.1	1.59	0.01	0.01	0.89	0.15	
10.5mS3	19702.84	8755.73	1698.08	2225.56	601.96	129.66	637.24	314.99	111.34	70.27	0.56	0.01	0.01	0.93	0.19	
12mS3	26877.03	9882.66	1660.93	3399.3	496.3	138.76	525.9	150.04	87.66	73.71	1.35	0.01	0.01	0.85	0.11	
13.5mS3	13596.66	7252.62	1519.89	3595.97	210.89	141.33	491.49	201.01	56.36	84.72	0.01	0.01	0.01	1.84	0.38	
15mS3	29150.09	10802.6	3062.35	5198.46	1597.67	204.15	754.06	150.95	53.86	81.81	2.24	0.78	0.05	0.52	0.13	
16.5mS3	30598.78	13826.93	1646.58	7013.71	494.4	66.79	747.91	369.51	158.39	61.81	1.32	0.01	0.01	0.82	0.18	
18mS3	15713.68	10246.57	1907.1	3516.43	651.05	165.55	809.45	149.67	62.49	47.12	1.05	0.18	0.01	0.69	0.12	
19.5mS3	19950.69	13473.07	3950.85	3377.75	129.78	12.35	360.14	173.99	83.1	42.4	0.65	0.01	0.01	0.92	0.16	
21mS3	22020.16	13538.15	2414.22	3888.54	343.25	50.56	943.15	88	52.91	66.45	0.01	0.01	0.01	0.71	0.15	
22.5mS3	18551.08	11484.7	2964.48	2790.43	247.22	103.76	589.59	269.23	98.94	50.75	2.73	0.02	0	0.57	0.16	
S2_Fresh ashS2	13545.89	8328.45	2152.95	1996.23	404.45	98.03	653.33	262.53	138.72	40.51	1.96	0.41	1.65	0.97	0.55	
SurfaceS2	7562.3	8809.17	1109.5	1139	50.82	37.37	977.28	31.11	32.34	41.81	1.34	0.01	1.67	0.01	0.01	
1.5mS2	7426.87	9279.38	1012.04	1307	39.98	36.11	706.87	34.38	42.82	40.17	2.64	0.01	1.51	0.36	2.51	
3mS2	5159.44	9142.43	1014.07	1256.51	52.62	54.65	606.96	71.79	45.75	24.66	0.8	0.01	1.82	0.28	4.24	
4.5mS2	5583.99	8878.72	1048.28	1202.97	49.54	47.37	738.44	82.66	43.99	39.07	1.57	0.2	1.86	0.35	0.26	
6mS2	5111.68	8658	1061.99	1286.93	37.79	36.68	551.49	74.45	33.64	36.27	1.47	0.01	1.14	0.07	2.23	
7.5mS2	15666.56	9546.14	928.27	1103	49.58	36.96	738	149.75	59.12	26.65	2.49	0.02	1.68	1.02	4.02	
9mS2	10366.54	9680.84	1045.41	1244.3	51.93	50.29	760.05	104.58	54.42	29.34	0.4	0.01	1.6	0.61	0.19	
10.5mS2	10512.58	9953.6	1056.51	1134.12	48.88	33.77	629.73	194.95	65.1	23.94	1.77	0.01	1.99	0.8	3.09	
12mS2	9409.06	9776.01	969.24	1178.74	51.14	41.11	674.23	162.14	68.38	24.27	1.98	0.17	1.65	0.67	0.01	
13.5mS2	9101.43	9454.2	959.87	1093.59	60.28	36.81	576.81	154.26	79.46	16.24	2.35	0.08	1.84	0.8	0.28	
15mS2	5842.96	8614.78	869.61	1006.27	48.76	32.47	612.28	77.94	40.27	17.89	1.08	0.01	1.18	0.73	1.52	
16.5mS2	16929.34	9813.62	1122.93	1183.89	48.5	55.16	586.37	196.84	71.98	19.14	2.37	0.36	1.38	0.84	4.44	
18mS2	9373.93	9540.83	1016.05	1183.02	47.69	50.71	559.15	143.55	61.05	17.9	1.35	0.36	1.89	0.75	3.35	

http://etd.uwc.ac.za/

19.5mS2	8619.44	9322.98	1077.66	1082.15	60.42	44.31	573.12	173.64	70.81	20.32	2.79	0.24	2.25	1.15	3.02
21mS2	8526.76	9971.56	1126.6	1190.71	62.72	67.89	652.29	178.89	75.54	15.85	1.79	0.01	1.75	1.18	1.22
22.5mS2	7223.23	8958.04	1123.23	1237.16	46.75	67.94	756.07	90.01	38.65	17.4	2.31	0.01	0.99	0.55	1.51

APPENDIX E: Gold tailings whole data

Sample_No	Sample_ID	Depth_from_M	Depth_to_M	LOI	SiO2	Al2O3	Fe2O3	CaO	MgO	Na2O	K2O	MnO	TiO2	P2O5	Cr2O3	TOTC	TOTS	Ba	Co	Cs	Ga	Hf	Nb	Rb	Sn	Sr
MT001	T008	1	1.2	2.02	90.3	4.63	1.42	0.28	0.41	0.03	0.28	0.005	0.24	0.02	0.041	0.02	0.26	41	3.6	0.9	5.2	3	5.7	7.2	2	14.1
MT002	T008	1.9	2.1	1.72	90.2	4.56	0.86	0.3	0.29	0.02	0.26	0.005	0.24	0.01	0.025	0.05	0.26	38	2.9	1.1	5.2	2.6	4.8	7.2	2	16.1
MT003	T008	3	3.2	5.54	83.4	5.33	3.4	0.24	0.54	0.03	0.25	0.005	0.18	0.03	0.038	0.03	2	39	49.7	0.9	5.7	3.2	4.3	7.4	2	18.2
MT004	T008	4	4.2	3.6	85	5.96	2.69	0.27	0.59	0.03	0.25	0.02	0.26	0.02	0.035	0.03	1.25	46	36.9	0.9	6.4	3	3.9	8.6	2	18.9
MT005	T008	5	5.2	5.55	79.2	8.25	3.66	0.53	0.58	0.09	0.4	0.04	0.27	0.03	0.037	0.08	1.61	67	69.3	1.5	8.8	2.9	4	13.8	2	32.3
MT006	T008	6	6.2	5.38	78.5	7.82	3.73	0.85	0.81	0.16	0.39	0.3	0.29	0.04	0.04	0.13	1.53	144	65.7	1.4	8.6	3	4.2	13.3	2	48.9
MT007	T008	7	7.1	5.57	77	8.46	3.05	1.7	0.58	0.11	0.37	0.65	0.28	0.04	0.046	0.2	1.75	264	57.1	2.7	9	3.8	5	13.6	3	67.8
MT007-1	T008	7.5	7.6	4.62	70.7	9.08	8.77	1.64	0.6	0.14	0.55	0.45	0.28	0.04	0.049	0.22	1.78	172	97.1	3	9.7	3.4	4.8	18.1	4	64.8
MT008	T008	8	8.2	2.35	89	3.83	2.34	0.51	0.34	0.05	0.17	0.25	0.25	0.02	0.035	0.09	0.96	115	33.6	1.4	4.8	4.1	4.3	6.2	1	35.6
MT008-1	T008	8.6	8.8	2.71	85.9	5.11	4	0.19	0.3	0.04	0.19	0.11	0.28	0.02	0.038	0.03	2.19	34	51.7	0.8	5.7	5.1	4	6.3	1	19.9
MT008-2	T008	8.9	9.1	7.26	75.7	7.26	2.9	2.75	0.31	0.13	0.34	0.56	0.21	0.04	0.047	0.16	2.1	235	94.1	2.9	9.1	3.4	4.7	12.9	4	70.2
MT009	T008	9.9	10.1	2.59	88.6	4.69	2.1	0.4	0.31	0.03	0.21	0.08	0.23	0.02	0.034	0.04	0.96	58	25.2	1	5.5	3.1	4.6	6.7	2	23.2

http://etd.uwc.ac.za/

MT010	T009	1	1.2	3.76	84.1	6.73	2.11	1.03	0.09	0.07	0.3	0.005	0.22	0.03	0.038	0.07	0.67	53	4.4	1.1	7.8	3.4	4.6	10.7	1	34.8
MT011	T009	2	2.1	2.82	87.9	5.37	1.37	0.37	0.28	0.02	0.27	0.005	0.23	0.02	0.029	0.04	0.64	45	14.1	0.9	6.4	2.8	3.5	7.6	1	16.8
MT012	T009	3	3.2	3.43	84.4	6.55	2.5	0.48	0.56	0.04	0.33	0.01	0.21	0.03	0.033	0.05	1.17	51	21.4	1.2	7.2	3.1	3.8	10.1	2	22
MT013	T009	4	4.2	2.23	87.1	6.05	2.21	0.27	0.31	0.05	0.24	0.005	0.24	0.02	0.028	0.03	0.98	40	23.7	0.9	6.6	3.2	3.1	8.4	2	22
MT014	T009	5	5.2	3.59	82.1	8.45	2.59	0.54	0.64	0.12	0.35	0.02	0.29	0.03	0.036	0.05	1.28	61	44.4	1.2	8.2	3	3.5	12	2	36
MT015	T009	6	6.2	4.47	80.9	7.49	3.55	0.52	0.56	0.08	0.36	0.06	0.27	0.03	0.035	0.06	1.51	62	69.6	1.1	8	2.9	3.1	12.2	1	31.6
MT016	T009	7	7.1	4.49	81.6	7.21	3.52	0.55	0.49	0.11	0.35	0.05	0.29	0.03	0.035	0.04	1.58	65	68.5	1.1	8	3.3	3.9	11.9	2	33
MT017	T009	8	8.2	3.97	79	5.25	9.01	0.55	0.38	0.06	0.23	0.04	0.22	0.02	0.036	0.22	1.47	60	114	0.9	5.7	3.9	4.1	7.5	2	23
MT018	T009	8.5	8.6	3.18	85.3	5.71	3.51	0.48	0.39	0.05	0.22	0.02	0.27	0.03	0.037	0.04	1.94	40	41.1	0.9	6	3.9	3.4	7.7	1	24
MT018-1	T009	9	9.1	3.42	82.4	9.85	1.75	0.19	0.4	0.1	0.4	0.02	0.35	0.02	0.057	0.05	0.31	71	10.4	1.3	10	3.8	3.7	13.1	2	42.8
MT019	T009	10	10.1	3.23	82.6	7.78	3.21	0.4	0.46	0.15	0.35	0.02	0.26	0.03	0.035	0.09	1.63	55	45.3	1	8.1	3.3	3.1	11.5	1	34.2
MT020	T010	1	1.2	2.49	87.9	6.29	1.63	0.06	0.1	0.15	0.4	0.005	0.23	0.01	0.044	0.01	0.26	64	0.9	1	6.8	3.5	3.2	11.9	1	36.7
MT021	T010	2	2.2	2.78	86.4	7.04	1.83	0.31	0.13	0.17	0.44	0.005	0.23	0.02	0.041	0.04	0.37	75	1.3	1.3	7.3	2.6	3.1	13.2		40.4
MT021-1	T010	2.2	2.4	2.59	87.2	6.73	1.2	0.35	0.12	0.16	0.4	0.005	0.28	0.02	0.045	0.02	0.34	73	0.9	1.2	7.3	3.8	3.6	12.9	1	41.9
MT023	T010	4	4.2	3.21	82.8	9.4	1.49	0.48	0.11	0.28	0.65	0.005	0.29	0.03	0.044	0.05	0.39	104	1.3	1.7	10	2.9	4.1	20.5	2	61.2
MT024	T010	5	5.2	2.24	88.4	4.55	2.76	0.21	0.17	0.09	0.23	0.01	0.3	0.02	0.047	0.02	1.5	35	27.6	0.5	5.6	5.5	4.1	7.1	1	27.5
MT025	T010	6	6.2	3.14	83.9	9.21	1.61	0.36	0.23	0.22	0.55	0.01	0.24	0.05	0.062	0.04	0.86	89	26.2	1.5	9.4	3.1	3.5	17.8		55.7
MT026	T010	7	7.2	2.41	86.2	7.51	1.55	0.17	0.19	0.19	0.43	0.005	0.22	0.05	0.048	0.01	0.81	65	24.5	1.1	7.6	2.8	3.5	13.5		44.3
MT027-1	T010	8.5	8.6	4.43	76.5	6.97	9.31	0.54	0.48	0.11	0.39	0.04	0.24	0.03	0.044	0.08	1.53	69	125.9	1.1	7.1	3.5	3.9	12.4	4	33.2
MT028	T010	9	9.2	3.73	82.3	9.78	1.58	0.47	0.27	0.27	0.57	0.005	0.26	0.04	0.055	0.06	1.04	89	30.7	1.5	8.9	2.6	3.1	17.3	1	56.7
MT029	T011	1	1.2	4.6	86.2	4.21	3.13	0.44	0.41	0.06	0.36	0.02	0.22	0.03	0.084	0.21	0.65	63	10.5	0.6	4.9	2.9	2.8	9.6	5	23.4
MT030	T011	2	2.1	2.1	90.1	3.06	2.59	0.28	0.66	0.04	0.24	0.02	0.26	0.01	0.045	0.03	1.03	35	29.2	0.3	3.4	3.5	3.3	5.7		17
MT031	T011	3	3.2	2.6	86.7	4.12	3.12	0.52	0.86	0.04	0.31	0.03	0.3	0.02	0.046	0.07	1.06	43	37.9	0.6	4.8	3.5	3.3	6.7	1	18.5
MT032	T011	4	4.2	2.81	87.6	4.96	2.39	0.7	0.23	0.05	0.35	0.02	0.24	0.02	0.042	0.14	0.94	49	31.1	0.8	5.7	3	3.4	10.6	2	30.3
MT033	T011	5	5.2	2.35	88.7	5.76	1.69	0.37	0.13	0.08	0.26	0.005	0.26	0.02	0.037	0.03	0.83	41	18.6	0.9	7.2	4.3	6.3	8.6	2	25.3

http://etd.uwc.ac.za/

MT034	T011	6	6.2	2.96	87.7	5.76	1.97	0.34	0.19	0.12	0.31	0.005	0.24	0.02	0.046	0.01	1.05	47	19.3	0.9	6.6	3.6	5.3	9.5	1	31.5
MT035	T011	7	7.1	2.49	86.7	6.28	2.44	0.32	0.48	0.02	0.35	0.01	0.2	0.02	0.045	0.04	1.09	48	36.2	0.9	6.2	2.3	4.4	8.9	2	16.9
MT036	T011	8	8.2	2.56	87	5.95	2.38	0.35	0.47	0.05	0.28	0.01	0.19	0.02	0.038	0.04	1.11	42	34.6	1.1	6.2	2.5	4.7	8	2	18.3
MT037	T011	9	9.2	2.41	87.2	5.68	2.48	0.3	0.58	0.03	0.25	0.02	0.21	0.02	0.038	0.04	1.17	35	36.7	0.8	6.4	2.9	4.3	7.1	1	16.4
MT038	T004	0.9	1.1	3.42	84.8	6.94	1.97	0.62	0.52	0.05	0.5	0.005	0.2	0.02	0.04	0.08	0.44	60	7	0.9	6.9	2.6	4.4	11.6	2	23
MT039	T004	1.7	2	4.14	85.7	5.92	2.38	0.41	0.43	0.06	0.31	0.005	0.19	0.03	0.041	0.04	1.03	46	17.3	0.9	6.1	2.5	3.5	8.4	2	18.5
MT040	T004	3	3.2	3.09	85.6	6.43	2.6	0.32	0.48	0.04	0.36	0.01	0.19	0.02	0.046	0.04	1.02	47	17.8	0.9	6	3.1	4.1	10.1	2	20
MT041	T004	4	4.2	3.65	83.6	8.25	2.31	0.4	0.43	0.07	0.38	0.01	0.23	0.03	0.049	0.11	1.08	63	39.4	1.3	7.4	3	3.9	12.6	2	27.1
MT042	T004	5	5.2	4.02	82.8	6.74	3.47	0.79	0.67	0.14	0.36	0.04	0.25	0.03	0.045	0.08	1.29	61	49.9	1	6.7	3.6	3.6	11.3	1	31
MT042-1	T004	5.3	5.4	4.93	80.6	7.64	3.68	0.7	0.56	0.1	0.41	0.05	0.24	0.03	0.034	0.08	1.49	63	65.1	1.1	6.9	3.1	3.5	12.7	2	30.5
MT043	T004	6	6.2	3.53	85.1	6.02	2.95	0.4	0.42	0.09	0.29	0.03	0.23	0.02	0.037	0.04	1.2	46	44.7	0.8	5.1	2.9	4	8.8	2	25
MT044	T004	7	7.2	3.15	79.7	5.56	9.05	0.63	0.39	0.07	0.25	0.02	0.23	0.02	0.047	0.03	1.34	41	89.7	1.2	4.9	3.9	4.1	8.1	3	24.2
MT045	T004	8	8.2	2.88	88.1	4.59	3.17	0.26	0.27	0.04	0.19	0.01	0.19	0.02	0.041	0.04	1.58	29	34.7	0.6	4.1	3.3	3.2	6	1	18.7
MT046	T004	9	9.2	3.25	85.1	6.14	3.37	0.47	0.4	0.07	0.27	0.02	0.22	0.03	0.043	0.07	1.72	40	38.5	0.9	5.5	2.6	3.9	9	2	23.5

UNIVERSITY of the
WESTERN CAPE

http://etd.uwc.ac.za/

APPENDIX F : Gold tailings Water fraction

Sample_no	Sample No	Sample ID	Depth from (M)	Depth from real(M)	Ca	Ce	Mg	Na	K	Pb	Th	Y	Rb	Nb	Cu	As
MT001	MT001	T008	1	1	149.279	0.00983	2.54224	0.76669	27.8598	0.05466	0.07633	0.0031	0.00787	0.00426	0.0118	0.0198
MT002	MT002	T008	1.9	2	57.0505	0.04329	1.04941	0.08014	21.15	0.10533	0.05692	0.00206	0.00885	0.00397	0.06066	0.12313
MT003	MT003	T008	3	3	30.6081	0.06841	20.6371	0.00642	38.743	0.0011	0.21412	0.04396	0.0133	0.0025	6.2681	0.04737
MT004	MT004	T008	4	4	455.149	0.3294	95.0745	2.81239	56.8638	0.00584	0.46367	0.40501	0.00146	0.00199	1.72586	0.04109
MT005	MT005	T008	5	5	674.278	2.51788	246.798	2.74438	73.1707	0.89633	2.44659	1.63364	0.00138	0.00365	5.47568	1.06473
MT006	MT006	T008	6	6	98.444	0.24223	37.1545	0.7262	35.5761	0.05007	2.41137	0.09484	0.00352	0.00211	1.25137	0.14471
MT0071	MT007-1	T008	7.5	7.5	521.907	0.93548	95.158	3.1267	63.3177	0.42353	4.90998	0.32672	0.00251	0.00183	2.50776	4.12491
MT009	MT009	T008	9.9	10	131.89	0.0681	0.61165	0.12082	25.2991	0.08063	0.09724	0.00385	0.00393	0.00197	0.03724	0.08812
MT010	MT010	T009	1	1	771.862	0.10235	122.259	2.38376	59.856	0.1089	0.37347	0.03621	5.4E-05	0.00166	1.59445	0.21625
MT011	MT011	T009	2	2	552.24	0.14723	144.022	2.07793	68.6433	0.22239	1.79341	0.07421	0.00483	0.00151	2.67185	0.90301
MT012	MT012	T009	3	3	488.548	0.2204	91.5135	2.98117	50.4849	0.13574	1.26606	0.16109	0.00038	0.00184	3.6601	0.02888
MT013	MT013	T009	4	4	499.254	1.13674	18.5652	2.80871	95.1368	1.40259	0.7276	0.36998	0.0046	0.00739	1.8456	0.06398
MT014	MT014	T009	5	5	659.122	2.75194	231.182	1.8768	108.503	0.77376	6.01668	2.9402	0.01008	0.0051	4.10736	1.27064
MT016	MT016	T009	7	7	13.0087	0.08501	12.5543	0.09432	40.7075	0.10881	0.31063	0.02101	0.01768	0.00012	0.30098	0.20763
MT017	MT017	T009	8	8	1105.91	0.93756	212.989	2.34981	62.9833	0.57005	1.96421	0.37691	0.00041	0.00255	4.06894	1.90671
MT018	MT018	T009	8.5	8.5	361.317	0.55377	94.7724	3.86734	61.2692	0.06707	0.74214	0.23621	0.01072	0.00205	0.68749	0.03204
MT0181	MT018-1	T009	9	9	409.363	0.49045	82.1717	3.12973	59.3373	0.02283	2.34297	0.17546	0.00684	0.0019	1.72403	0.02353
MT019	MT019	T009	10	10	906.293	1.01127	197.556	4.41545	62.2534	0.7441	2.35105	0.29496	0.00718	0.00376	5.01915	6.1596

http://etd.uwc.ac.za/

MT020	MT020	T010	1	1	14.7688	0.07013	0.4889	0.23123	24.5774	0.07422	0.06239	0.00418	0.00636	0.00342	0.02126	0.10796
MT021	MT021	T010	2	2	694.257	0.01899	10.1174	3.98047	55.5247	0.09343	0.00601	0.0043	0.00405	0.00061	0.16655	0.0049
MT0211	MT021-1	T010	2.2	2.4	72.0405	0.03616	1.35511	0.38365	31.1591	0.14005	0.04963	0.0038	0.00474	0.00218	0.02397	0.0498
MT023	MT023	T010	4	4	451.6	0.05856	32.1095	3.24677	69.635	0.09255	1.20758	0.0148	0.00632	0.00013	0.43911	0.02646
MT025	MT025	T010	6	6	53.3955	0.07902	9.0729	0.07119	47.4719	0.04554	0.32721	0.05806	0.00028	0.00048	11.3367	1.12068
MT0271	MT027-1	T010	8.5	8.5	322.168	1.06874	259.128	2.31736	51.5733	0.81125	3.24342	0.43537	0.00116	0.00462	3.78447	1.43215
MT029	MT029	T011	1	1	206.711	0.10767	89.1048	16.498	37.11	0.01679	0.14334	0.06735	0.0002	0.00035	1.14374	0.00229
MT030	MT030	T011	2	2	200.996	0.02088	66.7244	13.357	40.0529	0.08136	0.13519	0.01354	0.00138	0.00202	0.04362	0.03255
MT033	MT033	T011	5	5	351.843	0.10751	15.6137	12.5165	53.5871	0.09743	0.02756	0.11259	0.00079	0.00222	1.37293	
MT036	MT036	T011	8	8	227.171	0.25447	71.5611	24.9282	42.3344	0.1202	0.15824	0.25971	0.00625	0.00206	1.28964	0.0228
MT037	MT037	T011	9	9	250.811	0.16456	30.7082	27.445	50.0347	0.0816	0.10576	0.14635	0.0041	0.00274	0.61096	0.0165
MT039	MT039	T004	1.7	2	319.935	0.02968	79.6586	11.2138	38.7052	0.21871	0.06782	0.02032	0.00057	0.00126	0.47165	0.02954
MT041	MT041	T004	4	4	459.854	1.17367	68.4335	13.9405	86.9935	0.24143	0.24421	0.26466	0.00236	0.00106	4.28505	0.02244
MT042	MT042	T004	5	5	332.325	0.68604	86.7433	11.5262	59.3674	0.22451	0.53414	0.88325	0.00487	0.00097	2.74656	0.03656
MT0421	MT042-1	T004	5.3	5.4	320.214	0.55128	87.8507	14.2507	46.9602	0.23273	0.42884	0.17382	0.00192	0.00061	2.19874	0.07971

UNIVERSITY of the
WESTERN CAPE

http://etd.uwc.ac.za/

APPENDIX G : Gold tailings Carbonate fraction

Sample No	Sample ID	Depth from (M)	Depth from real(M)	Sample_ID	Ca	Si	Ce	Mg	Na	K	Pb	Nb	Th	Y	Rb	Cu	Cu_327	As	Zn	Mo	Co
MT001	T008	1	1	T008	185.715	95.2852	0.23128	12.7055	5.10753	44.263	0.526	0.02314	0.30038	0.00921	0.06069	0.2339	0.17909	0.96288	0.01515	0.15979	0.34994
MT002	T008	1.9	2	T008	114.35	30.05	0.15208	10.168	2.50749	61.5887	0.66695	0.00081	0.08156	0.00537	0.06537	0.04299	0.02035	0.6614	0.38454	0.05025	0.00895
MT003	T008	3	3	T008	169.931	104.882	0.14974	47.5711	6.34526	38.4514	0.10901	0.00444	0.16126	0.02393	0.11364	2.06383	2.04338	2.05388	2.16712	0.04465	1.04593
MT004	T008	4	4	T008	296.985	25.7014	0.21817	31.099	8.011	32.9723	0.04113	0.00418	0.29592	0.0349	0.12655	0.18102	0.22412	0.84816	2.94934	0.0391	1.00769
MT005	T008	5	5	T008	748.606	37.8913	0.305	83.812	6.22561	82.5709	0.1528	0.01219	0.27254	0.03167	0.17118	0.06643	0.01553	0.58736	2.53933	0.0341	1.55096
MT006	T008	6	6	T008	983.245	28.4743	0.0218	96.6727	7.39031	158.874	0.80431	0.01662	1.40709	0.01725	0.13821	0.04683	0.02488	1.19361	0.08148	0.00512	0.91089
MT007	T008	7	7	T008	1258.21	53.703	0.51302	69.0294	8.77901	546.977	1.27207	0.01223	2.83736	0.27796	0.14252	0.28487	0.37508	1.21021	3.57735	0.0221	1.0934
MT007-1	T008	7.5	7.5	T008	384.523	18.0088	0.1512	16.005	10.8448	59.3303	0.67248	0.01178	0.88131	0.0235	0.14792	0.08154	0.03975	0.80198	0.85696	0.07214	0.5323
MT008	T008	8	8	T008	121.018	43.7741	0.15927	22.9092	5.46421	23.1253	0.10341	0.01378	0.39129	0.00946	0.14876	0.01765	0.02511	1.60617	0.71036	0.09739	0.632
MT008-1	T008	8.6	8.5	T008	1280.83	40.5445	0.12878	9.21283	5.93745	385.97	0.18892	0.01801	0.37688	0.0052	0.1945	0.00526	0.0018	1.04718	0.45073	0.06453	0.14716
MT010	T009	1	1	T009	360.438	48.2836	0.25907	26.7741	5.91801	136.365	0.76126	0.01432	0.39435	0.01211	0.11758	0.02079	0.04179	1.17629	0.39066	0.10404	0.91278
MT011	T009	2	2	T009	564.927	25.2976	0.03172	31.4567	4.8968	244.026	0.01319	0.01835	0.16475	0.01387	0.12167	0.05758	0.06111	0.96742	0.25132	0.02695	0.27662
MT012	T009	3	3	T009	120.004	7.93328	0.10526	15.3048	3.39647	10.0881	0.76981	0.01991	0.24791	0.01339	0.13308	0.00558	0.03614	0.55729	0.13751	0.04927	0.03176
MT013	T009	4	4	T009	855.875	23.7126	0.18684	10.4794	6.23177	416.772	2.33337	0.02299	0.14433	0.01538	0.1421	0.08968	0.15767	0.81167	0.1935	0.08821	0.33033
MT015	T009	6	6	T009	335.372	25.0006	0.08428	52.7893	2.59371	111.627	0.36913	0.02216	0.02773	0.03552	0.26858	0.02008	0.03435	0.63657	0.87659	0.04092	0.60473
MT016	T009	7	7	T009	417.885	25.0012	0.36062	41.7514	2.08749	269.257	0.85809	0.00851	0.40093	0.0008	0.04816	0.01464	0.07207	1.88472	0.43465	0.21361	0.41782
MT017	T009	8	8	T009	240.796	18.7517	0.26571	35.8521	0.88741	140.004	1.07792	0.00158	0.04155	0.01011	0.09144	0.00743	0.15262	1.84526	0.09273	0.16979	0.5738
MT018	T009	8.5	8.5	T009	88.9163	21.2528	0.26454	23.1389	1.16161	113.315	0.47207	0.00688	0.09807	0.00246	0.06103	0.01857	0.10487	2.34822	0.0311	0.06404	0.27651

http://etd.uwc.ac.za/

MT019	T009	10	10	T009	368.296	22.7058	0.32294	34.6255	0.42836	313.477	0.62017	0.002	0.14071	0.00528	0.02932	0.03679	0.11716	1.82642	0.53474	0.17713	0.34323
MT020	T010	1	1	T010	34.6075	31.5525	0.15385	10.4392	0.96082	25.4865	0.28994	0.01067	0.04302	0.01274	0.06891	0.06548	0.07419	1.14429	0.04004	0.14568	0.02056
MT021	T010	2	2	T010	90.2572	38.3345	0.21747	10.2754	1.20468	232.887	0.43109	0.00649	0.57322	0.00257	0.07501	0.02017	0.11798	2.1822	0.05754	0.02451	0.04631
MT021-1	T010	2.2	2.4	T010	101.169	46.8021	0.16642	10.1097	1.51532	190.726	1.67386	0.00919	0.15854	0.01507	0.10651	0.03912	0.0983	1.89306	0.01143	0.19722	0.03126
MT023	T010	4	4	T010	157.565	40.1611	0.27355	10.5387	1.06932	110.974	0.76734	0.00764	0.28963	0.00296	0.07273	0.05937	0.11258	2.33727	0.04616	0.06567	0.06563
MT024	T010	5	5	T010	65.131	44.3375	0.30054	12.5174	0.95562	83.1675	0.50587	0.00247	0.02014	0.00956	0.06953	0.00328	0.10423	2.67402	0.03223	0.11954	0.10568
MT025	T010	6	6	T010	87.2145	20.9028	0.42118	17.8486	1.18097	166.563	0.29317	0.01367	0.32981	0.01262	0.0036	2.14818	2.43964	2.0756	0.75179	0.21323	0.35179
MT026	T010	7	7	T010	58.7289	26.6213	0.22755	17.3025	2.40961	77.6146	0.11459	0.00964	0.26556	0.00563	0.00675	0.38006	0.21627	0.50883	0.43363	0.294	0.16707
MT027-1	T010	8.5	8.5	T010	105.164	11.9344	0.37035	19.6759	0.62261	60.0704	0.31714	0.00527	0.66279	0.00231	0.02639	1.79588	2.10526	2.66872	0.78356	0.01999	0.37485

APPENDIX H : Gold tailings Hydroxylamine fraction

Sample No	Sample ID	Depth from (M)	Depth from real(M)		ppm	Ca	Si_	Si_28	Ca_3	Ce	Mg	Na	K	Pb	Nb	Th	Y	Rb	Nb	Cu	Cu
MT001	T008	1	1		MT1	87.88975	13.2671	12.87635	11.58925	0.445921	29.9476	76.425	24.3799	0.19138	0.474628	0.119644	0.542814	0.114918	0.438583	0.683948	0.4
MT002	T008	1.9	2		h11.1	8.5435	16.919	16.8535	94.12	0.189829	25.9238	52.84	81.139	0.66375	0.8643	0.286975	0.36967	0.111924	0.424153	0.7973	0.
MT003	T008	3	3		h3	94.933	12.5485	12.38325	19.85875	0.933325	3.964375	51.7425	16.11957	0.376	0.144735	0.111852	0.238639	0.5561	0.313128	0.162847	0.

http://etd.uwc.ac.za/

MT004	T008	4	4		h4	97.715	7.247525	7.163225	111.2425	0.538817	3.6855	36.98425	1.538923	0.919223	0.2655	0.316	0.481448	0.23319	0.958743	0.126345	0.
MT006	T008	6	6		h6	9.41625	28.242	28.29425	13.681	0.427118	28.8235	5.718325	19.81825	0.349223	0.262482	0.391872	0.616559	0.154359	0.142375	0.156132	0.
MT007	T008	7	7		h7	129.8775	45.25725	45.63735	146.358	0.557885	39.88875	97.9875	23.45	3.928	0.216413	2.13674	0.358517	0.37325	0.445785	1.581313	1.
MT007-1	T008	7.5	7.5		h8	87.59	13.97128	13.92775	1.32925	0.5699	29.98443	11.78475	5.339953	0.496525	0.348963	0.189558	0.197175	0.393764	0.21888	0.194125	0.
MT008	T008	8	8		h8.2	93.99575	17.67213	17.567	19.42225	0.544673	3.55425	83.77175	36.5377	0.151325	0.417529	0.177	0.116771	0.932228	0.171883	0.914248	0.
MT010	T009	1	1		h11	84.86575	21.25238	2.9711	97.57	0.1361	28.93123	13.512	45.3255	0.118985	0.5875	0.152793	0.253255	0.156274	0.114683	0.3225	0.
MT011	T009	2	2		h12	96.57175	17.5588	17.5485	11.128	0.164292	31.54425	78.12175	13.7536	0.545316	0.27375	0.133173	0.578272	0.224814	0.754398	0.223589	0.
MT012	T009	3	3		h13	15.6935	14.9961	14.8835	12.419	0.42535	36.795	189.931	3.28835	0.16422	0.588465	0.142777	0.417715	0.9977	0.139195	0.95155	0.
MT013	T009	4	4		h14	12.527	26.84115	26.18668	117.9645	0.986733	31.96313	83.9125	54.583	1.346983	0.16518	0.242241	0.168358	0.153814	0.121714	0.444716	0.
MT014	T009	5	5		h15	93.87	11.95275	11.7864	16.3975	0.294663	32.25625	11.81625	11.92775	0.271243	0.158464	0.276415	0.23198	0.326226	0.241613	0.229266	0.
MT016	T009	7	7		h97.1	9.335	13.8873	13.8249	85.21875	0.756363	6.44325	319.847	68.16	0.621814	0.141794	0.365925	0.264287	0.885725	0.463333	0.39879	0.
MT018	T009	8.5	8.5		h98.11	114.3885	19.96825	19.7238	132.5835	0.82493	36.1926	54.1415	59.4935	0.275178	0.414673	0.173731	0.157455	0.22749	0.15748	0.852	0.
MT018-1	T009	9	9		h99.1	112.77	17.4472	16.96355	129.565	0.63327	33.9385	128.351	34.86725	0.7378	0.5277	0.216544	0.567515	0.156165	0.9235	0.17239	0.
MT021	T010	2	2		h12.1	235.672	23.3727	22.9556	266.1325	0.466916	74.14	279.11	31.77115	0.464759	0.145795	0.16563	0.45915	0.5311	0.446958	0.816575	0.

http://etd.uwc.ac.za/

MT021-1	T010	2.2	2.4		h13	118.4685	26.1675	25.39315	136.7938	0.115625	35.445	154.8383	38.93383	0.295228	0.56397	0.153725	0.259744	0.673448	0.428875	0.491359	0.
MT023	T010	4	4		h14	94.2345	24.738	24.29815	19.14275	0.251638	27.62525	138.2663	35.239	0.36428	0.136843	0.26425	0.444383	0.226248	0.485222	0.572275	0.
MT024	T010	5	5		h15	91.12575	9.68275	9.616775	15.85225	0.149345	29.41725	69.63645	67.93275	0.452314	0.14117	0.154125	0.82975	0.113958	0.285869	0.95115	0.
MT025	T010	6	6		h16	1.95	19.6671	19.61623	114.4473	0.629373	32.717	81.51125	43.27978	0.246575	0.444544	0.26562	0.294525	0.62489	0.483425	0.59965	0.
MT026	T010	7	7		h17	86.368	14.16538	14.937	1.32925	0.545978	3.15	19.445	53.71213	0.181923	0.234562	0.41386	0.339875	0.346665	0.656653	0.282686	0.
MT027-1	T010	8.5	8.5		h18	81.92825	18.35318	18.44825	94.39	0.78925	26.65425	95.58865	35.7215	0.366728	0.213518	0.118968	0.243894	0.11185	0.166535	1.49275	0.
MT029	T011	1	1		h111	89.1395	12.42685	12.35225	89.97625	0.376473	6.49475	225.25	22.74175	0.91575	0.441979	0.345775	0.869433	0.627399	0.2249	0.533816	0.
MT030	T011	2	2		h112	74.1925	9.5445	9.372175	75.15975	0.232118	5.61685	16.62915	21.27213	0.578175	0.152555	0.193468	0.2451	0.419747	0.144965	0.272648	0.
MT031	T011	3	3		h113	94.59775	42.79223	41.119	89.227	0.6776	66.75575	357.5175	21.2325	6.198525	0.129387	0.12525	0.162563	0.121928	0.828618	4.37485	6.
MT032	T011	4	4		h114	156.587	55.52225	54.95388	152.8788	0.251124	59.641	16.6558	4.8425	1.181425	0.139488	0.54782	0.126489	0.112525	0.692718	1.838613	2.
MT033	T011	5	5		h115	87.49725	15.51555	15.83375	8.86275	0.671475	6.164675	377.58	11.6293	0.56244	0.766468	0.226365	0.74883	0.829928	0.115147	0.44284	0.
MT034	T011	6	6		h116	9.9195	32.8663	33.57455	89.16	0.295828	24.99218	26.77322	23.28	3.349618	0.896295	0.495538	0.121783	0.2591	0.174388	2.768883	3.
MT036	T011	8	8		h118	74.767	14.1112	13.65113	68.984	0.527355	5.51137	182.4853			0.68589	0.918325	0.892756	0.439989	0.566853	0.342487	0.
MT037	T011	9	9		h119	74.14425	15.51325	15.22865	75.2865	0.184248	5.46315	27.615	38.81168	0.272267	0.321475	0.264863	0.244133	0.156145	0.134836	0.361977	0.

http://etd.uwc.ac.za/

MT038	T004	0.9	1		h41	92.525	2.552	19.812	94.2465	0.432695	6.6416	22.8275	12.6675	0.229384	0.411788	0.163	0.589965	0.255822	0.8492	0.67644	0.
MT039	T004	1.7	2		h42	81.7475	19.48635	19.4218	82.7825	0.168553	6.12115	59.25783	9.925775	0.368357	0.373978	0.157597	0.142596	0.129748	0.15244	0.677688	0.
MT042-1	T004	5.3	5.4		h46	85.45175	16.87918	16.3484	76.66525	0.55249	6.631	322.9158	39.4267	1.2173	0.983383	0.29262	0.128537	0.472159	0.128895	0.492963	0.
MT043	T004	6	6		h47	92.862	27.8675	27.82638	93.714	0.284648	6.528725	142.1339	12.56718	0.12784	0.197529	0.235938	0.241665	0.157185	0.154718	0.474445	0.
MT046	T004	9	9		h49	112.325	15.99835	15.41145	14.935	0.134185	7.771325	329.8883	3.914575	0.51955	0.132648	0.32173	0.8974	0.123275	0.177213	0.658834	0.

UNIVERSITY of the
WESTERN CAPE

APPENDIX I: Coal fly ash and gold tailings sampling location

BH ID	Easting	Northings	Elevation	Method	Hole type

http://etd.uwc.ac.za/

S1	711112	7060505	1636	GPS	RC
S2	711084	7060651	1635	GPS	RC
S3	711076	7060792	1610	GPS	RC

Sample ID	East	North	Latitude	Longitude	Elevation (M)	Method	Hole type	Depth
T008	576129,3	7109896	-26,1282	27,76152	1776	GPS	RC	10,2
T009	576023,5	7110328	-26,1243	27,76043	1779	GPS	RC	10,2
T010	576021,8	7109749	-26,1295	27,76045	1738	GPS	RC	10,2
T011	576189,2	7110169	-26,1257	27,7621	1772	GPS	RC	10,2
T004	576049,1	7110149	-26,1259	27,7607	1779	GPS	RC	10,2

APPENDIX J: Coal fly ash lithology based on Discriminant analysis

SampleID	DepthFrom	depthTo	Lon	Lat	Discriminant	Elevation
S1	0	7,8	-26,5604	29,11935	D1	1636
S1	7,8	16,8	-26,5604	29,11935	D2	1628,2
S1	16,8	18,5	-26,5604	29,11935	D3	1619,2
S1	18,5	19,2	-26,5604	29,11935	D2	1617,5
S1	19,2	22,8	-26,5604	29,11935	D3	1616,8

UNIVERSITY of the WESTERN CAPE
http://etd.uwc.ac.za/

S2	0	0,25	-26,5591	29,11904	D1	1635
S2	0,25	1,2	-26,5591	29,11904	D2	1634,75
S2	1,2	5	-26,5591	29,11904	D1	1633,8
S2	5	9,5	-26,5591	29,11904	D2	1630
S2	9,5	12,5	-26,5591	29,11904	D1	1625,5
S2	12,5	17	-26,5591	29,11904	D2	1622,5
S2	17	23	-26,5591	29,11904	D1	1618
S2	23	31,8	-26,5591	29,11904	D2	1612
S3	0	0,25	-26,5578	29,11894	D1	1610
S3	0,25	1,2	-26,5578	29,11894	D2	1609,75
S3	1,2	5	-26,5578	29,11894	D1	1608,8
S3	5	9,5	-26,5578	29,11894	D2	1605
S3	9,5	12,5	-26,5578	29,11894	D1	1600,5
S3	12,5	17	-26,5578	29,11894	D2	1597,5
S3	17	23	-26,5578	29,11894	D1	1593
S3	23	31,8	-26,5578	29,11894	D2	1587

UNIVERSITY of the WESTERN CAPE
http://etd.uwc.ac.za/

UNIVERSITY of the
WESTERN CAPE

APPENDIX K: Discriminant analyses of coal fly ash samples

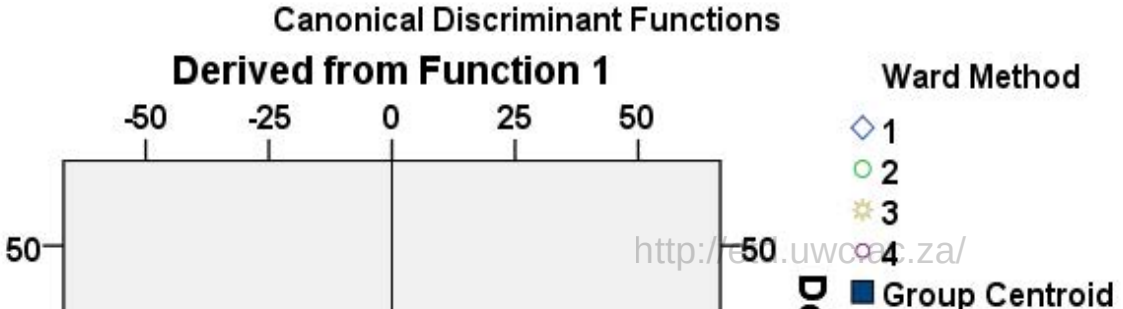

http://etd.uwc.ac.za/

UNIVERSITY of the
WESTERN CAPE

Classification Results[a]

			Predicted Group Membership				
		Ward Method	1	2	3	4	Total
Original	Count	1	16	0	0	0	16
		2	2	38	0	0	40
		3	0	0	3	0	3
		4	0	0	0	2	2
	%	1	100,0	0,0	0,0	0,0	100,0

http://etd.uwc.ac.za/

2	5,0	95,0	0,0	0,0	100,0
3	0,0	0,0	100,0	0,0	100,0
4	0,0	0,0	0,0	100,0	100,0

a. 96.7% of original grouped cases correctly classified.

Structure Matrix

	Function		
	1	2	3
K2O	-.396*	,097	,146
SiO2	-,109	.554*	-,174
MnO	-,113	,032	.783*
Al2O3	,181	,458	-.690*
Na2O[b]	-,025	,009	.610*
CaO[b]	,141	,087	.571*
TiO2	,045	,184	.521*
MgO[b]	-,105	,177	.467*
P2O5[b]	,018	,108	.415*
Fe2O3	-,039	-,032	.344*
%S[b]	-,131	-,183	.226*

Pooled within-groups correlations between discriminating variables and standardized canonical discriminant functions
Variables ordered by absolute size of correlation within function.

UNIVERSITY of the WESTERN CAPE
http://etd.uwc.ac.za/

*. Largest absolute correlation between each variable and any discriminant function
b. This variable not used in the analysis.

UNIVERSITY of the
WESTERN CAPE

APPENDIX L: Summary of gold tailings whole data

	Gold tailings' data				Oxidized Layer	Transition Layer	Reddish layer	Un-oxidised layer
Variables	**Min**	**Max**	**G.Mean**	**Std. D**	**G.Mean**	**G.Mean**	**G.Mean**	**G.Mean**
Major Elements	**%wt**							
LOI	**1.72**	**7.26**	**3.28**	**1.12**	**2.82**	**3.37**	**4.00**	**3.36**

http://etd.uwc.ac.za/

SiO_2	70.70	90.30	84.24	4.11	87.32	84.48	76.39	84.09
Al_2O_3	3.06	9.85	6.25	1.60	5.43	6.35	6.56	6.57
Fe_2O_3	0.86	9.31	2.64	1.93	1.75	2.64	9.03	2.60
CaO	0.06	2.75	0.43	0.44	0.34	0.41	0.74	0.44
MgO	0.09	0.86	0.35	0.18	0.25	0.41	0.45	0.37
Na_2O	0.02	0.28	0.07	0.06	0.06	0.07	0.09	0.08
K_2O	0.17	0.65	0.32	0.10	0.33	0.33	0.33	0.31
MnO	0.01	0.65	0.02	0.14	0.01	0.01	0.06	0.03
TiO_2	0.18	0.35	0.24	0.04	0.23	0.25	0.24	0.24
P_2O_5	0.01	0.05	0.02	0.01	0.02	0.02	0.03	0.03
Cr_2O_3	0.03	0.08	0.04	0.01	0.04	0.04	0.04	0.04
Leco A.	(%wt)							
TOT/C	0.01	0.22	0.05	0.05	0.04	0.05	0.10	0.05
TOT/S	0.26	2.19	1.00	0.51	0.48	1.13	1.52	1.23
Trace elements	(ppm)							
Ba	29.00	264.00	58.59	45.96	52.25	52.08	73.51	63.59
Co	0.90	125.90	23.99	29.36	4.71	27.09	105.74	37.70
Cs	0.30	3.00	1.04	0.52	0.87	0.98	1.37	1.12
Th	3.60	54.10	8.61	8.07	4.89	8.71	10.43	10.84
U	4.00	655.50	25.53	90.46	6.88	34.71	38.62	37.40
Zr	92.70	233.80	122.80	26.69	112.26	121.05	152.81	124.41
Mo	1.20	6.40	3.57	1.39	3.74	3.31	4.45	3.50
Cu	3.80	308.80	35.43	58.70	13.20	36.24	65.05	50.47
Pb	15.40	150.20	42.91	29.26	46.70	41.69	52.67	40.41

UNIVERSITY of the WESTERN CAPE
http://etd.uwc.ac.za/

Zn	**4.00**	**817.00**	**73.02**	**143.50**	**19.69**	**88.87**	**142.55**	**108.88**
Ni	**3.80**	**274.10**	**69.31**	**71.17**	**19.85**	**77.44**	**164.88**	**101.83**
As	**15.30**	**471.40**	**105.28**	**75.47**	**61.63**	**97.99**	**167.39**	**130.68**
Au	**58.10**	**1417.50**	**189.19**	**227.93**	**154.60**	**226.48**	**625.72**	**152.87**
Sb	**0.40**	**2.30**	**0.73**	**0.38**	**0.55**	**0.66**	**1.86**	**0.75**
Bi	**0.70**	**3.60**	**1.43**	**0.63**	**1.27**	**1.38**	**2.65**	**1.39**
Hg	**0.05**	**2.51**	**0.21**	**0.47**	**0.24**	**0.21**	**0.13**	**0.21**
Static test								
Paste pH	**2.61**	**8.69**	**4.28**	**1.52**	**3.85**	**4.20**	**3.82**	**4.64**
EC (mS/cm)	**0.43**	**3.99**	**1.09**	**0.79**	**0.92**	**1.15**	**1.79**	**1.06**

UNIVERSITY of the
WESTERN CAPE

http://etd.uwc.ac.za/